Université de Montréal

Synthesis, diversification and biomedical applications of 4,5-substitued *N*-aminoimidazol-2-ones

by

Julien Poupart

Département de Chimie, Faculté des Arts et Sciences

Thesis presented to the Faculté des études supérieures et postdoctorales for the obtention of a Ph.D. degree in chemistry

January 2020

Université de Montréal

Unité académique : Département de Chimie, Faculté des Arts et Sciences

---

This Thesis titled:

Synthesis, diversification and biomedical applications of 4,5-substitued N-aminoimidazol-2-ones

Presented by

Julien Poupart

Was evaluated by a Jury composed of:

Samy Cecioni
President of the Jury

William D. Lubell
Research Director

Stephen Hanessian
Jury Member

David M. Chenoweth
External Examiner

Résumé

Le développement de mimes de tours peptidiques pose un intérêt particulier en chimie médicinale, en raison de leur importance dans la reconnaissance moléculaire. Dans ce contexte, les résidus *N*-aminoimidazol-2-one (Nai) ont démontré une tendance à occuper la position centrale de repliements peptidiques. De plus, la présence de l'unité imidazolone offre un potentiel de fonctionnalisation en position 4 et 5 pouvant jouer le rôle de chaînes latérales rigidifiées dans l'espace χ.

Des méthodes ont été développées pour rendre possible l'utilisation de résidus Nai en chimie peptidique. Par le passé, des esters de dipeptide Nai possédant un substituant à la position 4 de l'hétérocycle ont été synthétisés de manière racémique. L'utilisation de groupement *C*-terminaux a permis de grandement réduire l'épimérisation due à l'utilisation de base forte utilisée durant l'étape de cyclisation. La fonctionnalisation de la position 5 du cycle après la cyclisation a aussi été rendue possible par le développement de nouvelles conditions réactionnelles. Par exemple, des conditions de formylation ont donné des résidus (4-Me, 5-Aldéhyde)Nai. La fonction aldéhyde a été réduite et oxydée, donnant accès a des fonctions alcool et acide carboxylique. L'amination réductrice du squelette (4-Me, 5-Aldéhyde)Nai en utilisant des amines primaires et secondaires ainsi que l'amino-méthylation de résidus (4-Me)Nai ont donné accès à des résidus d'acide diaminobutyrique rigidifiés. Dans le but de préparer des analogues Nai pouvant servir de mimes rigidifiés de résidus phénylalanine, la catalyse au palladium a rendu possible l'installation de groupements 5-aryle par couplage croisé avec différents iodoaryles. Dans un modèle de peptide, le résidu (4-Me, 5-aryl)Nai a été soumis à une analyse par dynamique moléculaire qui a révélé le positionnement de la portion Nai à la position *i*+1 d'un tour β de type II', avec la chaine latérale aryle adoptant une conformation *gauche* (-).

Ayant en main des conditions de synthèse énantioenrichie ainsi que de diversification de la position 5, la construction de peptides Nai possédant un intérêt biologique a été entreprise. Des dérivés du peptide *Growth hormone releasing peptide-6* (GHRP-6) ont été ciblés car les analogues semicarbazide correspondant ont précédemment démontré avoir à la fois de la sélectivité et une affinité relativement grande pour le *Cluster of differentiation receptor* (CD36).

Ils ont ainsi le potentiel de moduler l'inflammation attribuable aux macrophages dans des conditions menant à la dégénérescence maculaire liée à l'âge, l'athérosclérose et l'angiogenèse. Des études précédentes ont démontré que le remplacement du résidu Trp^4 du GHRP-6 par un semicarbazide possédant une chaîne latérale aromatique favorisait l'adoption d'un repliement de la chaîne peptidique et une affinité sélective envers le récepteur CD36. Une méthode de synthèse sur phase solide d'analogues [(4-Me, 5-Aryle)Nai^4]-GHRP-6 a été développée et utilisée pour synthétiser quatre différents peptides Nai en utilisant la résine Rink amide. Les quatre analogues se sont montrés efficaces à réduire la surproduction d'oxide nitrique (NO) dans les cellules macrophages traitées avec un agoniste du *Toll-like receptor 2* (TLR2). Malgré le fait que l'évaluation biologique des analogues [(4-Me, 5-Aryle)Nai^4]-GHRP-6 soit toujours en cours, leur habilité à moduler la surproduction d'oxide nitrique montre qu'ils possèdent la bonne géométrie quant à la chaîne principale et la chaîne latérale aromatique pour interagir avec le récepteur.

En somme, la présente thèse a fourni des méthodes efficaces de synthèse de nouveaux analogues de peptides rigidifiés pour mimer les chaînes principale et latérales de tours β. Les résidus Nai énantioenrichis ont été synthétisés, introduits dans des séquences peptidiques d'intérêt sur phase solide et fonctionnalisés à la $4^{ième}$ et $5^{ième}$ position. L'utilisation de ces analogues Nai 4,5-disubstitués en chimie médicinale et peptidique offre un potentiel considérable dans l'exploration de la relation structure-activité de peptides d'intérêt biologique pour identifier et mimer les conformères bioactifs.

Mots clef: *N*-Aminoimidazolone, azapeptides, GHRP-6, CD36, peptidomimétisme, tours-β, arylation catalysée au palladium, réaction de Vilsemeier, réaction de Mannich, semicarbazone

Abstract

In peptide-based medicinal chemistry, mimicry of turn conformations is important because of the significance of such secondary structures for molecular recognition. In this context, *N*-aminoimidazol-2-one (Nai) residues have demonstrated ability to mimic the central residue of turn conformers. Moreover, potential to functionalize the 4- and 5-positions of the Nai heterocycle offer opportunities to add and orient side chain functionalities with constrained c-geometry.

Methods have been developed to employ Nai residues for peptide mimicry. Previously, Nai dipeptide esters with substituents at the imidazol-2-one 4-position were obtained as racemic mixtures. By employing alternative *C*-terminal groups, epimerization has now been minimized. Functionalization of the Nai 5-position after cyclization has also been achieved by novel chemistry. For example, (4-Me, 5-aldehyde)Nai residues were obtained by 5-position formylation. The aldehyde was then reduced and oxidized to provide alcohol and acid functionality. Reductive aminations on (4-Me, 5-aldehyde)Nai residues using different primary and secondary amines and amino methylation of (4-Me)Nai residues were also used to prepare constrained diaminobutyric acid analogs. In the interest to prepare Nai analogs that can serve as constrained phenylalanine residues, palladium-catalyzed chemistry was developed to cross-couple different aryl iodides at the 5-position. In model peptides, the (4-Me, 5-aryl)Nai residues were predicted by molecular dynamic calculations to be located at the *i*+1 position of type II' β-turn conformations with the aryl side chain positioned in the *gauche* (–).

The synthesis of biologically relevant Nai peptides was next explored using methods for accessing enantioenriched residues and conditions for their 5-position arylation. Peptide derivatives of growth hormone releasing peptide-6 (GHRP-6) were targeted using the Nai residues because the corresponding semicarbazide analogs had exhibited selective and relatively high binding affinity for the cluster of differentiation receptor (CD36) receptor and potential to mediate macrophage-driven inflammation in conditions leading to age-related macular degeneration, atherosclerosis and angiogenesis. Previous studies with GHRP-6 analogs demonstrated that replacement of Trp^4 with a semicarbazide possessing an aromatic side chain

favored a turn conformation and selective CD36 binding affinity. Solid-phase methodology was developed to synthesize [(4-Me, 5-Aryl)Nai^4]-GHRP-6 analogs and used to prepare four different Nai peptides on Rink amide resin. All four analogs were effective at mediating nitric oxide (NO) overproduction in macrophages cells treated with a Toll-like receptor 2 (TLR2) agonist. Although biological evaluation of the [(4-Me,5-Aryl)Nai^4]-GHRP-6 analogs is still being performed, their ability to modulate NO overproduction strongly indicated backbone and side chain conformational requirements for biological activity.

In sum, this thesis has provided effective methods for preparing novel constrained peptide analogs for mimicry of the backbone and side chain geometry in β-turns. Enantiomerically enriched Nai residues were synthesized, introduced into peptide sequences, and functionalized at the 4- and 5-positions. Employment of the 4,5-disubstituted Nai analogs in the study of peptide medicinal chemistry offers powerful potential for exploring structure-activity relationships to identify and replicate biologically active conformers.

Keywords: *N*-Aminoimidazolone, azapeptides, GHRP-6, CD36, peptide mimicry, β-turns, palladium-catalyzed arylation, Vilsmeier formylation, Mannich reaction, semicarbazone

Note

This thesis describing synthesis, diversification and biomedical application of *N*-aminoimidazolone residues is written by articles. The individual contribution of each co-authors is specified before each article. The Chapter one, Introduction and background, and unless otherwise specified below, the other chapters were all written by me and edited by Professor William D. Lubell.

The first article to appear (Chapter 2), entitled "Synthesis of steroenriched 4,5-disubstituted *N*-aminoimidazol-2-one (Nai) peptide turn mimic" describes the conditions and *C*-terminal groups that were used in order to achieve cyclization of aza-propargyl-glycine dipeptides with minimal epimerization. Following ring synthesis, a variety of functional groups are introduced at the 5-position including aldehyde, alcohol, acid and aminomethyl functionalities. This article has been submitted to *Can. J. Chem.* to feature in a special edition dedicated to Professor James D. Wuest and is currently being reviewed.

The second article to appear (Chapter 3), entitled "Palladium-catalyzed Arylation of *N*-aminoimidazol-2-ones Towards Synthesis of Constrained Phenylalanine Dipeptide Mimics" describes conditions to insert aryl groups at the 5-position of the Nai residue using palladium-catalyzed cross coupling. The solution phase approach tolerates a wide range of aryl moieties. Molecular dynamic analysis of model peptides showed that the (4-Me, 5-Aryl)Nai residues adopted the central position of β-turns conformation. This article has been published in *Heterocycles*. The third article entitled "4,5-Disubstituted *N*-aminoimidazol-2-one mimics of peptide turn backbone and side chain conformation" describes the synthesis of the first example of 5-aryl substituted Nai residue and has been published as a proceeding for the 24th American Peptide Symposium (APS).

The fourth article (Chapter 4), entitled "Application of *N*-aminoimidazol-2-one Turn Mimics to Study the Backbone and Side-chain Orientation of Peptide-based CD36 Modulators" describes methodology to synthetize [(4-Me, 5-Aryl)Nai^4]-GHRP-6 analogs. Four Nai-peptides were synthetized and evaluated for their ability to modulate macrophage-driven inflammation. The biological evaluation was done by Dr Mukadila Mulumba under the direction of Professor

Huy Ong at the Faculté de Pharmacie de l'Université de Montréal. Other biological experiments are still being done; therefore, the article is presented as *Manuscript in preparation*.

Other work and perspective will be presented in chapter 5, followed by a conclusion.

Table of content

List of tables

List of Schemes

List of figures

List of abbreviations

$[\alpha]_D$	Specific rotation (sodium D-line) [in (degmL/gdm)]
Ac	Acetyl
Ac_2O	Acetic anhydride
AcOH	Acetic acid
Agl	α-amino-γ-lactam
Ala	Alanine
Ar	Aryl
Arg	Arginine
Asn	Asparagine
Asp	Aspartic Acid
AzaXaa	Aza Amino acid
Bn	Benzyl
Bgl	β-amino-γ-lactam
Boc	*tert*-butyloxycarbonyl
Boc_2O	Di-*tert*-butyl dicarbonate
Br	*broad* (in NMR)
BTC	bis(trichloromethyl)carbonate
i-Bu	*iso*-butyl
t-Bu	*tert*-butyl
c	Concentration

^{o}C	degrees Celsius
Calcd	Calculated
Cbz	Benzyloxycarbonyl
CD	Circular Dichroism
CD36	Cluster of differentiation 36
COSY	Correlated Spectroscopy
Cys	Cysteine
δ	Chemical displacement (in NMR)
d	Doublet (in NMR)
Dab	Diaminobutyric acid
DABCO	1,4-diazabicyclo[2.2.2]octane
DCM	Dichloromethane
Dd	Doublet of doublet (in NMR)
DEAD	Diethyl azodicarboxylate
Deg	Degrees
DIC	*N,N*-diisopropylcarbodiimide
DIEA	*N,N*-diisopropylethylamine
DMAP	4-dimethylaminopyridine
DMF	Dimethylformamide
DMSO	dimethylsulfoxide
er	enantiomeric ratio
ESI	Electrospray ionization

Et	Ethyl
Et_3N	Triethylamine
Et_2O	Ethyl ether
EtOAc	Ethyl Acetate
EtOH	Ethanol
FA	Formic Acid
Fmoc	Fluorenylmethyloxycarbonyle
FTIR	Fourier Transformed Infra-red
g	Gramme(s)
GH	Growth hormone
GHRH	Growth hormone releasing hormone
GHRP-6	Growth hormone releasing peptide 6
Gln	Glutamine
Glu	Glutamic Acid
Gly	Glycine
GPCR	G protein-coupled receptor
h	hour(s)
HATU	1-[bis(dimethylamino)methylene]-1H-1,2,3-triazolo[4,5-b]pyridinium 3-oxide hexafluorophosphate
HBTU	3-[bis(dimethylamino)methyliumyl]-3*H*-benzotriazole-1-oxide hexafluorophosphate
His	Histidine

HOAt	Hydroxy-azabenzotriazole
HOBt	Hydroxybenzotriazole
HPLC	High performance liquid chromatography
HRMS	High-resolution mass spectrometry
Hse	Homoserine
IBC	*Iso*-butyl chloroformate
IGF-1	Insulin growth factor 1
Ile	Isoleucine
J	Coupling constant (in NMR)
Kcal	kilocalorie
l, L	Liter(s)
LC-MS	Liquid chromatography-mass spectrometry
Leu	Leucine
Lys	Lysine
M	Mole per litre
mM	millimole per litre
Me	Methyl
Met	Methionine
MHz	MegaHertz
Min	Minute(s)
Mol	Mole

mmol	mmole
m	multiplet (in NMR)
mp	Melting point
MS	mass spectrometry, molecular sieves
Nai	*N*-aminoimidazol-2-one
nM	nanomolar
nm	nanometer
NMM	*N*-methylmorpholine
NMR	Nuclear Magnetic Resonance
nOe	Nuclear Overhauser effect
NOESY	Nuclear Overhauser effect spectroscopy
Nu	Nucleophile
Obs	Observed
oxLDL	Oxidized low-density lipoprotein
PEG	polyethylene glycol
Ph	Phenyl
Phe	Phenylalanine
ppm	parts per million (in NMR)
Pr	Propyl
i-Pr	*iso*-propyl
Pro	Proline

PyOXIM	[Ethylcyano(hydroxyimino)acetato-O^2]tri-1-pyrrolidinylphosphonium hexafluorophosphate
q	Quartet (in NMR)
R*f*	Retention factor (in TLC)
rt	Room temperature
RT	Retention time
RP	Reverse-phase
s	Singlet (in NMR)
SAR	Structure-activity relationship
SEM	Standard error of the mean
Ser	Serine
SFC	Supercritical-fluid chromatography
SPPS	Solid-phase peptide synthesis
t	Triplet (in NMR)
T	Temperature
TEA	Triethylamine
TES	Triethylsilane
TFA	Trifluoroacetic acid
Theor.	Theoretical
THF	Tetrahydrofuran
Thr	Threonine
TLC	Thin-layer chromatography

TMS	Tetramethylsilane
Tosyl	*para*-toluenesulfonyl
Tr	Triphenylmethyle (Trityl)
Tyr	Tyrosine
UV	Ultraviolet light
Val	Valine

To Gabrielle

Acknowledgements

First and foremost, I would like to thank my research director, Professor William Lubell, for his support throughout my studies. I joined the group in 2012 as a master's student, and I never regretted my decision. Thanks to Bill's support, I had the opportunity to attend international conferences and present my work to some of the experts in the fields of organic chemistry and peptide science. Most importantly, thanks Bill for your outspoken style and for helping me achieve my full potential. You were always a great mentor.

I would like to thank my thesis committee, Professor Joëlle Pelletier and Professor Stephen Hanessian for their guidance throughout my doctoral studies. Your comments and suggestions were much helpful for the development of the project and the way it is being presented.

I would like to thank Lubell's Group member, both current and former, for the friendly atmosphere that was always present. Special thanks to Cynthia Criffard with whom I shared a laboratory for most of my Ph.D. I'm also thankful to the undergraduate who worked with me during my graduate studies, particularly to Yousra Hamdane, now a master's student in the group, who worked on the project for two summers and helped review the thesis. Thanks also to former group members Dr. Caroline Proulx and Dr. Ngoc-Duc Doan who initiated the project.

I would like to thank Dr. Alexandra Fürtos, Karine Gilbert, Marie-Christine Tang and Louiza Mahrouche from the Laboratoire de spectrommétrie de masse de l'Université de Montréal for their help with HRMS and LC-MS analyses. Thanks to Dr. Pedro Aguiar, Sylvie Bilodeau, Antoine Hamel and Cédric Malveau for their help with NMR analysis.

I am also very thankful to the Département de chimie for a travel award which helped me present at the 2019 American Peptide Symposium. Thanks to Dr. Gaétan Caron, Denis Deschaines, Kevin Delormes and Lorraine Phang from the teaching laboratory who helped keep things running smoothly during my T.A. sessions.

I had the chance to have many friends who supported me during my studies. They both encouraged me and allowed me to take some time off and relax. Their support meant a lot.

Thanks also to my martial art instructor Shihan Jacques Dupont, who gave me an opportunity to concentrate on something other than research for a few hours per day.

Finally, I would like to thank my family; My mother Lucie Florent, my father Dr. Marc-André Poupart and my sister Amélie Poupart. Their love and support have been essential.

Chapter 1

Introduction and background

1. Introduction

1.1 Peptides

Peptides are naturally occurring polyamides generally comprising less than 50 residues. In the animal kingdom, 21 amino acids are typically used to construct peptides.[1] Other than selenocysteine, the other 20 amino acid residues are genetically encoded.[2] The amino acids are typically of *L*-configuration;[3] however, certain *D*-amino acids are produced due to the action of isomerase enzymes.[4]

1.2 Peptides as therapeutic agents

Peptides have significant utility as therapeutic agents.[5-7] For example, the peptide drugs Sarenin®, Fuzeon® and Sermorelin® are respectively used to treat hypertension,[8] to combat antiretroviral resistant HIV strains,[9] and to diagnose growth hormone (GH) hypo-secretion.[10, 11] Atosiban® is used to delay preterm labor in industrialized countries.[12, 13] Neospect® acts as a tumor contrast agent and used to diagnose lung cancer by scintigraphy.[14] Copaxone® reduces the incidence of immune attack in patients suffering from multiple sclerosis.[15]

These representative examples are peptides approved for clinical use by North American and European regulatory agencies. They benefit typically from high binding affinity and specificity which is often associated with natural peptides.[16-18] In the pursuit of peptide therapeutics, solid-phase peptide synthesis (SPPS) can also offer effective means to prepare large combinatorial libraries of analogs for studying structure-activity relationships.[19] The pharmacodynamic, pharmacokinetic and physicochemical properties of peptides can however limit their use in clinical settings.

In many cases, peptides have poor metabolic stability due to rapid degradation by the plethora of proteases and peptidases present in the blood and other biological settings.[18] With few exceptions,[20-22] peptides are not suitable for oral administration and require parenteral

administration. Aqueous solubility and chemical stability may also be problems with certain peptide sequences.[18] Peptide-based drug discovery thus wield a double edge sword: benefiting from potency and selectivity, yet encumbered by inherent issues related to the metabolism and bioavailability of these natural polyamide structures.

1.3 Conformational properties of peptides

Peptides can adopt different secondary structures in solution,[23] which are classified according to the values of their backbone dihedral angles, namely phi (ϕ), psy (ψ) and omega (ω, Figure 1.1).[24] Side chain orientations are defined by the chi (χ) dihedral angles.[25, 26] Amide bonds adopt usually the (*Z*)-*trans* conformation, in which the ω value is normally 180°.[27, 28] The three most often encountered secondary structures in peptides and proteins are α-helices, β-sheets and β-turns.[29, 30]

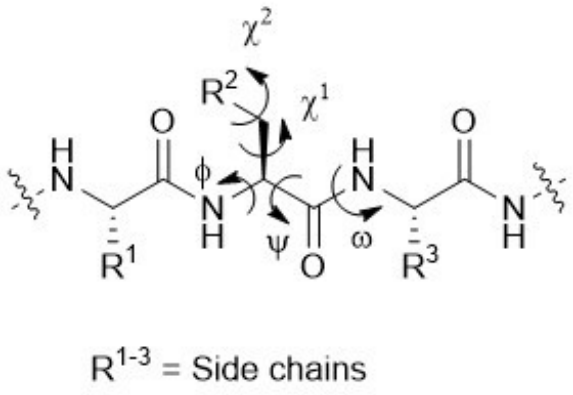

Figure 1.1: Peptide chain and relevant dihedral angles

Considering that the ω value is normally 180°, the relationship of ϕ and ψ dihedral angle values may be the plotted to portray the conformations adopted by the peptide backbone, which are often said to exist inside Ramachandran space.[24, 25] The α-helical, β-sheet and poly-proline type II conformers, which feature repeating unites with similar dihedral angles, occupy specific locations in the Ramachandran plot. The preference for a peptide to adopt a specific secondary structure is governed by many factors, including the sequence, presence of intramolecular hydrogen bonds and interactions between the different side chains. The geometry of the side

chain defined by their preferred dihedral angle values has been coined “Chi space”.[24-26] The backbone secondary structure and side chain orientations are crucial for the activity and binding affinity of peptide analogs which interact with biological targets.[31]

1.4 Beta (β)-turns

β-Turns are secondary structures composed of four consecutive amino acid residues, which reverse the direction of the peptide backbone (Figure 1.2).[32] β-Turns position the α-carbons of the residues at the *i* and *i*+3 positions within a distance inferior or equal to 7 Å. The different types of β-turns are classified using the values of the ϕ and ψ dihedral angles of the two central residues at the *i*+1 and *i*+2 positions.[32-34] Type I, II, IV and VIII β-turns are most often encountered in natural peptide and protein structures;[25, 35] type VI β-turns are less frequent.[32] Certain amino acids (e.g., glycine and proline) have strong potential to adopt the central residues of specific β-turns.[32] An intramolecular hydrogen bond may be present between the amide carbonyl of the *i* residue and the amide nitrogen of residue *i*+3.[36] Although the resulting ten-membered ring formed by such a hydrogen bond may stabilize the turn conformation, this factor is not a major force governing turn formation.[36]

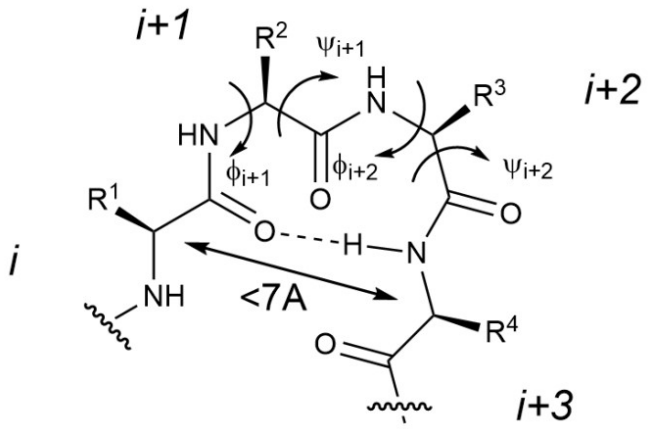

Figure 1.2: β-Turn and relevant dihedral angles

Type of turn	ϕ_{t+1}	ψ_{t+1}	ϕ_{t+2}	ψ_{t+2}
I	-60	-30	-90	0
II	-60	120	80	0
VIII	-60	-30	-120	120
I’	60	30	90	0
II’	60	-120	-80	0
VIa1	-60	120	-90	0
VIa2	-120	120	-60	0
VIb	-135	135	-75	160
IV	-61	10	-53	-17

Table 1.1: Ideal values (in degrees) for the different types of β-turns

β-Turns are often regions involved in molecular recognition and protein folding.[32] β-Turns are therefore attractive targets for the rational design of therapeutic peptides and related

synthetic analogs, so called peptidomimetics. In the interest of replicating β-turns by such synthetic analogs, many strategies have been examined (Figure 1.3).

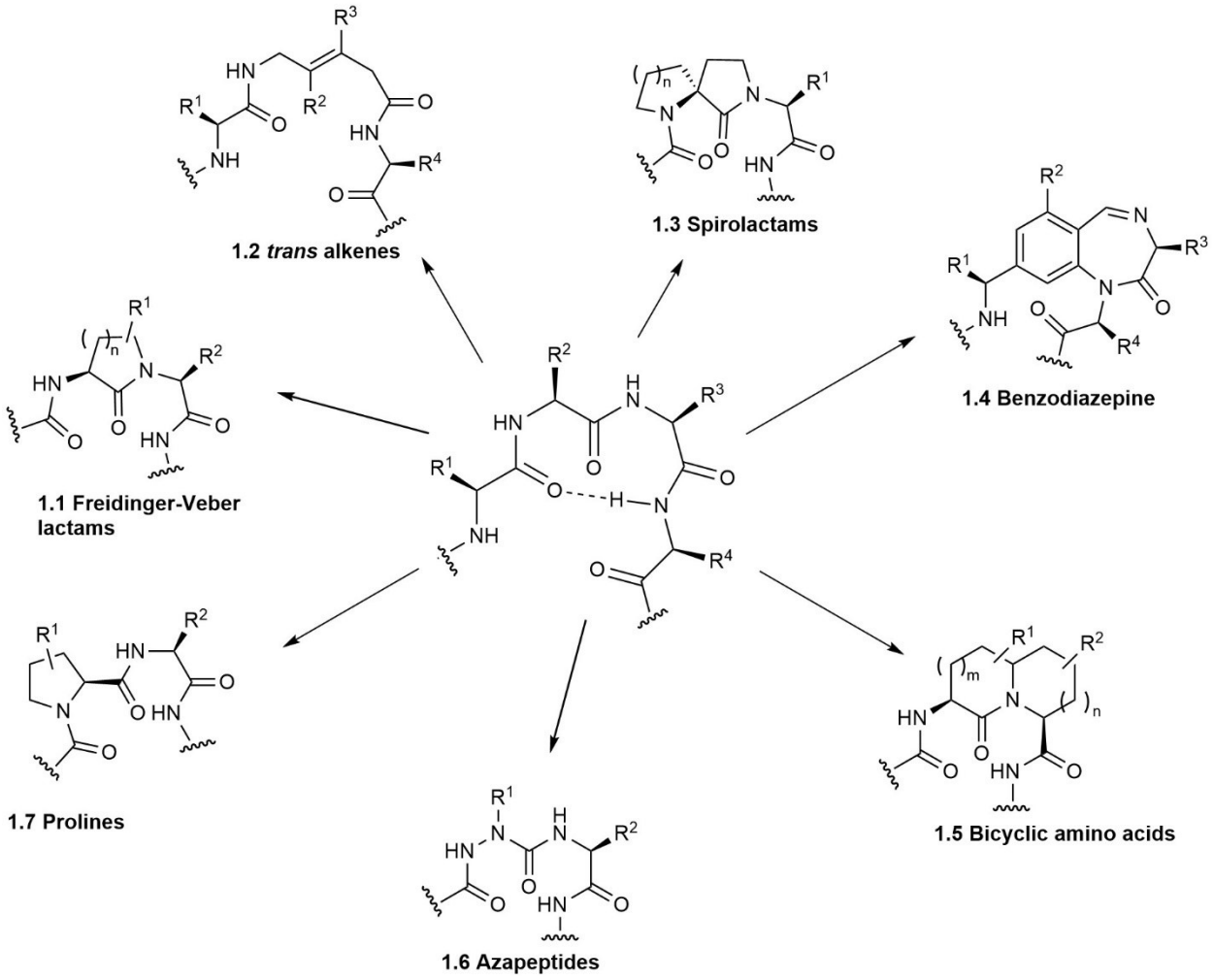

Figure 1.3: β-turns mimics

As mentioned, the natural amino acid proline has been known to favor β-turns in a wide array of different proteins with a preference to situate at the *i*+1 position.[32] Scanning in which each amino acid in the peptide sequence is replaced by proline has been used to detect the location of β-turns responsible for biological activity.[37-39]

The first example of the use of a covalent modification of the peptide chain to favor a β-turn conformation has been attributed to the laboratory of R. Freidinger and D. Veber at Merck.[40, 41] By introducing an α-amino-γ-lactam into the sequence of luteinizing hormone-releasing

hormone [gonadotropin releasing hormone (GnRH)], a rigid analog was produced that exhibited greater activity than the parent peptide, likely due to stabilization of an active β-turn conformation. Following this example, efforts have been pursued to examine different lactam ring sizes and to introduce ring substituents.[42-47] For the introduction of a variety of functional groups onto the lactam ring by way of a common intermediate, displacement of the alcohol of an α-amino-β-hydroxy-γ-lactam residue using Mitsunobu chemistry and cyclic sulfamidate ring opening has procured a wide range of stereocontrolled α-amino-γ-lactam analogs possessing heteroatomic β-substituents.[47]

Various other approaches have been used to induce the β-turn geometry. For example, replacement of a dipeptide moiety by a *trans*-5-amino-3,4-dimethylpent-3-enoate unit has been used to induce β-turn and β-hairpin geometry by way of $A^{1,2}$ and $A^{1,3}$ allylic strain.[48] Alternative covalent constraints in spirolactam,[49-51] benzodiazepine, benzotriazepine,[52, 53,54] as well as azabicyclo[X.Y.0]alkanone amino acids,[55-59] all have been successfully used to induce β- and γ-turn conformations within different peptide structures.

1.5 Azapeptides

Azapeptides (Figure 1.4) are peptide analogs in which one or more of the amino acid α carbons has been replaced by a nitrogen atom.[60-64] Aza-residues can induce β-turn secondary structure by stereo-electronic constraints from their semicarbazide components by implicating the planarity of the urea portion to control the ψ dihedral angle and the lone pair-lone pair repulsion between the neighboring nitrogen to restrict the rotational barrier around the ϕ dihedral angle. The combination of these effects to stabilize β-turns has been observed in model azapeptides using x-ray diffraction and NMR spectroscopy,[65, 66] and by computational analyses.[67, 68] Moreover, modeling of *N*,*N*'-diformylhydrazine by ab initio analysis has revealed that an energy minimum existed in which the two lone pairs were at an angle of 90°.[69] Scanning by systematic replacement of each amino acid in a sequence with an aza-amino acid residue has been used to probe for evidence of a β-turn in a peptide of biological interest.[70]

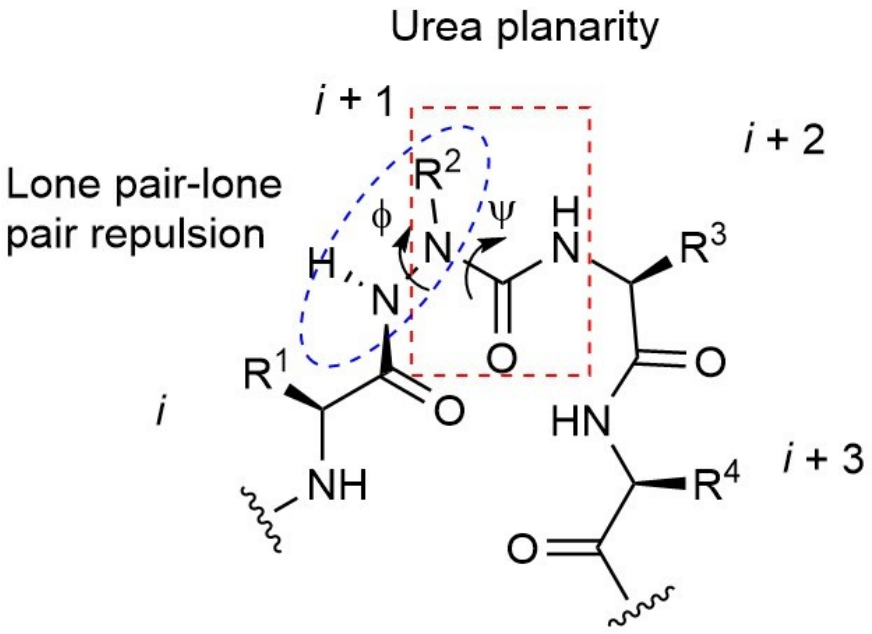

Figure 1.4: Azapeptide residue in a β-turn

One example of a successful use of an azapeptide in medicinal chemistry is the drug Zoladex®, which features a *C*-terminal aza-glycine residue (Figure 1.5). Zoladex® acts as a gonadotropin releasing hormone (GnRH) agonist, is administered by subcutaneous injection, and is used clinically for sexual hormone suppression in treatments of prostate and breast cancer.[71] Incorporation of the aza-residue improves the pharmacokinetic profile of the peptide extending duration of action by reducing susceptibility to proteases-mediated degradation.[72]

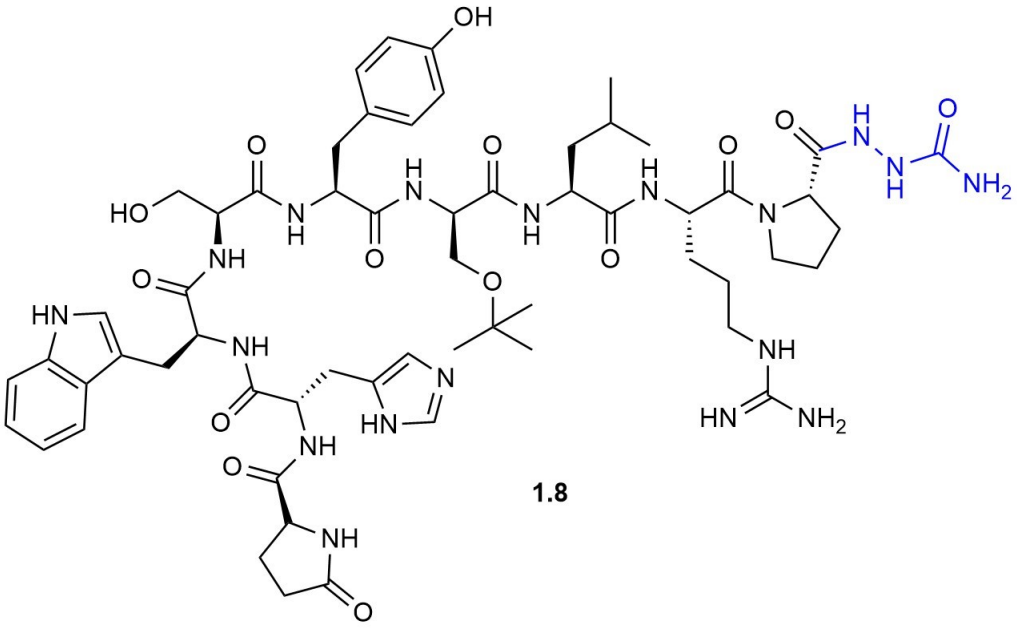

Figure 1.5: Zoladex® structure

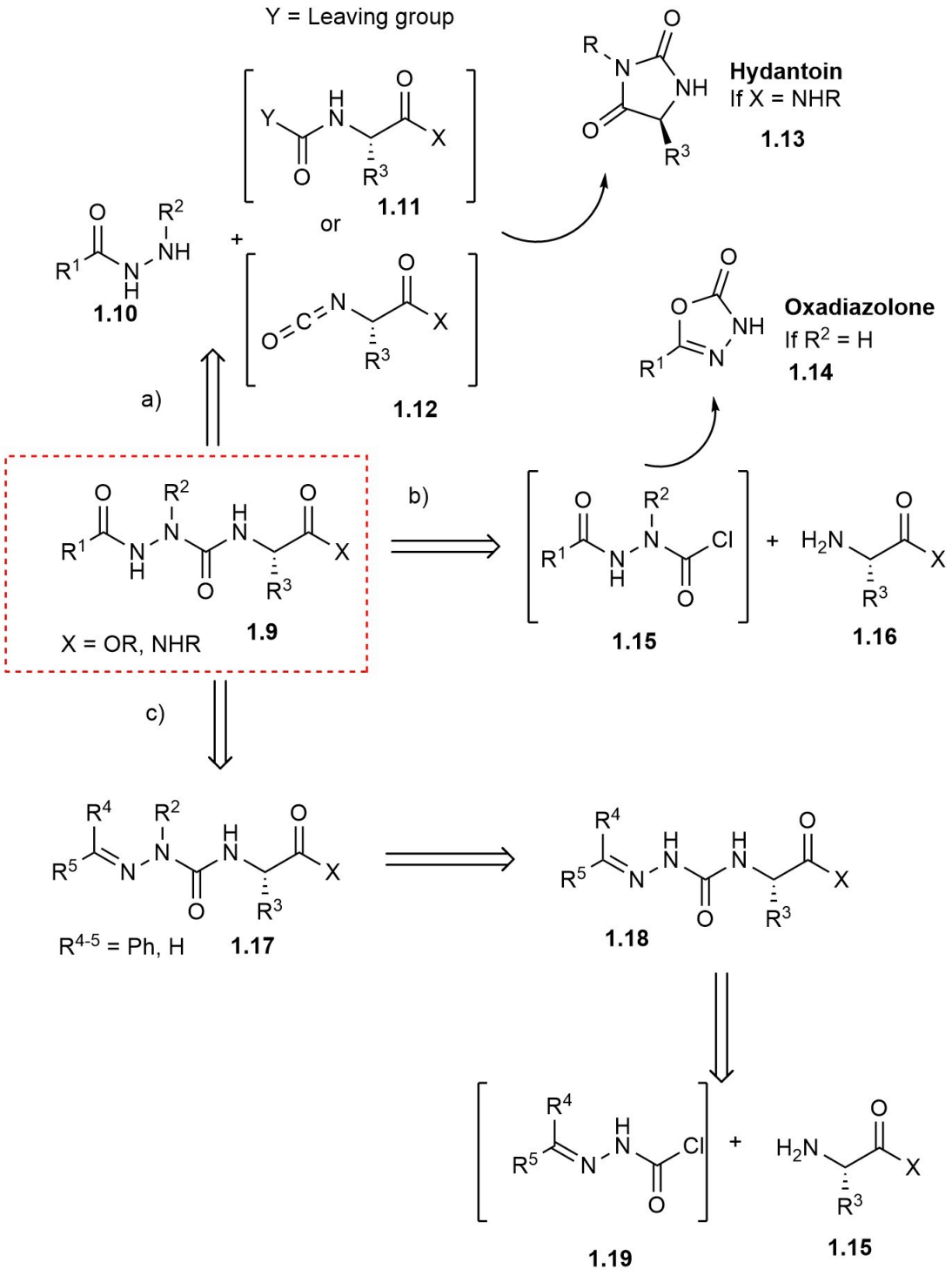

Figure 1.6: Different retrosynthetic strategies to azapeptides

Many strategies have been used to synthesize azapeptides (Figure 1.6).[64, 73] The *N*-termini of protected amino acid and peptide structures have been activated with a carbonyl donor, such

as an activated carbamate **1.11** or isocyanate **1.12**, and reacted with a protected hydrazide **1.10** to give the azapeptide residue (Strategy a). In this strategy, the presence of a *C*-terminal secondary amide can lead to an intramolecular reaction on the carbonyl donor to yield hydantoin side-products **1.13**. Alternatively, hydrazides **1.10** can be activated with carbonyl donors, such as a phosgene equivalent or carbonyldiimidazole to yield activated carbazate equivalents **1.15** that reacted with the amine of a protected amino acid or peptide (Strategy b). In this strategy, an unsubstituted carbazate **1.15** (R^2 = H) can react intramolecularly to form of oxadiozolone **1.14** as a significant side-product. Finally, hydrazones **1.17** can be converted to methylidene carbazates **1.19** upon reaction with carbonyl donors, such as a phosgene equivalent, disuccinimidyl carbonate or 4-nitrophenylchloroformate, and reacted with the amine of a protected amino acid or peptide to form semicarbazones **1.18** (Strategy c). The latter can be selectively alkylated in presence of various bases (e.g., Et_4NOH) owing to resonance stabilization of the anion intermediate **1.18b**, without concomitant epimerization of chiral centers present in the peptide (Figure 1.7).[74] The semicarbazone protection has been removed using both aqueous HCl and hydroxylamine hydrochloride in pyridine.[75]

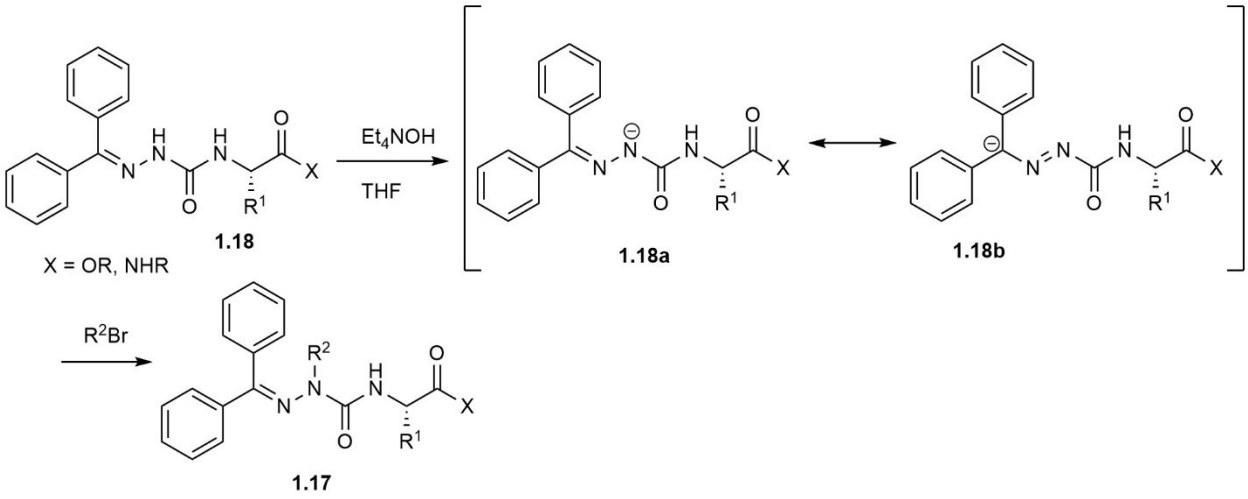

Figure 1.7: Semicarbazone alkylation

Aza-residues have been functionalized with a wide range of groups to mimic natural side chains and to incorporate reactive appendages onto the azapeptide. For example, alkyl, benzyl and propargyl functionalities have been introduced onto semicarbazones **1.18** by alkylation

under basic conditions (Figure 1.8a).[76, 77] A wide range of aryl and heteroaryl groups have been installed onto azapeptides **1.18** using copper catalysis (Figure 1.8b) to give aza-aryl glycines **1.20**.[78] Alkylation using propargyl bromide has given aza-propargyl glycine (azaPra) residues **1.21** which can be used to construct different aryl triazolo-aza-alanines **1.22** by copper-catalyzed Huisgen coupling (Figure 1.8c),[79] and tertiary amino-alkynes **1.23** using copper-mediated triple A (A^3) reactions using different secondary amines and formaldehyde as a carbon donor (Figure 1.8d).[59] The latter reaction will be discussed again in Chapter 5.

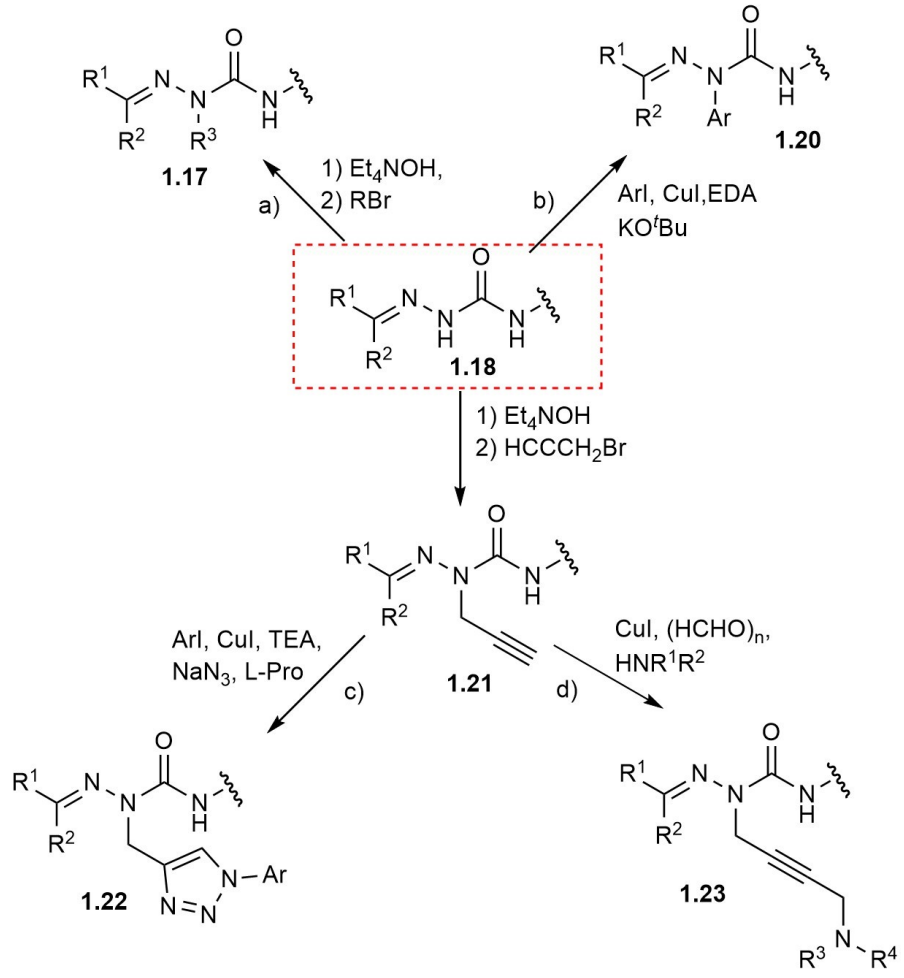

Figure 1.8: Introduction and diversification of aza-glycine **1.18**

1.6 Aid and Nai residues

Aza-aminoimidazolidine (Aid) residues **1.25** have been obtained by bisalkylation of semicarbazones **1.18**, such as aza-Gly peptides **1.24**, with ethylene bromide after treatment with Et_4NOH. The Aid residues are covalently constrained aza residues and may be viewed as the aza counterpart of Freidinger-Veber lactams. The heterocycle further restricts the accessible Ramachandran and Chi space that may be occupied by the amino acid residue in the peptide chain (Figure 1.9).[80, 81] Systematic replacement of Aid residues for the amino acids in a peptide sequence (Aid-scanning) has been achieved using a solid-phase approach to study conformation-biological activity relationships.[80] The synthesis of substituted Aid residues merits further study, because the absence of side chain functionality on the heterocycle surrogate, like the α-amino-γ-lactam counterpart, may have a detrimental consequence on biological activity.

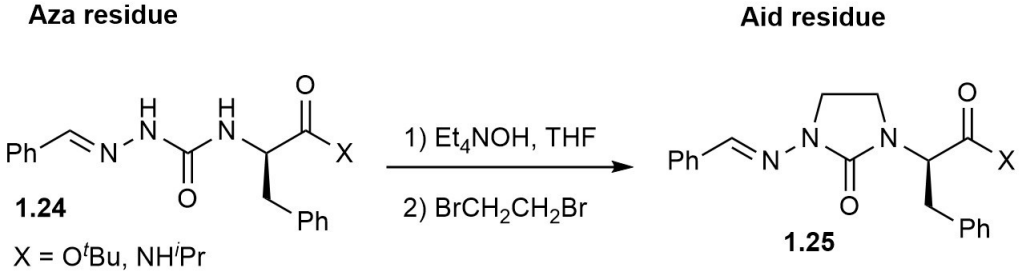

Figure 1.9: Synthesis of Aid residues

N-Aminoimidazolones (Nai) residues are unsaturated counterparts of Aid residues.[75, 81, 82] 4-Substituted Nai residues have been obtained by base promoted cyclization of aza-Pra residues (Figure 1.10). Contingent of the 4-position substituent, Nai residues have been shown to adopt the central residues of type II' β- and inverse γ-turns in X-ray analyses of model peptides (e.g., **1.31**, Figure 1.11). Although type II' β-turns are relatively rare in peptides, they garner significant interest due to their role in the formation of β-hairpins.[32]

Relative to the saturated Aid counterpart, the unsaturated Nai residue possesses a flatter heterocycle with an alkene component that enables functionalization at both the ring 4- and 5-positions. The addition of functional groups onto the imidazole-2-one ring especially at the 5

position is of particular interest for side chain mimicry. As mentioned, β-turn secondary structures are often associated with peptide recognition events, 5-substituted Nai analogs may offer advantages for mimicry of both backbone and side chain geometry and function. The absence of chirality at the Nai ring 4- and 5-positions may further simplify the synthesis of substituted analogs. The rigidity brought by the imidazole-2-one core, and the steric interactions of a 4-position substituent make 4,5-disubstitued Nai residues promising candidates for probing χ-space, due to the relatively limited conformational freedom of the 5-position substituent.[83]

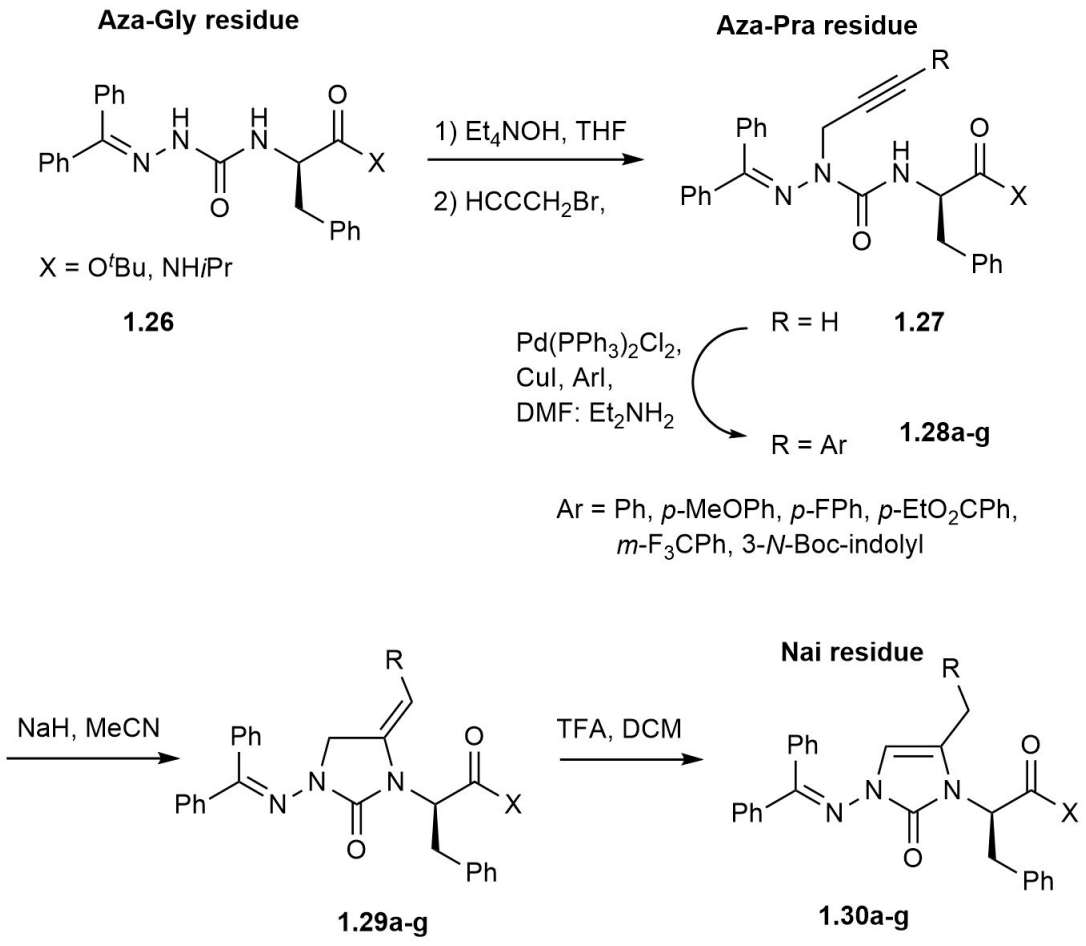

Figure 1.10: 4-Substitued Nai synthesis[75]

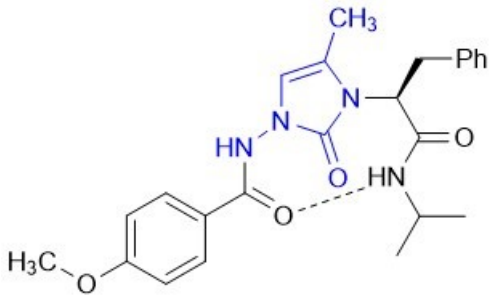

Figure 1.11: Nai-peptide mimic **1.31** in a β-turn

The base promoted cyclisation of aza-Pra residues **1.27** and **1.28** using sodium hydride gave typically a mixture of *exo* and *endo* double bond isomers. The former isomerized to the thermodynamically more stable latter in the presence of silica and acid to give a single structural isomer **1.30**. Esters **1.27** and **1.28** (X = OR) cyclized with concomitant epimerization to give a racemized Nai-dipeptide enantiomers, which could be separated using chiral supercritical fluid chromatography (SFC).[84]

1.7 Enantioenriched Nai synthesis, 5-position functionalization and biomedical applications of 4,5-disubstutited Nai containing peptides

The Nai residue offers potential for inducing turn conformations in peptides and for modification with substituents at both the 4 and 5 positions. Insertion of substituted Nai residues into bioactive peptides merits study to examine effects on efficacy, selectivity and pharmacokinetic properties. The rigidity induced by the imidazole-2-one ring and the steric interactions between the alkene substituents offers potential to probe the Chi space of different side chains.

This thesis presents the development of methods to obtain enantiomerically enriched Nai residues. Subsequently, methods are described for introducing different substituents at the Nai 5-position, to mimic the orientation and functional groups of natural amino acid side chains

(Figure 1.11). Finally, the introduction of (4-methyl,5-aryl)Nai residues into peptides has been achieved using a solid-phase approach.

Different *C*-terminal groups and cyclization conditions were explored to enable synthesis of enantiomerically enriched Nai dipeptides in Chapter 2a. For example, Nai dipeptides having up to 98:2 *er* were obtained by employing aza-Pra dipeptide acids. Modification of (4-methyl)Nai by formylation and aminomethylation chemistry using Vilsmeier-Haack and Mannich conditions gave respectively give (4-methyl,5-formyl)Nai and (4-methyl,5-morpholinomethyl)Nai dipeptide analogs. The aldehyde of the (4-methyl,5-formyl)Nai analog was respectively oxidized and reduced to provide carboxylic acid and hydroxymethyl Nai residues with potential to serve as constrained aspartate (Asp) and homo-serine (Hse) mimics . Reductive amination reactions on the (4-methyl,5-formyl)Nai analog using different amines provided a set of Nai peptides with 4-position *N*-alkylaminomethyl substituents (Chapter 2b).

In Chapter 3, palladium-catalysis was explored to add a wide range of aryl groups to the 4-position of (4-methyl)Nai analogs. Employing a set of aryl iodides, a series of Nai peptides cross-couplings were performed using a palladium diacetate mediated reaction. The conformational impact of the 5-aryl group in both Ramachandran and Chi space was studied using molecular dynamics. Finally, a dipeptide mimic featuring a (4-methyl,5-*p*-nitrophenyl)Nai unit was synthetized in solution.[83]

In Chapter 4, the aryl addition chemistry has been adopted to solid-support to make [(5-aryl)Nai^4]-growth hormone releasing peptide-6 (GHRP-6) analogs. Based on results with azapeptide counterparts, the [(5-aryl)Nai^4]-GHRP-6 analogs were targeted to modulate the cluster of differentiation receptor (CD36). The roles of this scavenger receptor in innate immunity and lipid metabolism have attracted attention for development of CD36 ligands as potential treatments of age-related macular degeneration (AMD) as well as atherosclerosis.[85] Protected (4-methyl)Nai-D-Phe was coupled to H-Lys(Boc)-NH-Rink amide resin and the resulting Nai tripeptide resin was arylated using different aryl iodides, deprotected and elongated.[86] After removal of the protecting groups, resin cleavage and purification by HPLC, the [(5-aryl)Nai^4]-

GHRP-6 analogs were examined for ability to minimize nitric oxide production in RAW macrophages cells treated with a Toll-like receptor (TLR)-2 agonist.

As concluded in Chapter 5, Nai residues can be effectively functionalized with different groups to mimic the side chain of amino acids present in turn conformations. The *N*-aminoimidazole ring causes covalent and electronic constraints to restrict movement about the ϕ, ψ and χ^1 dihedral angles. Moreover, the 4-methyl substituent may cause steric interactions on a 5-position substituent that may rigidify the χ^2 dihedral angle. The combination of these constraints on the backbone and side chain of the Nai surrogate has been predicted by computational analysis to favor positioning at the *i*+1 residue of a type II' β-turn with a *gauche* (–) side chain orientation. The 4,5-disubstituted Nai residues offer thus interesting potential for biomedical applications, because of their ability to restrict the Ramachandran[24] and Chi[26] space of bioactive peptides.

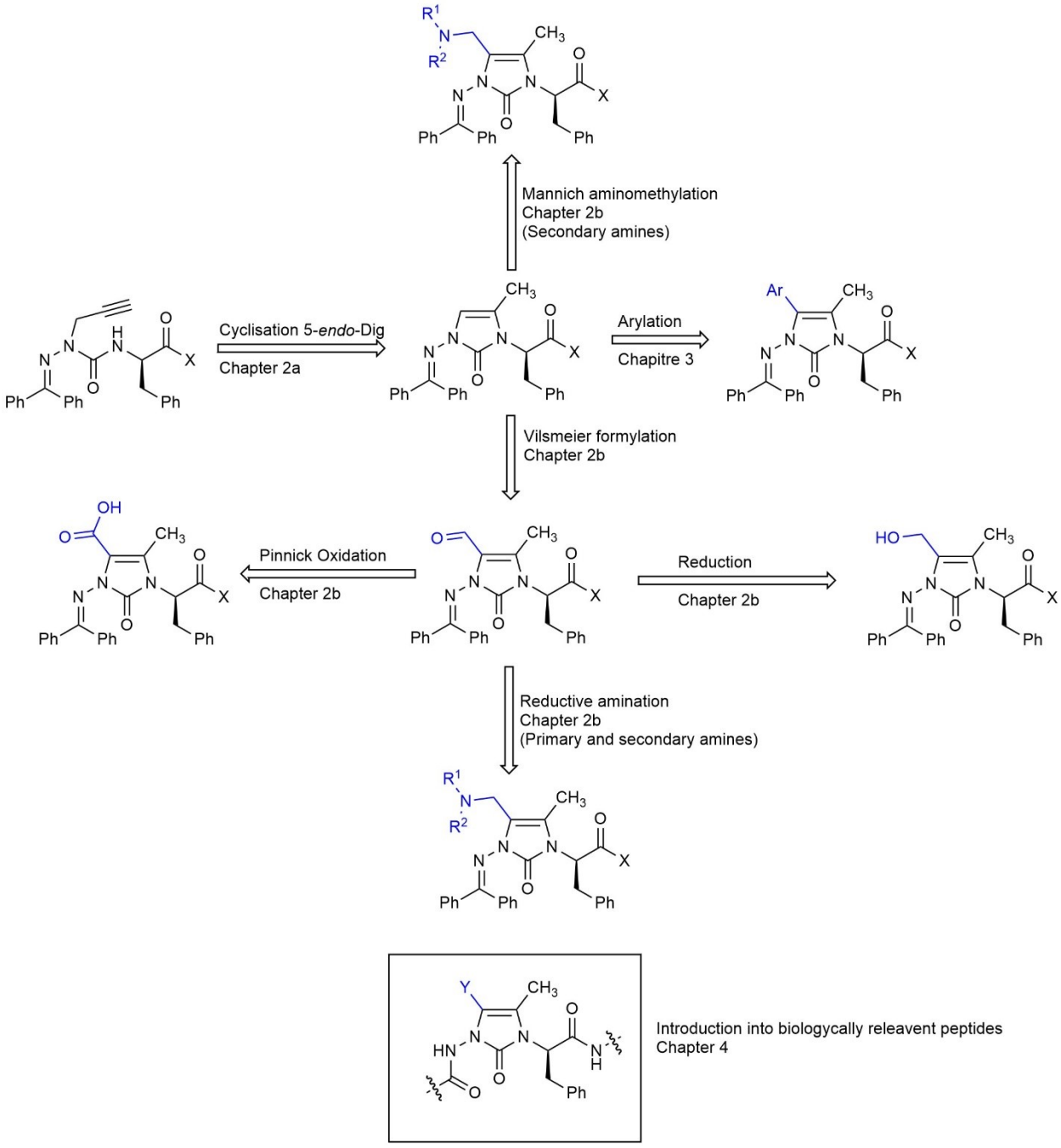

Figure 1.12: Schematic representation of Chapters 2-4

Chapter 2

Stereoenriched Nai residues synthesis, acylation and formyl group derivatization

2.1 Imidazolone relevance

Imidazolones are present as pharmacophores in many natural products.[87, 88] Imidazolone analogs display a wide range of biological activity, including antioxidant,[89] anti-hypotensive,[90] pro-β-adrenergic,[91] anti-inflammatory,[92] anti-oncogenic,[93] anti-Parkinsonian and immunomodulatory properties (Figure 2.1).[94] Accessible from different starting materials, imidazolones are important tools in medicinal chemistry.

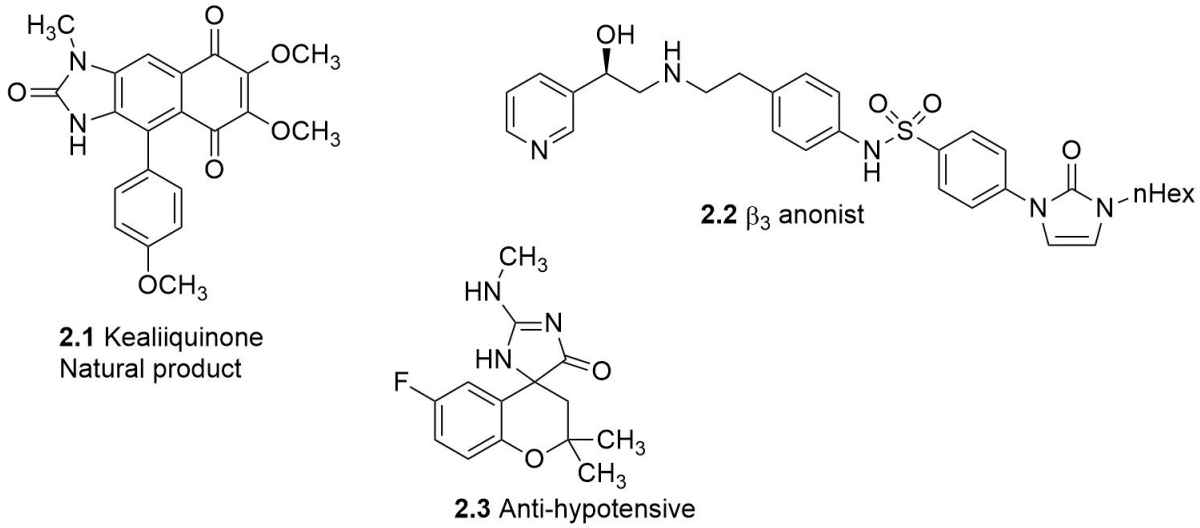

Figure 2.1: Examples of natural and synthetic imidazolones[87, 90, 91]

2.2 Synthesis of imidazolone subunit

Driven by the interest for imidazole-2-ones (e.g., **2.4**) as components of various active molecules, different methods for their synthesis have been explored. For example, oxidation of imidazolium salts (e.g. **2.5**) have provided direct access to the imidazole-2-one system (Figure 2.1a).[95, 96] Tetra-substituted imidazolones and iminoimidazoles have been prepared by treating imidazolium salts with aqueous sodium hydroxide followed by *N*-chlorosuccinimide.[95] Tetra-substituted imidazolium salts have been converted to imidazolones using aqueous potassium

hydroxide in toluene at reflux, likely by a mechanism proceeding through 2-hydroxylation, ring opening and closure via C-N coupling.[96]

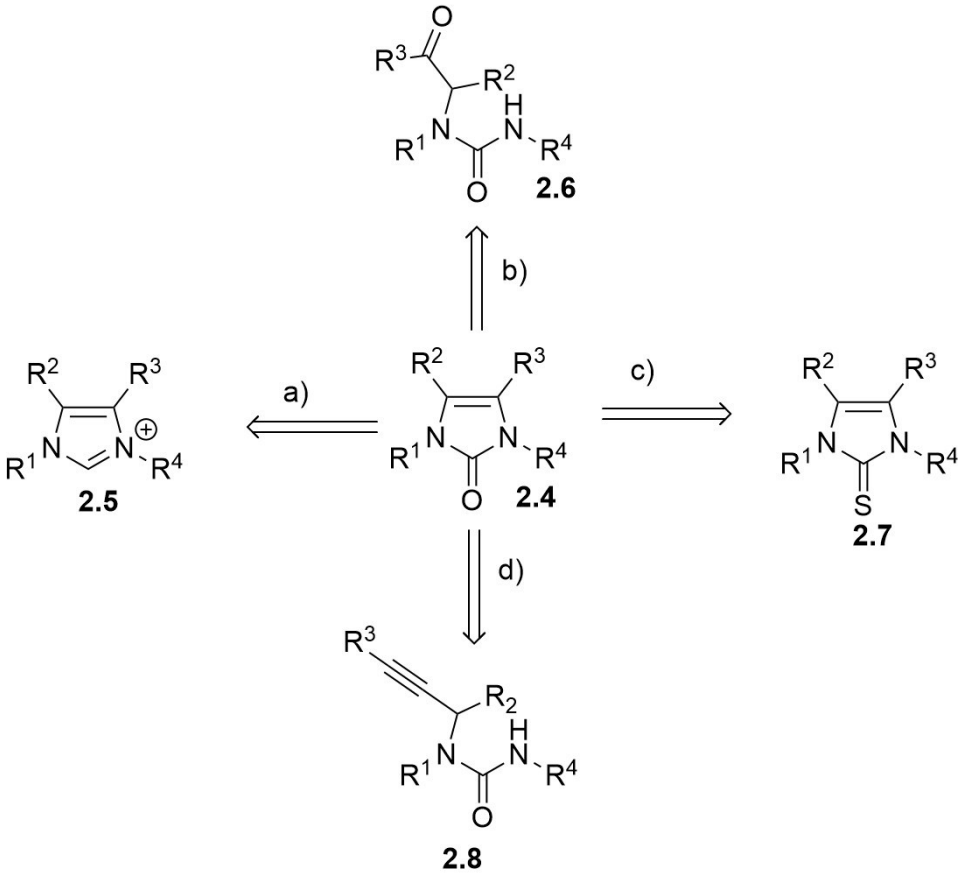

Figure 2.2: Different strategic disconnections for imidazol-2-one synthesis

β-Keto and β-aldehyde urea (e.g., **2.6**) have been cyclized under both acidic[97] and basic[98] conditions to access functionalized imidazolone subunits (Figure 2.1b). Oxidations of imidazol-2-thiones (e.g., **2.7**) to imidazolones have used nitrous oxide in a mechanism likely implicating a stabilized carbene intermediate (Figure 2.1c).[99] Finally, propargyl urea (e.g., **2.8**) have been cyclized under various conditions to yield 4- and 5-substituted imidazolones (Figure 2.1d).[75, 100-104] In the latter case, different reaction conditions that can effectively promote cyclization onto the alkyne may be divided into three distinct categories. Transition metal (e.g., Ag^{+}, Au^{+}) catalysts may activate the triple bond and form a metal-alkyne intermediate that undergoes cyclization.[100-102] The triple bond may be activated as a π-cation type intermediate using reagents such as tetrabutylammonium fluoride (TBAF).[103, 104] Finally, base promoted cyclisation may entail alkyne

isomerization to an allene intermediate which undergoes a 5-*exo*- or 5-*endo*-dig cyclisation, followed by alkene isomerization.[105]

2.3 Synthesis of Nai residues

N-aminoimidazol-2-one (Nai) residues can be synthesized from aza-propargylglycine (aza-Pra) residues by base-promoted cyclization using sodium hydride; however, C_α epimerization is observed in the case of *C*-terminal esters.[75, 84] The epimerization can be limited significantly using *C*-terminal amides, likely due to the formation of an amide anion (e.g., **2.9**) which resists epimerization (Figure 2.3).[75] Amides are however difficult to hydrolyze for further functionalization and peptide elongation.

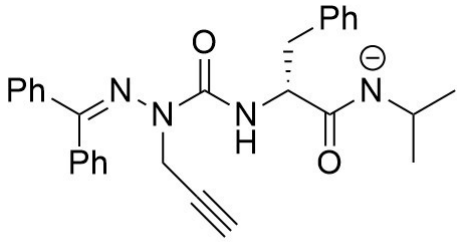

2.9

Figure 2.3: Protective effect of negative charge on the amide group

Enantiomerically enriched Nai dipeptides were pursued by cyclization of aza-Pra residues possessing *C*-terminal groups that could disfavor epimerization and serve for further derivatization. Initial evidence showed that *O*-methyl hydroxamate **2.11** could be cyclized with minimal epimerization to imidazolone **2.12** in presence of stoichiometric amounts of potassium *tert*-butoxide, likely due to the presence of the acidic hydroxamate N-H, but subsequent derivatization proved ineffective using ^{t}BuONO in H_2O,[106] and this approach was abandoned (Figure 2.4). Alternatively, as described in Chapter 2 (submitted for publication to *Can. J. Chem*.), different *N*-terminal groups proved effective for avoiding epimerization and enabling further carboxylate functionalization.

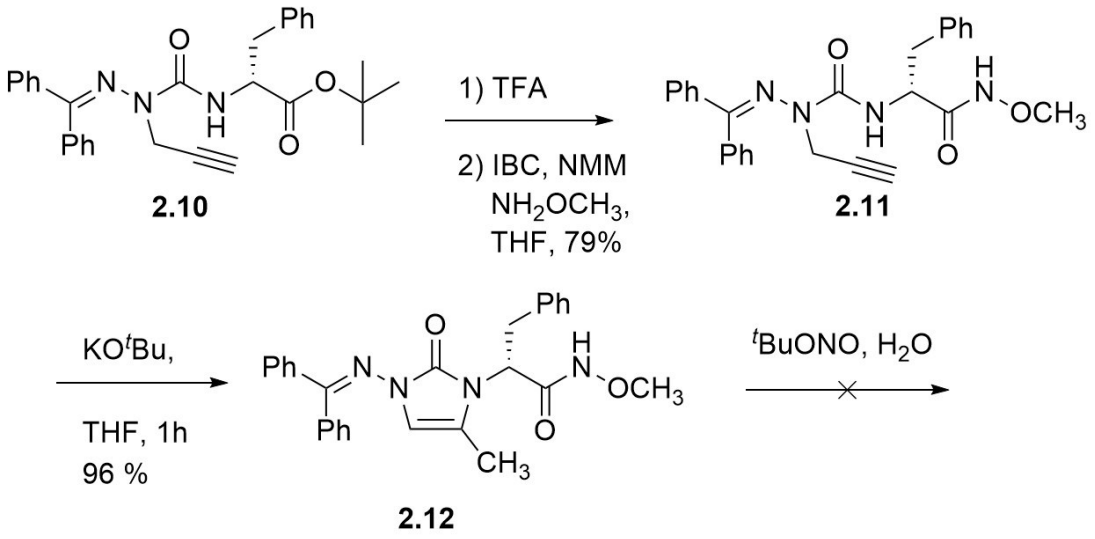

Figure 2.4: *O*-Methyl hydroxamate as *C*-terminal protecting group

2.4 Aldehydes in peptide motifs

Examples of biologically active peptides bearing *C*-terminal aldehydes include inhibitors of cysteine,[107] HIV,[108] and coronavirus proteases.[109] In theses inhibitors, the aldehyde can mimic the natural substrate amide carbonyl and form a covalent linkage with a nucleophilic sulfur or oxygen side chain in the active site of the protease inactivating the enzyme.[110] Such aldehydes may be considered suicide inhibitors, because of the slow off rate of the resulting tetrahedral intermediate in their mechanism of action.[111]

Masked aldehydes have been used during solid-phase synthesis (SPPS) to prepare peptides, which upon liberation of the carbonyl group form iminium ions with neighboring amide nitrogen and other side chain nucleophiles to form bi-, tri- and tetracyclic heterocyclic systems.[112, 113] For example, protected amino acid residues featuring acetal groups have been introduced into peptides using standard SPPS, exposed to acidic conditions to liberate the aldehyde for the formation of different heterocycles.[114]

Methods to prepare peptide aldehydes at both *C*- and *N*-terminal positions have also been used to install different functional groups, such as unsaturated bonds by olefination reactions.[115, 116] Capacity to add aldehyde functionality to peptide frameworks has thus significant utility.

2.5 Context

As mentioned in the previous chapter (sections 1.5 and 1.6), 4,5-disubstitued Nai residues are of particular interest for mimicking β-turns while maintaining side chain diversity. The importance of the 4-methyl group for control of χ^2 dihedral angle will be discussed further in chapter 3.[83] Methods for introducing a variety of 4-substituents on the imidazolone ring have been discussed in chapter 1.[75] 4-Position functionalization is thus pertinent; however, 5-position substituents may better mimic natural amino acid side chain orientations. Ability to introduce functional groups at both ring positions is of general interest from a diversity-oriented standpoint. In this context, enantiomerically enriched material is desired for further incorporation in peptides. This chapter, along with chapters 3 and 4 will address the above issues.

Chapter 2 has been submitted to a *Can. J. Chem*. special issue in honor of Professor James D. Wuest. The synthesis of enantiomerically enriched Nai dipeptides has been studied by cyclization routes featuring substrates with *C*-terminal groups that minimize α-carbon epimerization and enable carboxylate functionalization. In the cyclization mechanism, isomerization of the propargyl urea to an allenyl urea intermediate proceeds likely by deprotonation of the more acidic propargylic methylene proton to give propargyl anion **2.14a**.[117] Isomerization to allene anion **2.14b** is likely followed by urea proton extraction to give anion **2.15** prior to nucleophilic attack on the β-carbon of the alkene (Figure **2.4**).[118] In principle, substrate **2.13** may isomerize unproductively to ynamide anion **2.14c**,[119] the protonated product of which was however not observed.[118] To minimize epimerization during allene formation, the originally used sodium hydride (pK_a ~35)[120] was switched to the weaker base potassium *tert*-butoxide (pK_a ~17);[121] moreover, the solvent was changed from MeCN to the less polar THF. Product from cyclization using the new conditions exhibited only the *endo* double bond. Since the exocyclic double bond was observed by crude [1] Although ester epimerization remained significant,

racemization was minimized by application of two *C*-terminal groups, namely the carboxylic acid and hydrazide. Attempts using alternative cyclization conditions will be discussed further in Chapter 5.

With the enantiomerically enriched material in hand, functionalization of the 5-position of the imidazolone ring was explored. Considering the importance of aldehyde containing peptides as discussed above, the Vilsmeier reaction was pursued using $POCl_3$ in DMF and provided the 5-formyl imidazolone. Modification of the aldehyde was subsequently pursued to provide constrained amino acid chimeras with side chains of different amino acids [(e.g., aspartic acid (Asp), homoserine (Hse) and diaminobutyric acid (Dab)]. Moreover, Mannich chemistry was also shown to provide a means to amino methylate the imidazalone to obtain Dab analogs. Finally, incorporation of 4,5-disubstituted Nai residues into peptides was subsequently pursed as described in Chapters 4 and 5.

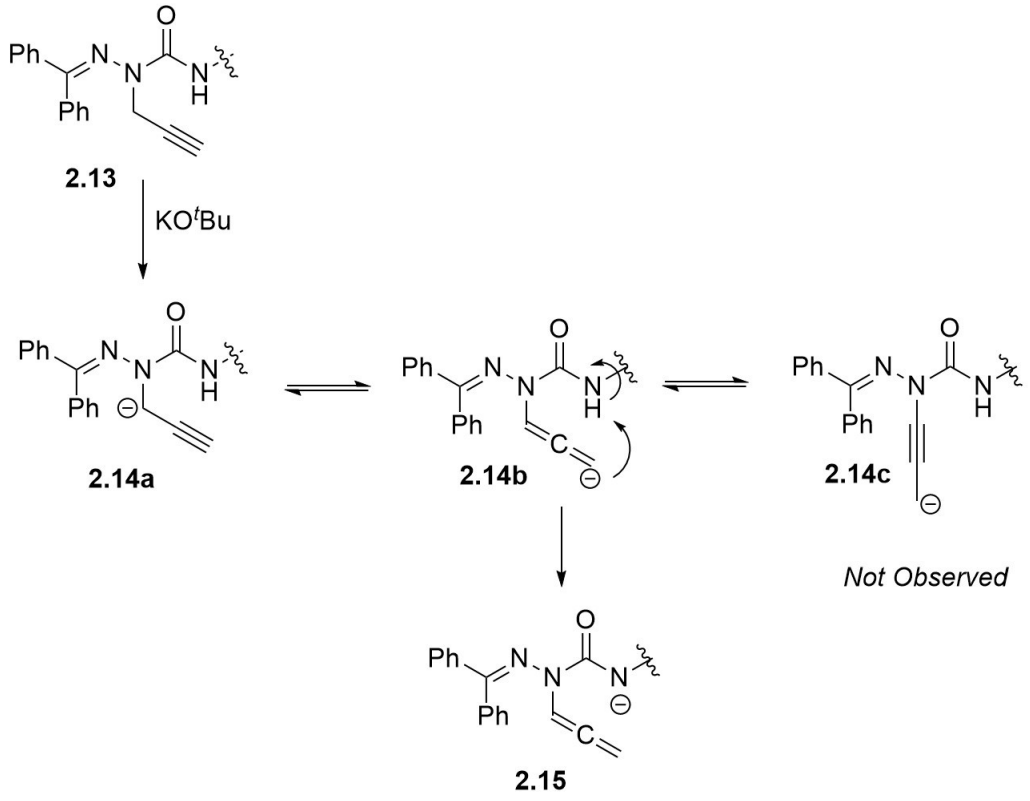

Figure 2.4: Plausible mechanism for the prototropic rearrangement of propargyl urea and subsequent cyclization

Article 1:

Poupart, J.; Hamdane, Y.; Lubell, W. D.; Synthesis of enantiomerically enriched 4,5-disubstituted N-aminoimidazol-2-one (Nai) peptide turn mimics, *Can. J. Chem.* **2019**, *98*: 278.

Special Issue dedicated to Professor James D. Wuest

Authors contribution

Yousra Hamdane, an undergraduate student who worked under my supervision, worked on analog **2.20**, synthesized and described the compound and scaled up the synthesis up to gram scale.

All other synthetic work was done by me.

The manuscript was written by me and edited by Professor William Lubell.

Synthesis of enantiomerically enriched 4,5-disubstituted *N*-aminoimidazol-2-one (Nai) peptide turn mimics

Julien Poupart, Yousra Hamdane and William D. Lubell*

Département de Chimie, Université de Montréal, C.P. 6128, Succursale Centre-Ville, Montréal, Québec, H3C3J7, Canada

Abstract

N-Aminoimidazolone (Nai) peptide mimics were synthesized with minimal epimerization by base-promoted 5-endo-dig cyclisation of aza-propargylglycine dipeptide acids and hydrazides followed by olefin migration. 5-Position functionalization using Mannich amino methylation and Vilsmeier–Haack formylation has given access to a set of restrained side chain analogs of Asp, Dab and Hse residues for mimicry of turn form and function.

Introduction

The therapeutic potential of peptides is well recognized, because of their ease of synthesis, minimal toxicity and efficacy against a wide variety of biological targets. Limited selectivity, metabolic stability and bioavailability are however drawbacks, which impede the development of peptides as therapeutics.[122, 123] Strategies for peptide mimicry offer means to retain the advantages of natural peptides while improving selectivity and pharmacokinetic properties.[37, 124] Among the different secondary structures implicated in biomolecular recognition,[125, 126] peptide turns have received particular attention as targets for mimicry due to the abundance of these natural folded sequences.[6]

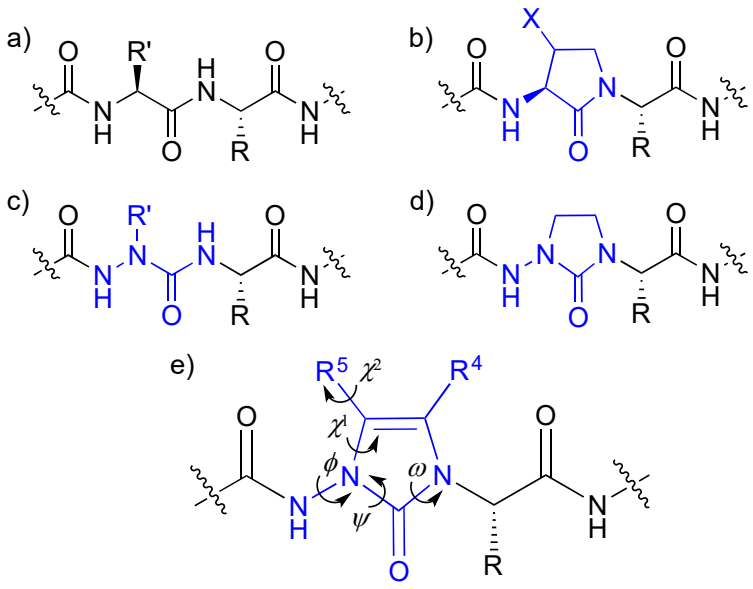

Figure 2.5. (a) Natural peptide, (b) Agl (X = H), Hgl (X = OH), (c) azapeptide, (d) Aid and (e) Nai residues, the latter depicted with relevant dihedral angles.

Among strategies to favor peptide turn geometry, the α-amino-β-lactam (Agl, Figure 2.5) residue, so-called Friedinger-Veber lactam, employs covalent restriction between the side chain and amine of the *N*- and *C*-terminal residues in a dipeptide to rigidify the geometry of the backbone φ- and ψ-dihedral angles.[40, 127, 128] Although challenging, the introduction of side chain diversity onto Agl residues has been achieved by stereoselective synthesis,[7] including alcohol alkylation and displacement from β-hydroxyl-Agl (Hgl, Figure 2.5b, X = OH) counterparts.[46, 47,11] Alternatively, stereo-electronic restriction using semicarbazide residues can favor turn geometry in azapeptides, due to the combination of urea planarity and adjacent nitrogen lone pair-lone pair repulsion (Figure 2.5c).[12,13] Although relatively flexible, azapeptide residues can be effectively embellished with diverse side chains by alkylation and arylation chemistry.[13] By merging the covalent and stereo-electronic strategies of Agl and azapeptide mimicry, the *N*-aminoimidazolidin-2-one (Aid)[14,15] and *N*-aminoimidazolone (Nai)[16-18] residues were conceived and have shown potential to induce turn conformations in model peptides (Figures 2.5d and 2.5e).[7] The Nai residues offer accessible sites for effective ring functionalization to mimic both the backbone and side chain orientations of peptide turns. For example, 4-methyl and 4-benzyl

Nai residues have been previously synthesized and shown by X-ray crystallography to induce type II' β- and inverse γ-turns in model dipeptides.[16,17]

Previously, 4-substituted Nai peptides were synthesized by routes commencing with alkylation of an azaGly semicarbazone with propargyl bromide to prepare an aza-propargylglycine (azaPra) residue.[19] Sonogashira cross-couplings on the azaPra analogs were used to install various aryl moieties.[16] 4-Substituted Nai peptides were prepared by base-promoted 5-*endo*-dig cyclisation of the azaPra analogs, presumably by way of an allene intermediate,[20,21] followed by olefin isomerization.[16] Epimerization was however observed in cases of *C*-terminal esters, necessitating purification of enantiomers by preparative supercritical fluid chromatography (SFC) on a chiral stationary phase.[22]

Substituents at the 4-position of the Nai residue mimic the *trans* χ^1 dihedral angle orientation, as observed in X-ray structures of model peptides in which they influence the χ-dihedral angle of the neighboring *C*-terminal residue.[17] The *gauche* (*+*) and (–) χ^1 orientations may however be better mimicked by an appendage at the Nai 5-position. In combination with a 4-position substituent, the 5-position substituent may experience additional steric interactions that restrict the χ^2 dihedral angle (Figure 2.5e). Previously, palladium-catalyzed Heck chemistry was employed to install aryl substituents at the 5 position of (4-methyl)Nai residues in solution.[83] Furthermore, computational analysis revealed that *p*-MeOBz-(4-methyl,5-aryl)Nai-D-Phe-NH*i*-Pr analogs (aryl = 5-phenyl and 5-*p*-hydroxphenyl) adopted type II' β-turn geometry with the χ dihedral angles of the groups situated in the *gauche* (–) conformation. Side chain *gauche* (+) and (–) orientations have been suggested to be preferred by natural side chains particularly in molecular recognition events.[23,24]

Aiming to broaden the utility and diversity of Nai peptide mimics, approaches are herein reported for minimizing epimerization during cyclization and for adding a variety of substituents to the heterocycle 5-position. Employing azaPra peptides with *C*-terminal carboxylic acid and hydrazide groups, cyclization with minimum epimerization was achieved. Moreover, 4,5-disubstituted Nai analogs with various hetero-alkyl appendages at the 5-position have been prepared by routes commencing respectively with Vilsmeier–Haack formylation and Mannich amino methylation.

Results and Discussion

Previously, attempts were unsuccessful to convert azaPra peptides into their Nai counterparts using various conditions featuring catalysis with transition metal (e.g., Au and Ag) complexes[25,26] or with cation-π activation using tetra-*n*-butylammonium fluoride (TBAF).[27,28] Successful 5-*endo*-dig cyclization was promoted using relatively strong base (e.g., NaH), but plagued by *C*-terminal ester epimerization.[16,22]

The employment of alternative carboxylate derivatives has been explored to provide Nai analogs suitable for peptide synthesis without epimerization (Table 2.1). Although potassium *tert*-butoxide in THF was found to be an effective relatively less basic condition than NaH in MeCN for cyclization, *C*-terminal ester epimerization was observed even under conditions using catalytic amounts of base (entries 1 and 2). Switching the *C*-terminal residue to the corresponding carboxylic acid **2.16b** and hydrazide **2.16c** minimized epimerization under conditions featuring short reaction times and excess base (entries 5 and 6). Removal of the acidic protons of the hydrazide and carboxylic acid groups by ^{t}BuOK may likely protect the chiral center from epimerization under the rapid cyclization conditions.

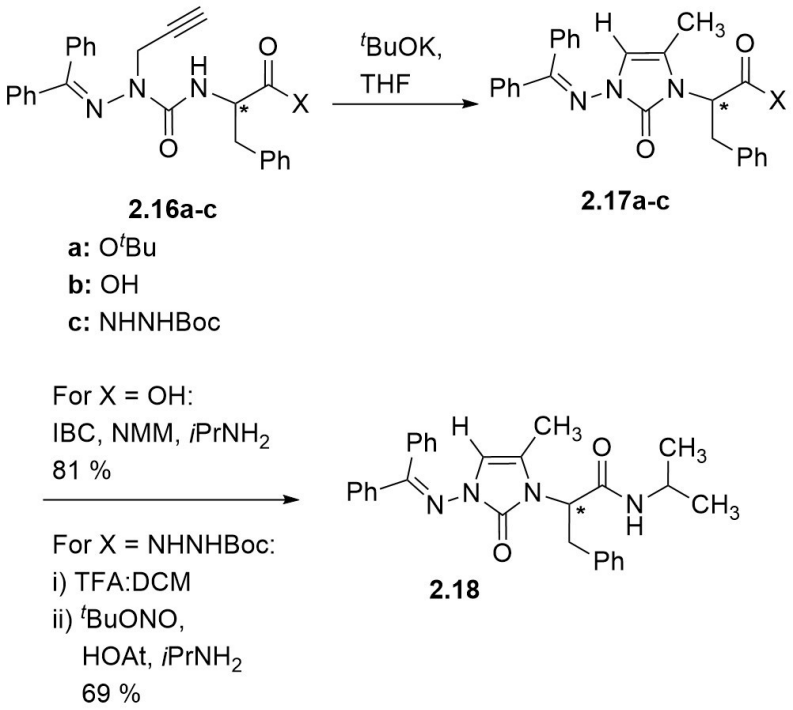

Scheme 2.1. Examination of AzaPra dipeptide carboxylate analogs for cyclisation to Nai residues without epimerization

Entry	X	^{t}BuOK equiv.	time (h)	% yield **2.17**[a]	*er* **2.18**
1	O^{t}Bu	0.3	12	21	1:1
2	O^{t}Bu	1.1	12	45	1:1
3	OH	0.3	18	0	N/A
4	OH	1.5	12	69	1:1
5	OH	3	0.25	60	98:2[b]

6	NHNHBoc	3	0.5	96	96:4[b]

*a: Isolated yield; b: Determined by chiral SFC of amide **2.18**.*

Table 2.1. Influences of substrate **2.16** and cyclization conditions on enantiomeric purity

The enantiomeric purities of Nai carboxylic acid **2.17b** and hydrazide **2.17c** were ascertained after conversion to *iso*-propyl amide **2.18** and analysis using SFC and a chiral column to measure the enantiomeric ratio (*er*). Acid **2.17b** was coupled to *iso*-propyl amine by way of a mixed anhydride intermediate using *iso*-butyl chloroformate (IBC) and *N*-methylmorpholine in THF.[29] Hydrazide **2.17c** was converted to amide **2.18** by cleavage of the Boc protection, oxidation to the acyl azide using *tert*-butyl nitrite,[30] and displacement using HOAt and *iso*-propyl amine in DMF.

With access to enantiomerically enriched Nai dipeptides **2.17**, different methods were examined to add a variety of substituents to the 5-position of (4-methyl)Nai dipeptides **2.17a-c**. the biological activity of 1,3-dihydro-2H-imidazol-2-one derivatives has inspired considerable effort to synthesize analogs of the parent heterocycle; however, few methods have been developed for adding functionality to the 4- and 5-positions under mild conditions.[31,32] For example, Friedel-Crafts acylation using $AlCl_3$ in nitrobenzene has been a common method for adding ketone substituents to 1,3-dihydroimidazolones;[31] however, (4-methyl)Nai dipeptides **2.17a-c** may not tolerate such harsh conditions.

The Vilsmeier–Haack formylation was explored to add a carbonyl function to the 5-position of (4-methyl)Nai dipeptides **2.17a-c**. Aldehydes **2.19a-d** were synthesized in 66-81% using DMF and phosphoryl chloride (Scheme 2.2). Starting material was returned however after attempts to use similar conditions with *N*,*N*-dimethyl acetamide and benzamide. Acylation with trichloro- and trifluoroacetic anhydride gave products, which were observed to degrade rapidly by TLC and mass spectrometry and could not be isolated.

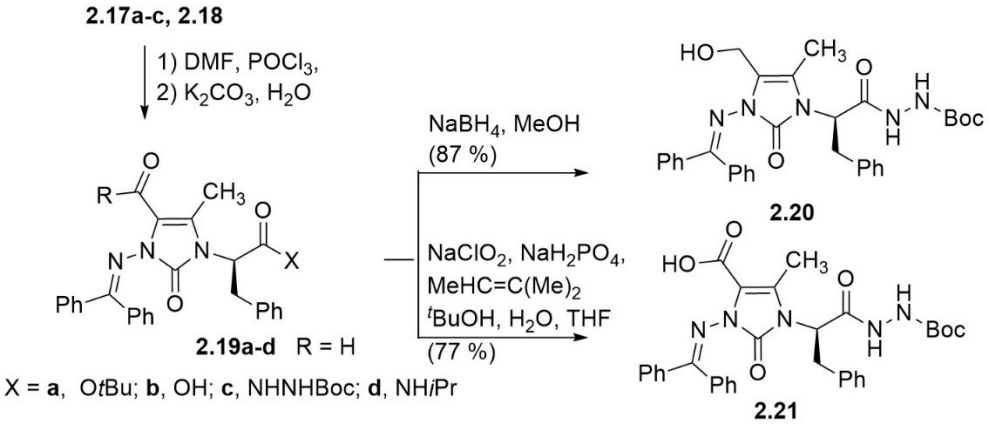

Scheme 2.2. Synthesis of aldehydes **2.19a-d** by way of Vilsmeier-Haack formylation and conversion to constrained Hse and Asp dipeptides

With (5-formyl)Nai **2.19c** in hand, the aldehyde was converted to (5-hydroxmethyl)Nai and (5-carboxy)Nai peptides **2.20** and **2.21**. Constrained homo-serine (Hse) dipeptide **2.20** was prepared in 87 % yield by hydride addition to aldehyde **2.19c** using sodium borohydride in MeOH. Restrained aspartate dipeptide **2.21** was obtained in 77 % yield **2.19c** by oxidation of aldehyde using sodium chlorite and potassium phosphate monobasic in presence of a 2 M solution of 2-methyl-2-butene in THF in a 9:1 ^{t}BuOH:water mixture (Scheme 2.2).[33] The reaction sequences to **2.20** and **2.21** were scalable and performed on multiple gram scale (experimental section).

A set of constrained diaminobutyric acid (Dba) analogs **2.22-2.25** was next synthesized by reductive amination of primary and secondary amines on (5-formyl)Nai **2.19c** (Scheme 2.3). Imine was generated by reaction of aldehyde **2.19c** with the amine and a catalytic amount of acetic acid in a 1:1 THF:MeOH mixture, and reduced *in situ* by the addition of sodium cyanoborohydride. Secondary and tertiary amines **2.22-2.25** were synthesized in 43-68 % yields employing allyl, methoxyethyl, and benzyl amines, and morpholine.

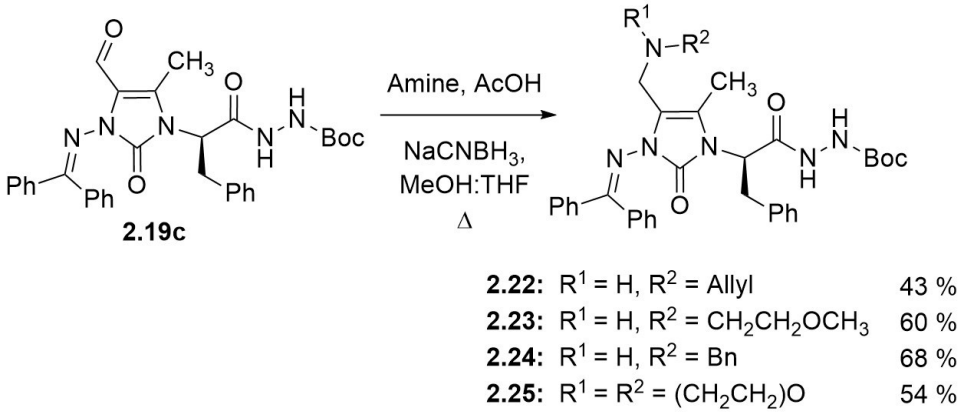

Scheme 2.3. Synthesis of constrained Dab analogs **2.22-2.25** by reductive amination

Based on the successful Vilsmeier-Haack formylation of (4-methyl)Nai **2.17a**, the Mannich reaction was explored using this ester substrate to provide an alternative one-step protocol to prepare the constrained Dba analogs. Amino methylation of imidazalone **2.17a** was initially studied using different acids, morpholine and paraformaldehyde in THF (Table 2.2). The mineral acid, HCl gave low yields of product, probably due to a competing retro-Mannich reaction (Table 2.2, entries 1 and 2). To support this hypothesis, morpholine **2.26** was treated with HCl in THF for 4h at 60°C; afterwards, TLC analysis showed formation of (4-methyl)Nai **2.17a**. Acetic acid gave relatively low yield. The Lewis acid, zinc chloride provided morpholine adduct **2.26** in 60% yield (entry 4). Subsequent attempts to employ alternative solvents (e.g., MeOH and dioxane) as well as aqueous formaldehyde under the $ZnCl_2$ conditions, all gave lower yields. With Mannich conditions in hand, (4-methyl)Nai hydrazide **2.17c** was reacted with morpholine to give constrained Dba analog **2.25** in 45% yield (Scheme 2.4).

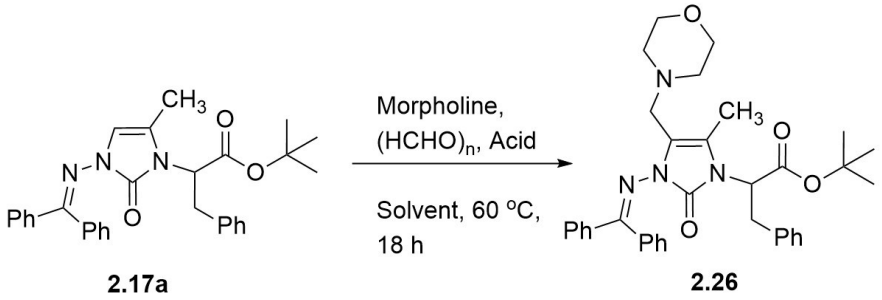

2.17a **2.26**

Entry	Acid (equiv.)	Solvent	% **2.26**[a]
1	HCl (1)	THF	trace[b]
2	HCl (3)	THF	19
3	AcOH (3)	THF	15
4	$ZnCl_2$ (3)	THF	60
5	$ZnCl_2$ (3)	MeOH	0[c]
6	$ZnCl_2$ (3)	Dioxane	31
7	$ZnCl_2$ (3)	THF	28[d]

a: Isolated yield. b: Observed by TLC. c: Starting material was recovered. d: Reaction performed with 40% aq. $H_2C=O$.

Table 2.2. Influence of conditions on Mannich reaction

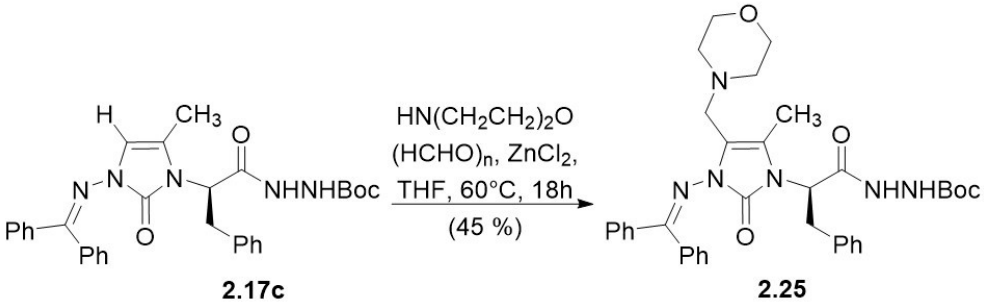

2.17c **2.25**

Scheme 2.4. Synthesis of amine **2.25** by Mannich reaction

In conclusion, 4,5-disubstituted Nai residues were synthetized by a route featuring 5-*endo*-dig cyclisation of azaPra dipeptide acid and hydrazide derivatives to provide enantiomerically enriched (4-methyl)Nai analogs **2.17b** and **2.17c**. Subsequently, different hetero-alkyl functional groups were introduced onto the 5- position of (4-methyl)Nai residue using Vilsmeier-Haak formylation and Mannich protocols to give respective access to (5-formy)Nai **2.19** and tertiary (5-aminomethyl)Nai **2.25-2.26** analogs. Modification of (5-formy)Nai **2.19** by oxidation, reduction and reductive amination has given further entry into Nai residues bearing alcohol, acid and secondary and tertiary amine 5-position substituents to provide constrained Hse, Asp and Dab analogs **2.20-2.25**. Efforts are currently being pursued towards the introduction of 4,5-disubstituted Nai residues into biologically relevant peptides and will be reported in due time.

Experimental Section

General

Unless specified, all reactions were performed under argon atmosphere. All glassware was stored in the oven or flame-dried and let cool under inert atmosphere prior to use. Anhydrous solvents were obtained either by filtration through drying columns (DCM, THF, MeCN, DMF) in a GlassContour system (Irvine, CA) or by distillation over CaH_2 (MeOH, $CHCl_3$). *tert*-Butyl 2-(3-((diphenylmethylene)amino)-5-methyl-2-oxo-2,3-dihydro-1*H*-imidazol-1-yl)-3-phenylpropanoate was synthesized according to the literature procedure.[16] All other starting materials, reagents and chemicals were purchased from commercial suppliers and used without further purification. Reaction progress was monitored by thin layer chromatography (TLC) on silica gel plates, which were visualized under UV light (254 nm) and by staining with $KMnO_4$, 2,4-dinitrophenylhydrazine (DNPH) and bromocresol green. Flash chromatography[34] was performed using either 230-400 mesh silica gel from SiliCycle Inc. or on a CombiFlash instrument from Teledyne using RediSep Gold columns. Nuclear magnetic resonance spectra (^1H, ^{13}C and COSY NMR) were recorded either on Bruker AMX 300, AV 400, AVII 400 or AMX 500 spectrometers. Specific rotations were determined on a Perkin-Elmer 341 polarimeter at 589 nm sodium-D line using a 0.5 dm cell and are reported as follow $[\alpha]_{\lambda}^{\text{temperature (°C)}}$, concentration (*c* in g/100 mL), and solvent. High resolution mass spectrometry (HRMS) was performed by the Centre régional de

spectroscopie de masse de l'Université de Montréal. Analytical supercritical fluid chromatography (SFC) was perfomed by the Laboratoire d'analyse et de separation chirale par SFC de l'Université de Montréal and reported as follow: temperature, backpressure and retention time (R*t*).

(2-(Diphenylmethylene)-1-(prop-2-yn-1-yl)hydrazine-1-carbonyl)-*D*-phenylalanine (2.16b)

tert-Butyl (2-(diphenylmethylene)-1-(prop-2-yn-1-yl)hydrazine-1-carbonyl)-*D*-phenylalaninate (15.8 g, 32.8 mmol) was dissolved in DCM (164 mL), treated with TFA (164 mL), and stirred for 2h. The volatiles were evaporated. The residue was co-evaporated with DCM to remove residual TFA. Acid **2.16b** was obtained as dark yellow oil (14.0g, 33.8mmol, 100%) and was used directly in the next step without further purifications: R*f* = 0.16 (50 % EtOAc/hexanes revealed by bromocresol green).

***tert*-Butyl 2-((2-(diphenylmethylene)-1-(prop-2-yn-1-yl)hydrazine-1-carbonyl)-*D*-phenylalanyl)hydrazine-1-carboxylate (2.16c)**

(2-(Diphenylmethylene)-1-(prop-2-yn-1-yl)hydrazine-1-carbonyl)-*D*-phenylalanine (14 g, 32.9 mmol) was dissolved in THF (329 mL). The mixture was cooled to –15°C in a 1:4 MeOH:H_2O dry ice bath. 4-Methylmorpholine (10.9 mL, 98.7 mmol) and isobutyl chloroformate (5.12 mL, 39.5 mmol) were sequentially added to the mixture, which was stirred for 15 min, treated with *tert*-butyl carbazate (6.52 g, 49.4 mmol), and stirred for 1.5h at –15°C. The ice bath was removed, and the mixture warmed to room temperature with stirring overnight. The volatiles were evaporated. The residue was dissolved in EtOAc and washed twice with saturated $NaHCO_3$, twice with saturated NH_4Cl and once with brine. The organic layer was dried over $MgSO_4$, filtered and evaporated. The residue was purified by column chromatography on silica gel using 0-100 % EtOAc in hexanes as eluent. Evaporation of the collected fractions gave hydrazide **2.16c** as yellow oil (12.9 g, 32.9 mmol, 68%): R*f* = 0.48 (50 % EtOAc/hexanes). ^{1}H NMR (500 MHz, $CDCl_3$) δ 1.47 (s, 9H), 2.03-2.05 (m, 1H), 3.16 (dd, *J* = 8.2, 6.0 Hz, 1H), 3.28 (dd, J = 8.1, 6.1 Hz, 1H), 3.82 (br. d, *J* = 16 H, 1H), 4.07 (br. d. *J* = 18 Hz, 1H), 4.67 (d, *J* = 6.3 Hz, 1H) 6.48 (br. s. 1H), 6.89 (d, *J* = 7.3 Hz, 1H), 7.22-7.46 (m, 13H), 8.33 (br. s. 1H). ^{13}C NMR (126 MHz, $CDCl_3$) δ 28.3, 29.8, 35.5, 37.3, 54.6,

72.4, 78.2, 81.8, 127.1, 128.3, 128.8, 128.9, 129.2, 129.6, 130.1, 130.6, 135.3, 136.6, 138.3, 155.2, 158.6, 160.3, 171.2. HRMS calc. for $C_{31}H_{34}N_5O_4$ [M+H$^+$] 540.2605, found 540.2601.

(*R*)-2-(3-((Diphenylmethylene)amino)-5-methyl-2-oxo-2,3-dihydro-1*H*-imidazol-1-yl)-3-phenylpropanoic acid (2.17b)

Acid **2.16b** (2.66 g, 6.25 mmol) was dissolved in dry THF (40 mL) and treated with potassium *tert*-butoxide (1.12 g, 10.0 mmol), stirred for 15 min, and quenched carefully with saturated NH_4Cl until the dark brown color disappeared. The mixture was transferred to a separatory funnel and extracted with DCM (3 x 50 mL). The aqueous layer was acidified with 1N HCl to pH = 3 and extracted with DCM (50 mL). The organic layers were combined, washed with brine (100 mL), dried over $MgSO_4$, filtered and evaporated to a residue that was purified by column chromatography on silica gel eluting with 0-20 % MeOH in DCM. Evaporation of the collected fractions gave imidazolone **2.17b** as yellow oil (1.60 g, 60 %): R*f* = 0.29 (50 % EtOAc/hexanes); $[\alpha]_D^{23}$ 45.7 (*c* 0.75, $CHCl_3$), ^{1}H NMR (500 MHz, $CDCl_3$) δ 1.37 (s, 3H), 3.03 (dd, *J* = 10.7, 2.9 Hz, 1H), 3.57 (t, *J* = 12.8 Hz, 1H), 4.44 (dd, *J* = 13.5, 6.3 Hz, 1H), 5.56 (s. 1H), 6.93-766 (m, 15H). ^{13}C NMR (126 MHz, $CDCl_3$) δ 32.0, 37.1, 110.3, 126.2, 127.4, 128.4, 128.5, 128.9, 129.1, 129.2, 129.5, 130.2, 132.6, 137.7, 163.4, 169.2. HRMS calc. for $C_{26}H_{24}N_3O_3$ [M+H$^+$] 426.1812, found 426.1807.

(*R*)-*tert*-Butyl 2-(2-(3-((diphenylmethylene)amino)-5-methyl-2-oxo-2,3-dihydro-1*H*-imidazol-1-yl)-3-phenylpropanoyl)hydrazine-1-carboxylate (2.17c)

Hydrazide **2.16c** (2.35 g, 4.35 mmol) was dissolved in THF (90 mL), treated with potassium *tert*-butoxide (976 mg, 8.70 mmol), stirred for 30 min, and treated with water (90 mL). The reaction mixture was stirred for 5 min and extracted with EtOAc (3 x 100 mL). The combined organic layer was washed with brine (1 x 100 mL), dried with $MgSO_4$, filtered and evaporated to give a residue that was purified by column chromatography on silica gel using a gradient of 0-100 % EtOAc in hexanes. Evaporation of the collected fractions gave imidazolone **2.17c** as yellow low-melting solid (2.26 g, 96 %): $[\alpha]_D^{23}$ 106.3 (*c* 0.70, $CHCl_3$) ^{1}H NMR (400 MHz, $CDCl_3$) δ 1.46 (s, 9H), 1.50 (s, 3H), 3.30 (br. s., 1H), 3.63-3.70 (m, 1H), 4.50 (m, 1H), 5.44 (s, 1H), 6.48 (br s, 1H), 7.03-7.63 (m, 15H), 9.59 (br. s.,1H). ^{13}C NMR (75 MHz, $CDCl_3$) δ 10.4, 28.3, 35.1, 77.4, 81.5, 106.8,

119.2, 127.0, 128.3, 128.7, 128.8, 128.9, 129.1, 129.3, 131.1, 134.8, 137.1, 137.2 150.4, 155.0, 166.3, 170.0. HRMS calc. for $C_{31}H_{34}N_5O_4$ [M+H$^+$] 540.2605, found 540.2609.

(*R*)-2-(3-((Diphenylmethylene)amino)-5-methyl-2-oxo-2,3-dihydro-1*H*-imidazol-1-yl)-*N*-isopropyl-3-phenylpropanamide (2.18)

Acid 2.17b (60 mg, 0.14 mmol) was dissolved in THF (2 mL). The solution was cooled to –15 °C using a MeOH:water:dry ice bath. *Iso*-butyl chloroformate (28 µL, 0.14 mmol) was added dropwise to the cooled solution, which was stirred for 15 min, and treated with *iso*-propylamine (46 µL, 0.56 mmol). The ice bath was removed. The reaction mixture warmed to room temperature with stirring over 2h. The reaction mixture was partitioned between water (5 mL) and EtOAc (5 mL). The layers were separated. The aqueous layer was extracted with EtOAc (3 x 5 mL). The organic layers were combined, washed with saturated $NaHCO_3$ (3 x 10 mL), saturated NH_4Cl (3 x 10 mL) and brine (10 mL), dried with magnesium sulfate, filtered and evaporated to give a residue that was purified by column chromatography on silica gel eluting with 0-100 % EtOAc in hexanes. Evaporation of the collected fractions gave amide **2.18** as yellow low-melting solid (53 mg, 81 %). The characterisation of **2.18** was consistent with that previously reported.[16] The enantiomeric ratio of 98:2 was determined by chiral SFC analysis (OJ-H column, 5-90 % MeOH/H_2O over 15 min. Rt major = 5.20 min, Rt minor = 7.40 min).

Hydrazide 2.17c (50.0 mg, 0.09 mmol) was dissolved in dry CH_2Cl_2 (1 mL), treated with trifluoroacetic acid (140 µL, 1.85 mmol), and stirred at room temperature for 2h. The volatiles were evaporated. The residue was dissolved in DCM (10 mL), washed with saturated $NaHCO_3$ (3 x 5 mL) and brine (1 x 5 mL), dried over $MgSO_4$, filtered and evaporated. The residue was dissolved in DMF (1 mL), treated with *tert*-butyl nitrite (14 mL, 0.1 mmol) and HOAt (38 mg, 0. 3 mmol), stirred at room temperature for 30 min, treated with *iso*-propylamine (24 mL, 0. 3 mmol) and DIEA (48.4 µL, 0.3 mmol), and stirred for 18h. Water (5 mL) was added to the mixture, which was extracted with DCM (3 x 10 mL). The organic layers were combined, washed with saturated $NaHCO_3$ (3 x 10 mL), saturated NH_4Cl (3 x 10 mL) and brine (10 mL), dried over magnesium sulfate and evaporated to a residue that was purified by column chromatography on silica gel eluting with 0-100 % EtOAc in hexanes. Evaporation of the collected fractions gave amide **2.18** as yellow low-melting solid (30 mg, 69 %). The characterisation of **2.18** was consistent with that previously

reported.[16] The enantiomeric ratio of 96:4 was determined by chiral SFC analysis using the same conditions described above (Rt major = 5.15 min Rt minor = 7.51).

***tert*-Butyl 2-(3-(benzhydrylidene)amino)-4-formyl-5-methyl-2-oxo-2,3-dihydro-1*H*-imidazol-1-yl)-3-phenylpropanoate (2.19a)**

A solution of Nai ester **2.17a** (1 g, 2.08 mmol) in DMF (20 mL) was cooled to 0 °C, and treated dropwise with $POCl_3$ (0.60 mL, 6 mmol) over 10 min. The cooling bath was removed. The reaction mixture warmed to room temperature. After stirring for 1h, the reaction mixture was treated with K_2CO_3 (1.39 g, 10.0 mmol), stirred for 1h, and poured into saturated ammonium chloride (40 mL). The phases were separated. The aqueous layer was extracted with EtOAc (3 x 20 mL). The organic layers were combined, washed with saturated ammonium chloride (3 x 20 mL) and brine (30 mL), dried over magnesium sulfate, filtered and evaporated to a residue, that was purified by column chromatography on silica gel eluting with 0-100% EtOAc in hexanes. Evaporation of the collected fractions afforded aldehyde **2.19a** (826 mg, 81%) as orange oil; R*f* = 0.76 (50 % EtOAc/hexanes); ^{1}H NMR (300 MHz, $CDCl_3$) δ 1.47 (s, 9H), 1.78 (s, 3H), 3.23 (dd, *J* = 11.0, 3.1 Hz, 1H), 3.34 (dd, *J* = 9.9, 4.1 Hz, 1H), 4.37 (dd, *J* = 6.8, 4.0 Hz, 1H), 6.67-7.72 (m, 15H), 9.59 (s, 1H). ^{13}C NMR (126 MHz, $CDCl_3$) δ 8.9, 28.0, 34.8, 58.4, 83.2, 119.5, 127.0, 128.1, 128.3, 128.7, 128.8, 129.1, 129.4, 129.6, 130.0, 131.8, 135.6, 136.6, 137.2, 146.0, 162.7, 167.0. HRMS calc. for $C_{31}H_{32}N_3O_4$ $[M+H]^+$ 510.2393, found 570.2389.

(*R*)-2-(3-((Diphenylmethylene)amino)-4-formyl-5-methyl-2-oxo-2,3-dihydro-1*H*-imidazol-1-yl)-3-phenylpropanoic acid (2.19b)

Employing the protocol for the synthesis of (4-methyl,5-formyl)Nai **2.19a**, acid **2.17b** (1.00 g, 2.21 mmol) in DMF (25 mL) was reacted with $POCl_3$ (0.63 mL, 6.63 mmol). The residue was purified by column chromatography on silica gel eluting with 0-100 % EtOAc in hexanes. Evaporation of the collected fractions afforded aldehyde **2.19b** as orange solid (236 mg, 66%): R*f* 0.21 (80 % EtOAc/hexanes); $[\alpha]_D^{23}$ 229.1 (*c* 0.75, $CHCl_3$); mp = 134-13.8 °C. ^{1}H NMR (300 MHz, $CDCl_3$) δ 1.46 (s, 3H), 3.21-3.35 (m, 2H), 4.52-4.55 (m, 1H), 6.66-765 (m, 15H), 9.15 (br. s., 1H), 9.44-9.47 (m, 1H). ^{13}C NMR (125 MHz, $CDCl_3$) δ 27.6, 27.8, 29.7, 53.4, 87.2, 111.2, 113.5, 115.7, 118.0, 127.9, 128.5, 128.6, 129.0, 129.1, 129.2, 129.3, 133.4, 136.9, 159.7, 160.0, 160.3, 199.9. HRMS calc. for $C_{27}H_{24}N_3O_4$ $[M+H]^+$ 454.1767, found 454.1812.

***tert*-Butyl (*R*)-2-(2-(3-((diphenylmethylene)amino)-4-formyl-5-methyl-2-oxo-2,3-dihydro-1*H*-imidazol-1-yl)-3-phenylpropanoyl)hydrazine-1-carboxylate (2.19c)**

Employing the protocol for the synthesis of (4-methyl,5-formyl)Nai **2.19a**, hydrazide **2.17c** (880 mg, 1.63 mmol) in DMF (8 mL) was reacted with $POCl_3$ (0.49 mL, 4.89 mmol). The residue was purified by column chromatography on silica gel eluting with 0-100 % EtOAc in hexanes. Evaporation of the collected fractions afforded aldehyde **2.19c** as orange oil (236 mg, 66%): R*f* = 0.41 (50 % EtOAc/hexanes); $[\alpha]_D^{23}$ 173.2 (*c* 1.30, $CHCl_3$); ^{1}H NMR (500 MHz, $CDCl_3$) δ 1.46 (s, 9H), 1.82 (s, 3H), 3.34 (br s, 2H), 4.60 (br s, 1H) 6.69 (br. s, 2H), 7.12-7.69 (m, 14H) 9.17 (br. s, 1H) 9.40 (s, 1H). ^{13}C NMR (126 MHz, $CDCl_3$) δ 8.9, 28.3, 34.9, 57.4, 81.94, 82.3, 119.9, 127.4, 127.7, 128.3, 128.5, 129.0, 129.2, 129.3, 129.7, 130.0, 132.2, 135.4, 136.1, 146.8, 151.3, 154.3, 155.0, 168.4. HRMS calc. for $C_{32}H_{34}N_5O_5$ [M+H$^+$] 568.2555, found 568.2550.

(*R*)-2-(3-((Diphenylmethylene)amino)-4-formyl-5-methyl-2-oxo-2,3-dihydro-1*H*-imidazol-1-yl)-*N*-isopropyl-3-phenylpropanamide (2.19d)

Employing the protocol for the synthesis of (4-methyl,5-formyl)Nai **2.19a**, amide **2.18** (1g, 0.50 mmol) in DMF (5 mL) was reacted with $POCl_3$ (0.15mL, 1.50 mmol). The residue was purified by column chromatography on silica gel eluting with 0-100 % EtOAc in hexanes. Evaporation of the collected fractions afforded aldehyde **2.19d** as orange oil (236 mg, 66%): R*f* = 0.31 (35 % EtOAc/hexanes); $[\alpha]_D^{23}$ 102 (*c* 0.51, $CHCl_3$); ^{1}H NMR (400 MHz, $CDCl_3$) δ 1.41 (d, *J* = 6.6 Hz, 3H), 1.47 (d, *J* = 6.5 Hz, 3H), 2.27 (s, 3H), 3.55 (dd, *J* = 13.7, 3.9 Hz, 1H), 3.77 dd, *J* = 13.4, 2.2 Hz, 1H), 4.29. (sext, *J* = 6.7 Hz, 1H), 4.73 (dd, *J* = 6.6, 4.1 Hz, 1H), 7.1-8.0 (m, 15H), 9.81 (s, 1H). ^{13}C NMR (100 MHz, $CDCl_3$) δ 9.2, 22.5, 35.4, 40.1, 77.0, 119.9, 127.2, 128.3, 128.5, 128.6, 128.8, 129.0, 129.7, 130.0, 132.1, 135.5, 136.4, 136.8, 167.9. HRMS calc. for $C_{30}H_{31}N_4O_3$ [M+H$^+$] 495.2391, found 495.2401.

***tert*-Butyl (*R*)-2-(2-(3-((diphenylmethylene)amino)-4-(hydroxymethyl)-5-methyl-2-oxo-2,3-dihydro-1*H*-imidazol-1-yl)-3-phenylpropanoyl)hydrazine-1-carboxylate (2.20)**

A round bottomed flask containing a solution of aldehyde **2.19c** (12.00 g, 21.1 mmol) in MeOH (200 mL) was cooled to 0^{o}C using an ice bath. The solution was treated portion-wise with sodium borohydride (800 mg, 21.1 mmol). The cooling bath was removed. The reaction mixture warmed to room temperature. After stirring over 1h, water (300 mL) was added to the mixture,

which was extracted with EtOAc (3 x 200 mL). The organic layers were combined, washed with brine (300 mL), dried over $MgSO_4$, filtered and evaporated to a residue, that was purified by column chromatography on silica gel eluting with 0-100 % EtOAc in hexanes. Evaporation of the collected fractions afforded alcohol **2.20** (10.0 g, 77%) as dark yellow oil: R*f* = 0.20 (50% EtOAc/hexane); $[\alpha]_D^{23}$ 45.9 (*c* 0.60, $CHCl_3$); ^{1}H NMR (300 MHz, $CDCl_3$) δ 1.47 (s, 9H), 1.63 (s, 3H), 2.43 (br. s, 1H), 3.14-3.18 (m, 1H), 3.37-3.45 (m, 1 H), 4.36 (m, 3H), 6.18 (br. s, 1H), 6.67-7.67 (m, 15H) 9.08 (br. s, 1H). ^{13}C NMR (75 MHz, $CDCl_3$) δ 8.5, 28.1, 34.9, 81.5, 77.2 117.0, 118.5, 126.9, 128.1, 128.3, 128.6, 128.7, 128.9, 129.4, 131.8, 135.7, 136.6, 137.0, 146.4, 154.8, 169.7, 174.9. HRMS calc. for $C_{32}H_{36}N_5O_5$ [M+H$^+$] 570.2711, found 570.2683.

(*R*)-3-(1-(2-(*tert*-Butoxycarbonyl)hydrazinyl)-1-oxo-3-phenylpropan-2-yl)-1-((diphenylmethylene)amino)-4-methyl-2-oxo-2,3-dihydro-1*H*-imidazole-5-carboxylic acid (2.21)

A round bottomed flask containing a solution of aldehyde **2.19c** (2.00 g, 3.52 mmol) in a mixture of *tert*-butanol (32.0 mL) and H_2O (3.20 mL) was cooled to 0°C using an ice bath. The cooled solution was treated sequentially with potassium phosphate monobasic (1.03 mL, 17.60 mmol), a 2 M solution of 2-methyl-2-butene in THF (8.81 mL, 17.60 mmol) and sodium chlorite (technical grade 80%, 1.27 g, 14.1 mmol). The reaction mixture was stirred for 4h, at which point disappearance of starting material was observed by TLC and a new more polar product was observed near the baseline and stained yellow with bromocresol green. Saturated NH_4Cl (100 mL) was added to the reaction mixture. The phases were separated. The aqueous phase was extracted with EtOAc (3 x 10 mL). The organic layers were combined, washed with brine (100 mL), dried over $MgSO_4$, filtered, and evaporated to a residue, which was purified by column chromatography on silica gel eluting with 0-20 % MeOH in DCM. Evaporation of the collected fractions gave **2.21** as yellow solid (1.58 g, 77%): R*f* = 0.29 (60% EtOAc/hexanes); $[\alpha]_D^{23}$ 215.0 (*c* 0.60, $CHCl_3$); mp 153.7-157.2 °C. ^{1}H NMR (400 MHz, $CDCl_3$) δ 1.44 (overlapping s, 3H and 9H), 3.25-3.35 (m, 2H), 4.49-4.50 (m, 1H), 6.17 (br. s, 1H) 6.49-7.63 (m, 15H), 9.15 (br. s, 1H). ^{13}C NMR (75 MHz, $CDCl_3$) δ 9.9, 28.1, 29.7, 34.6, 77.2, 81.9, 113.3, 127.1, 128.1, 128.4, 128.6, 128.7, 128.8, 129.0, 129.5, 129.8, 132.0, 123.8, 135.4, 136.1, 136.3, 155.1, 162.2, 168.6. HRMS calc. for $C_{32}H_{34}N_5O_6$ [M+H$^+$] 584.2504, found 584.2504.

***tert*-Butyl (*R*)-2-(2-(4-(allylaminomethyl)-3-((diphenylmethylene)amino)-5-methyl-2-oxo-2,3-dihydro-1*H*-imidazol-1-yl)-3-phenylpropanoyl)hydrazine-1-carboxylate (2.22)**

Aldehyde **2.19c** (150 mg, 0.26 mmol) was reacted with allylamine (58 µL, 0.79 mmol), sodium cyanoborohydride (82 mg, 1.3 mmol) and acetic acid (1 µL, 0.02 mmol), in a 1:1 THF/MeOH mixture (1 mL). The mixture was heated to 65°C for 4 h and then quenched with water (1 mL). The reaction mixture was cooled to room temperature and extracted with EtOAc (3 x 5 mL). The combined organic layers were washed with saturated $NaHCO_3$ (1 x 10 mL) and brine (1 x 10 mL). The organic layer was dried over magnesium sulfate and evaporated to a residue that was purified by column chromatography on silica gel eluting with a gradient of 0-100 % EtOAc in hexanes. Evaporation of the collected fraction gave amine **2.22** as yellow oil (67 mg, 43%).R*f* = 0.22 (60% EtOAc/hexanes); $[\alpha]_D^{23}$ 177.9 (*c* 0.95, $CHCl_3$); ^{1}H NMR (300 MHz, $CDCl_3$) δ 1.48 (s, 9H), 1.55 (s, 3H), 2.96-3.17 (m, 3H), 3.41-3.63 (m, 3H), 4.32-4.35 (m, 1H), 5.05-5.11 (m, 2H), 5.78-5.87 (m, 1H), 6.14 (br. s, 1H), 6.78-7.69 (m, 15H); ^{13}C NMR (125 MHz, $CDCl_3$) δ 8.6, 28.3, 35.1, 40.9, 51.7, 81.5, 116.7, 117.2, 126.9, 127.0, 127.8, 128.1, 128.4, 128.7, 128.8, 129.1, 129.3, 129.5, 129.8, 131.8, 135.8, 136.8, 137.4, 139.8, 146.6, 154.9, 170.0, 175.1. HRMS calc. for $C_{35}H_{40}N_6O_4Na$ [M+Na^+] 631.3003, found 631.3001.

***tert*-Butyl (*R*)-2-(2-(4-(methoxyethylaminomethyl)-3-((diphenylmethylene)amino)-5-methyl-2-oxo-2,3-dihydro-1*H*-imidazol-1-yl)-3-phenylpropanoyl)hydrazine-1-carboxylate (2.23)**

Employing the protocol for the synthesis of amine **2.22**, aldehyde **2.19c** (50 mg, 0.10 mmol) was reacted with methoxyethylamine (38 µL, 0.44 mmol), sodium cyanoborohydride (27 mg, 0.44 mmol) and acetic acid (1 µL, 0.02 mmol) in a 1:1 THF/MeOH mixture (1 mL). The residue was purified by column chromatography on silica gel eluting with a gradient of 0-100 % EtOAc in hexanes. Evaporation of the collected fraction gave amine **2.23** as yellow oil (40 mg, 60%). R*f* = 0.16 (80 % EtOAc/hexanes); $[\alpha]_D^{23}$ 173.4 (*c* 0.60, $CHCl_3$); ^{1}H NMR (300 MHz, $CDCl_3$) δ 1.47 (s, 11H), 1.56, 3H), 2.55 (t, *J* = 5.5 Hz, 2H), 3.08-3.18 (m, 1H), 3.32 (s, 3H), 3.38-3.66 (m, 5H), 4.31-4.34 (m, 1H), 6.17 (br.s, 1H), 6.76-6.77 (m, 2H), 7.14-7.53 (m, 11H), 7.66-7.69 (m, 2H). ^{13}C NMR (125 MHz, $CDCl_3$) δ 1.9, 8.6, 28.1, 35.0, 40.7, 49.9, 77.3 (overlapping with the $CDCl_3$ signal but confirmed by Dept), 81.5, 116.2, 116.4, 126.8, 128.0, 128.3, 128.6, 128.7, 129.0, 129.3, 129.7, 131.7, 135.7,

136.3, 136.6, 137.2, 146.7, 154.8, 169.9, 175.0. HRMS calc. for $C_{35}H_{42}N_6O_5Na$ [M+Na$^+$] 649.3109, found 649.3120.

***tert*-Butyl (*R*)-2-(2-(4-(benzylaminomethyl)-3-((diphenylmethylene)amino)-5-methyl-2-oxo-2,3-dihydro-1*H*-imidazol-1-yl)-3-phenylpropanoyl)hydrazine-1-carboxylate (2.24)**

Employing the protocol for the synthesis of amine **2.22**, aldehyde **2.19c** (50 mg, 0.10 mmol) was reacted with benzylamine (48 µL, 0.44 mmol), sodium cyanoborohydride (27 mg, 0.44 mmol) and acetic acid (1 µL, 0.02 mmol) in a 1:1 THF/MeOH mixture (1 mL). The residue was purified by column chromatography on silica gel eluting with a gradient of 0-100 % EtOAc in hexanes. Evaporation of the collected fraction gave benzylamine **2.24** (43 mg, 68 % yield). R*f* = 0.11 (80 % EtOAc/hexanes); $[\alpha]_D^{23}$ 181.5 (*c* 0.95, $CHCl_3$); ^{1}H NMR (500 MHz, $CDCl_3$) δ 1.37 (s, 3H), 1.45 (s. 9H), 3.165 (br. s. 1H) 3.45 (d, *J* 14.1 Hz)), 3.14-3.58)m, 2H), 6.03 (br. s, 1H). 6.29 (br. s, 1H), 6.80-7.68 (m, 20H). ^{13}C NMR (126 MHz, $CDCl_3$) δ 8.5, 28.2, 30.0, 40.8, 58.6, 81.4, 116.06, 117.1, 126.8, 127.7, 128.0, 128.03, 128.6, 128.7, 129.1, 1292, 109.4, 129.7, 135.8, 136.67, 138.67, 146.5, 154.8, 169.9, 175.0 HRMS calc. for $C_{39}H_{42}N_6O_4$ [M+H$^+$] 659.3340, found 659.3343.

***tert*-Butyl (*R*)-2-(2-(4-(morpholinomethyl)-3-((diphenylmethylene)amino)-5-methyl-2-oxo-2,3-dihydro-1*H*-imidazol-1-yl)-3-phenylpropanoate (2.26)**

In a sealed vessel, a solution of paraformaldehyde (325 mg, 4.0 mmol) and morpholine (0.35 mL, 4.04 mmol) in THF (5 mL) was heated to 60 °C, and stirred for 15 min. The vessel was cooled to room temperature, the cap was exchanged for a rubber stopper under nitrogen, and the reaction mixture was treated with a solution of Nai ester **2.17a** (241 mg, 0.5 mmol) in THF (2 mL), that was transferred by syringe. The reaction mixture was treated with $ZnCl_2$ (76 mg, 0.56 mmol), heated to 60^{o}C, stirred for 4 h, cooled to room temperature, and quenched with water (1 mL). The reaction mixture was transferred to a separatory funnel and partitioned between EtOAc (50 mL) and water (25 mL). The layers were separated. The organic layer was washed with saturated $NaHCO_3$ (3 x 30 mL) and brine (30 mL), dried over magnesium sulfate, filtered, and evaporated to a residue, that was purified by column chromatography on silica gel eluting with 30-100% EtOAc in hexane as eluent. Evaporation of the collected fractions gave morpholine **2.26** as yellow oil (174 mg, 60 %) as yellow oil. R*f* = 0.16 (80 % EtOAc/hexanes); $[\alpha]_D^{23}$ 173.4 (*c* 0.60,

$CHCl_3$); ^1H NMR (300 MHz, $CDCl_3$) δ 1.40 (s, 9H), 1.51 (s, 3H), 2.25-2.28 (m, 4H), 3.05-3.9 (m, 1H), 3.19-3.22 (m, 2H), 3.38-3.43 (m, 1H), 3.65-3.69 (m, 4H), 4.27-4.4.33 (m, 1H), 6.69-7.66 (m, 15H); ^{13}C NMR (100 MHz, $CDCl_3$) δ 8.7, 28.0, 34.9, 50.9, 53.0, 57.6, 67.0, 82.0, 114.3, 117.2, 126.2, 127.5, 128.0, 128.2, 128.8, 129.2, 129.3, 129.6, 131.0, 136.4, 137.5, 138.1, 146.4, 168.4, 174.3. HRMS calc. for $C_{35}H_{40}N_6O_5{}^{107}Ag$ [M+Ag^+] 687.2095, found 687.2017; calc. for $C_{35}H_{40}N_6O_5{}^{109}Ag$ [M+Ag^+] 689.2097, found 689.2119.

tert-Butyl (_R_)-2-(2-(3-((diphenylmethylene)amino)-5-methyl-4-(morpholinomethyl)-2-oxo-2,3-dihydro-1_H_-imidazol-1-yl)-3-phenylpropanoyl)hydrazine-1-carboxylate (2.25)

Employing the protocol described for the synthesis of amine **2.22**, aldehyde **2.19c** (60 mg, 0.11 mmol) was reacted with morpholine (46 mL, 0.53 mmol), sodium cyanoborohydride (33 mg, 0.53 mmol) and acetic acid (1 µL, 0.02 mmol) in a 1:1 THF/MeOH mixture (1 mL). The residue was purified by column chromatography on silica gel eluting with a gradient of 0-100 % EtOAc in hexanes. Evaporation of the collected fraction gave amine **2.25** as yellow oil (38 mg, 54%). R*f* = 0.25 (60 % EtOAc/hexanes); $[\alpha]_D^{23}$ 105.8 (*c* 0.75, $CHCl_3$); ^1H NMR (500 MHz, $CDCl_3$) δ 1.46 (s, 9H), 1.51 (s, 2H), 1.62 (s, 1H), 2.20 (br.s, 3H), 2.80-3.43 (m, 3H), 3.34-3.43 (m, 2H), 3.65-3.69 (m, 4H), 3.90-3.92 (m, 1H), 4.33-4.38 (m, 1H), 6.61 (br.s, 1H), 6.77 (br.s, 1H), 7.07-7.17 (m, 3H), 7.37-7.51 (m, 7H), 7.62-7.7 (m, 4H). ^{13}C NMR (126 MHz, $CDCl_3$) δ 8.8, 28.3, 29.8, 35.2, 50.8, 50.9, 53.0, 65.4, 67.0, 81.6, 126.7, 127.9, 128.4, 128.6, 129.1, 129.3, 129.7, 129.9, 131.6, 136.2, 137.0, 137.4, 147.0, 154.9, 170.1, 175.5. HRMS calc. for $C_{36}H_{42}N_6O_5Na$ [M+Na^+] 639.3289, found 639.3274.

Employing the protocol for **2.26**, paraformaldehyde (328 mg, 4.04 mmol), morpholine (0.35 mL, 4.04 mmol), Nai peptide **2.17c** (243 mg, 0.51 mmol) and $ZnCl_2$ (76 mg, 0.56 mmol) were reacted. After aqueous work up and purification by column chromatography on silica gel eluting with 30-100% EtOAc in hexane as eluent, evaporation of the collected fractions gave morpholine **2.25** as yellow oil (147 mg, 45%), which exhibited identical characteristics as material made by the reductive amination protocol described above.

Supplementary information

Supplementary data is available through the journal web site

Acknowledgments

This research was supported by the Natural Sciences and Engineering Research Council of Canada (NSERC) and the Canadian Institute of Health Research (CIHR). The authors thank Dr. Alexandra Fürtös and Karine Gilbert (Université de Montréal) for assistance with mass spectrometry and SFC analysis.

References

[1]. Fosgerau, K.; Hoffmann, T., Peptide therapeutics: current status and future directions. *Drug Discov. Today*. **2015**, *20* (1), 122-8. doi: 10.1016/j.drudis.2014.10.003.

[2]. Sawyer TK. Renaissance in peptide drug discovery: the third wave. In: Peptide-Based Drug Discovery: Challenges and New Therapeutics. Srivastava V (Ed.). Royal Society of Chemistry, Cambridge, UK, 2017, pp. 1-34. doi: 10.1039/9781788011532-00001

[3]. Marshall, G. R., A hierarchical approach to peptidomimetic design. *Tetrahedron* **1993**, *49* (17), 3547-3558.

[4]. Ung, P.; Winkler, D. A., Tripeptide motifs in biology: targets for peptidomimetic design. *J. Med. Chem.* **2011**, *54* (5), 1111-25. doi: 10.1021/jm1012984.

[5]. Cooper, W. J.; Waters, M. L., Molecular recognition with designed peptides and proteins. *Curr. Opin. Chem. Biol.* **2005**, *9* (6), 627-631. doi: 10.1016/j.cbpa.2005.10.015

[6]. Tyndall, J.D.; Pfeiffer, B.; Abbenante, G.; Fairlie, D.P. Over one hundred peptide-activated G protein-coupled receptors recognize ligands with turn structure. *Chem. Rev.* **2005**, 105 (3), 793-826. doi: 10.1021/cr040689g

[7]. St-Cyr D.J., García-Ramos Y., Doan ND., Lubell W.D. (2017) Aminolactam, N-Aminoimidazolone, and N-Aminoimdazolidinone Peptide Mimics. In: Lubell W. (eds) Peptidomimetics I. Topics in Heterocyclic Chemistry, vol 48. Springer, Cham. pp 125-175. doi.org/10.1007/7081_2017_204

[8]. Freidinger, R. M.; Perlow, D. S.; Veber, D. F., Protected lactam-bridged dipeptides for use as conformational constraints in peptides. *J. Org. Chem.* **1982**, *47* (1), 104-109. doi.org/10.1021/jo00340a023

[9]. Freidinger, R. M.; Veber, D. F.; Perlow, D. S.; Saperstein, R. Bioactive conformation of luteinizing hormone-releasing hormone: evidence from a conformationally constrained analog. *Science* **1980**, *210* (4470), 656-658. doi: 10.1126/science.7001627

[10]. St-Cyr, D. J.; Jamieson, A. G.; Lubell, W. D. α-Amino-β-hydroxy-γ-lactam for constraining peptide Ser and Thr residue conformation. *Org. Lett.* **2010**, *12* (8), 1652-5. doi: 10.1021/ol1000582.

[11]. Geranurimi, A.; Lubell, W. D. Diversity-oriented syntheses of β-substituted α-amino γ-lactam peptide mimics with constrained backbone and side chain residues. *Org. Lett.* **2010**, *12* (8), 1652-1655. doi.org/10.1021/ol1000582

[12]. Proulx, C.; Sabatino, D.; Hopewell, R.; Spiegel, J.; Garcia Ramos, Y.; Lubell, W. D. Azapeptides and their therapeutic potential. *Future Med. Chem.* **2011**, *3*, 1139−1164. doi: 10.4155/fmc.11.74.

[13]. Chingle, R.; Proulx, C.; Lubell, W. D. Azapeptide synthesis methods for expanding side-chain diversity for biomedical applications. *Acc. Chem. Res.* **2017**, *50* (7), 1541-1556. doi: 10.1021/acs.accounts.7b00114.

[14]. Doan, N. D.; Hopewell, R.; Lubell, W. D. N-Aminoimidazolidin-2-one peptidomimetics. *Org. Lett.* **2014**, *16* (8), 2232-5. doi: 10.1021/ol500739k.

[15]. Doan, N. D.; Lubell, W. D. X-ray structure analysis reveals β-turn mimicry by N-amino-imidazolidin-2-ones. *Biopolymers, Peptide Sci.* **2015**, *104* (5), 629-35. doi: 10.1002/bip.22646.

[16]. Proulx, C.; Lubell, W. D. N-Amino-imidazolin-2-one Peptide Mimic Synthesis and Conformational Analysis. *Org. Lett.* **2012**, *14* (17), 4552-5. doi: 10.1021/ol302021n.

[17]. Proulx, C.; Lubell, W. D. Analysis of N-amino-imidazolin-2-one peptide turn mimic 4-position substituent effects on conformation by X-ray crystallography. *Biopolymers, Peptide Sci.* **2014**, *102* (1), 7-15. doi: 10.1002/bip.22327.

[18]. Poupart, J. D., Ngoc-Duc, D.; Bérubé, D.; Hamdane, Y.; Medena, C.; Lubell, W. D. Palladium-Catalyzed Arylation of N-Aminoimidazol-2-ones towards Synthesis of Constrained Phenylalanine Dipeptide Mimics. *Heterocycles* **2019**, *99* (1), 279-293. doi: 10.3987/COM-18-S(F)22

[19]. Garcia-Ramos, Y.; Proulx, C.; Lubell, W. D. Synthesis of hydrazine and azapeptide derivatives by alkylation of carbazates and semicarbazones. *Can. J. Chem.* **2012,** *90* (11), 985-993. doi.org/10.1139/v2012-070

[20]. Casnati, A.; Perrone, A.; Mazzeo, P. P.; Bacchi, A.; Mancuso, R.; Gabriele, B.; Maggi, R.; Maestri, G.; Motti, E.; Stirling, A.; Della Ca, N. Synthesis of Imidazolidin-2-ones and Imidazol-2-ones via Base-Catalyzed Intramolecular Hydroamidation of Propargylic Ureas under Ambient Conditions. *J. Org. Chem.* **2019**, *84*, 3477-3490. doi.org/10.1021/acs.joc.9b00064

[21]. Menges, N.; Sari, O.; Abdullayev, Y.; Erdem, S. S.; Balci, M. Design and synthesis of pyrrolotriazepine derivatives: an experimental and computational study. *J. Org. Chem.* **2013**, *78* (11), 5184-95. doi: 10.1021/jo4001228.

[22]. García-Ramos, Y.; Proulx, C.; Camy, C.; Lubell, W.D. Synthesis and purification of enantiomerically pure N-aminoimidazolin- 2-one dipeptide. Proceedings of the 32nd Europ. Peptide Symp. (2012) George Kokotos, Violetta Constantinou-Kokotou, John Matsoukas (Editors) European Peptide Society, pp. 366-367.

[23]. Hruby, V. J.; Li, G.; Haskell-Luevano, C.; Shenderovich, M. Design of peptides, proteins, and peptidomimetics in chi space. *Peptide Sci.* **1997,** *43* (3), 219-266. doi: 10.1002/(SICI)1097-0282(1997)43:3<219::AID-BIP3>3.0.CO;2-Y

[24]. Swindells, M. B.; MacArthur, M. W.; Thornton, J. M. Intrinsic ϕ, ψ propensities of amino acids, derived from the coil regions of known structures. *Nat. Struct. Biol.* **1995**, *2* (7), 596-603. doi: 10.1038/nsb0795-596

[25]. Peshkov, V.A.; Pereshivko, O.P.; Sharma, S.; Meganathan, T.; Parmar, V.S.; Ermolat'ev, D.S.; Van der Eycken, E.V. Tetrasubstituted 2-imidazolones via Ag (I)-catalyzed cycloisomerization of propargylic ureas. *J. Org. Chem.* **2011**, *76* (14), 5867-72. doi: 10.1021/jo200789t.

[26]. Pereshivko, O. P.; Peshkov, V. A.; Peshkov, A. A.; Jacobs, J.; Van Meervelt, L.; Van der Eycken, E. V. Unexpected regio-and chemoselectivity of cationic gold-catalyzed cycloisomerizations of propargylureas: access to tetrasubstituted 3, 4-dihydropyrimidin-2 (1 H)-ones. *Org. Biomol. Chem.* **2014**, *12* (11), 1741-1750.

[27]. Yasuhara, A.; Kanamori, Y.; Kaneko, M.; Numata, A.; Kondo, Y.; Sakamoto, T. Convenient synthesis of 2-substituted indoles from 2-ethynylanilines with tetrabutylammonium fluoride. *J. Chem. Soc., Perkin Trans. 1*, **1999**, (4), 529–534.

[28]. Huguenot, F.; Delalande, C.; Vidal, M. Metal-free 5-exo-dig cyclization of propargyl urea using TBAF. *Tetrahedron Lett.* **2014**, *55* (33), 4632-4635.

[29]. Anderson, G. W.; Zimmerman, J. E.; Callahan, F. M., Reinvestigation of the mixed carbonic anhydride method of peptide synthesis. *J. Am. Chem. Soc.* **1967**, *89* (19), 5012-7. doi: 10.1021/ja00995a032

[30]. Honzl, J.; Rudinger, J. Amino-acids and peptides. XXXIII. Nitrosyl chloride and butyl nitrite as reagents in peptide synthesis by the azide method; Suppression of amide formation. *Collect. Czech. Chem. Commun.* **1961**, *26* (9), 2333–2344. doi:10.1135/cccc19612333

[31]. Zav'yalov, S. I.; Ezhova, G. I.; Kravchenko, N. E.; Kulikova, L. B.; Dorofeeva, O. V.; Rumyantseva, E. E.; Zavozin, A. G. 1,3-Dihydro-2H-imidazol-2-one Derivatives: Synthesis and Applications (A Review). *Pharm. Chem. J.* **2004**, *38* (5), 256–260. doi:10.1023/b:phac.0000042090.73921.72

[32]. Lu, J.; Tan, X.; Chen, C. Palladium-catalyzed direct functionalization of imidazolinone: synthesis of dibromophakellstatin. *J. Am. Chem. Soc.* **2007**, 129 (25), 7768-9. doi: 10.1021/ja072844p

[33]. Bal, B.S.; Childers, W.E.; Pinnick, H.W. Oxidation of α,β-unsaturated aldehydes. *Tetrahedron* **1981**, *37*, 2091-2906

[34]. Still, W. C.; Kahn, M.; Mitra, A., Rapid chromatographic technique for preparative separations with moderate resolution. *J. Org. Chem.*, **1978**, *43* (14), 2923-2925. doi: 10.1021/jo00408a041

Chapter 3:

Solution-phase synthesis of (4-Me, 5-Aryl)Nai residues

3.1 Importance of aromatic residues in turn structure

Aromatic residues (Phe, Tyr, His and Trp) are known to stabilize β-turn conformers, due to steric, hydrophobic and amide (*n*-π*) interactions.[129-135] In the case of histidine, especially at the *i* and *i*+2 positions, turn conformation stabilization may result from intramolecular hydrogen bonds with the imidazole side chain.[32, 136] Aromatic residues in β-turns are featured in the active conformations of many biologically relevant peptides. For example, the opioid neuropeptides, Met- and Leu-enkephalin (H-Tyr-Gly-Gly-Phe-Met-OH and H-Tyr-Gly-Gly-Phe-Leu-OH) have been suggested to adopt β-turn conformers with tyrosine and phenylalanine residues at the *i* and *i+3* positions, respectively.[137] Angiotensin II (H-Asp-Arg-Val-Tyr-Ile-His-Pro-Phe-OH) is a vasoconstrictive peptide hormone purported to feature a β-turn with the tyrosine residue at the *i*+1 position.[138] Somatostatin (H-Ala-Gly-Gly-Lys-Asn-Phe-Phe-Trp-Lys-Phe-Thr-Ser-Cys-OH) is a peptide hormone which inhibits insulin and glucagon secretion, and is rigidified by a disulfide bridge that favors a β-turn conformer with the Phe^7 and Trp^8 at the *i* and *i*+1 positions, respectively.[139] Bradykinin (H-Arg-Pro-Pro-Ser-Pro-Phe-Arg-OH) is another vasoconstrictive peptide hormone in which the Phe residue is predicted to sit at the *i*+3 position of a β-turn.[140] β-Turn peptide mimics possessing suitably oriented aromatic moieties may offer utility as tools to study the backbone and side chains of such biologically active peptides in programs oriented towards peptide-based drug discovery.

3.2 Chi Space

The orientations of backbone (φ, ω and ψ) and side chain (χ) dihedral angles are critical for peptide recognition by target receptors. The term "Chi space" was introduced by Professor Victor Hruby to describe the ensemble of side chain locations within a peptide (Figure 3.1).[26] Notably, rotation about the χ^1 dihedral angle provides three major energy minima: *gauche* (-), *trans* and *gauche* (*+*) (Figure 3.2). The energy differences between the three minima is relatively low. Most *L* amino acids adopt preferably the *gauche* (-) conformation.[26]

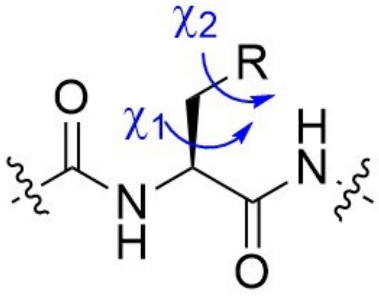

Figure 3.1: Different χ dihedral angles

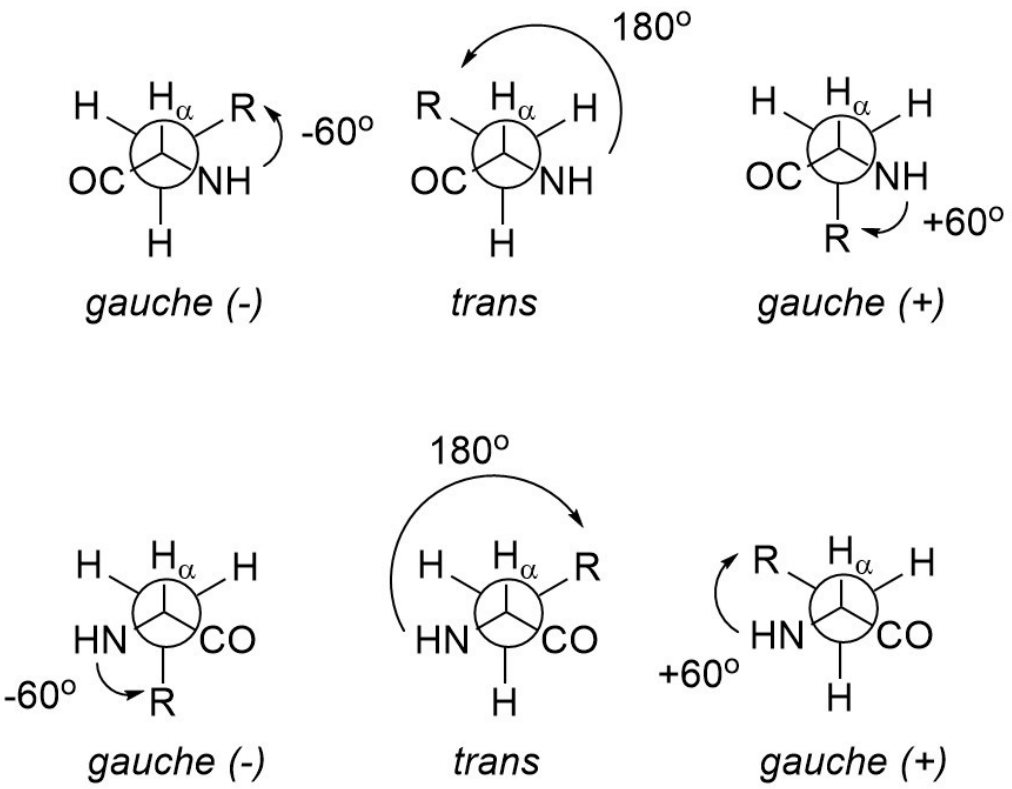

Figure 3.2: Different conformers around the χ^1 dihedral angle for *L* (top) and *D* (bottom) amino acids

Introduction of a β-substituent onto the side chain and cyclisation, both have been used to increase rotational barriers giving rise to significant populations of certain conformers.[25, 26] For mimicry of natural amino acid side chain orientations, the *gauche* (–) conformation is of particular interest. Several phenylalanine mimics have been designed to prefer the *gauche* (–) conformation (Figure 3.3).[141] For example, introduction of a (3*S*)-methyl group on the β-carbon of phenylalanine

3.1 rigidified the χ^1 dihedral angle by steric constraint to yield the *gauche* (–) conformer. Indanyl glycine (Ing) **3.2** locks χ^1 and χ^2 dihedral angles by a covalent constraint to favors the *gauche* (–) conformer.[141] Covalent constraint by cyclisation between the C_α and aromatic C_{ortho} of Phe has provided carboxyl-aminotetraline (Atc) **3.3**, which cannot adopt the *gauche* (*+*) and prefers the *gauche* (–) and *trans* conformations with equal energy levels.[141]

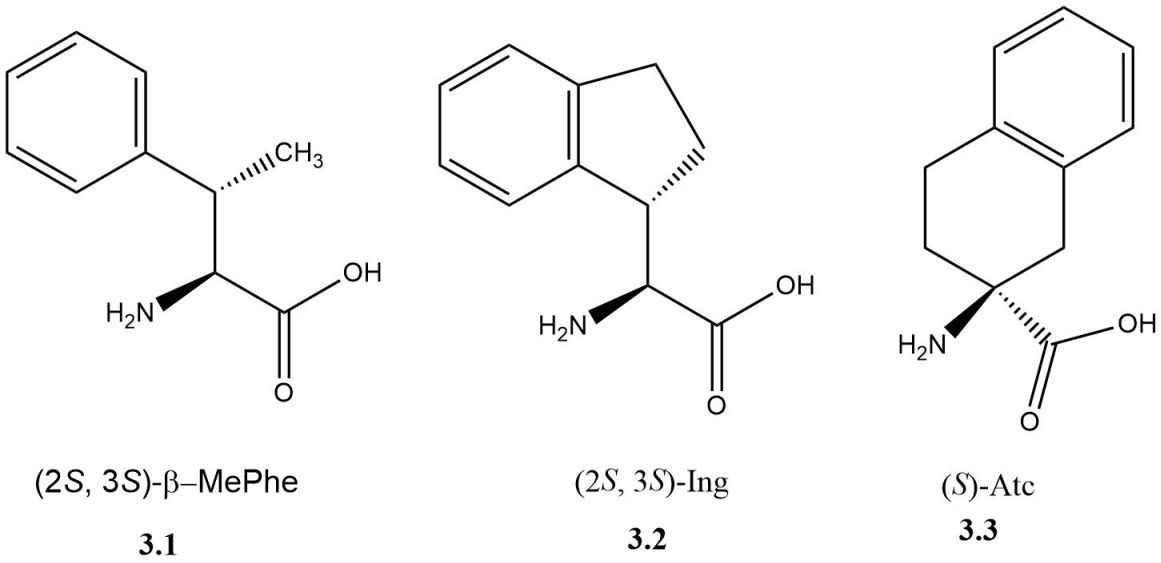

(2*S*, 3*S*)-β–MePhe **3.1**

(2*S*, 3*S*)-Ing **3.2**

(*S*)-Atc **3.3**

Figure 3.3. Rigidified phenylalanine mimics with a preference for the *gauche* (–) conformation

3.3 Aryl Imidazolones

The imidazolone is a structural motif possessing a wide range of different biological properties, and utility in medicinal chemistry.[89, 93, 94] Substitution onto the imidazolone heterocycle core is however challenging. Previously, 4-arylmethyl-*N*-aminoimidazol-2-ones (4-arylmethyl-Nai) analogs were synthesized by a route featuring Sonogashira cross-coupling onto an aza-propargylglycine (aza-Pra) residue (e.g., **3.4**) to give an aryl alkyne (e.g., **3.5**) followed by base promoted cyclisation, and acid mediated ester solvolysis to yield the Nai dipeptide acid (e.g., **3.6**, Figure 3.4).[75, 82] Epimerization of the *C*-terminal ester was however caused by the relatively strong base (sodium hydride) which was needed to accomplish the cyclisation. The arylmethyl substituent in the 4-position of the Nai product (e.g., **3.6**) is oriented in *trans* χ-geometry. On the other hand,

an aryl group at the 5-position of the heterocycle may effectively mimic *gauche* χ-geometry characteristic of natural amino acid side chain orientations.

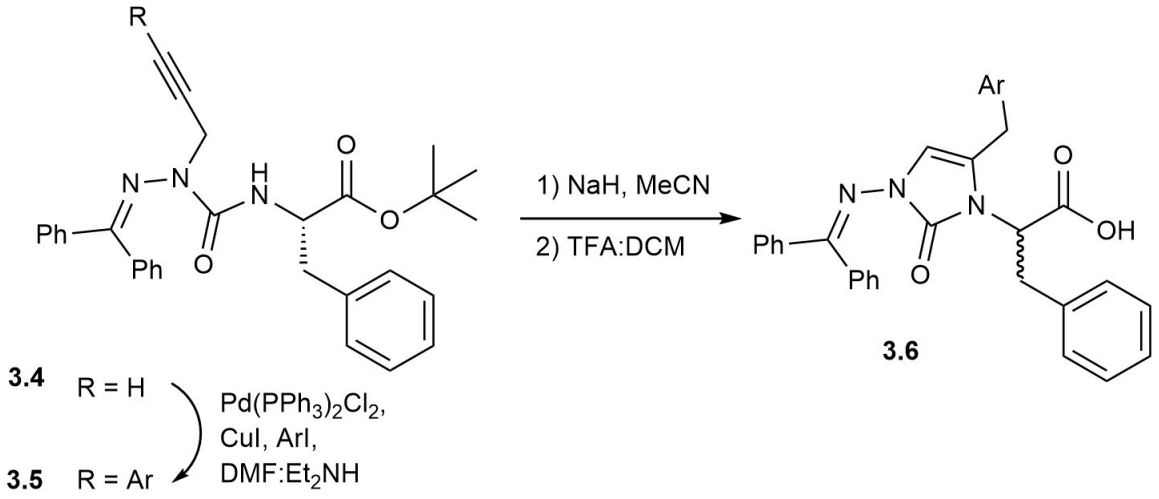

Figure 3.4: 4-arylmethyl-Nai synthesis[75]

Aryl iodides have previously been reacted with ordinary imidazole-2-ones **3.7** using palladium catalysis (Figure 3.5).[142] Experimental and computational analysis of the aryl addition reaction revealed that the mechanism was not a typical Heck cross-coupling. Instead, C-H activation of the alkene proton of imidazole-2-one **3.7** was suggested to be assisted by sodium acetate followed by reductive elimination to give the arylated product **3.8**.[142] Although aryl bromides reacted with **3.7**, longer reaction times were needed for the aryl addition and lower yields were obtained.[142]

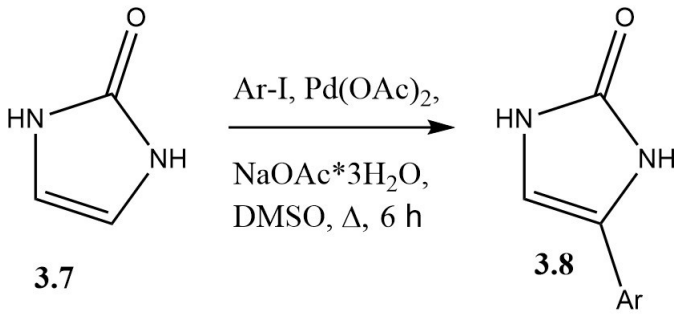

Figure 3.5: Arylation of imidazole-2-one **3.7** by palladium-catalyzed C-H activation

In the arylation, certain alkyl substituents were tolerated on the nitrogen of urea **3.7**; however, imidazole-2-ones with alkene substituents were not studied by the authors.[142] The utility of the method was demonstrated by the synthesis of dibromophakellstatin (**3.9**, Figure 3.6), an alkaloid isolated from the marine sponge *Phakellia Mauritania.*[131]

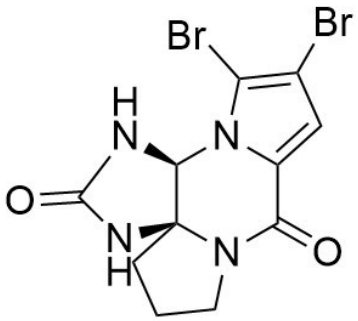

3.9

Figure 3.6: *Rac*-dibromophakellstatin (**3.9**)

3.4 Context

This chapter has been published in the journal *Heterocycles* and in a Proceeding of the 24th American Peptide Symposium. Synthetic methods are presented for the preparation of (5-aryl)Nai residues. Solution-phase chemistry has been developed employing a palladium-catalyzed arylation reaction on (4-methyl)Nai residues. A wide range of coupling partners has been introduced to prepare a diverse series of (4-methyl-5-aryl)Nai peptides. To the best of our knowledge, the described process constitutes the first synthetic route to (5-aryl)Nai residues and the first example of imidazolone arylation in presence of a 4-position substituent. Among the coupling conditions which were explored, best results were obtained using recrystallized palladium diacetate in the absence of a ligand with anhydrous sodium acetate as base in DMSO. Employing structural data from the reported X-ray crystallographic analysis of a model Nai peptide which was shown to adopt a type II' β-turn conformation, a computational analysis was performed on the 5-aryl counterpart.[75] The *in silico* molecular dynamic study revealed a type II' β-turn in which the *N*-aminoimidazolone residue occupied the *i+1* position and the 5-position aryl substituent adopted a *gauche* (–) side chain

conformation. The computational analysis highlighted the potential of the (5-aryl)Nai residue to serve as aromatic β-turns mimics, both in Ramanchandran backbone and chi space. The (5-aryl)Nai residue is rigidified by three different constraints: the backbone and side chain dihedral angles, both are rigidified by covalent and stereo-electronic forces from the imidazolone core, and the χ^2 torsion angle is restricted by steric interactions from the neighboring 4-methyl substituent. The effective means described herein for adding aryl groups to the 5-position of Nai residues have thus broadened the potential of this class of peptide analogs for mimicry of β-turn backbone and side chain geometry.

Article 2:

Poupart, J.; Doan N. D.; Bérubé D., Hamdane Y.; Medena, C; Lubell, W.D. Palladium-Catalyzed Arylation of *N*-aminoimidazol-2-ones Towards Synthesis of Constrained Phenylalanine Dipeptide Mimics. *Heterocycles* **2019**, 99(1) 279-293.

DOI: 10.3987/COM-18-S(F)22

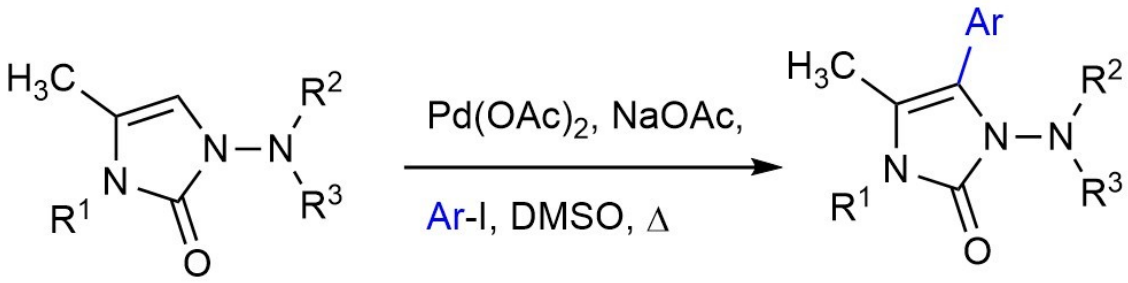

Dr. Ngoc-Duc Doan made compounds **3.22-3.36** with the help of the visiting scientist Caleb Medena.

Damien Bérubé and Yousra Hamdane, undergraduate students working under my direction, helped develop compounds **3.31** and **3.21** respectively.

The rest of the synthetic work, including the optimization table, and the computational chemistry was done by me.

The article was written by me and edited by Professor William D. Lubell.

Palladium-Catalyzed Arylation of *N*-aminoimidazol-2-ones Towards Synthesis of Constrained Phenylalanine Dipeptide Mimics

*Julien Poupart, Ngoc-Duc Doan, Damien Bérubé, Yousra Hamdane, Caleb Medena and William D. Lubell**

Département de chimie, Université de Montréal, C.P. 6128, Succursale Centre-Ville, Montréal, Québec H3C3J7, Canada. E-mail: William.Lubell@umontreal.ca

Abstract

N-Aminoimidazol-2-ones (e.g., **3.15**) offer potential to serve as constrained amino amide components that can induce turn conformation in peptide sequences. To add side chain functionality onto this amino amide surrogate, mild conditions have now been developed for palladium-catalyzed arylation of *N*-aminoimidazol-2-ones. A diverse array of aryl iodides reacted at the 5-position of *N*-aminoimidazol-2-one dipeptides **3.16** and **3.30** in a general approach for making constrained arylalanine dipeptide turn mimics (e.g., **3.17-3.28** and **3.31**).

Introduction

Imidazolones are valuable pharmacophores found in molecules exhibiting notable properties, including antioxidant,[1] anti-inflammatory,[2] anti-oncogenic,[3] anti-Parkinsonian and immunomodulatory activities.[4] For example, 4,5-diphenylimidazolone **3.10** displayed anticoagulant activity,[5] 4-butylimidazolone **3.11** exhibited activity as a potent angiotensin II receptor (AT2) antagonist,[6] 4-aminopyridine derivative **3.12** inhibited p38MAP kinase,[7] *N*,*N*-diacetyl-4-methylimidazol-2-one (**3.13**) inhibited TNF-α converting enzyme (TACE)[8] and 4-*p*-bromophenylimidazol-2-one **3.14** demonstrated antitumor activity.[3,9] Related *N*-aminoimidazolone analogs have also exhibited potential as immune-modulator, anti-Parkinsonian and anti-inflammatory agents.[10] Notably, imidazalones with 4- and 5-position aryl substituents (e.g., **3.10**, **3.12** and **3.14**) have displayed enhanced activity;[9] however, such aromatic moieties have typically been introduced during heterocycle synthesis. Arylation of the imidazolone ring may thus offer advantages for combinatorial study of structure-activity relationships (SAR) in medicinal chemistry programs.[9,11]

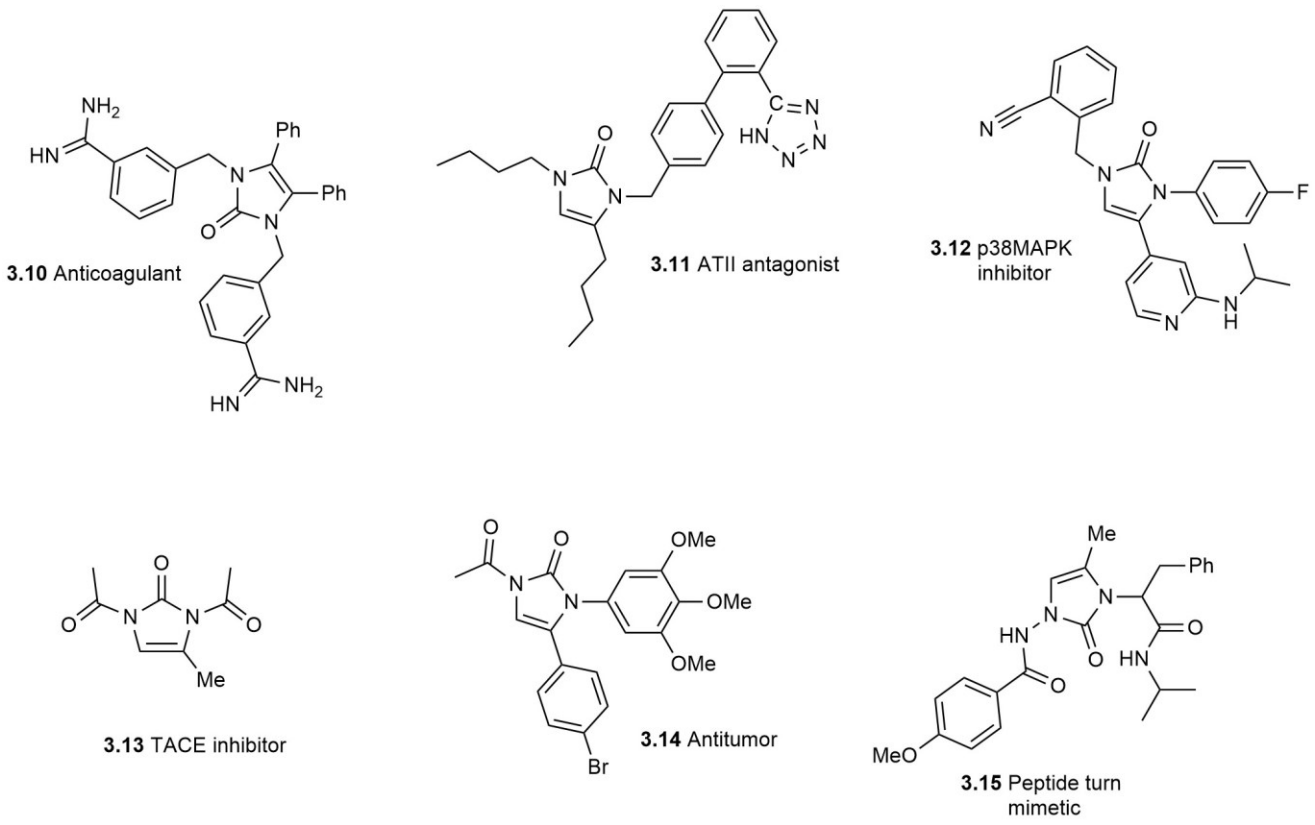

Figure 3.1. Biologically relevant imidazolones **3.10-3.14** and *N*-aminoimidazolone **3.15**

In the context of our program in peptide mimicry, *N*-aminoimidazolone (Nai)[12] residues have been explored as constrained amino amide surrogates. In particular, Nai residues have exhibited potential to induce type II' β-turn and inverse γ-turn geometry in model peptides (e.g., **3.15**).[13] 4-Substituted Nai analogs were prepared by 5-*exo*-dig cyclization of aza-propargylglycine derivatives.[14] Moreover, in model Nai peptides, the 4-position substituent was shown to influence the turn conformation and the χ-dihedral angle geometry of the adjacent *C*-terminal residue.[15]

Considering the normal orientations of amino acid side chains, modification of the Nai ring system at the 5-position has been pursued to improve capacity for mimicry of natural peptide geometry and function. Inspired by a recent report on palladium-catalyzed C-H activation and arylation of simple imidazolones,[16] we have pursued the application of similar conditions to add

aryl side chains at the 5-position of Nai residues. The success of this approach has now been validated by the preparation of a series of arylalanyl-phenylalanine dipeptides.

Results and Discussion

Arylation of 1,3-dihydro-2*H*-imidazol-2-one has previously been reported using aryl iodides and bromides with palladium acetate as catalyst.[16] To explore this method using *N*-aminoimidazalones, Nai residue **3.16** was synthesized by a route featuring aza-glycine alkylation followed by base promoted 5-*exo*-dig cyclisation.[13] Arylation was first examined with *p*-tosyloxyphenyl iodide under different conditions to prepare tyrosine mimic **3.17** (Figure 3.2 and Table 3.1).[17] Palladium acetate proved more effective than palladium chloride, and $Pd(PPh_3)_2Cl_2$. Moreover, palladium acetate alone reacted more effectively than in the presence of additives such as silver nitrate, triphenylphosphine and BINAP. Highest yields were obtained using 10 mol% palladium acetate in the presence of sodium acetate in DMSO at 80 °C. Acetonitrile and dioxane were ineffective as solvent.

The scope of the Pd-catalyzed arylation was next studied using Nai residue **3.16** and electron rich and poor aryl iodides. A wide array of *para* and *meta* substituted aryl iodides reacted successfully on *N*-aminoimidazolone **3.16** (Figure 3.2). Both electron rich and electron deficient aryl iodides were tolerated in the Pd-catalysed arylation, including methoxy, fluoride, trifluoromethyl, nitro and pyrrolo groups. Compared to 1,3-dihydro-2*H*-imidazol-2-one,[16] Nai residue **7** required longer reaction times (16 h vs 6 h) and higher catalyst loading (10 mol% vs 5 mol%) to give similarly good yields. On the other hand, 5-aryl-*N*-aminoimidazolones **3.17-3.28** were not produced using aryl bromides. The wide array of 5-aryl substituents that were introduced on Nai residue **3.16** offer potential for studying structure-activity relationships of a variety of relevant aromatic residues. Notably, phenylalanine Nai analogs **3.17-3.28** were effectively prepared; however, attempts failed to prepare histidine and tryptophan Nai analogs employing respectively 4-iodo-1-tritylimidazole and 3-iodo-*N*-(Boc)-indole as cross-coupling partners under similar conditions with *N*-aminoimidazalone **7**, which was recovered unchanged. Attempts to couple *p*-iodophenol provide unprotected phenol **3.20** after a longer reaction time

(48 h) without complete conversion. Finally, an attempt to prepare 5-phenyl-Nai **3.18** using only 1.2 equivalents of iodobenzene failed to go to completion after 72 h.

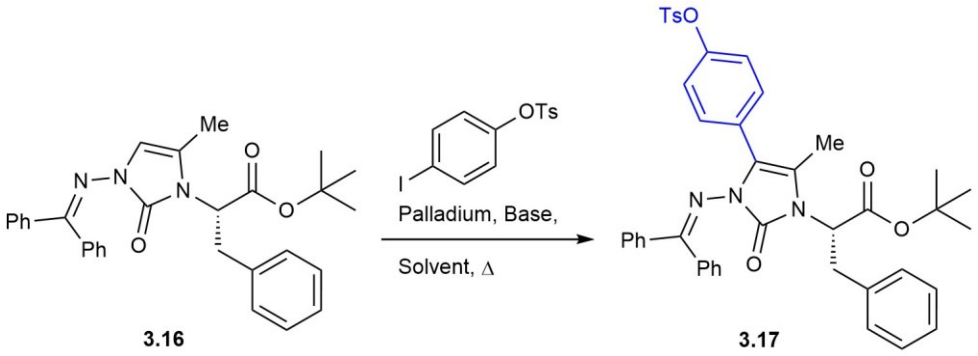

Entry	Catalytic system (mol%)	Solvent	Temperature (°C)	Time (h)	Base	Yield (%)[b]
1	$Pd(OAc)_2$ (10)	MeCN	80	48	NaOAc	Traces[c]
2	$Pd(OAc)_2$ (10)	DMSO	80	18	NaOAc	86
3	$Pd(OAc)_2$ (5)	DMSO	80	18	NaOAc	49
4	$Pd(OAc)_2$ (10)	DMSO	20	96	NaOAc	-[d]
5	$Pd(OAc)_2$ (5) $AgNO_3$ (20)	DMSO	80	48	NaOAc	20
6	$Pd(OAc)_2$ (5) *Rac*-BINAP (10)	DMSO	80	48	NaOAc	39
7	$Pd(OAc)_2$ (5) PPh_3 (10)	DMSO	80	48	NaOAc	traces
8	$Pd(PPh_3)_2Cl_2$ (10)	dioxane	100	72	KOAc	-[d]

9	$PdCl_2$ (10)	DMSO	80	72	NaOAc	-[d]

*a: Reagent and conditions: a mixture of **3.16**, 4-tosyloxyphenyl iodide (3 equiv), base (3 equiv), catalyst and degassed solvent [1 mM] was heated in a sealed tube under argon for the specified time. b: Isolated yield. c: Product detected on TLC but not isolated. d: No product observed.*

Table 3.1. Optimization of Nai **3.16** arylation to prepare constrained tyrosine analog **3.17**[a]

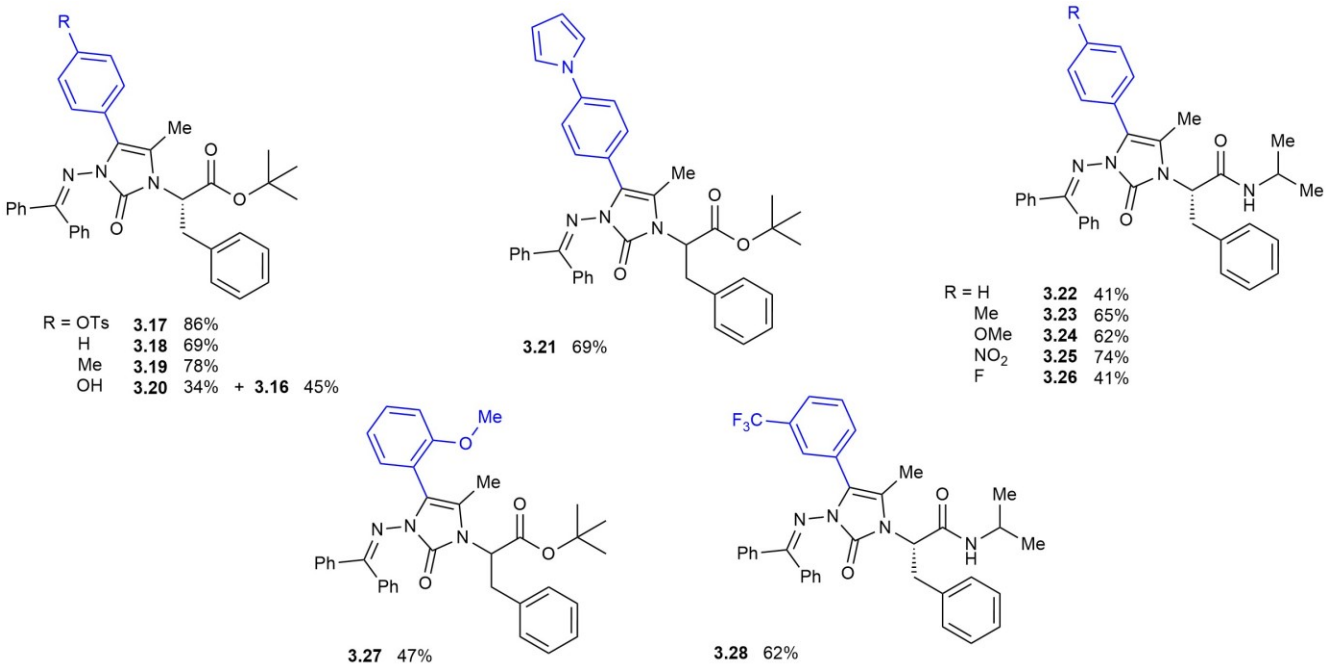

Figure 3.2. Arylation scope

The arylation conditions were also examined on a more peptide-like scaffold, dipeptide **3.30**, which was prepared by cleavage of the benzophenone protecting group under aqueous acidic conditions followed by semicarbazide acylation with *p*-methoxybenzoyl chloride. Treatment of Nai-peptide **3.30** with *p*-iodotoluene and palladium acetate (10 mol%) under the optimized conditions afford 5-arylated Nai-dipeptide **3.31** in modest yield.

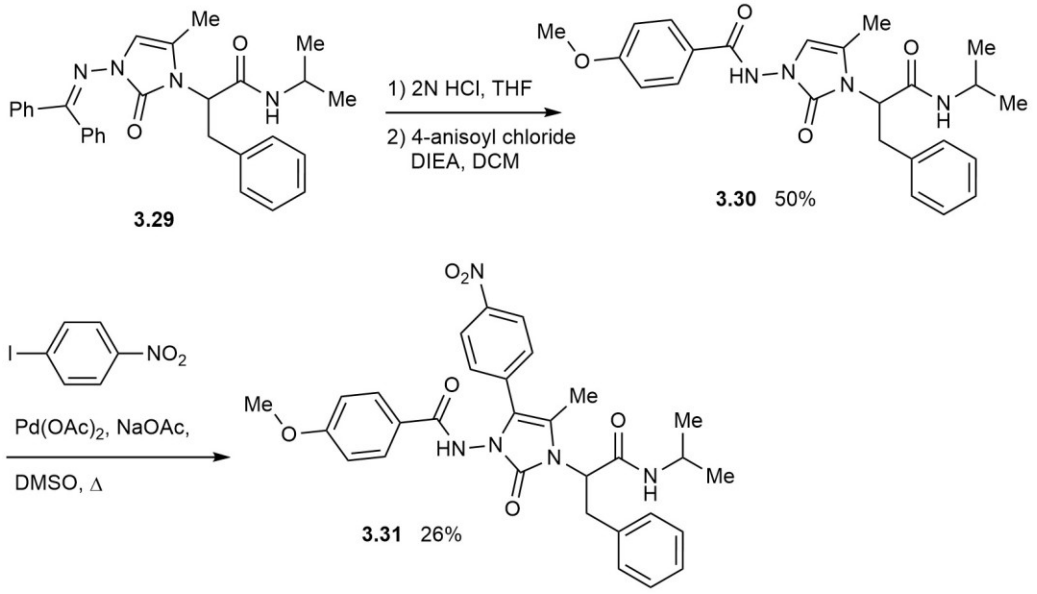

Figure 3.3. Synthesis of 5-aryl-Nai peptide **3.31**

To examine the potential of a 5-*p*-hydroxyphenyl Nai residue to serve as a constrained tyrosine residue, a geometry optimization of *p*-methoxybenzoyl-5-(*p*-hydroxyphenyl)-4-(methyl)Nai-Phe-NH*i*Pr **3.32** was performed using coordinates obtained from the crystal structure of the parent 4-(methyl)Nai peptide **3.30**.[13] Consistent with the parent structure, the backbone dihedral angles were coherent with a type II' β-turn.[14] Moreover, the side chain dihedral angles, χ_1 and χ_2, of the 5-position aryl substituent were in the *gauche* (–) conformation, due in part to steric interactions with the 4-position methyl group. Notably, the *gauche* (–) conformation is preferred for the aromatic side chain of L-amino acid residues.[18] The 5-(aryl)Nai residue was thus predicted to mimic both the backbone and side chain geometry of aromatic residues situated at the *i + 1* position of a type II' β-turn.

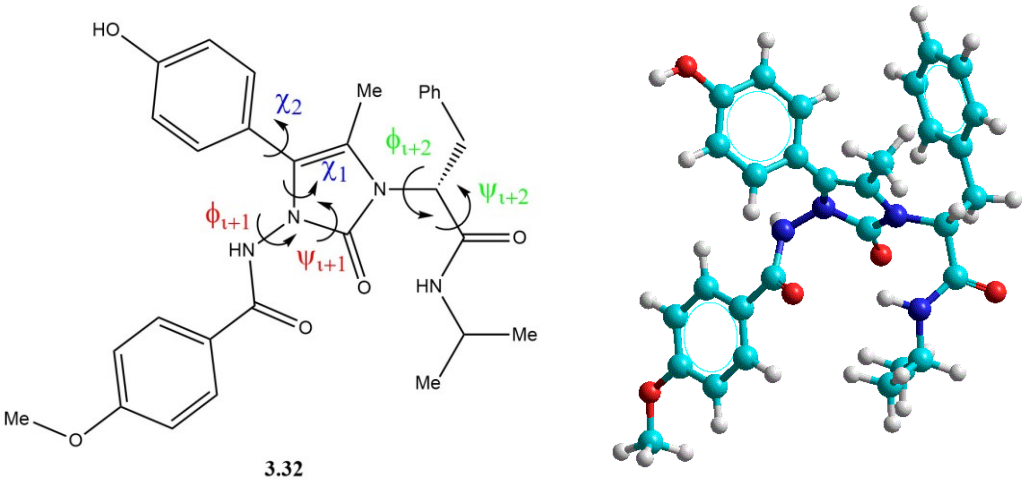

Figure 3.4. Left: Tetrapeptide mimic **3.32** and relevant dihedral angles, Right: Minimized structure

Conclusion

Mild and versatile palladium-catalyzed arylation of *N*-aminoimidazol-2-one (Nai) residues has been developed in an approach to synthesize mimics of peptide backbone turn conformation and side chain orientation. A wide variety of aryl iodides reacted successfully in the late-stage diversification of the Nai residues. Computational analysis of 5-aryl Nai peptide **3.32** predicted that the χ values of the side chain corresponded to a *gauche* (–) geometry within a type II' β-turn conformation. Considering the effectiveness of the arylation chemistry and the ability of the 5-aryl Nai residue to induce turn secondary structure, the described method offers strong potential for mimicry of natural peptide geometry.

Acknowledgements

This research was supported by the Natural Sciences and Engineering Research Council of Canada (NSERC) and the Canadian Institute of Health Research (CIHR). The authors thank Dr. Alexandra Fürtös and Karine Gilbert (Université de Montréal) for assistance with mass spectrometry and SFC analysis, as well as Sarah-Ève Papineau for help preparing starting materials.

Experimental

General chemistry

Unless specified, all reactions were performed under argon atmosphere. All glassware was stored in the oven or flame-dried and let cool under inert atmosphere prior to use. Anhydrous solvents were obtained either by filtration trough drying columns (DCM, THF, MeCN) in a GlassContour system (Irvine, CA) or by distillation over CaH_2 (dioxane). *tert*-Butyl 2-{3-[(diphenylmethylidene)amino]-5-methyl-2-oxo- 2,3-dihydro-1*H*-imidazol-1-yl}-3-phenylpropanoate,[13] 2-(3-((diphenylmethylene)amino)-5-methyl-2- oxo-2,3-dihydro-1*H*-imidazol-1-yl)-*N*-isopropyl-3- phenylpropanamide,[13] 4-iodophenyl 4-methylbenzenesulfonate[19] and *p*-methoxybenzoyl chloride[20] were synthesized using published procedures. All other starting materials, reagents and chemicals were purchased from commercial suppliers and used without further purification, except for silver nitrate which was recrystallised from boiling water. The progress of reaction was monitored by thin layer gel chromatography (TLC) plates, visualized under UV light (254 nm) or by staining with $KMnO_4$. Flash chromatography[21] was performed using 230-400 mesh silica gel from SiliCycle Inc. and distilled solvents. Nuclear magnetic resonance spectra (^1H and ^{13}C) were recorded either on a Bruker AMX 300, AV 400, AVII 400 or AMX 500 spectrometer. Specific rotations were determined on a Perkin-Elmer 341 polarimeter at 589, and are reported as follows $[\alpha]_\lambda^{temp}$, concentration (*c* in g/100 mL), and solvent. High resolution mass spectrometry (HRMS) was performed by the Centre regional de spectroscopie de masse de l'Université de Montréal. Analytical and preparative supercritical fluid chromatography (SFC) was performed at the Laboratoire d'analyse et de séparation chirale par SFC de l'Université de Montréal and data are reported as follow: temperature, backpressure and retentions times (R*t*).

Computational chemistry

The model of tetrapeptide mimic **3.32** was created using parameters from the published crystal structure of 4-(methyl)Nai peptide **3.30**,[13] and minimized using HyperChem 8™ (Molecular mechanics and a Polak-Ribiere conjugate gradient of 0.1 kcal/(Å*mol) in a 16.5 $Å^3$ periodic box.

Dihedral angles for ideal □-turn, the crystal structure of **3.30** and computed values for **3.32**:

Type of turn	φ_{i+1}	ψ_{i+1}	φ_{i+2}	ψ_{i+2}	$\chi_{1\ i+1}$	$\chi_{2\ i+1}$
Ideal β-II'[14]	60	-120	-80	0	-	-
3.30[13]	58.9	-153.3	-69.1	-4.6	-	-
3.32	48.6	-143.7	-62.4	33.6	-41.1	76.0

***tert*-Butyl (*R*)-2-(3-((diphenylmethylene)amino)-4-methyl-2-oxo-5-(4-(tosyloxy)phenyl)- 2,3-dihydro-1*H*-imidazol-1-yl)-3-phenylpropanoate (3.17)**

tert-Butyl (2*R*)-2-{3-[(diphenylmethylidene)amino]-5-methyl-2-oxo-2,3-dihydro- 1*H*-imidazol-1-yl}-3-phenylpropanoate (**7**, 67 mg, 0.14 mmol), 4-iodophenyl 4-methylbenzene-1-sulfonate (156 mg, 0.42 mmol), sodium acetate (34 mg, 0.42 mmol) and palladium acetate (3 mg, 0.014 mmol) were added to 1 mL of degassed DMSO in a pressure vessel. The vessel was purged with argon, sealed, heated to 80 °C and stirred overnight, when complete reaction was ascertained by TLC (disappearance of starting material, R*f* = 0.45 (30% EtOAc/hexanes). The reaction mixture was cooled and partitioned between DCM (10 mL) and a mixture of brine (8 mL) and 5% citric acid (2 mL). The phases were separated, and the aqueous layer was extracted with DCM (10 mL). The combined organic layers were washed with brine (10 mL), dried over magnesium sulfate, filtered and evaporated to a residue that was purified by column chromatography using 15-30% EtOAc/hexanes as eluent. Evaporation of the collected fractions gave 5-aryl Nai **3.17** as a yellow oil (87 mg, 86%): R*f* = 0.34 (30% EtOAc/hexanes); $[\alpha]_D^{25}$ –97.1 (*c* 0.22, $CHCl_3$). ^{1}H NMR (400 MHz, $CDCl_3$) δ 7.63 (d, *J* = 8.0 Hz, 2H), 7.54 (d, *J* = 8.0 Hz, 2H), 7.45-7.49 (m, 1H), 7.34-7.39 (m, 3H), 7.18-7.22 (m, 5H), 7.13 (d, *J* = 8.0 Hz, 2H), 7.00-7.02 (m, 2H), 6.81-6.92 (m, 6H), 4.64-4.68 (m, 1H), 3.39-3.43 (m, 2H), 2.40 (s, 3H), 1.49 (s, 9H); ^{13}C NMR (75 MHz, $CDCl_3$) δ 174.6, 168.4, 148.3, 148.1, 145.4, 137.8, 137.1, 135.0, 132.2, 131.2, 130.1, 129.7, 129.6, 129.2, 128.7, 128.4, 128.0, 127.8, 126.6, 122.1, 117.8, 116.1, 82.4, 57.6, 35.4, 29.7, 28.0, 21.7, 9.5. HRMS calcd. for $C_{43}H_{42}N_3O_6S$, $[MH^+]$ = 728.2789, found = 728.2802.

tert-Butyl (_S_)-2-(3-((diphenylmethylene)amino)-4-methyl-2-oxo-5-phenyl-2,3-dihydro- 1_H_-imidazol-1-yl)-3-phenylpropanoate (3.18)

Employing the protocol for the synthesis of 5-aryl-Nai **3.17**, Nai **3.16** (158 mg, 0.33 mmol) was reacted with iodobenzene (112 µL, 1 mmol), and the residue was purified by flash chromatography using 15% EtOAc/hexanes as eluent to provide 5-phenyl-Nai **3.18** as yellow foam (128 mg, 69%): R*f* = 0.48 (30% EtOAc in hexanes); $[\alpha]_D^{20}$ –191.7 (*c* 1.06, $CHCl_3$). ^{1}H NMR (400 MHz, $CDCl_3$) δ 7.60-7.58 (m, 2H), 7.48-7.43 (m, 1H), 7.38-7.18 (m, 11H), 7.09-6.99 (m, 6H), 4.68-4.63 (m, 1H), 3.48-3.59 (m, 2H), 1.64 (s, 3H), 1.50 (s, 9H); ^{13}C NMR (101 MHz, $CDCl_3$) δ174.9, 168.6, 148.1, 138.0, 137.2, 135.3, 131.2, 129.82, 129.4, 129.2, 128.8, 128.5, 128.2, 128.1, 127.9, 127.2, 126.7, 125.9, 119.3, 116.0, 116.0, 82.5, 57.9, 35.6, 28.1, 9.6. HRMS calcd. for $C_{36}H_{36}N_3O_3$, $[MH^+]$ = 558.2712, found = 558.2717.

tert-Butyl (_S_)-2-(3-((diphenylmethylene)amino)-4-methyl-2-oxo-5-(p-tolyl)-2,3-dihydro- 1_H_-imidazol-1-yl)-3-phenylpropanoate (3.19)

Employing the protocol for the synthesis of 5-aryl-Nai **3.17**, Nai **3.16** (101 mg, 0.21 mmol) was reacted with iodotoluene (83 µL, 0.64 mmol), and the residue was purified by flash chromatography using 15% EtOAc/hexanes as eluent to provide 5-tolyl-Nai **3.19** as yellow foam (92.1 mg, 78%): R*f* = 0.49 (30% EtOAc in hexanes); $[\alpha]_D^{20}$ –185.5 (*c* 1.06, $CHCl_3$). ^{1}H NMR (400 MHz, $CDCl_3$) □ 7.63 (dd*, J* = 1.0, 5.7 Hz, 2H), 7.46 (tt, *J* = 1.2, 6.0 Hz, 1H), 7.39-7.34 (m, 3H), 7.30-7.23 (m, 5H), 7.10-7.01 (m, 4H), 7.01-7.00 (m, 4H), 4.64-4.16 (m, 1H), 3.45-3.35 (m, 2H), 2.33 (s, 3H), 1.64 (s, 3H), 1.50 (s, 9H); ^{13}C NMR (101 MHz, $CDCl_3$) δ 174.6, 168.8, 147.9, 138.1, 137.4, 136.9, 135.5, 131.1, 129.9, 129.4, 129.2, 129.1, 128.9, 128.9, 128.5, 128.1, 127.8, 126.6, 126.3, 119.3, 115.3, 82.3, 57.8, 35.6, 28.1, 21.3, 9.6. HRMS calcd. for $C_{37}H_{38}N_3O_3$, $[MH^+]$ = 571.2837, found = 571.2835. An enantiomeric ratio of >99:1 *S*-**3.19**:*R*-**3.19** was ascertained by SFC analysis on a chiral stationary phase [Chiralcel AD-H 25 cm, 5 µm, 20% i-PrOH, 3 mL/min, 35 °C, 150 bar, R*t* = 9.5 min].

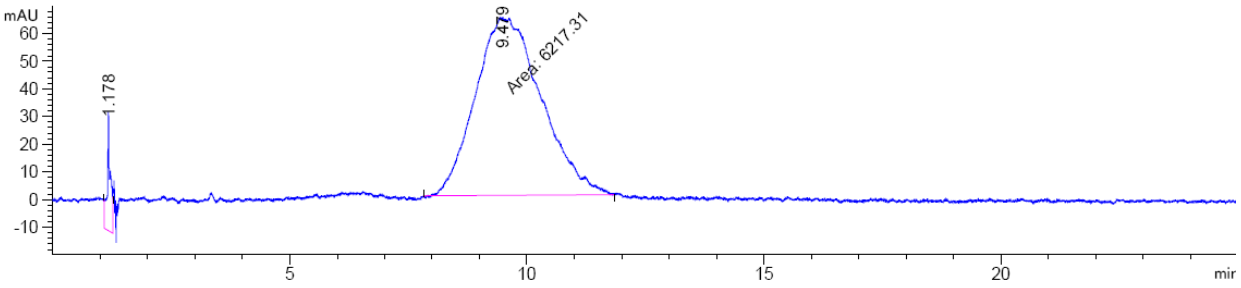

Co-injection of *S*-**3.19** and *R*-**3.19** gave two peaks that eluted at 9 min and 15.5 min.

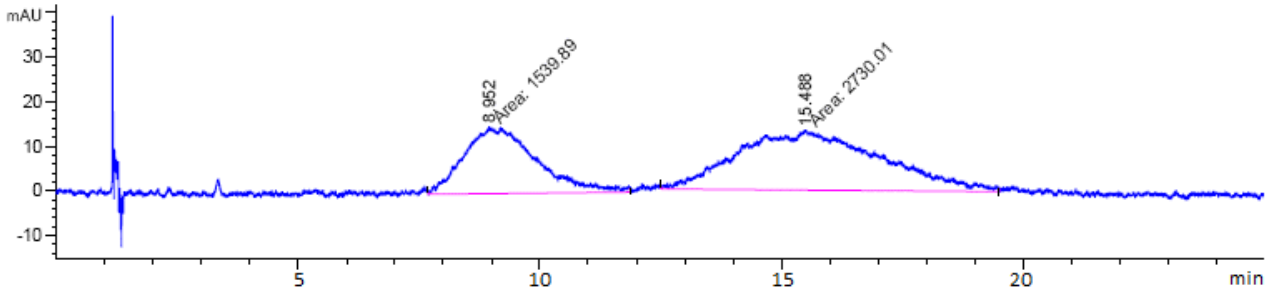

tert-Butyl (*S*)-2-(3-((diphenylmethylene)amino)-5-(4-hydroxyphenyl)-4-methyl-2-oxo- 2,3-dihydro-1*H*-imidazol-1-yl)-3-phenylpropanoate (3.20)

Employing the protocol for the synthesis of 5-aryl-Nai **3.17**, Nai **3.16** (61 mg, 0.13 mmol) was reacted with *p*-iodophenol (84 mg, 0.36 mmol), and the residue was purified by flash chromatography using 20% EtOAc in hexanes as eluent to provide 5-*p*-hydroxyphenyl-Nai **3.20** as orange low melting solid (25 mg, 34%): R*f* = 0.62 (50% EtOAc in hexanes); $[\alpha]_D^{25}$ –29.4 (*c* 0.18, $CHCl_3$). ^{1}H NMR (400 MHz, $CDCl_3$) □ 7.73 (t, *J* = 6 Hz, 1H), 7.54 (d, *J* = 7.7 Hz, 2H), 7.50-7.19 (m, 9H), 7.00-6.96 (m, 3H), 6.87 (d, *J* = 8.3 Hz, 2H), 6.65 (d, *J* = 8.5 Hz, 1H), 6.31-6.26 (m, 1H), 4.60-4.56 (m, 1H), 3.37-3.32 (m, 2H), 1.55 (s, 3H), 1.44 (s, 9H); ^{13}C NMR (75 MHz, $CDCl_3$) δ 155.2, 148.0, 138.0, 137.2, 130.8, 130.1, 129.8, 129.4, 129.2, 128.8, 128.5, 128.4, 128.2, 128.1, 127.9, 115.2, 115.0, 82.4, 57.8, 29.8, 28.1, 27.9, 22.8, 14.2, 9.5. HRMS calcd. for $C_{36}H_{35}N_3O_4$, $[M^+]$ = 574.2700, found = 574.2696. Starting Nai **3.16** was also recovered (27 mg, 45%).

tert-Butyl 2-(5-(4-(1H-pyrrol-1-yl)phenyl)-3-((diphenylmethylene)amino)-4-methyl-2-oxo- 2,3-dihydro-1*H*-imidazol-1-yl)-3-phenylpropanoate (3.21)

Employing the protocol for the synthesis of 5-aryl-Nai **3.17**, Nai **3.16** (67 mg, 0.14 mmol) was reacted with 1-(4-iodophenyl)-pyrrole (113 mg, 0.42 mmol), and the residue was purified by flash chromatography using 20% EtOAc in hexanes as eluent to provide 5-(4-(1*H*-pyrrol-1-yl)phenyl-Nai **3.21** as yellow low melting solid (60 mg, 69%): R*f* = 0.51 (40% EtOAc in hexanes). ^{1}H NMR (300 MHz, $CDCl_3$) δ 7.67-7.58 (m, 3H), 7.50-7.28 (m, 8H), 7.25-7.03 (m, 10H), 6.38 (t, *J* = 2.2 Hz, 1H), 6.32 (t, *J* = 2.2 Hz, 1H), 4.69-4.58 (m, 1H), 3.49-3.29 (m, 2H), 1.63 (s, 1H), 1.54 (d, *J* = 1.3 Hz, 2H), 1.46 (s, 9H); ^{13}C NMR (75 MHz, $CDCl_3$) δ 168.1, 138.5, 137.6, 136.7, 135.1, 131.4, 129.5, 129.3, 129.1, 128.9, 128.4, 128.4, 128.2, 128.1, 128.1, 128.0, 127.0, 126.6, 126.4, 125.7, 119.0, 118.8, 81.2, 53.9, 27.6, 22.0, 9.0. HRMS calcd. for $C_{40}H_{38}N_4O_3$, [M^+] = 623.3017, found = 623.3024.

(*S*)-2-(3-((Diphenylmethylene)amino)-4-methyl-5-phenylimidazolin-2-one-1-yl)-*N*-isopropyl-3-phenylpropanamide (3.22)

Employing the protocol for the synthesis of 5-aryl-Nai **3.17**, (*S*)-2-(3-((diphenylmethylene)amino)-5-methyl-2-oxo-2,3-dihydro-1*H*-imidazol-1-yl)-*N*-isopropyl-3-phenylpropanamide (54 mg, 0.12 mmol) was reacted with iodobenzene (70 mg, 0.35 mmol), and the residue was purified by flash chromatography using 20-30% EtOAc in hexanes as eluent to provide 5-phenyl-Nai amide **3.22** as yellow low melting solid (26 mg, 41 %): R*f* = 0.51 (50% EtOAc in hexanes); $[\alpha]_D^{20}$ –126.3 (*c* 1.06, $CHCl_3$). ^{1}H NMR (500 MHz, $CDCl_3$) δ 8.03 (br. s, 1H), 7.59 (dd, *J* = 1.2, 7.1 Hz, 2H), 7.48-7.44 (m, 1H), 7.38-7.33 (m, 4H), 7.26-7.20 (m, 8H), 7.05-6.97 (m, 6H), 4.48-4.46 (m, 1H), 4.02 (2 overlapping q, *J* = 7.5 Hz, 1H), 3.60-3.55 (m, 1H), 3.29 (dd, *J* = 4.3, 9.4 Hz, 1H) 1.64 (s, 3H), 1.17 (d, *J* = 6.6 Hz, 3H), 1.13 (d, *J* = 6.6 Hz, 3H); ^{13}C NMR (126 MHz, $CDCl_3$) δ 175.9, 169.6, 148.7, 137.7, 137.0, 135.2, 131.5, 129.9, 129.5, 129.4, 129.2, 128.6, 128.6, 128.3, 128.2, 128.0, 127.5, 126.9, 119.9, 116.4, 41.8, 35.8, 22.7, 22.6, 9.6. HRMS calcd. for $C_{35}H_{35}N_4O_2$, [MH^+] = 543.2755, found = 543.2759.

(*S*)-2-(3-((Diphenylmethylene)amino)-4-methyl-5-(*p*-methylphenyl)imidazolin-2-one-1-yl)-*N*-isopropyl-3-phenylpropanamide (3.23)

Employing the protocol for the synthesis of 5-aryl-Nai **3.17**, (*S*)-2-(3-((diphenylmethylene)amino)-5-methyl-2-oxo-2,3-dihydro-1*H*-imidazol-1-yl)-*N*-isopropyl-3-phenylpropanamide (310 mg, 0.67 mmol) was reacted with *p*-iodotoluene (259 μL, 2.00 mmol), and

the residue was purified by flash chromatography using 25% EtOAc in hexanes as eluent to provide 5-tolyl-Nai amide **3.23** as yellow low melting solid (251 mg, 65%): R*f* = 0.55 (50% EtOAc in hexanes); $[\alpha]_D^{20}$ –65.9 (*c* 1.06, $CHCl_3$). ^1H NMR (500 MHz, $CDCl_3$) 8.04 (br. s, 1H), 7.59 (dd, *J* = 1.1, 7.1 Hz, 2H), 7.47-7.44 (m, 1H), 7.36-7.27 (m, 4H), 7.24-7.18 (m, 4H), 7.06-6.99 (m, 6H), 6.80 (d, *J* = 8.2 Hz, 2H), 4.44-4.43 (m, 1H), 4.50 (2 overlapping q, *J* = 7.4 Hz, 1H), 3.55 (t, *J* = 11.4 Hz, 1H), 3.27 (dd, *J* = 4.2, 9.5 Hz, 1H), 2.29 (s, 3H), 1.61 (s, 3H), 1.16 (d, *J* = 6.6 Hz, 3H), 1.12 (d, *J* = 6.6 Hz, 3H); ^{13}C NMR (126 MHz, $CDCl_3$) 175.8, 169.7, 148.6, 137.8, 137.4, 137.0, 135.3, 131.4, 129.9, 129.5, 129.3, 129.2, 128.2, 128.5, 128.6, 128.2, 128.0, 126.8, 125.7, 119.9, 116.0, 41.7, 35.8, 22.6, 22.6, 21.3, 9.6. HRMS calcd. for $C_{36}H_{37}N_4O_2$, $[MH^+]$ = 557.2911, found = 557.2927. An enantiomeric ratio of >96:4 *S*- **3.23**:*R*-**3.23** was ascertained by SFC analysis on a chiral stationary phase [Chiralcel AD-H 25 cm, 5 µm, 15% i-PrOH, 3 mL/min, 35 °C, 150 bar, R*t* (major) 10.6 min; R*t* (trace) 15.1 min].

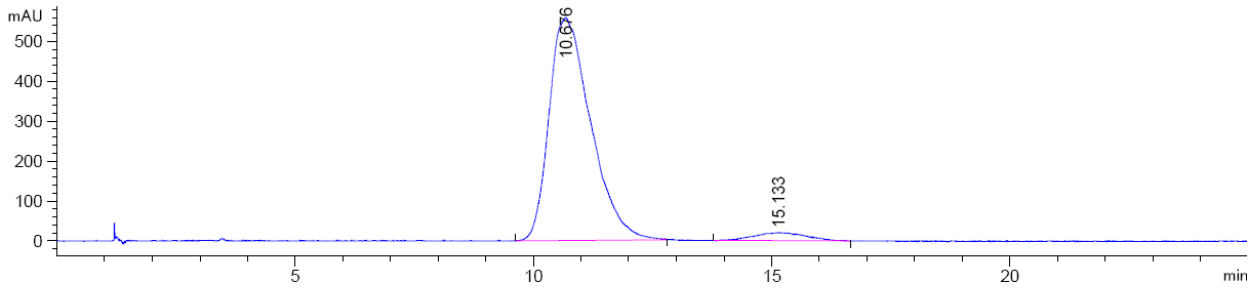

Injection of *R*-**3.23** gave a major peak (99%) at 15.1 min.

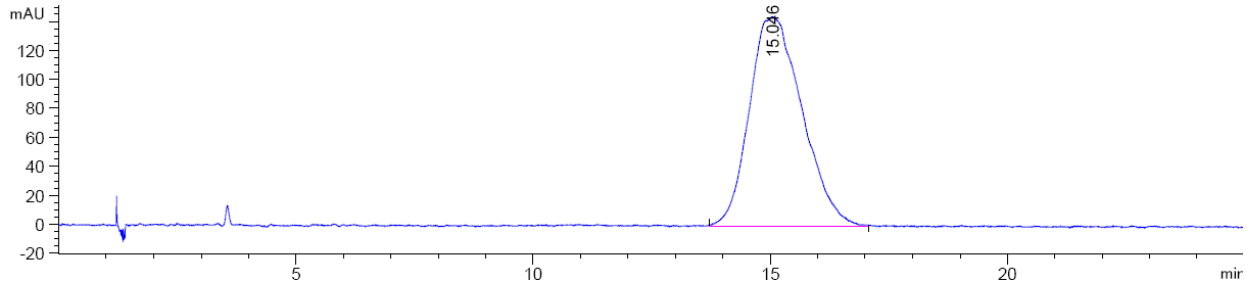

(*S*)-2-(3-((Diphenylmethylene)amino)-4-methyl-5-(*p*-methoxylphenyl)imidazolin-2-one-1-yl)-*N*- isopropyl-3-phenylpropanamide (3.24)

Employing the protocol for the synthesis of 5-aryl-Nai **3.17**, (*S*)-2-(3-((diphenylmethylene)amino)-5-methyl-2-oxo-2,3-dihydro-1*H*-imidazol-1-yl)-*N*-isopropyl-3-phenylpropanamide (54 mg, 0.12 mmol) was reacted with *p*-iodoanisole (81 mg, 0.35 mmol), and the residue was purified by flash chromatography using 20-35% EtOAc in hexanes as eluent to provide 5-*p*-methoxylphenyl-Nai amide **3.24** as yellow low melting solid (41 mg, 62%): R*f* = 0.49 (50% EtOAc in hexanes); $[\alpha]_D^{20}$ –93.9 (*c* 1.06, $CHCl_3$). ^{1}H NMR (500 MHz, $CDCl_3$) δ 8.04 (br. s, 1H), 7.58 (dd, *J* = 1.2, 7.2 Hz, 2H), 7.48-7.44 (m, 1H), 7.36-7.32 (m, 3H), 7.21-7.19 (m, 4H), 7.02-6.99 (m, 4H), 6.95-6.63 (m, 2H), 7.27 (d, *J* = 8.9 Hz, 2H), 4.44-4.43 (m, 1H), 4.00 (2 overlapping q, *J* = 6.7 Hz, 1H), 3.76 (s, 3H), 3.57-3.52 (m, 1H), 3.27 (dd, *J* = 4.3, 9.5 Hz, 1H), 1.59 (s, 3H), 1.16 (d, *J* = 6.6 Hz, 3H), 1.12 (d, *J* = 6.6 Hz, 3H); ^{13}C NMR (126 MHz, $CDCl_3$) δ 176.1, 169.8, 159.1, 148.7, 137.8, 137.0, 135.3, 132.6, 131.5, 130.8, 130.2, 129.9, 129.5, 129.2, 128.7, 128.6, 128.2, 128.0, 126.8, 121.0, 119.6, 115.8, 113.8, 55.4, 41.8, 35.9, 22.6, 9.5. HRMS calcd. for $C_{36}H_{36}N_4O_3$, $[M^+]$ = 573.2860, found = 573.2854.

(*S*)-2-(3-((Diphenylmethylene)amino)-4-methyl-5-(*p*-nitro-phenyl)imidazolin-2-one-1-yl)-*N*-isopropyl-3-phenylpropanamide (3.25)

Employing the protocol for the synthesis of 5-aryl-Nai **3.17**, (*S*)-2-(3-((diphenylmethylene)amino)-5-methyl-2-oxo-2,3-dihydro-1*H*-imidazol-1-yl)-*N*-isopropyl-3-phenylpropanamide (54 mg, 0.12 mmol) was reacted with *p*-nitroiodobenzene (84 mg, 0.35 mmol), and the residue was purified by flash chromatography using 20-35% EtOAc in hexanes as eluent to provide 5-*p*-nitrophenyl-Nai amide **3.25** as orange low melting solid (50 mg, 74%): R*f* = 0.58 (50% EtOAc in hexanes); $[\alpha]_D^{20}$ –124.2 (*c* 1.06, $CHCl_3$). ^{1}H NMR (500 MHz, $CDCl_3$) δ 8.11 (d, *J* = 9.0 Hz, 2H), 7.59 (dd, *J* = 1.2, 7.2 Hz, 2H), 7.49 (dt, *J* = 1.3, 7.4 Hz, 1H), 7.41-7.35 (m, 3H), 7.30-7.27 (m, 2H), 7.24-7.20 (m, 5H), 7.04-7.01 (m, 4H), 4.50-48 (m, 1H), 3.88 (2 overlapping q, *J* = 7.5 Hz, 1H), 3.54 (dd, *J* = 11.4, 2.4, Hz, 1H), 3.28 (dd, *J* = 4.5, 9.3 Hz, 1H), 1.17 (s, 3H), 1.15 (d, *J* = 6.6 Hz, 3H), 1.11 (d, *J* = 6.6 Hz, 3H); ^{13}C NMR (126 MHz, $CDCl_3$) δ 175.5, 169.0, 148.4, 146.4, 137.3, 136.5,

135.2, 134.9 129.8, 129.2, 129.0, 128.6, 128.5, 128.3, 128.1, 127.0, 123.6, 119.0, 118.4, 41.8, 35.5, 22.5, 22.4, 9.8. HRMS calcd. for $C_{35}H_{34}N_5O_4$, [MH^+] = 588.2605, found = 588.2615.

(*S*)-2-(3-((Diphenylmethylene)amino)-4-methyl-5-(*p*-fluoro-phenyl)imidazolin-2-one-1-yl)-*N*-isopropyl-3-phenylpropanamide (3.26)

Employing the protocol for the synthesis of 5-aryl-Nai **3.17**, (*S*)-2-(3-((diphenylmethylene)amino)-5-methyl-2-oxo-2,3-dihydro-1*H*-imidazol-1-yl)-*N*-isopropyl-3-phenylpropanamide (54 mg, 0.12 mmol) was reacted with *p*-fluoroiodobenzene (77 mg, 0.35 mmol), and the residue was purified by flash chromatography using 20-35% EtOAc in hexanes as eluent to provide 5-*p*-fluorophenyl-Nai amide **3.26** as yellow low melting solid (26 mg, 41%): R*f* = 0.43 (50% EtOAc in hexanes); $[\alpha]_D^{20}$ –117.4 (*c* 1.06, $CHCl_3$). ^{1}H NMR (500 MHz, $CDCl_3$) δ 8.01 (br. s, 1H), 7.58 (dd *J* = 1.3, 7.2 Hz, 2H), 7.47 (dt, *J* = 1.3, 7.5 Hz, 1H), 7.39-7.30 (m, 3H), 7.29-7.27 (m, 1H), 7.23-7.19 (m, 3H), 7.03-6.92 (m, 9H), 4.60-4.43 (m, 1H), 4.01 (2 overlapping q, *J* = 6.6 Hz, 1H), 3.56 (dd, *J* = 11.3, 2.3 Hz, 1H), 3.28 (dd, *J* = 4.4, 9.4 Hz, 1H), 1.61 (s, 3H), 1.17 (d, *J* = 6.6 Hz, 3H), 1.13 (d, *J* = 6.6 Hz, 3H); ^{13}C NMR (126 MHz, $CDCl_3$) δ 176.0, 169.6, 148.7, 137.7, 136.9, 135.2, 131.7, 131.3, 131.2, 129.9, 129.7, 129.2, 128.7, 128.3, 128.1, 126.9, 124.8, 118.9, 116.5, 115.5, 115.4, 41.8, 35.8, 22.7, 22.6, 9.5. HRMS calcd. for $C_{35}H_{34}FN_4O_2$, [MH^+] = 561.2667, found = 561.2660.

***tert*-Butyl 2-(3-((diphenylmethylene)amino)-5-(2-methoxyphenyl)-4-methyl-2-oxo-2,3-dihydro- 1*H*-imidazol-1-yl)-3-phenylpropanoate (3.27)**

Employing the protocol for the synthesis of 5-aryl-Nai **3.17**, Nai **3.16** (43 mg, 0.09 mmol)was reacted with 2-iodoanisole (36 μL, 0.27 mmol), and the residue was purified by flash chromatography using 15% EtOAc in hexanes as eluent to provide 5-(*p*-methoxyphenyl-Nai **3.27** as yellow oil (25 mg, 47%): R*f* = 0.72 (50% EtOAc in hexanes). ^{1}H NMR (400 MHz, $CDCl_3$) δ 7.51 (d, *J* = 4 Hz, 2H), 7.42-7.17 (m, 10H), 7.17 (d, *J* = 1.2 Hz, 2H), 7.05 (d, *J* = 5.9 Hz, 2H), 6.92 (d, *J* = 7.5 Hz, 1H), 6.82 (t, *J* = 7.6 Hz, 1H), 6.75 (d, *J* = 7.9 Hz, 1H), 4.65-4.62 (m, 1H), 3.63 (s, 3H), 3.40-3.30 (m, 2H), 1.53 (s, 3H), 1.44 (s, 9H); ^{13}C NMR (101 MHz, $CDCl_3$) δ 168.8, 157.5, 147.9, 138.1, 135.5, 132.5, 130.4, 129.7, 129.4, 129.3, 129.0, 128.8, 128.4, 127.8, 127.7, 126.4, 120.1, 116.2, 116.0,

110.9, 82.1, 57.5, 55.09, 35.5, 29.7, 28.0, 9.8. HRMS calcd. for $C_{37}H_{37}N_3O_4$, $[M^+]$ = 588.2857, found = 588.2864.

(*S*)-2-(3-((Diphenylmethylene)amino)-4-methyl-5-(*m*-trifluoromethyl-phenyl)-imidazolin-2-one-1- yl)-*N*-isopropyl-3-phenylpropanamide (3.28)

Employing the protocol for the synthesis of 5-aryl-Nai **3.17**, (*S*)-2-(3-((diphenylmethylene)amino)-5-methyl-2-oxo-2,3-dihydro-1*H*-imidazol-1-yl)-*N*-isopropyl-3-phenylpropanamide (54 mg, 0.12 mmol) was reacted with *m*-trifluoromethyl-iodobenzene (94 mg, 0.35 mmol), and the residue was purified by flash chromatography using 20-35% EtOAc in hexanes as eluent to provide 5-*m*-trifluoromethylphenyl-Nai amide **3.28** as yellow low melting solid (48 mg, 68%): R*f* = 0.52 (50% EtOAc in hexanes); $[\alpha]_D^{20}$ –121.8 (*c* 1.06, $CHCl_3$). ^{1}H NMR (500 MHz, $CDCl_3$) δ 7.96 (br. s, 1H), 7.57 (dd, *J* = 1.2, 7.1 Hz, 2H), 7.48-7.44 (m, 2H), 7.38-7.33 (m, 4H), 7.24-7.17 (m, 7H), 7.08-7.06 (m, 2H), 6.90 (dd, *J* = 1.0, 7.1 Hz, 2H), 4.51-4.48 (m, 1H), 4.03 (2 overlapping q, *J* = 6.6 Hz, 1H), 3.60 (dd, *J* = 11.4, 2.4 Hz, 1H), 3.31 (dd, *J* = 4.4, 9.5 Hz, 1H), 1.65 (s, 3H), 1.18 (d, *J* = 6.6 Hz, 3H), 1.15 (d. *J* = 6.6 Hz, 3H); ^{13}C NMR (126 MHz, $CDCl_3$) δ 176.3, 169.4, 149.1, 137.6, 136.7, 134.9, 132.3, 131.8, 129.9, 129.8, 129.5, 129.2, 128.8, 128.7, 128.6, 128.3, 128.1, 127.0, 126.1, 122.7, 118.5, 117.4, 62.4, 41.9, 36.0, 22.7, 22.6, 9.6. HRMS calcd. for $C_{36}H_{34}F_3N_4O_2$, $[MH^+]$ = 611.2628, found = 611.2635.

***N*-(3-(1-(*iso*-Propylamino)-1-oxo-3-phenylpropan-2-yl)-4-methyl-2-oxo-2,3-dihydro-1*H*-imidazol-1-yl)-4-methoxybenzamide (3.30)**

2-(3-((Diphenylmethylene)amino)-5-methyl-2-oxo-2,3-dihydro-1*H*-imidazol-1-yl)-*N*-isopropyl-3-phenyl-propanamide (**3.29**, 349 mg, 0.75 mmol) was dissolved in THF (8 mL) and treated with aqueous HCl (2M, 8 mL, 15 mmol). The mixture was stirred at room temperature for 2 h until complete conversion was ascertained by TLC. The mixture was concentrated under vacuum, diluted with a 4:1 mixture of acetonitrile/water (25 mL). The aqueous layer was separated, washed with hexanes (3 x 15 mL), and freeze-dried. The residue was dissolved in DCM (8 mL), treated with freshly prepared 4-anisoyl chloride (0.20 mL, 1.5 mmol) and DIEA (0.37 mL, 2.25 mmol) and stirred overnight. The reaction mixture was diluted with DCM (10 mL), washed with 5% citric acid (3 x 5 mL) and brine (10 mL), dried over magnesium sulfate and evaporated to

a residue that was purified by column chromatography using 20-70% EtOAc in hexanes to give amide **3.30** as yellow foam (164 mg, 50%): R*f* = 0.41 (80% EtOAc in hexanes). ^{1}H NMR (300 MHz, $CDCl_3$) δ 10.87 (s, 1H), 7.79 (d, *J* = 8.9 Hz, 2H), 7.15-7.10 (m, 6H), 6.71 (d, *J* = 9.0 Hz, 2H), 6.03 (s, 1H), 4.53 (dd, *J* = 4.5, 6.8 Hz, 1H), 4.10, (2 overlapping q, *J* = 1.0 Hz, 1H), 3.81 (s, 3H), 3.71 (dd, *J* = 2.4, 11.5 Hz, 1H), 3.51 (dd, *J* = 4.5, 9.3 Hz, 1H), 1.75, (s, 3H), 1.21 (d, *J* = 6.6 Hz, 3H), 1.15 (d, *J* = 6.6 Hz, 3H); ^{13}C NMR (75 MHz, $CDCl_3$) δ 168.5, 166.2, 162.8, 154.3, 137.7, 129.8, 129.1, 128.8, 127.0, 122.9, 119.3, 113.6, 110.9, 61.2, 55.5, 42.0, 35.1, 22.6, 22.4, 10.5. HRMS calcd. for $C_{24}H_{29}N_4O_4$, [MH^+] = 436.2183, found = 437.2188.

_N_-(3-(1-(Isopropylamino)-1-oxo-3-phenylpropan-2-yl)-4-methyl-5-(4-nitrophenyl)-2-oxo-2,3-dihydro-1H-imidazol-1-yl)-4-methoxybenzamide (3.31)

Employing the protocol for the synthesis of 5-aryl-Nai **3.17**, *N*-(3-(1-(isopropylamino)-1-oxo-3-phenylpropan-2-yl)-4-methyl-2-oxo-2,3-dihydro-1*H*-imidazol-1-yl)-4-methoxybenzamide (**3.30**, 84 mg, 0.19 mmol) was reacted with *p*-iodonitrobenzene (144 mg, 0.58 mmol) with stirring for 48 h, and purification by column chromatography using 30-70% EtOAc in hexanes gave 5-*p*-nitrophenyl-Nai peptide **3.31** as orange low melting solid (28 mg, 26%): R*f* = 0.11 (50% EtOAc in hexanes). ^{1}H-NMR (400 MHz, MeOD-d_4) δ 8.22 (d, *J* = 8.6 Hz, 2H), 7.79 (d, *J* = 8.2 Hz, 2H), 7.46 (d, *J* = 8.4 Hz, 2H), 7.32-7.22 (m, 5H), 6.98 (d, *J* = 8.7 Hz, 2H), 4.13- 4.07 (m, 1H), 3.84 (s, 3H), 3.54-3.51 (m, 1H), 3.33-3.27 (m, 2H), 1.80 (s, 1H), 1.73 (s, 2H), 1.20-1.19 (m, 6H); ^{13}C NMR (75 MHz, $CDCl_3$) δ 169.8, 162.9, 148.3, 139.1, 138.7, 135.8, 130.8, 130.8, 130.6, 130.4, 129.7, 128.0, 124.7, 115.0, 79.5, 56.0, 53.2, 43.2, 22.4, 22.4, 7.5. HRMS calcd. for $C_{30}H_{31}N_5O_6$, [M^+] = 558.2347, found = 558.2355.

References

[1]. R. C. Smith and J. C. Reeves, *Biochem. Pharmacol.*, 1987, **36**, 1457.

[2]. K. Pande, R. Kalsi, T. Bhalla, and J. Barthwal, *ChemInform*, 1987, **18**.

[3]. A. Kamal, G. Ramakrishna, P. Raju, A. Viswanath, M. J. Ramaiah, G. Balakishan, and M. Pal-Bhadra, *Bioorg. Med. Chem. Lett.*, 2010, **20**, 4865.

[4]. K. M. Khan, U. R. Mughal, N. Ambreen, Samreen, S. Perveen, and M. I. Choudhary, *J. Enzyme Inhib. Med. Chem*., 2010, **25**, 29.

[5]. R. Mohan and M. M. Morrissey, U.S. Patent No. 5, 612, 363. 1997.

[6]. J. J. Egan, E. G. McMahon, G. M. Olins, and J. R. Schuh, U.S. Patent No. 6, 984, 633. 2006.

[7]. A. Kubo, R. Imashiro, H. Sakurai, H. Miyoshi, A. Ogasawara, H. Hiramatsu, T. Nakajima, and T. Nakane, U.S. Patent No. 7, 473, 695. 2009.

[8]. J. Sheppeck, J. L. Gilmore, X.-T. Chen, and X. He, U.S. Patent No. 7, 211, 671. 2007.

[9]. N. Xue, X. Yang, R. Wu, J. Chen, Q. He, B. Yang, X. Lu, and Y. Hu, *Bioorg. Med. Chem.*, 2008, **16**, 2550.

[10]. M. J. Broadhurst, W. H. Johnson, and D. S. Walter, U.S. Patent No. 6, 235, 787. 2001.

[11]. K. P. Cusack, H. F. Koolman, U. E. Lange, H. M. Peltier, I. Piel, and A. Vasudevan, *Bioorg. Med. Chem. Lett.*, 2013, **23**, 5471.

[12]. D. J. St-Cyr, Y. García-Ramos, N.-D. Doan, and W. D. Lubell, 'Aminolactam, *N*-Aminoimidazolone, and *N*-Aminoimdazolidinone Peptide Mimics', ed. by W. D. Lubell, Peptidomimetics I. Topics in Heterocyclic Chemistry vol 48, Springer, Cham, 2017.

[13]. C. Proulx and W. D. Lubell, *Org. Lett.*, 2012, **14**, 4552.

[14]. C. M. Wilmot and J. M. Thornton, *J. Mol. Biomol.*, 1088, **203**, 221.

[15]. J. Bezenšek, U. Grošelj, K. Stare, J. Svete, and B. Stanovnik, *Tetrahedron*, 2012, **68**, 516; C. Neochoritis, C. A. Tsoleridis, and J. Stephanidou-Stephanatou, *Tetrahedron*, 2008, **64**, 3527; Y. Zhu and Y. Shi, *Chem. Eur. J.*, 2014, **20**, 13901; G. Crank and H. Khan, *Aust. J. Chem.*, 1985, **38**, 447.

[16]. J. Lu, X. Tan, and C. Chen, *J. Am. Chem. Soc.*, 2007, **129**, 7768.

[17]. J. Poupart, D. Doan-Ngoc, and W. D. Lubell, *Proceedings of the 24th Am. Peptide Symp.*, American Peptide Society, 2015, 272.

[18]. V. J. Hruby, G. Li, C. Haskell-Luevano, and M. Shenderovich, *J. Pept. Sci.*, 1997, **43**, 219; S. Cowell, Y. Lee, J. Cain, and V. Hruby, *Curr. Med. Chem.*, 2004, **11**, 2785.

[19]. H. Abas, S. M. Linsdall, M. Mamboury, H. S. Rzepa, and A. C. Spivey, *Org. Lett.*, 2017, **19**, 2486.

[20]. C. A. Snyder, J. P. Selegue, N. C. Tice, C. E. Wallace, M. T. Blankenbuehler, S. Parkin, K. D. Allen, and R. T. Beck, *J. Am. Chem. Soc.*, 2005, **127**, 15010.

[21]. W. C. Still, M. Kahn, and A. Mitra, *J. Org. Chem.*, 1978, **43**, 2923.

Article 3:

Poupart, J.; Doan, N. D.; Lubell, W. D. 4,5-Disubstituted *N*-aminoimidazol-2-one mimics of peptide turn backbone and side chain conformation. *Proceedings of the 24th Am. Peptide Symp. (2015),* Ved Srivastava, Andrei Yudin and Michal Lebl (Editors), American Peptide Society, 2015, 272.

DOI: 10.17952/24APS.2015.272

All the synthetic work was done by me, based on work initiated by Dr. Duc Ngoc-Doan.

The article was written by me and edited by Professor William D. Lubell

4,5-Disubstituted *N*-aminoimdazol-2-one mimics of peptide turn backbone and side chain conformation

Julien Poupart, Duc Doan-Ngoc, William D. Lubell

Department of chemistry, Université de Montréal, Montreal, Canada,

Introduction: *N*-aminoimdazol-2-one (Nai) residues

Nai residues have been shown by NMR spectroscopy and X-ray crystallography to adopt turn conformations, and have been incorporated into biologically active peptides to study structure-activity relationships (Figure 3.5).[1,2]

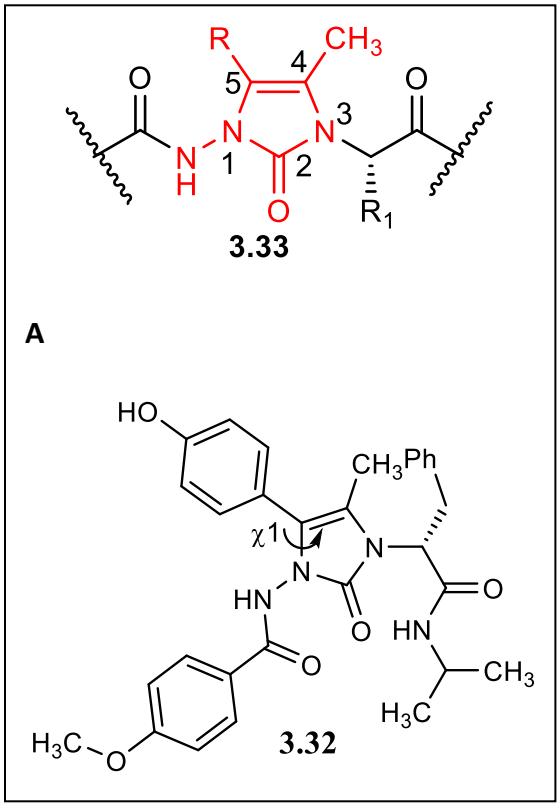

Figure 3.5: 4,5-disubstituted Nai residue in a peptide **3.33** (A) and model Nai peptide **3.32** (B)

The synthesis of Nai residues has entailed alkylation of aza-glycinyl dipeptides with propargyl bromide using tetraethyl ammonium hydroxide, followed by sodium hydride induced 5-*exo*-dig cyclisation and *exo*- to *endo*-alkene epimerization. By performing a Sonogashira reaction on the aza-propargylglycine residue prior to ring formation, various aromatic and heteroaromatic ring systems have been introduced at the 4-position of the aminoimdazol-2-one residue. Although the use of strong base led to epimerization of aza-glycinyl dipeptide *C*-terminal α-amino esters, the Nai dipeptide enantiomers were effectively separated by chiral supercritical fluid chromatography.[3] After liberation of the carboxylic acid, the resulting Nai dipeptide building blocks have been inserted into longer peptide structures by standard coupling methods.[1,2]

The current method for Nai peptide construction offers effective means for introducing substituents at the 4-position to mimic different amino acid side chains. Moreover, the 4-position substituents have been observed by crystallographic analyses to influence the conformation of the *C*-terminal α-amino acid residue side chain in model Nai peptides.[2] Considering the natural orientation of amino acid side chains in chi-space,[4] the Nai 5-position represents a promising location for the attachment of substituents for peptide mimicry.[5] Evidence that the backbone and side chain geometry of natural amino acids involved in β-turns may be mimicked by 5-aryl Nai residues was derived from molecular modelling using HyperChem 8^{TM}, which predicted that model Nai peptide 3.32 adopted a type II´ β-turn conformation in which the aromatic side chain χ^1 torsion angle was oriented in a *gauche* (–) conformation (Figure 3.5).

Aromatic residues are abundant at the central positions of turn conformations of naturally occurring bioactive peptides, such as somatostatin.[6] Constrained mimics of aryl amino acids that adopt turn conformations may thus offer interesting potential for studying structure-activity relationships.[7] Arylation of the Nai 5-position is thus being studied to provide rigidified aryl and heteroarylalanine residues for turn mimicry.

Results and Discussion

Palladium catalyzed arylation was performed in solution on a protected Nai analog to functionalize the 5-position. For example, employing Nai dipeptide *S*-**3.16**,[1] the palladium-catalyzed arylation with 4-iodophenyl-4-methylbenzenesulfonate gave 5-aryl Nai dipeptide **3.17**

in 86% yield (Figure 3.6). In the interest of studying the conformation of the 5-aryl Nai residue, efforts are now being pursued to incorporate Nai dipeptide **3.17** into model peptides as a constrained aza-tyrosine surrogate. Moreover, the scope of the palladium-catalyzed arylation will be explored to assess its tolerance to different functionalities on both the alkene and aryl iodine.

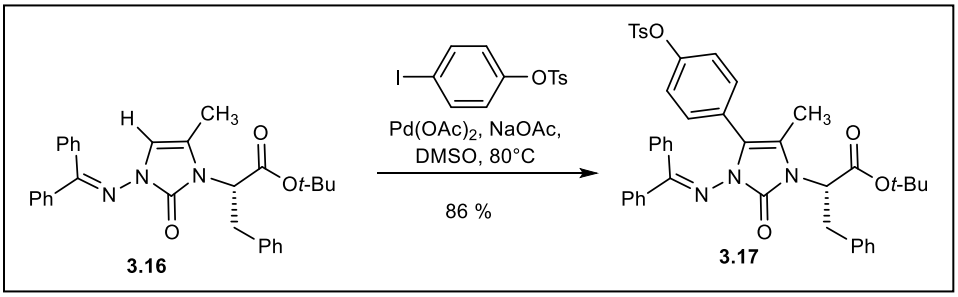

Figure 3.6: Synthesis of peptide **3.17**

Experimental

(*S*)-*tert*-butyl 2-(3-((diphenylmethylene)amino)-5-methyl-2-oxo-4-(4-(tosyloxy)phenyl)-2,3-dihydro-1H-imidazol-1-yl)-3-phenylpropanoate (3.17)

tert-Butyl (2*R*)-2-{3-[(diphenylmethylidene)amino]-5-methyl-2-oxo-2,3-dihydro-1H-imidazol-1-yl}-3-phenylpropanoate (1 eq., 67 mg, 0.14 mmol, prepared according to reference 8), 4-iodophenyl 4-methylbenzene-1-sulfonate (3 eq., 156 mg, 0.42 mmol, prepared according to reference 9), sodium acetate (3 eq., 34 mg, 0.42 mmol) and palladium acetate (10 mol%, 3 mg, 0.014 mmol) were dissolved in degassed DMSO (1 mL) in a pressure vessel. The vessel was purged with argon, heated to 80°C, and stirred overnight, when complete reaction was observed by TLC (disappearance of starting material, Rf 0.45, 30% EtOAc/Hexanes). The reaction mixture was partitioned between DCM (10 mL) and a mixture of brine (8 mL) and 5% citric acid (2 mL). The phases were separated, and the organic layer was washed with brine (3 x 5 mL). The combined organic phases were dried over magnesium sulfate, filtered and evaporated to a residue that was purified by column chromatography on silica gel using 15-30% EtOAc in hexanes as eluent.

Evaporation of the collected fractions gave 5-aryl Nai **3** as a yellow oil (87 mg, 86%): R_f 0.34 (30 % EtOAc / hexanes); ^{1}H NMR (400 MHz, $CDCl_3$) δ 1.49 (9H, s), 1.61 (3H, s), 2.40 (3H, s), 3.39-3.43 (2H, m), 4.64-4.68 (1H, m), 6.81-6.92 (5H, m), 7.00-7.02 (2H, m), 7.13 (2H, d, *J* = 8 Hz), 7.18-7.22 (5H, m), 7.34-7.39 (3H, m), 7.45-7.49 (2H, m), 7.54 (3H, d, *J* = 8 Hz), 7.63 (2H, d, *J* = 8 Hz). ^{13}C NMR (75 MHz, $CDCl_3$) δ 174.6, 168.4, 148.3, 148.1, 145.4, 137.8, 137.1, 135.0, 132.2, 131.2, 130.1, 129.7, 129.6, 129,2, 128.7, 128.4, 128.0, 127.8, 126.6, 122.1, 117.8, 116.1, 82.4, 57.6, 35.4, 29.7, 28.0, 21.7, 9.5. HRMS Calcd. $C_{43}H_{42}N_3O_6S$ $[M+H]^+$ = 728.2789, found = 728.2802.

Acknowledgments

The authors would like to thank the Natural Sciences and Engineering Research Council of Canada (NSERC), the Canadian Institutes of Health Research (CIHR), the Ministère du développement économique de l'innovation et de l'exportation du Quebec (#878-2012, Traitement de la dégénerescence maculaire), Amorchem and the NSERC Collaborative Research and Training Experience Program (CREATE) in Continuous Flow Science.

References

[1]. Proulx, C.; Lubell, W. D., "Analysis of N-amino-imidazolin-2-one peptide turn mimic 4-position substituent effects on conformation by X-ray crystallography." *Biopolymers, Pep. Sci.*, **2014**, 102(1):7-15. DOI: 10.1002/bip.22327

[2]. Proulx, C.; Lubell, W. D., "N-Amino-imidazolin-2-one Peptide Mimic Synthesis and Conformational Analysis." *Org. Lett.,* **2012,** 14 (17), 4552-55. DOI: 10.1021/ol302021n

[3]. Yésica García-Ramos, Caroline Proulx, Christophe Camy, William D. Lubell "Synthesis and purification of enantiomerically pure N-aminoimidazolin- 2-one dipeptide" Proceedings of the 32nd Europ. Peptide Symp. (2012) George Kokotos, Violetta Constantinou-Kokotou, John Matsoukas (Editors) European Peptide Society, 2012, pp. 366-67.

[4]. Hruby, V. J., Li, G., Haskell-Luevano, C., Shenderovich, M. "Design of peptides, proteins, and peptidomimetics in chi space." *Peptide Science*, **1997** 43(3): 219-66. DOI: 10.1002/(SICI)1097-0282(1997)43:3<219::AID-BIP3>3.0.CO;2-Y

[5]. Doan, N. D.; Hopewell, R.; Lubell, W. D., “N-aminoimidazolidin-2-one peptidomimetics.” *Org. Lett.,* **2014,** *16* (8), 2232-35. DOI: 10.1021/ol500739k

[6]. Mattern, R.H., Tran, T.A., Goodman, M. “Conformational analyses of cyclic hexapeptide analogs of somatostatin containing arylalkyl peptoid and naphthylalanine residues.” *J. Pept. Sci.*, **1999**, 5(4):161-75. DOI: 10.1002/(SICI)1099-1387(199904)5:4<161::AID-PSC177>3.0.CO;2-F

[7]. Makwana, K. M.; Mahalakshmi, R., “Comparative analysis of cross strand aromatic-Phe interactions in designed peptide [small beta]-hairpins.” *Org. Biomol. Chem.,* **2014,** 12 (13), 2053-61. DOI: 10.1039/C3OB42247J

Chapter 4

Biomedical application of (4-Me, 5-Aryl)Nai residues : [(4-Me, 5-Aryl)Nai^{4}]-GHRP-6

4.1 GHRP-6: development and biochemistry

Growth hormone releasing hormone-6 (GHRP-6, **4.4**, H-His-D-Trp-Ala-Trp-D-Phe-Lys-NH_2) was reported in 1984.[143] In studies of the opioid peptide Met-enkephalin (H-Tyr-Gly-Gly-Phe-Met-OH, **4.1**), Gly^2 was replaced by $D\text{-}Trp^2$ and the *C*-terminal acid group was changed to an amide (**4.2**) to provide a peptide devoid of opioid activity but able to cause growth hormone release.[144] Further optimization featuring the removal of the Met residue and replacement of Gly^3 with Ala gave peptide **4.3** that had a thousand fold ability to cause growth hormone release.[145] Structure-activity relationship (SAR) studies revealed the importance of aromatic ring stacking and a favored alternation of L- and D-stereochemistry for activity. Replacement of Tyr^1 by His and addition of a *C*-terminal lysine amide gave GHRP-6 (**4.4**) which performed better both *in vitro* and *in vivo* with an activity of about 30 times peptide **4.3**.[143]

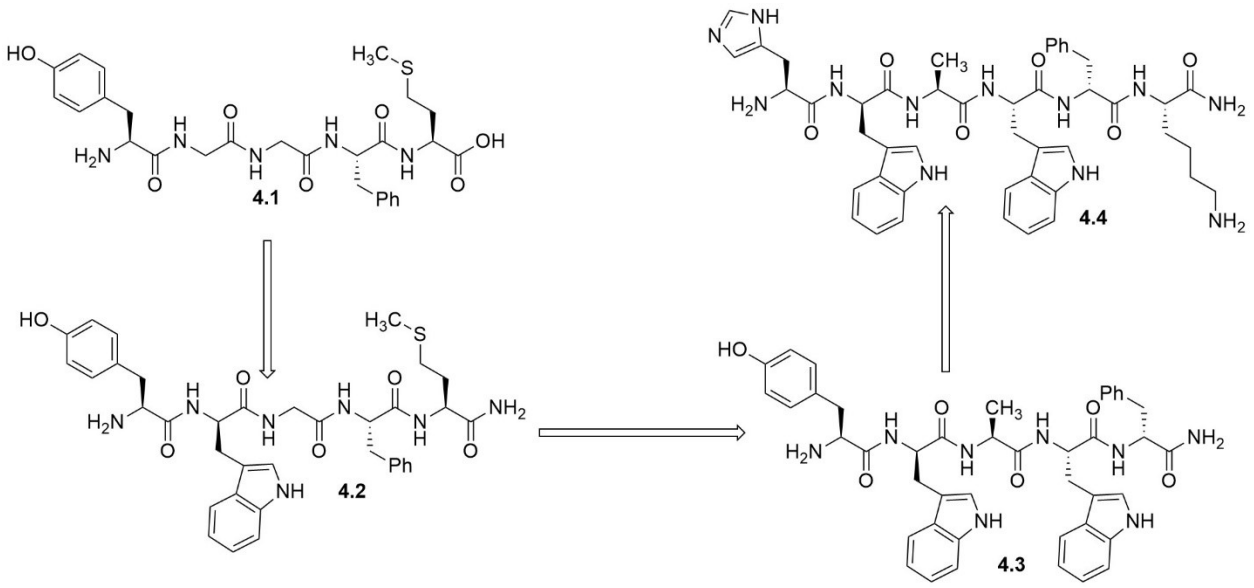

Figure 4.1: Conception of GHRP-6 (**4.4**) from Met-enkaphalin (**4.1**)

The mechanism of action of GHRP-6 (**4.4**) remained unclear until the growth hormone secretagogue receptor-1a (GHS-R1a) was cloned.[144] A G-coupled protein receptor (GPCR) that bound the natural peptide ghrelin as ligand, GHS-R1a was identified as a target of GHRP-6.[146, 147]

Moreover, GHS-R1a was shown to stimulate production of growth hormone by a distinct pathway than that of the growth hormone secretion receptor (GHSR). Both, GHS-R1a and GHSR receptors are mainly present in hypothalamic cells.

Subsequently, GHRP-6 was shown to exhibit cardioprotective properties, which were attributed to binding to a second receptor.[148] The alternative receptor was identified as the cluster of differentiation-36 receptor (CD36). A type B scavenger receptor, CD36 features a large extracellular domain. Present on many cells, including macrophages, dendrites and cardiac cells, CD36 binds a variety of molecules including oxidized low-density lipoproteins (oxLDL). With roles in the internalization of oxLDL and plaque formation, CD36 has been pursued as a promising target for pharmaceutical intervention to treat artherosclerosis.[149, 150] Furthermore, ligands targeting the scavenger receptor may find promise for the treatment of age-related macular degeneration (AMD), the major cause of irreversible central vision loss in the elderly, because of the importance of CD36 in neovascularization and in the accumulation of oxLDL in the cellular layers between the retina and choroid in the eye.[151]

4.2 Development of aza^4-GHRP-6

In search of a selective peptide ligand for CD36, GHRP-6 analogs without GHRS-R1a binding affinity were targeted. Azapeptide analogs of GHRP-6 were prepared by insertion of semicarbazide residues in place of the different amino amides in the GHRP-6 sequence.[152] Among a variety of analogs, [aza-Tyr^4]- and [Ala^1, aza-Phe^4]-GHRP-6 (**4.5** and **4.6**) maintained CD36 binding affinity yet exhibited a considerable (>1000 fold) loss of ability to engage the GHS-R1a receptor.[85] The study shed light on the importance of aza-residues at the peptide 4-position. Moreover, circular dichroism (CD) spectroscopy revealed that azapeptides **4.5** and **4.6**, which differentiated between GHS-R1a and CD36, exhibited curve shapes indicative of β-turn structure in contrast to GHRP-6 (**4.4**) which possessed a random coil spectrum in water. The CD study led to the hypothesis that azapeptides **4.5** and **4.6** bound CD36 in an active β-turn conformation. Further optimization of the aza-GHRP-6 ligands concentrated on the 1- and 4-positions, examining angiogenic activity in a mouse choroidal explant model.[85] Although [Ala^1, aza-Phe^4]-

GHRP-6 (**4.6**) lacked angiogenic activity, [aza-Tyr[4]]- and [aza(4-F)Phe[4]]-GHRP-6 (**4.5** and **4.7**) exhibited significant antiangiogenic activity.[85] The aromatic side chain of the aza-residue at the 4-position was shown to be important for activity. The results of the latter study correlated with those employing α- and β-amino-γ-lactam (Agl and Bgl) residues to constrain GHRP-6.[45] Although certain analogs (e.g. [(3*S*)-Agl[3]]- and [(3*R*)-Bgl[3]]-GHRP-6) exhibited promising selective CD36 binding affinity, peptides with lactam substitutions at the 4-position engaged neither GHS-R1a nor CD36, likely due in part to the absence of the aromatic side chain.

4.3 [(4-Me,5-Ar)Nai[4]]-GHRP-6

A β-turn conformation and a 4-position residue with aryl (Ar) side chain, both seem essential for binding to CD36. Constraint of the aza-reside of GHRP-6 has been explored using [(4-Me,5-Ar)Nai[4]]-GHRP-6 analogs **4.8a-d** (Figure 2). The Nai residue has already been shown to induce β- and γ-turn conformers in X-ray crystallographic and computational studies.[75, 83] Methods for adding aryl groups at the 5-position of the imidazole-2-one heterocycle of the Nai residue were described in Chapter 3. In the present chapter, such chemistry has been extended to introduce aryl groups to Nai residues linked to solid supports. Installation of the Nai residue on solid support was performed using the enantioenriched Nai dipeptide acid, which was synthesized from an aza-Pra dipeptide acid using the method described in Chapter 2. Among challenges encountered in the synthesis of [(4-Me,5-Ar)Nai[4]]-GHRP-6 analogs on solid phase, novel chemistry was developed for the removal of the benzhydrylidene protection and the acylation of the resulting semicarbazide moiety.

The purified peptides were evaluated for their ability to reduce R-FSL-1 induced nitric oxide (NO) production in macrophages. R-FSL-1 is a Toll-like receptor 2 (TLR-2) agonist, which initiates an inflammatory cascade. CD36 is co-express with the heterodimeric receptor TLR-2/6 complex.[153] Previously, reduction of NO production in macrophages after treatment with a TLR-2 agonist was correlated to peptide binding to CD36.[85, 153] Modulators of CD36 that reduce the cascade to NO are attractive because of their potential to curb macrophage driven inflammation in diseases such as atherosclerosis and AMD. For example, [aza-Tyr[4]]-GHRP-6 (**4.5**) has been

shown to induce dissociation of the CD36-TLR-2 oligomeric complex, decrease inflammasome activation, and reduce immune responses to alleviate subsequent inflammation-dependent neuronal injury characteristic of retinal disorders such as AMD.[153]

Aza-amino acid residues exhibit preferences to situate in the central regions of β-turns at either the *i* + 1 or *i* + 2 positions as demonstrated by computation, X-ray crystallography and spectroscopic methods (Figure 2).[63] In the case of GHRP-6 analogs with aza-residues in the 4-position, the aza-residue has been suggested to situate at the *i* + 2 position based on NMR spectroscopic analysis.[154] Moreover, [(3*S*)-Agl^3]- and [(3*R*)-Bgl^3]-GHRP-6 have been suggested to adopt β-turn conformations in which the lactam occupies at the *i* + 1 position.[45] In spite support for an active conformer with the third and fourth amino acid residues at the central positions of a β-turn, potential exists for an alternative conformation in which the aza-residue adopts the *i* + 1 position and the fourth and fifth residues are in the middle of the turn. Although [(3*S*)-Agl^4]- and [(3*R*)-Bgl^4]-GHRP-6 would adopt the latter conformer, their lack of binding affinity may be due to the absence of the aromatic side chain. The Nai residue could similarly locate at the *i* + 1 position of a β-turn due to the covalent constraints of the imidazole-2-one ring. Moreover, the (5-Aryl)Nai residue enables placement of an aromatic residue at the *i* + 1 position with a *gauche* (-) side chain orientation. Although their binding affinity remains to be evaluated, [(4-Me,5-Ar)Nai^4]-GHRP-6 analogs **4.9-4.12** tempered effectively NO overproduction in macrophages treated with a TLR-2 agonist indicates the potential for such an active conformation with the fourth and fifth amino acid residues in the center of the β-turn.

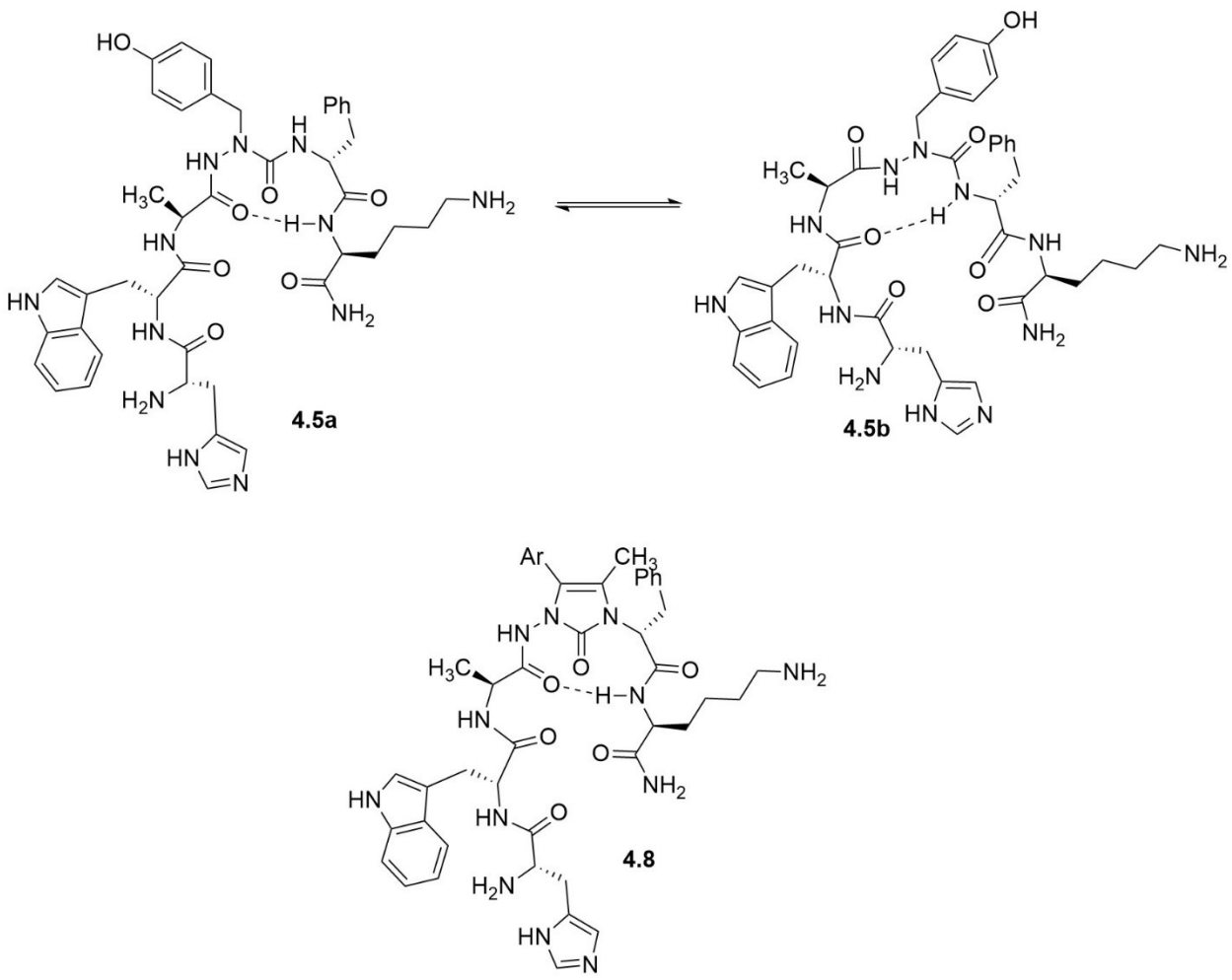

Figure 4.2: Two conformers of azapeptide **4.5**. It can form two different types of β-turns, while only one is accessible for Nai **4.8**

Therefore, (4-Me,5-Ar)Nai residues have the potential to help probe receptors of bioactive peptides and help understanding the SAR. In the case of [(4-Me,5-Ar)Nai[4]]-GHRP-6 analogs, preliminary biological results indicate they effectively mimic the GHRP-6 active conformation for interacting with CD36. As such, they represent a step forward in both understanding the structural properties needed for correct binding and developing CD36 peptidomimetic modulators.

Article 4:

Poupart, J.; Mulumba, M.; Doan, N. D.; Ong, H.; Lubell, W. D.: Application of *N*-Aminoimidazol-2-one Turn Mimics to Study the Backbone and Side-chain Orientations of Peptide-based CD36 Modulators, *Article in preparation,* **2020**.

KEYWORDS

GHRP-6, CD36, *N*-aminoimidazol-2-one, solid-phase synthesis, palladium-catalyzed cross-coupling, β-turn

All synthetic work was done by me. Dr. Duc Ngoc-Doan helped with conceptualization.

All biological work was done by Dr. Mukandila Mulumba, under the direction of Professor Huy Ong.

The manuscript was written by me and edited by Professor William D. Lubell.

Application of *N*-Aminoimidazol-2-one Turn Mimics to Study the Backbone and Side-chain Orientations of Peptide-based CD36 Modulators

Julien Poupart,[a] Dilan Mulumba,[b] Duc Ngoc-Doan,[a] Huy Ong[b] and William D. Lubell[a]*

[a] Département de Chimie and [b] Département de Pharmacie, Université de Montréal, C.P. 6128, Succursale Centre-Ville, Montréal, Québec, H3C3J7, Canada

Keywords

GHRP-6, CD36, *N*-aminoimidazol-2-one, solid-phase synthesis, palladium-catalyzed cross-coupling, β-turn

Abstract

N-Aminoimidazol-2-one (Nai) residues induce turn conformations in model peptides. Four [(4-methyl,5-aryl)Nai4]-growth hormone releasing peptide-6 (GHRP-6) analogs were synthesized using a solid-phase approach featuring insertion of a (4-Me)Nai residue into a resin-bound peptide followed by palladium-catalyzed 5-position C-H activation and coupling with different aryl iodides. Relative to the azapeptide cluster of differentiation receptor 36 (CD36) modulator [azaY4]-GHRP-6 (**4.5**), all four [(4-methyl,5-aryl)Nai4]-GHRP-6 (**4.9-4.12**) analogs exhibited similar and in one case better activity in mediating nitric oxide overproduction in macrophages treated with a Toll-like receptor-2 agonist. Considering the covalent, stereo-electronic and steric constraints induced by the amino acid surrogate, the biologically active conformer of the [(4-methyl,5-aryl)Nai4]-GHRP-6 analogs features likely a β-turn with the Nai residue at the *i* + 1 position and the 5-position aromatic ring in a gauche χ-space orientation. Their effective diversity-oriented solid-phase synthesis and preferred backbone and side chain orientations

designate (4-methyl,5-aryl)Nai residues as privileged go-to-scaffolds for exploring aromatic residues in biologically active peptides.

Introduction

The cluster of differentiation receptor 36 (CD36) is a promising target for the treatment of inflammatory and angiogenic diseases including atherosclerosis,[1] cardiovascular disease[2] and age-related macular degeneration (AMD).[3] A glycoprotein, CD36 is present in the membranes of various tissues, as well as red blood cells and macrophages.[4] A type B scavenger receptor, CD36 plays a key role in the internalization of oxidized low density lipoproteins (oxLDL).[5-6] Co-expressed with the Toll-like receptor (TLR)-2-TLR-6 complex, CD36 modulates the latter during inflammatory responses implicated in innate immunity.[7-8]

Growth hormone releasing peptide-6 (GHRP-6, H-His-D-Trp-Ala-Trp-D-Phe-Lys-NH_2) has been shown to bind both CD36 and the growth hormone secretagogue receptor 1a (GHSR-1a). Analogs of GHRP-6 with GHSR-1a activity have been studied for the development of treatments of impaired growth hormone (GH) secretion,[9] short stature and aging.[10] Towards the conception of CD36 specific ligands without GHSR-1a receptor binding affinity, certain constrained analogs of GHRP-6 have shown notable selectivity likely due to a favored turn geometry about the central amino acid residues.[11] For example, CD36-selective azapeptide analogs of GHRP-6 have been made by replacing specific amino amide residues by a semicarbazide which induced turn conformers due to stereo-electronic effects from urea planarity and lone pair-lone pair repulsion between neighboring hydrazine nitrogen.[12] Notably, circular dichroism (CD) spectroscopy of [aza-phenylalanine^4]-GHRP-6 analogs displayed curve shapes indicative of turn geometry in contrast to the random coil spectrum exhibited by the parent peptide in water. Moreover, relative to the parent peptide, the [Ala^1, aza-Phe^4]- and [aza-Tyr^4]-GHRP-6 (**4.7** and **4.5**) retained binding affinity for CD36 but exhibited significantly diminished ability to interact with the GHSR-1a receptor.[13] The CD36 selective azapeptide ligand [aza-Tyr^4]-GHRP-6 (**4.5**) exerted anti-inflammatory properties through the TLR2-inflammasome pathway and shifting the metabolic rate of mononuclear phagocytes to increase oxygen consumption by influencing the PPAR-γ pathway.[14]

A combination of α- and β-amino-γ-lactam (Agl and Bgl) residues have also been employed in a positional scan that delivered [(*S*)-Agl^3]- and [(*R*)-Bgl^3]-GHRP-6, both of which retained significant binding affinity for CD36, but were a thousand-fold less capable of engaging the GHSR-1a receptor relative to the parent peptide.[15] In contrast, the diasteromeric [(*R*)-Agl^3]- and [(*S*)-Bgl^3]-GHRP-6 analogs lost binding affinity to both receptors, likely due to their unfavorable conformations for receptor engagement. Moreover, insertion of (*R*)- and (*S*)-α- and β-amino-γ-lactam residues at the 4-position of GHRP-6 resulted consistently in significant losses of binding affinity to both receptors possibly due to the removal of a key aromatic side chain.

Considering the relevance of the turn geometry and aromatic side chain for CD36 selective azapeptide ligand binding affinity and activity, an investigation was launched to restrain the aryl group of the aza-residue. *N*-Aminoimidazol-2-one (Nai) residues combine the stereo-electronic effects of aza-residues with the covalent constraints of an α-amino-γ-lactam.[16] In model peptides, Nai residues have been shown by X-ray crystallography and NMR spectroscopy to induce β- and γ-turn geometry.[17-18] Moreover, various aryl iodides have been added to the 5-position of the imidazole-2-one ring of a variety of (4-Me)Nai residues using palladium-catalysis in solution.[19] Computational analysis has predicted that *p*-MeOBz-(4-Me,5-*p*-HOPh)Nai-D-Phe-NH*i*-Pr (**4.13**) adopted a type II' β-turn and positioned the aryl group in the *gauche* (–) conformation.[19] Aryl (Ar) side chain χ dihedral angle rigidity resulted from a combination of steric interactions with the neighboring 4-methyl group and the covalent and stereo-electronic constraints of the imidazole-2-one heterocycle (Figure 4.3).[19]

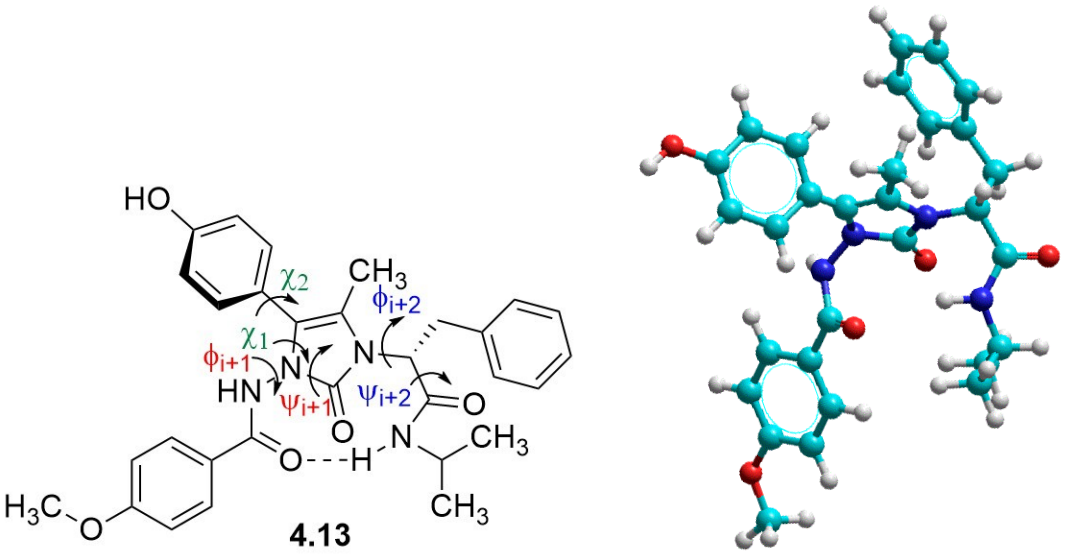

Figure 4.3. Representations of (4-Me,5-Ar)Nai residue in model peptide **4.13** with relevant dihedral angles (left) and in minimum energy conformer from molecular dynamics simulations (right).

Employing palladium-catalyzed aryl addition chemistry on (4-Me)Nai analogs, (4-Me,5-Ar)Nai building blocks have been prepared effectively in solution.[19] Although such constrained phenylalanine building blocks may be used to synthesize sets of (4-Me,5-Ar)Nai peptides, a solid-phase approach from a common late stage intermediate would enhance efficiency for their diversity-oriented construction. Installation of the aryl substituent onto the 5-position of a common (4-Me)Nai peptide linked to Rink amide resin has now been pursued using palladium-catalysis. Based on [aza-Phe[4]]-GHRP-6 analogs that have previously exhibited CD36 binding affinity and activity in reducing nitric oxide (NO) production in cells treated with a TLR-2 agonist, four [(4-Me,5-Ar)Nai[4]]-GHRP-6 analogs was pursued possessing phenyl (**4.9**), 4-methoxyphenyl (**4.10**), 4-hydroxyphenyl (**4.11**) and 4-fluorophenyl (**4.12**) 5-position aryl substituents.

The [(4-Me,5-Ar)Nai[4]]-GHRP-6 analogs (**4.9**-**4.12**) were evaluated for capacity to modulate CD36 mediated overproduction of nitric oxide (NO) in macrophage cells after treatment with the TLR-2-agonist fibroblast-stimulating lipopeptide (R-FSL-1). Measured as nitrite, NO is an inflammatory pathway modulation marker, which plays an important role as mediator of macrophage responses to defend against pathogens. Chronic NO production may

however lead to damage of host tissues.[20] Reduction of nitrite production has been correlated with CD36 binding affinity and decreased production of pro-inflammatory cytokines and chemokines in macrophages.[21] The CD36 binding affinity of the [(4-Me,5-Ar)Nai^4]-GHRP-6 analogs will be examined using a competitive binding assay against photoactivatable [^{125}I]-Tyr-Bpa-Ala-hexarelin (H-[^{125}I]-Tyr-Bpa-Ala-His-D-2-methyl-Trp-Ala-Trp-D-Phe-Lys-NH_2) as radiotracer.[21]

Results and discussion

Chemistry

Enantioenriched (4-Me)Nai-D-Phe-OH (**4.15**) was synthesized by base promoted cyclisation of aza-propargylglycinyl-D-phenylalanine (**4.14**) using potassium *tert*-butoxide in THF (Scheme 1).[17] Imidazole-2-one **4.15** is most likely formed by a 5-endo-*dig* cyclization, followed by double bond isomerization.[22] Initial carboxylic acid deprotonation under the basic conditions and short reaction times minimize racemization of the D-Phe residue such that the Nai dipeptide was obtained in a 98:2 enantiomeric ratio as determined by supercritical fluid chromatographic analysis on a chiral support.[17]

Dipeptide acid **4.15** was coupled onto H-Lys(Boc)-rink amide resin using O-[(cyano(ethoxycarbonyl)-methyliden)amino]yloxytripyrrolidinophosphonium hexafluorophosphate (PyOxim) and DIEA in DMF to give Nai tripeptide resin **4.16**. Among different conditions investigated to install an aryl substituent at the 5-position of (4-Me)Nai **4.16**, sonication of the resin at 60°C in the presence of aryl iodide, palladium acetate and sodium acetate in degassed DMSO for 18h gave full conversion to (4-Me,5-Ar)Nai resins **4.17-4.20** (Scheme 1).[19] Aryl iodides with both electron withdrawing (-F, -O_2CO*t*-Bu) and donating (-OCH_3) groups reacted successfully. 4-Iodophenol was protected with an acid labile Boc group, because the unprotected phenol retarded the cross-coupling reaction in solution.[19] For the installation of the aryl substituent, diphenyl ketamine protection was essential for high conversion. Rink amide

resins possessing Fmoc-Ala-(4-Me)Nai-D-Phe-Lys(Boc)- and Boc-Ala-(4-Me)Nai-D-Phe-Lys(Boc)-peptides reacted with low conversion and degradation of starting material.

With (4-Me,5-Ar)Nai semicarbazone resins **4.17-4.20** in hand, conditions were investigated for the removal of the benzhydrylidene protection. Commonly employed methods for liberating semicarbazides from semicarbazones, such as hydroxylamine hydrochloride in pyridine,[23] and acidic conditions,[24] either returned starting material or gave concomitant resin cleavage. The additional steric hindrance imposed by the 5-position substituent retarded significantly transimination and solvolysis of the benzhydrylidene group. Successful removal of the benzhydrylidene protection without resin cleavage was achieved by using a modification of the transimination conditions. Semicarbazones **4.17-4.20** reacted with methoxyamine hydrochloride and citric acid in a mixture of dioxane and water using sonication at 60°C. Contingent on the aromatic substituent, (4-Me,5-Ar)Nai semicarbazide resins **4.21-4.24** were obtained after 18-72 h. Methoxyamine was chosen with the expectation of increasing nucleophilicity relative to hydroxyl amine.[25] Citric acid, which had previously been employed in transamination reactions of benzhydrylidene protected amino esters,[26] proved strong enough to facilitate the reaction of the semicarbazone with methoxyamine without causing resin cleavage.[26-27]

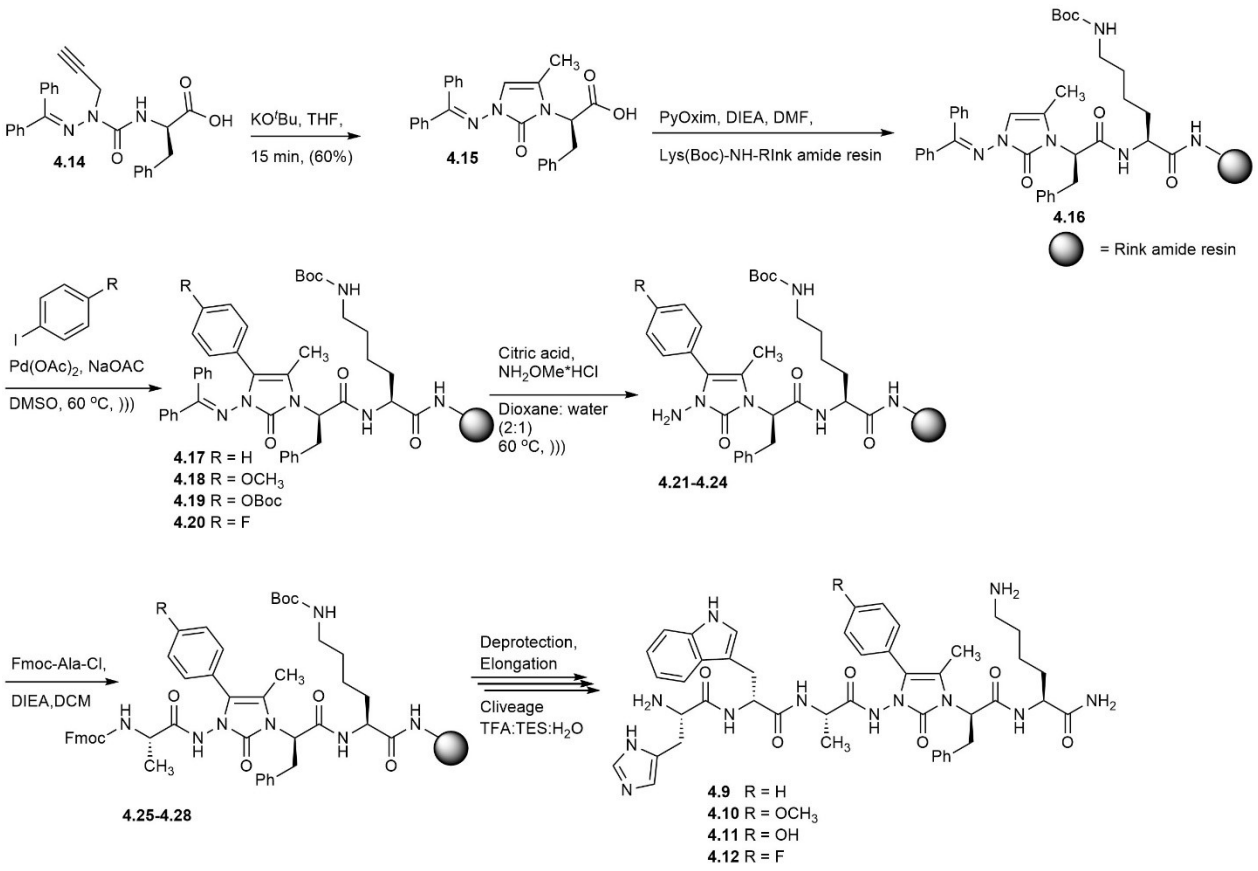

Scheme 4.1. [(4-Me,5-Ar)Nai^4]-GHRP-6 analog

Acylation of the sterically hindered and electronically deficient (4-Me,5-Ar)Nai semicarbazide resins **4.21-4.24** was effectively achieved using Fmoc-Ala-Cl, which was prepared by treatment of Fmoc-Ala-OH with bis-(trichloromethyl)carbonate (BTC) in DCM.[28-29] Elongation of Nai peptides **4.25-4.28** was performed using Fmoc group deprotections employing piperidine in DMF, and sequential peptide couplings with Fmoc-D-Trp(Boc)-OH and Fmoc-His(Tr)-OH using (2-(1H-benzotriazol-1-yl)-1,1,3,3-tetramethyluronium hexafluorophosphate (HBTU) and DIEA in DMF. The final [(4-Me,5-Ar)Nai^4]-GHRP-6 analogs **4.9-4.12** were cleaved from the resin and deprotected using a TFA:TES:H_2O (95:2.5:2.5 v/v/v) cocktail, and purified by RP-HPLC (Table 4.1).

Peptides 4.9-4.12 were isolated using RP-HPLC in sufficient yields for biological analyses. Overall yields were based on the measured resin loading. Yields were reduced in part due to H-His-Trp-Ala-NH_2 contaminant [m/z = 412.3 ($M+H^+$)], which appears to arrive from liberation of

capped resin under the conditions to remove the semicarbazone and subsequent peptide synthesis.

[(4-Me,5-Ar)Nai[4]]-GHRP-6 Ar = (4-X-Ph)	R*t* (Min)		Purity	HRMS [M+1]		Overall yield (%)[c]
	MeCN[a]	MeOH[b]		*Calc.*	*Experimental*	
4.9 (X = H)	7.49	7.32	>99	859.4662	859.4371	15
4.10 (X = OCH_3)	5.20	7.71	>90	889.4468	889.4468	3
4.11 (X = OH)	4.63	6.62	>90	875.4311	875.3819	9
4.12 (X = F)	5.17	7.47	>85	877.4278	977.4262	1

a: 10-90 % MeCN/H_2O; b: 10-90 % MeON/H_2O; c: isolated yield based on resin loading

Table 4.1. Retention times, purity and exact masses of [(4-Me,5-Ar)Nai[4]]-GHRP-6 analogs

Biology

Peptides **4.9-4.12** were evaluated for ability to attenuate overexpression of nitric oxide (NO) in RAW macrophage cells treated with the TLR-2 agonist R-FSL-1.[30] The selective and relatively potent CD36 ligand [azaY^4]-GHRP-6 was also tested as positive control.[13, 21] All four peptides **4.9-4.12** were able to modulate NO production in a statistically significant manner with similar potency as [azaY^4]-GHRP-6 (Figure 4.5). The [(4-Me,5-*p*-HOPh)Nai^4]-GHRP-6 analog (**4.11**) featuring a *para*-hydroxyl group was the least potent among [(4-Me,5-Ar)Nai^4]-GHRP-6 analogs **4.9-4.12**. On the other hand, [(4-Me,5-*p*-H_3COPh)Nai^4]-GHRP-6 (**4.10**) exhibited significantly higher activity than [azaY^4]-GHRP-6 in the nitric oxide assay (Figure 4.6). Moreover, [(4-Me,5-Ph and *p*-FPh)Nai^4]-GHRP-6 analogs (**4.9** and **4.12**) exhibited trends suggesting better performance than [azaY^4]-GHRP-6, but they were not statistically significant. In all cases, conformational constraint by the (4-Me,5-Ar)Nai^4 residue on the backbone and the χ-dihedral angles of the aza-GHRP-6 peptides appeared to retain or optimize ability to attenuate overexpression of NO in RAW macrophage cells treated with the TLR-2 agonist R-FSL-1.

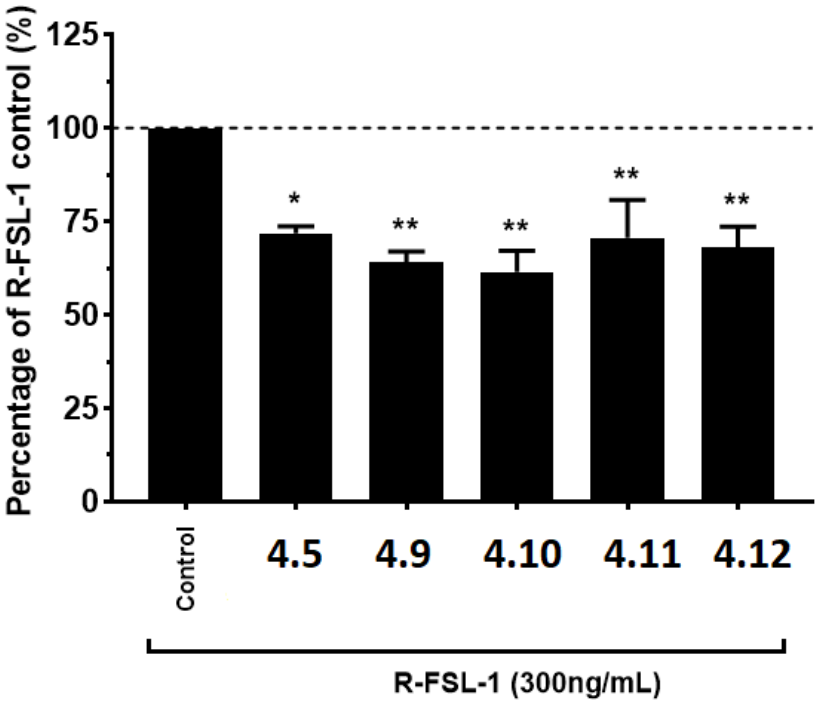

Fig. 4.5: Percentage of NO production reduction of peptides [aza-Tyr[4]]-GHRP-6 and **4.9-4.12**. ** p = 0.05; ** p = 0.01. n* = 18**.**

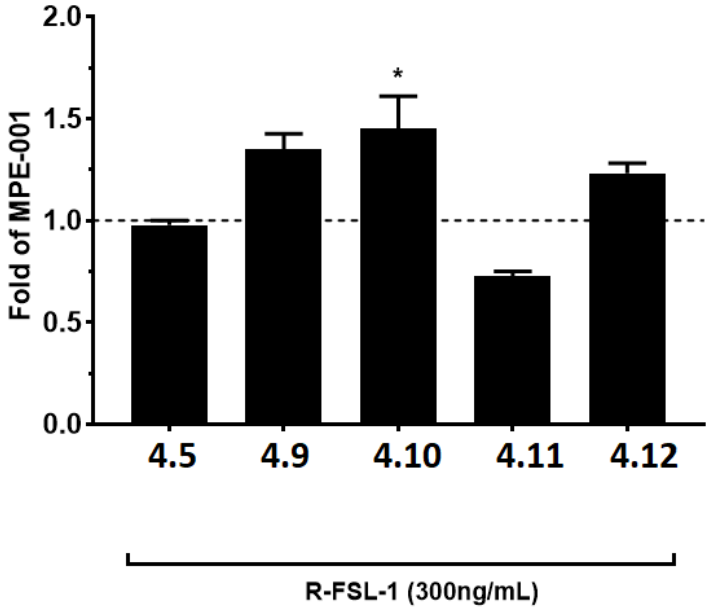

Figure 4.6: Activity of peptides **4.9-4.12** compared to [azaY[4]]-GHRP-6 (**4.5**, MPE-001). * *p = 0.05.*

The CD36 binding affinity of [(4-Me,5-Ar)Nai[4]]-GHRP-6 analogs **4.9-4.12** is currently being evaluated. In a typical experiment,[21] the [(4-Me,5-Ar)Nai[4]]-GHRP-6 analog will be examined in a competition displacement study with the photoactivable CD36 ligand [^{125}I]-Bpa-Ala-hexarelin. The competitions curves will reflect the relative binding affinities of [(4-Me,5-Ar)Nai[4]]-GHRP-6 analogs **4.9-4.12** against the high affinity binder hexarelin.

Discussion

Four [(4-Me,5-Ar)Nai[4]]-GHRP-6 analogs (**4.9-4.12**) were synthesized by a sequence commencing with introduction of benzhydrylidene protected (4-Me)Nai-D-Phe-OH dipeptide **4.15** into a peptide sequence bound to solid phase. Palladium catalysis proved effective for reacting both electron-rich and -deficient aryl iodides onto the 5-position of the imdazol-2-one residue on solid phase. Subsequently, the application of methoxyamine hydrochloride and citric acid in the transimination reaction removed the diphenylketimine protection and revealed the amine of the Nai residue, which upon acylation, peptide elongation and resin cleavage delivered the [(4-Me,5-Ar)Nai[4]]-GHRP-6 analogs.

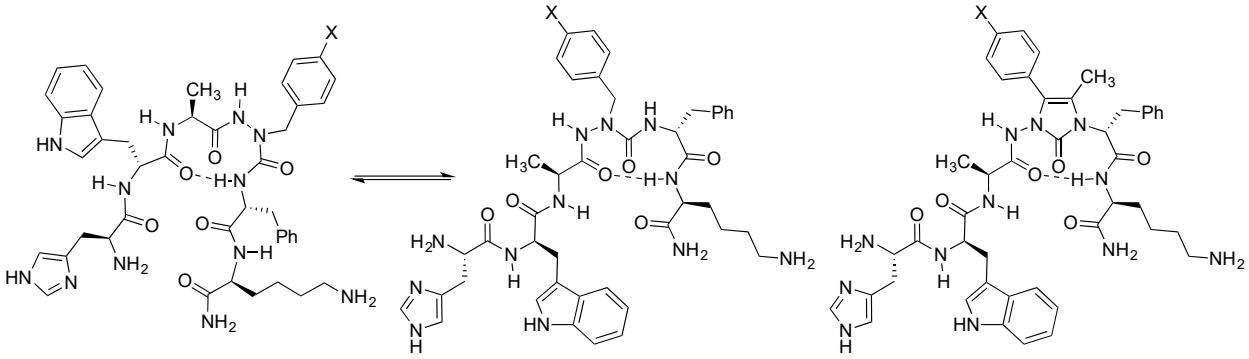

Figure 4.7: Possible conformations of [azaPhe[4]]-GHRP-6 analogs in which the semicarbazide adopts either the *i* + 2 (left) or *i* + 1 (center) positions of the central residues of a β-turn, and preferred conformer of [(4-Me,5-Ar)Nai[4]]-GHRP-6 analogs **4.9-4.12** (right) with Nai residue at *i* + 1 position.

Peptides **4.9-4.12**, all exhibited ability to modulate NO production in RAW macrophages cells treated with TLR-2 agonist R-FSL-1. Moreover peptide 4.10 featuring a 4-methoxyphenyl side chain was significantly more active than the reference compound [azaY[4]]-GHRP-6 (**4.5**).[13, 21]

Although their binding affinity is currently under investigation, the activity of peptides **4.9-4.12** indicate an active β-turn in which the Nai residue adopts the *i* + 1 location and the aryl 5-position substituent is situated in the *gauche* (-) orientation.

Azapeptides are known to adopt β-turn conformations in which the aza-residue situates in one of two central positions (*i* + 1 or *i* + 2, Figure 4.7).[31] Conformational analysis of [azaPhe^4]-GHRP-6 analogs by NMR spectroscopy has previously indicated amide temperature dependencies and long-range side chain interactions consistent with a turn geometry in which the D-Phe residue NH is engaged in an intramolecular hydrogen bond in aqueous solution.[11] Although such a conformation would situate the semicarbazide at the *i* + 2 position in a β-turn, its relevance for receptor binding has not been elucidated.[11] Moreover, related conformers in which the lactam residue is situated at the *i* + 1 position of a β-turn may account for the selectivity and CD36 binding affinity of [(*S*)-Agl^3]- and [(*R*)-Bgl^3]-GHRP-6.[15] In conflict with support for the semicarbazide at the *i* + 2 position in the active [azaPhe^4]-GHRP-6 conformer, [(4-Me,5-Ar)Nai^4]-GHRP-6 analogs **4.9-4.12** are expected to adopt an alternative β-turn conformation in which the Nai residue is situate at the *i* + 1 position. The activity of [(4-Me,5-Ar)Nai^4]-GHRP-6 analogs **4.9-4.12** appear to support a conformational dynamic for the [azaPhe^4]-GHRP-6 analogs in which the semicarbazide may toggle to the *i* + 1 position of a β-turn when receptor-bound.

Conclusion

N-Aminoimidazol-2-one (Nai) residues unite the stereo-electronic constraints of azapeptides and the covalent restrictions of α-amino γ-lactams to favor β-turn geometry in peptides.[11] Moreover, modification of the 4- and 5-positions of the Nai residue offers potential for adding substituents to mimic side chains with specific orientations. In peptides, (4-Me,5-Ar)Nai residue are predicted to adopt the *i* + 1 position of a β-turn with the aromatic substituent in the *gauche* (-) orientation.[19] Palladium-catalyzed arylation of the Nai 5-position by the solid-phase method presented herein offers an effective means to synthesize (4-Me,5-Ar)Nai peptides for studying the conformational preferences of aromatic amino acid residues. The synthesis and study of [(4-Me,5-Ar)Nai]-GHRP-6 analogs **4.9-4.12** has provided insight into the biologically active conformer of CD36 ligands. Considering the wealth of peptides possessing aromatic amino

acid residues, this solid-phase method for (4-Me,5-Ar)Nai peptide synthesis should find significant application for studying their purported turn conformers.

Experimental

General

Unless otherwise specified, all non-aqueous reactions were run under argon atmosphere. Analytical thin-layer chromatography (TLC) was performed on glass-backed silica gel-plates (Merck 60 F254). Visualization of the developed plates was performed by UV absorbance or staining with potassium permanganate, 2,4-dinitrophenyl hydrazine or bromocresol green. High resolution mass spectrometry was performed at the Centre régional de spectrométrie de masse de l'Université de Montréal. Polystyrene Rink Amide resin was purchased form Combi-Blocks, Inc. (San Diego, CA) and the extent of attachment of the first residue was ascertained by the Fmoc group loading test.[32] Reagents including methoxyamine hydrochloride, citric acid, trifluoroacetic acid (TFA), PyOxim™, sodium acetate, iodobenzene, 4-iodotoluene and 4-iodofluorobenzene, all were purchased from Sigma-Aldrich and used without further purification; $Pd(OAc)_2$ was purchased from Sigma-Aldrich and recrystallized from benzene. 4-Iodophenol was purchased from Combi-Blocks, Inc. and used without further purification. All solvents were obtained from VWR international except for dimethyl sulfoxide (Sigma-Aldrich). Anhydrous solvents (THF, MeCN, DCM and DMF) were obtained by passage through solvent filtration systems (Glass-Contour, Irvine, CA). Analytical LCMS analyses were performed on a C18 column using a gradient of 10-90% MeCN (0.1% FA) in water (0.1% FA) over 15 min (System A) and 10-90% MeOH (0.1% FA) in water (0.1% FA) (System B) over 15 min.

Solid-Phase Peptide Synthesis: Fmoc group deprotections and peptide couplings

Peptide syntheses were performed under standard conditions on polystyrene rink amide resin with agitation using an orbital shaker.[32] Couplings of amino acids (Fmoc-D-Trp(Boc)-OH and Fmoc-His(Tr)-OH, 3 equiv) were performed in DMF using either HBTU (3 equiv) and DIEA (6 equiv) in DMF for 2 hours. Following the first residue attachment, the resin was capped with a mixture of pyridine and acetyl anhydride (3:2) for 20 min. The Fmoc group was removed by treating the

resin with a 20% piperidine solution in DMF for 30 min. After each coupling and Fmoc-group removal step, the resin was washed sequentially with DMF (3 x 10 mL), ^{i}PrOH (3 x 10 mL) and DCM (3 x 10 mL). The purity of peptide fragments was ascertained by LCMS analyses after cleavage and deprotection of an aliquot (ca. 10 mg) of resin as described below.

***tert*-Butyl (4-iodophenyl) carbonate**

4-Iodophenol (2.00 g, 9.09 mmol) in DCM (18 mL) was treated with 4-dimethylaminopyridine (222 mg, 1.82 mmol) and di-*tert*-butyl dicarbonate (5.95 g, 27.3 mmol). After stirring for 18 h, the reaction mixture was poured into water (30 mL) and agitated. The organic layer was separated. The aqueous layer was extracted with DCM (2x 20 mL). The organic layers were combined, washed with 1 N NaOH (30 mL), sat. NH_4Cl (30 mL) and brine (40 mL), dried over magnesium sulfate, filtered and evaporated to a residue that was purified on silica gel using a Combiflash instrument and a gradient of 0-20% EtOAc in hexanes. Evaporation of the collected factions gave *tert*-butyl (4-iodophenyl) carbonate (contaminated with 50 % di-*tert*-butyl dicarbonate) as white low melting solid: R*f* = 0.55 (10 % EtOAc in hexanes); ^{1}H NMR (500 MHz, $CDCl_3$) δ 1.58 (s, 9H), 6.95-6.98 (m, 2H), 7.69-7.71 (m, 2H); $^{13}C[^{1}H]$ NMR (125 MHz, $CDCl_3$) δ 28.0, 67.1, 84.0, 89.8, 123.6, 138.5, 151.0, HRMS calc. for $C_{11}H_{14}IO_3$ $[M+H^+]$ = 320.9987 found = 320.9893.

Benzhydrylidene-(4-Me)Nai-D-Phe-Lys(Boc)-NH-Rink amide resin (4.16)

The Fmoc group was removed from Fmoc-Lys(Boc)-NH-Rink amide resin (1.0 g, 0.51 mmol/g, prepared according to reference[33]) using the conditions described above. The resin was swollen in DMF and treated sequentially with (*R*)-2-(3-((diphenylmethylene)amino)-5-methyl-2-oxo-2,3-dihydro-1H-imidazol-1-yl)-3-phenylpropanoic acid (**4.15**, 326 mg, 0.77 mmol, prepared according to reference[34]), PyOxim™ (405 mg, 0.77 mg) and DIEA (267 µL, 1.54 mmol). After agitation for 12h, the resin was filtered, washed as described above and freeze-dried. Complete coupling was indicated by examination of an aliquot of resin, which exhibited a negative Kaiser test.[35]

Benzhydrylidene-(4-Me,5-Ph)Nai-D-Phe-Lys(Boc)-NH-Rink amide resin 4.17

Resin **4.16** (0.1 mmol, 234 mg) was swollen in DMSO (2 mL) and treated successively with $Pd(OAc)_2$ (5 mg, 0.02 mml), NaOAc (25 mg, 0.3 mmol) and iodobenzene (63 mg, 0.3 mmol). The reaction mixture was treated with argon bubbles for 1 minute. The reaction vessel was flushed with argon, capped and agitated with sonication in a bath at 60 °C for 12 h. The vessel was cooled to room temperature. The resin was filtered and washed as described above. An aliquot of resin was cleaved with agitation in a 95:5 TFA:TIS mixture for 30 min, filtered, and the filtrate was evaporated to a residue that was dissolved in acetonitrile and analyzed by LCMS, which indicated complete conversion to benzhydrylidene-(4-Me,5-Ph)Nai-D-Phe-Lys-NH_2 (m/z = 729.7 ($M+H^+$), RT = 6.76 (System A). Using the respective iodides, (4-Me,5-Ar)Nai resins **4.18-4.20** were prepared by the same protocol, which gave complete conversion.

H-(4-Me,5-Ph)Nai-D-Phe-Lys(Boc)-NH-Rink amide resin 4.25

In a 7-mL vial, resin **4.17** (241 mg, 0.1 mmol) was swollen in dioxane (2 mL) and treated with 1 mL of a freshly prepared aqueous solution of citric acid (2M) and $MeONH_2{\cdot}HCl$ (2M). The vial was sealed, agitated with sonication and heated in a bath at 60 °C for 72 h. The vial was cooled to room temperature. The resin was filtered and washed as described above. An aliquot of resin was cleaved with agitation in a 95:5 TFA:TIS mixture for 30 min, filtered, and the filtrate was evaporated to a residue that was dissolved in MeCN and analyzed by LCMS, which indicated complete conversion to H-(4-Me,5-Ph)Nai-D-Phe-Lys-NH_2 (m/z = 565.1 ($M+H^+$)), RT = 4.36 min (System A). The corresponding (4-Me,5-Ar)Nai resins **4.22-4.24** were prepared using the same protocol which gave complete conversion after the respective times: **4.22**: 72 h; **4.23**: 24 h; **4.24**: 18 h.

Fmoc-Ala-(4-Me,5-Ph)Nai-D-Phe-Lys(Boc)-NH-Rink amide resin 4.25

A solution of Fmoc-Ala-OH (94 mg, 0.3 mmol) in DCM (3 mL) was treated with BTC (33 mg, 0.11 mmol), stirred for 30 minutes, treated with DIEA (89 µL, 0.5 mmol) and transferred to a syringe containing (4-Me,5-Ph)Nai peptide resin **4.21** (219 mg, 0.1 mmol). The syringe was capped and agitated for 6 h. The resin was filtered, washed with MeOH (3 x 10 mL) to destroy excess BTC, washed as described above and freeze-dried. An aliquot of resin was cleaved with agitation in a 95:5 TFA:TIS mixture for 30 min, filtered, and the filtrate was evaporated to a residue that was dissolved in MeCN and analyzed by LCMS, which indicated complete conversion

to Fmoc-Ala-(4-Me,5-Ph)Nai-D-Phe-Lys-NH_2 [m/z = 859.3 ($M+H^+$)], RT = 6.01 min (system A). The respective (4-Me,5-Ar)Nai resins **4.26-4.28** were prepared using the same protocol which gave complete conversions.

H-His-D-Trp-Ala-(4-Me,5-Ph)Nai-D-Phe-Lys-NH_2 (4.9)

Starting from resin **4.25** (248 mg, 0.1 mmol), sequential Fmoc group removals and peptide couplings with Fmoc-D-Trp(Boc)-OH and Fmoc-His(Tr)-OH using HBTU, DIEA and DMF as described above gave H-Ala-(4-Me,5-Ph)Nai-D-Phe-Lys(Boc)-NH-Rink amide resin, which was exposed to a solution of 90% TFA, 2.5 % H_2O and 2.5% TIS (3 mL) for 2h. The resin was filtered and washed twice with TFA. The filtrate and washings were combined and concentrated under vacuum and the concentrate was added to 50 mL of cold (–20°C) ethyl ether. The precipitated peptide was recovered by filtration, washed with cold ether (2 x 10 mL) and dried under vacuum for 1 h. Peptide **4.9** was purified by RP-HPLC using 5-90 % MeCN (0.1 % FA) in water (0.1 % FA). The collected fractions were concentrated under vacuum and freeze-dried to give peptide **4.9** as white solid.

Associated content

Supporting Information ^{1}H-NMR and ^{13}C spectra *tert*-butyl (4-iodophenyl) carbonate and LC-MS trace for Nai peptides **4.9-4.12**.

The following files are available free of charge. ^{1}H-NMR and ^{13}C spectra *tert*-butyl (4-iodophenyl) carbonate and chromatograms for Nai peptide **4.9-4.12** (PDF)

Author information

Corresponding Author

Phone, 514-343-7339; fax, 514-343-7586; E-mail, william.lubell@umontreal.ca.

ORICiD

Julien Poupart: 0000-0003-1164-5931

Duc Ngoc-Doan: 0000-0001-9672-2064

Mukandila Mulumba: 0000-0001-7708-7480

Huy Ong: 0000-0001-8459-2645

William D. Lubell: 0000-0002-3080-2712

Funding Sources

Natural Sciences and Engineering Research Council of Canada (NSERC) Discovery Research Project no. 04079.

Canadian Institutes of Health Research (CIHR) and NSERC for the Collaborative Health Research Project no. 462488.

Ministère du développement économique de l'innovation et de l'exportation du Québec (no. 878-2012, Traitement de la dégénerescence maculaire)

Amorchem

Fonds de recherche nature et technologie Quebec for the Centre in Green Chemistry and Catalysis (FRQNT-2020-RS4-265155-CCVC).

Acknowledgment

The authors thank the Natural Sciences and Engineering Research Council of Canada (NSERC) for funding for a Discovery Research Project no. 04079, the Canadian Institutes of Health Research (CIHR) and NSERC for the Collaborative Health Research Project no. 462488, the Ministère du développement économique de l'innovation et de l'exportation du Québec (no. 878-2012, Traitement de la dégénerescence maculaire) and Amorchem. The authors thank the Fonds de recherche nature et technologie Quebec for the Centre in Green Chemistry and Catalysis (FRQNT-2020-RS4-265155-CCVC). The authors thank the Universitéde Montreal and staff members of the regional center for Mass Spectrometry, Dr. Alexandra Fürtös and Karine Gilbert (Université de Montréal) for assistance with mass spectrometry.

Abbreviations

CD36, cluster of differentiation 36; DCM, Dichloromethane; DIEA, Diisopropilethylamine; DMF, Dimethylformamide; EtOAc, ethyl acetate; GPCR, G-protein-coupled receptor; MeCN, Acetonitrile; MeOH, Methanol; NO, nitric oxide; RP-HPLC, reverse-phase high-performance liquid chromatography; THF, Tetrahydrofuran; TLC, thin layer chromatography; TLR-2, Toll-like receptor 2

References

[1]. Park, Y. M., CD36, a scavenger receptor implicated in atherosclerosis. *Exp. Mol. Med.* **2014,** *46* (6), e99.

[2]. Stephen, S. L.; Freestone, K.; Dunn, S.; Twigg, M. W.; Homer-Vanniasinkam, S.; Walker, J. H.; Wheatcroft, S. B.; Ponnambalam, S., Scavenger receptors and their potential as therapeutic targets in the treatment of cardiovascular disease. Int. *J. Hypertens.* **2010,** *2010*, 1-21.

[3]. Mwaikambo, B.; Yang, C.; Ong, H.; Chemtob, S.; Hardy, P., Emerging roles for the CD36 scavenger receptor as a potential therapeutic target for corneal neovascularization. *Endo. Metab. Imm. Disord. Drug Targets (Formerly Current Drug Targets-Immune, Endocrine & Metabolic Disorders)* **2008,** *8* (4), 255-272.

[4]. Bujold, K.; Mellal, K.; Zoccal, K. F.; Rhainds, D.; Brissette, L.; Febbraio, M.; Marleau, S.; Ong, H., EP 80317, a CD36 selective ligand, promotes reverse cholesterol transport in apolipoprotein E-deficient mice. *Atherosclerosis* **2013,** *229* (2), 408-414.

[5]. Marleau, S.; Harb, D.; Bujold, K.; Avallone, R.; Iken, K.; Wang, Y.; Demers, A.; Sirois, M. G.; Febbraio, M.; Silverstein, R. L., EP 80317, a ligand of the CD36 scavenger receptor, protects apolipoprotein E-deficient mice from developing atherosclerotic lesions. *FASEB J.* **2005,** *19* (13), 1869-1871.

[6]. Bodart, V.; Bouchard, J.; McNicoll, N.; Escher, E.; Carriere, P.; Ghigo, E.; Sejlitz, T.; Sirois, M.; Lamontagne, D.; Ong, H., Identification and characterization of a new growth hormone–releasing peptide receptor in the heart. *Circ. Res.* **1999,** *85* (9), 796-802.

[7]. Triantafilou, M.; Gamper, F. G.; Haston, R. M.; Mouratis, M. A.; Morath, S.; Hartung, T.; Triantafilou, K., Membrane sorting of toll-like receptor (TLR)-2/6 and TLR2/1 heterodimers at the cell surface determines heterotypic associations with CD36 and intracellular targeting. *J. Biol. Chem.* **2006,** *281* (41), 31002-31011.

[8]. Yu, L.; Wang, L.; Chen, S., Endogenous toll-like receptor ligands and their biological significance. *J. Cell. Mol. Med.* **2010,** *14* (11), 2592-2603.

[9]. Imbimbo, B.; Mant, T.; Edwards, M.; Amin, D.; Dalton, N.; Boutignon, F.; Lenaerts, V.; Wüthrich, P.; Deghenghi, R., Growth hormone-releasing activity of hexarelin in humans. *Eur. J. Clin. Pharmacol.* **1994,** *46* (5), 421-425.

[10]. Frutos, M. G. a.-S.; Cacicedo, L.; Fernández, C.; Vicent, D.; Velasco, B.; Zapatero, H.; Sánchez-Franco, F., Insights into a role of GH secretagogues in reversing the age-related decline in the GH/IGF-I axis. *Am. J. Physiol. Endocrinology and Metabolism* **2007,** *293* (5), E1140-E1152.

[11]. Sabatino, D.; Proulx, C.; Pohankova, P.; Ong, H.; Lubell, W. D., Structure–Activity Relationships of GHRP-6 Azapeptide Ligands of the CD36 Scavenger Receptor by Solid-Phase Submonomer Azapeptide Synthesis. *J. Am. Chem. Soc.* **2011,** *133* (32), 12493-12506.

[12]. Boeglin, D. R.; Bodas, M. S.; Galaud, F.; Lubell, W. D., Positional Scanning for Peptide Secondary Structure by Solid Phase Synthesis with Aza-Amino Acids and Freidinger Lactams. In *Understanding Biology Using Peptides*, Springer: 2006; pp 47-49.

[13]. Proulx, C.; Picard, E.; Boeglin, D.; Pohankova, P.; Chemtob, S.; Ong, H.; Lubell, W. D., Azapeptide analogues of the growth hormone releasing peptide 6 as cluster of differentiation 36 receptor ligands with reduced affinity for the growth hormone secretagogue receptor 1a. *J. Med. Chem.* **2012,** *55* (14), 6502-6511.

[14]. Mellal, K.; Omri, S.; Mulumba, M.; Tahiri, H.; Fortin, C.; Dorion, M.-F.; Pham, H.; Ramos, Y. G.; Zhang, J.; Pundir, S., Immunometabolic modulation of retinal inflammation by CD36 ligand. *Sci. Rep.* **2019,** *9* (1), 1-18.

[15]. Boutard, N.; Jamieson, A. G.; Ong, H.; Lubell, W. D., Structure–Activity Analysis of the Growth Hormone Secretagogue GHRP-6 by α-and β-Amino γ-Lactam Positional Scanning. *Chem Biol Drug Des.* **2010,** *75* (1), 40-50.

[16]. St-Cyr, D. J.; García-Ramos, Y.; Doan, N.-D.; Lubell, W. D., Aminolactam, N-aminoimidazolone, and N-aminoimdazolidinone peptide mimics. In *Peptidomimetics I*, Springer: 2017; pp 125-175.

[17]. Proulx, C.; Lubell, W. D., N-Amino-imidazolin-2-one Peptide Mimic Synthesis and Conformational Analysis. *Org. Lett.* **2012,** *14* (17), 4552-4555.

[18]. Proulx, C.; Lubell, W. D., Analysis of N-amino-imidazolin-2-one peptide turn mimic 4-position substituent effects on conformation by X-ray crystallography. *Peptide Science* **2014,** *102* (1), 7-15.

[19]. Poupart, J.; Doan, N.-D.; Berube, D.; Hamdane, Y.; Medena, C.; Lubell, W. D., Palladium-Catalyzed Arylation of N-aminoimidazol-2-ones Towards Synthesis of Constrained Phenylalanine Dipeptide Mimics. *Heterocycles* **2019,** *99* (1), 279-293.

[20]. Korhonen, R.; Lahti, A.; Kankaanranta, H.; Moilanen, E., Nitric oxide production and signaling in inflammation. *Curr. Inflamm. Allergy Drug Targets* **2005,** *4* (4), 471-479.

[21]. Chignen Possi, K.; Mulumba, M.; Omri, S.; Garcia-Ramos, Y.; Tahiri, H.; Chemtob, S.; Ong, H.; Lubell, W. D., Influences of Histidine-1 and Azaphenylalanine-4 on the Affinity, Anti-inflammatory, and Antiangiogenic Activities of Azapeptide Cluster of Differentiation 36 Receptor Modulators. *J. Med. Chem.* **2017,** *60* (22), 9263-9274.

[22]. Casnati, A.; Perrone, A.; Mazzeo, P. P.; Bacchi, A.; Mancuso, R.; Gabriele, B.; Maggi, R.; Maestri, G.; Motti, E.; Stirling, A. s., Synthesis of Imidazolidin-2-ones and Imidazol-2-ones via Base-Catalyzed Intramolecular Hydroamidation of Propargylic Ureas under Ambient Conditions. *J. Org. Chem.* **2019,** *84* (6), 3477-3490.

[23]. Sabatino, D.; Proulx, C.; Klocek, S.; Bourguet, C. B.; Boeglin, D.; Ong, H.; Lubell, W. D., Exploring side-chain diversity by submonomer solid-phase aza-peptide synthesis. *Org. Lett.* **2009,** *11* (16), 3650-3653.

[24]. Horoiwa, S.; Yokoi, T.; Masumoto, S.; Minami, S.; Ishizuka, C.; Kishikawa, H.; Ozaki, S.; Kitsuda, S.; Nakagawa, Y.; Miyagawa, H., Structure-based virtual screening for insect ecdysone receptor ligands using MM/PBSA. *Biorg. Med. Chem.* **2019,** *27* (6), 1065-1075.

[25]. Mayr, H.; Ofial, A. R., Do general nucleophilicity scales exist? *J. Phys. Org. Chem.* **2008,** *21* (7-8), 584-595.

[26]. Lygo, B.; Beynon, C.; McLeod, M. C.; Roy, C.-E.; Wade, C. E., Application of asymmetric phase-transfer catalysis in the enantioselective synthesis of cis-5-substituted proline esters. *Tetrahedron* **2010,** *66* (46), 8832-8836.

[27]. Johnston, H. J.; McWhinnie, F. S.; Landi, F.; Hulme, A. N., Flexible, phase-transfer catalyzed approaches to 4-substituted prolines. *Org. Lett.* **2014,** *16* (18), 4778-4781.

[28]. Thern, B.; Rudolph, J.; Jung, G., Triphosgene as highly efficient reagent for the solid-phase coupling of N-alkylated amino acids—total synthesis of cyclosporin O. *Tetrahedron Lett.* **2002,** *43* (28), 5013-5016.

[29]. Falb, E.; Yechezkel, T.; Salitra, Y.; Gi1on, C., In situ generation of Fmoc-amino acid chlorides using bis-(trichloromethyl) carbonate and its utilization for difficult couplings in solid-phase peptide synthesis. *J. Pept. Res.* **1999,** *53* (5), 507-517.

[30]. Zhang, J.; Mulumba, M.; Ong, H.; Lubell, W. D., Diversity-Oriented Synthesis of Cyclic Azapeptides by A3-Macrocyclization Provides High-Affinity CD36-Modulating Peptidomimetics. *Angew. Chem.* **2017,** *56* (22), 6284-6288.

[31]. Proulx, C.; Sabatino, D.; Hopewell, R.; Spiegel, J.; García Ramos, Y.; Lubell, W. D., Azapeptides and their therapeutic potential. *Future med. chem.* **2011,** *3* (9), 1139-1164.

[32]. Lubell, W.; Blankenship, J.; Fridkin, G.; Kaul, R., Peptides. Science of Synthesis 21.11, Chemistry of Amides. Thieme: Stuttgart, Germany: 2005.

[33]. Marine, J. E.; Liang, X.; Song, S.; Rudick, J. G., Azide-rich peptides via an on-resin diazotransfer reaction. *Peptide Science* **2015,** *104* (4), 419-426.

[34]. Poupart, J. Hamdane, Y.; Lubell, W. D., Synthesis of enantiomerically enriched 4,5-disubstituted N-aminoimidazol-2-one (Nai) peptide turn mimics. *Under revision* **2019**.

[35]. Kaiser, E.; Colescott, R.; Bossinger, C.; Cook, P., Color test for detection of free terminal amino groups in the solid-phase synthesis of peptides. *Anal. Biochem.* **1970,** *34* (2), 595-598.

Chapter 5

Perspectives and Conclusion

5.1 Significance of the thesis

Having tools to mimic turn conformers is crucial to map receptors and help get an idea on SAR, and eventually for the development of peptide-based drugs. Many approaches are now available.[45, 59, 63, 80, 155-157] Among them, the Nai residue offers potential to promote the formation of both type II' β-turns as well as inverse γ-turns.[75, 82, 83] These particular heterocycles have many advantages over other methods, partly due to the high rigidity brought on by the *N*-aminoimidazolone ring. The other advantage is that substitution on both side of the alkene is possible. In the case of the more interesting 5- position, where the side chain of a natural amino acid would be located, functionalization can be made after ring synthesis, and on solid support in many cases. Finally, the steric interactions between the two substituents rigidify the side chain surrogate and offer the opportunity to explore χ-space.[26]

Among challenges for introducing Nai residue into peptides, the cyclization reaction of azaPra residues had previously given racemic material. Chiral SFC could be employed to obtain enantiomerically pure product. The necessity for specialized equipment and the maximum 50% theoretical yield for a desired enantiomer are however limitations that restricted applications of Nai residues in studies of biologically active peptides.[158]

Another drawback of the pre-existing methods was lack of access to 5-position substituents. Cyclization of aza-propargyl residues had provided access to Nai residues with 4-position substituents, which may mimic the *trans* side chain geometry. Ability to place side chain functionality at the 5-position of the heterocycle would offer access to *gauche* orientations commonly adopted by amino acids in natural peptides.

In the first part of this thesis, strategies have been pursued to obtain (4-Me)Nai residues without loss of enantiomeric purity. Changes in reaction conditions and the use of different *C*-terminal groups has increased the enantiomeric ratio (*er*) of product from 90:10,[75] up to 98:2.[159] In cyclization of aza-Pra dipeptide esters, experiments using the relatively weaker base (KO^tBu), shorter reaction times and THF as a less polar solvent, all had limited effects on minimizing racemization. On the other hand, changing from a *C*-terminal ester to the corresponding aza-Pra

dipeptide acid and hydrazide reduced racemization and enabled potential for further functionalization.

For the functionalization of the 5-position of Nai residue imidazol-2-ones, three novel synthetic methods have been presented in the thesis. As discussed in Chapter 2, formylation of the Nai 5-position was made possible using the Vilsmeier-Haack reaction conditions to afford the corresponding aldehyde. The aldehyde offered a gateway to other substituents including alcohol, carboxylic acid and amine substituents. Furthermore, amino alkylation of the Nai 5-position under Mannich conditions was used to introduce amine substituents. In addition, palladium-catalyzed chemistry has enabled aryl substituents to be added to the Nai 5-position.

With the ultimate goal of introducing sets of Nai resides possessing side chain functional groups into peptides, several challenges associated with sequence diversification and elongation were surmounted in Chapter 4. Employing a solid-phase strategy, multiple aryl groups were added to a Nai peptide linked to resin; however, the diphenylketamine protection proved essential for obtaining high yields in the palladium-catalyzed aryl addition chemistry. Cleavage of the diphenylketamine protection was explored using a variety of conditions and achieved by treating the (5-aryl)Nai resin using a mixture of citric acid and $MeONH_2$ in aqueous dioxane. Elongation of the resulting sterically hindered and electronically deficient semicarbazide was accomplished by employing *N*-(Fmoc)amino acid chlorides. Subsequent elongation using standard solid-phase peptide synthesis afforded a set of (5-aryl)Nai peptides.

The chemistry of imidazole-2-ones has been significantly advanced in the context of the thesis. Several paths of inquiry were explored during these studies. The promise of certain directions merits some discussion in this chapter, which is designed to give an outlook onto other potential projects featuring the Nai residue.

5.2 Earlier attempt at cyclization

As mentioned in chapter 2, other cyclisation strategies were attempted to avoid de the use of base and associated epimerization. For example, TBAF was completely ineffective and

starting material was recovered quantitatively. A promising result occured from using a combination of silver and gold catalysis (figure 5.1). Treatment of aza-Pra peptide **5.1** with silver nitrate caused cleavage of the diphenylketimine protection producing benzophenone which was identified by both TLC and LC-MS analyses. On the contrary, aza-Pra peptide **5.1** failed to cyclize in the presence of 2-(di-tert-butylphosphino)biphenyl (JohnPhos) gold(I) chloride and starting material was recovered. Employing both JohnPhos gold(I) chloride and silver nitrate in the reaction of **5.1** in THF at room temperature gave (4-Me)Nai dipeptide **5.3**. Best conditions were achieved using 300 mol% of both silver and gold salts relative to aza-Pra peptide **5.1** which provided (4-Me)Nai dipeptide **5.3** in 23% yield along with recovered alkyne **5.1** (30%). Use of lower amounts of both silver and gold salts decreased the yield of Nai dipeptide **5.3**. The conditions appear to support a mechanism featuring a Ag^{+}/Au^{+} bimetallic catalyst.[160] Notably, the specific rotation of Nai dipeptide **5.3** ($[\alpha]_D^{23}$ = 23.6, *c* 1.2, MeOH) prepared using the combination of gold and silver catalysis suggested that no epimerization occurred. Although further optimization of the gold and silver catalysis conditions may be merited, the stoichiometry and high price of the metals involved in the reaction conditions restrict the current method's practical utility.

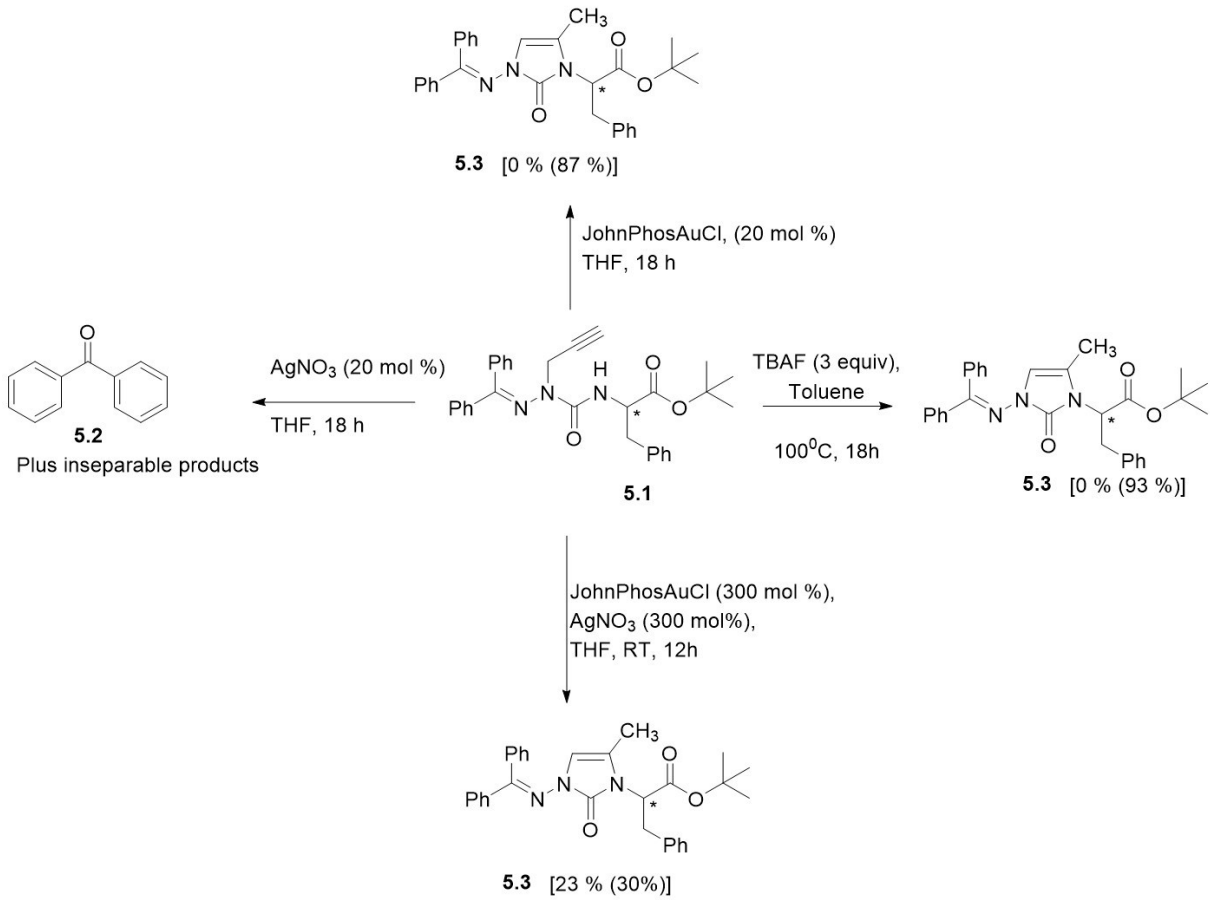

Figure 5.1: Synthesis of (5-Me)Nai peptide **5.3** using a combination of gold and silver catalysis.

5.3 Introduction of aminomethyl substituents at the 4-position

The copper catalyzed alkyne-aldehyde-amine (A^3) reaction on aza-Pra substrate has provided a variety of aza-4-aminobut-2-ynylglycine residues.[59, 161] Cyclization of the latter substrates would afford (4-aminomethyl)Nai residues to complement the (5-aminomethyl)Nai analogs prepared by reductive amination and Mannich reactions presented in Chapter 2. Towards this objective, Fmoc and benzhydrylidene protected aza-4-aminobut-2-ynylglycine residues **5.9** and **5.10** were respectively synthesized by A^3 reactions using the respective aza-Pra substrates, diallylamine and paraformaldehyde in dioxane (Scheme 5.1).[59]

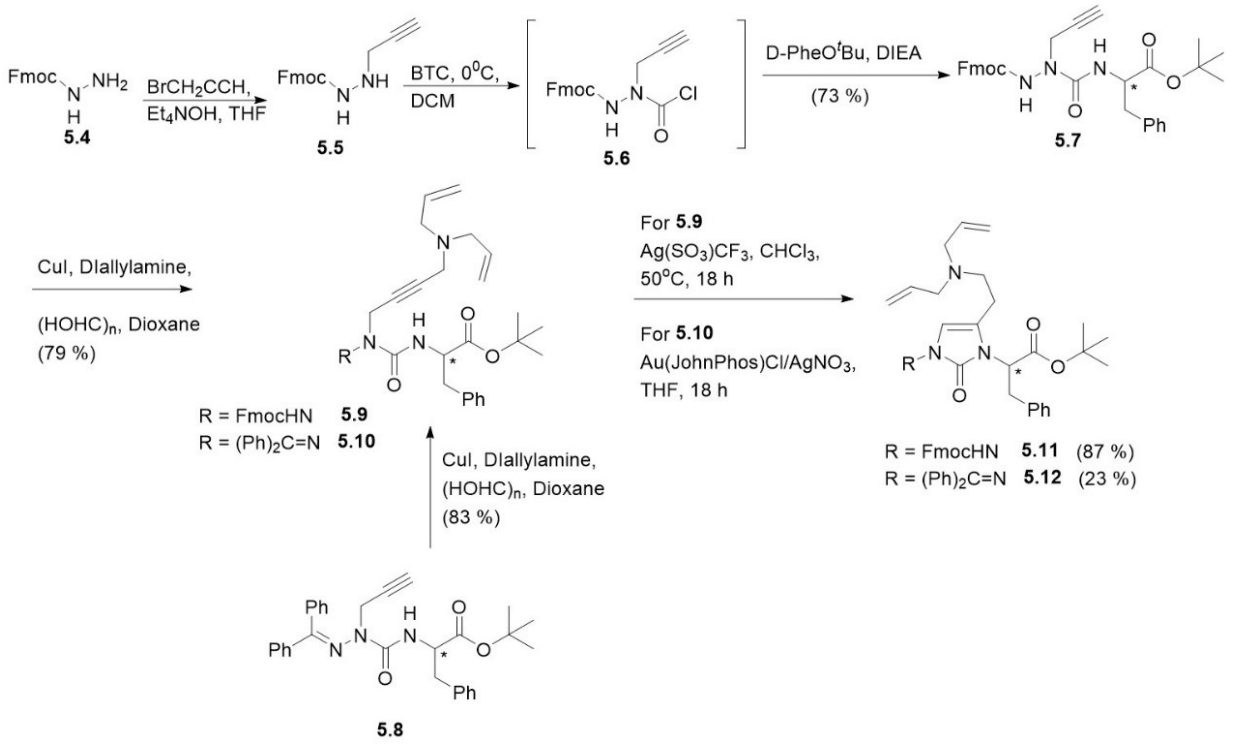

Scheme 5.1: Synthesis of (4-*N*,*N*-diallylaminoethyl)Nai peptides **5.11** and **5.12**

Diphenylketimine protection has been used effectively in A^3 reactions of aza-Pra residues.[59, 161] Attempts to cyclize benzhydrylidene protected aza-4-aminobut-2-ynylglycine **5.10** were however unsuccessful under basic conditions such as potassium *tert*-butoxide in THF, as well as sodium hydride in acetonitrile (Table 5.1).[75] On the other hand, cyclization of benzhydrylidene and Fmoc protected aza-4-aminobut-2-ynylglycine residues **5.9** and **5.10** occurred using transition metal catalysis. The Fmoc protected aza-dipeptide **5.9** was prepared by alkylation of carbazate **5.4** using propargyl bromide in THF,[162] activation of the resulting carbazate **5.5** as the corresponding aza-amino acid chloride **5.6** using bis-(trichloromethyl)carbonate (BTC), and amino ester acylation (Scheme 5.2).

Entry	**5.19/10 *N*-protection**	Conditions	% yield **5.11/12**
1	$(Ph)_2C=$	KO^{t}Bu (3eq), THF, 18 h	0

2	$(Ph)_2C=$	NaH (3eq), MeCN, 18 h	Traces
3	$(Ph)_2C=$	Au(JohnPhos)Cl (3eq)/$AgNO_3$ (3eq), THF, 18 h	23 %
4	Fmoc	Au(JohnPhos)Cl (3eq)/$AgNO_3$ (3eq), THF, 18 h	40 %
6	Fmoc	$AgNO_3$ (3eq), THF, 50^oC, 12h	30 %
7	Fmoc	AgO_3SCF_3 (3 eq), THF, 50^oC, 12h	87 %

Table 5.1: Synthesis of (4-aminomethyl)Nai peptides **5.11** and **5.12**.

Gold catalysis alone had little effect on cyclization, but in the presence of silver nitrate, JohnPhos gold(I) chloride caused cyclization of both Fmoc and benzylhydrene protected aza-4-aminobut-2-ynylglycine residues **5.9** and **5.10** in 40 % and 23 % (m/z = 613.3153, $M+Na^+$) respective yields. Moreover, silver nitrate alone induced cyclization of Fmoc protected aza-4-aminobut-2-ynylglycine residue **5.9** in 30 % yield. Silver triflate had previously been used to promote cyclization to form furan,[163] oxazole[164] and isoquinoline products.[165] Employment of silver triflate in the cyclization of aza-4-aminobut-2-ynylglycine **5.9** gave 87% isolated yield (entry 7). Attempts failed however to perform the reaction using catalytic amounts of silver triflate; instead, 3 equivalents were needed to complete the reaction in a timely fashion.

Although epimerization during cyclization was not examined, the silver promoted cyclization may likely afford enantiomerically enriched (4-aminoethyl)Nai residues for introduction into biologically interesting peptides. The 4-(*N*,*N*-diallyl)aminobut-2-ynylglycine residue has exhibited interesting activity in GHRP-6 analogs.[166] Cyclization of this residue may provide information regarding the conformer and structural requirements for biological activity. Moreover, the diallylamine protection may be removed using palladium catalysis to yield a primary amine.[167] In principle, (4-(*N*,*N*-diallyl)aminoethyl)Nai **5.11** may be introduced into peptides after removal of the *tert*-butyl ester using trifluoroacetic acid in dichloromethane. The synthesis of (4-aminoethyl)Nai peptides would then proceed by coupling to peptide bound to resin, Fmoc group cleavage using piperidine in DMF, acylation of the Nai residue using conditions described in Chapter 4, elongation and resin cleavage.

5.4 Introduction of Nai subunits on resin.

As described in Chapter 4, (4-Me)Nai dipeptides have been introduced into peptides bound to resin using standard coupling conditions and solid-phase chemistry. Many efforts were deployed to construct the Nai scaffold directly from aza-Pra residues in peptides attached to solid supports. Various attempts using transition metal catalysis have given little cyclized product. On the other hand, treatment of aza-Pra-D-Phe-Lys(Boc)-Rink amide resin with potassium *tert*-butoxide (3 eq.) in THF gave 20% conversion to the corresponding (4-Me)Nai peptide after 24 h; however, further treatment with alkoxide decreased purity without improving cyclisation yield. In addition, attempts to formylate (4-Me)Nai peptide bound to Rink amide resin were unsuccessful using various Vilsmeier-Haack reaction conditions.

As mentioned, the (4-Me,5-formyl)Nai residue has been used in reductive, oxidative and reductive amination chemistry. Aldehyde functions participate in a rich variety of chemistry.[168, 169] Several reactions may merit further investigation. For example, the Baylis-Hillman reaction on the Nai aldehyde could provide a conjugated system and in a preliminary experiment provided a diastereomeric mixture that was characterized by crude NMR and HRMS. The Henry reaction using nitromethane and sodium hydroxide gave mixtures of nitro olefin and 1,3-dinitro-2-propyl products, which were characterized by NMR. Mild conditions for Friedel-Crafts type acylation of pyrroles may prove effective for adding acyl substituents to the Nai 5-position.[170] The alcohol of (4-Me,5-hydroxymethyl)Nai dipeptide **2.20** was converted to the corresponding chloride **5.13** using *N*-chloro succinimide (NCS), triphenylphosphine and imidazole in DCM.[171] Chloride displacement with different nucleophiles merits further exploration.

5.5 Conclusions

The *N*-aminoimidazol-2-one (Nai) residue is a promising system for introducing conformational constraint into peptide structures. The combined roles of the imidazolone ring

and the azapeptide moiety gives an extremely rigid amino acid surrogate. Moreover, the ability to functionalize the 5 position after ring synthesis is a considerable asset.

This thesis has developed three pertinent synthetic advances for the effective application of Nai residues in peptide mimicry. First, methods for the synthesis of enantiomerically enriched Nai residues have been developed by employing aza-Pra dipeptide acids and hydrazides under base promoted cyclization conditions (Chapter 2). The resulting Nai dipeptide acids have subsequently been used to make enantiomerically pure peptides for biological studies.

Second, a variety of 5-position substituents have been added to the imidazol-2-one to mimic different amino acid side chains with *gauche* orientations in χ-space. For example, the Vilsmeier-Haack formylation provided a 5-position aldehyde group that was converted into acid, alcohol and amine analogs by oxidation, reduction or reductive amination chemistry yielding constrained Asp, Hse and Dab residues. The Mannich reaction provided an alternative entry to Dab analogs. Chemistry for aryl groups additions to Nai residues was demonstrated initially in solution and later on solid phase (Chapter 3). Palladium catalysis enabled a wide range of aryl groups to be introduced at the Nai 5-position to prepare constrained Phe and Tyr analogs.

Finally, effective methods were conceived for the solid-supported synthesis of 5-position substituted Nai peptides (Chapter 4). The palladium-catalyzed arylation conditions were adapted for solid-phase synthesis of (4-Me,5-Ar)Nai residues with high conversion. Solid-phase methods were also developed for the removal of the diphenylketimine protecting groups and for acylation of sterically demanding and electronically deficient semicarbazides. Four [(4-Me,5-Ar)Nai^4]-GHRP-6 analogs were prepared using these solid-phase protocols, which should be amenable to study a variety of other biologically active peptides.

Towards understanding the conformational preferences of 4,5-disubstituted Nai residues, this thesis has presented computational analyses of model (4-Me,5-Ar)Nai peptides. Employing coordinates from previously crystallized 4-Me-Nai dipeptide motifs, molecular modeling of the corresponding [4-Me,5-*p*-hydroxyphenyl)Nai dipeptide demonstrated that the aryl substituent had little impact on the backbone dihedral angles (φ and ψ) which maintained a β-turn geometry.[75] A combination of the location of the aryl group at the heterocycle 5-position and

steric interactions with the neighboring methyl group oriented the hydroxyphenyl substituent in a *gauche* (–) conformation.[26] The (4-Me,5-Ar)Nai residues employ covalent, stereo-electronic and steric constraints to predispose aromatic amino acids at the *i* + 1 position of β-turns with *gauche* (–) side chain geometry. The combined effect of inducing a turn conformation while placing the aromatic side chain in the natural geometry has tremendous potential to mimic natural aromatic turn structure. Moreover, since the arylation conditions can be employed with a wide range of aryl iodide coupling partner, Unnatural aromatic group can be introduced at the *i* + 1. This can be exploited by synthetizing libraries of peptidomimetic compounds and help understanding the SAR of a bioactive peptide featuring an aromatic β-turn.

In the context of peptide-based medicinal chemistry, this thesis has presented the synthesis of four [4-Me,5-Ar)Nai^4]-GHRP-6 analogs and preliminary study of their biological activity. Four different coupling partners featuring Phenyl, electron donating phenol (EDG) and 4-Methoxy phenyl and electron withdrawing group (EWG) 4-Fluoro phenyl. The choice of 4-substitued aryl groups is based upon previous work where substitution at other position on the ring were detrimental to binding.[85] In macrophages treated with the Toll-like receptor (TLR)-2 agonist R-FSL-1, the Nai analogs reduced overexpression of induced nitric oxide (NO). All four Nai peptides were active in this assay. Moreover, peptide **4.10** exhibited improved activity relative to [azaY^4]-GHRP-6, which has previously demonstrated both low micromolar activity for CD36 and a significant antiangiogenic action in mouse choroidal explants.[85] Combined with the conformational analysis described above, the activity of the [4-Me,5-Ar)Nai^4]-GHRP-6 analogs on NO production demonstrate the presence of an aromatic turn at the 4-position in the biologically active conformer responsible for CD36 modulation to mediate TLR-2 induced inflammation. These results are significant in order to acquire a better understanding of the active conformation needed to strongly bind CD36 and move towards the development of peptide or peptidomimetic drugs that could be used to treat angiogenic diseases, AMD and protect against cardiopathies by modulating CD36.

In conclusion, methodologies were developed to minimize epimerization during azaPra cyclization by using KO^{t}Bu in THF, short reaction times and varying the *C*-terminal group. Vilsmeier formylation allowed to install an aldehyde functionality at the 5-position which was

later derivatized to an alcohol, a carboxylate group and different substituted amine group. Mannich conditions also allowed acylation at the 5 position. Palladium-catalyzed arylation gave 4-Me, 5-Aryl-Nai where the aryl group could be substituted in *o*,*m* or *p* and bear both EWG and EDG. This methodology was then adapted to solid support and 4 different [4-Me, 5-Aryl-Nai[4]]-GHRP-6. Biological evaluation showed that they were all able to modulate CD36 by reducing Tlr2-mediated inflammation. These results demonstrate that Nai residues can be introduced in peptides whose active conformation feature a turn structure. Different substitution on the heterocycle can help map out SAR in both Ramachandran and Chi space. Considering this, the main objectives of the thesis, which were to develop Nai chemistry in order to have synthesis improved, introduce 5-substituents and put them in a biologically active peptide have been met. There is still work to be done to fully exploit some of the analogs made, as seen in this chapter, and possibly some other use to Nai residues. Those different potential analogs would be built upon the work presented in this thesis.

Experimental

General

Unless specified, all reactions were performed under argon atmosphere. All glassware was stored in the oven or flame-dried and let cool under inert atmosphere prior to use. Anhydrous solvents were obtained either by filtration through drying columns (DCM, THF, MeCN, DMF) in a GlassContour system (Irvine, CA) or by distillation over CaH_2 (MeOH, $CHCl_3$). *tert*-Butyl 2-(3-((diphenylmethylene)amino)-5-methyl-2-oxo-2,3-dihydro-1*H*-imidazol-1-yl)-3-phenylpropanoate was synthesized according to the literature procedure.[75] All other starting materials, reagents and chemicals were purchased from commercial suppliers and used without further purification. Reaction progress was monitored by thin layer chromatography (TLC) on silica gel plates, which were visualized under UV light (254 nm) and by staining with $KMnO_4$, 2,4-dinitrophenylhydrazine (DNPH) and bromocresol green. Flash chromatography[172] was performed using either 230-400 mesh silica gel from SiliCycle Inc. or on a CombiFlash instrument from Teledyne using RediSep Gold columns. Nuclear magnetic resonance spectra (^1H, ^{13}C and COSY NMR) were recorded either on Bruker AMX 300, AV 400, AVII 400 or AMX 500

spectrometers. Specific rotations were determined on a Perkin-Elmer 341 polarimeter at 589 nm sodium-D line using a 0.5 dm cell and are reported as follow $[\alpha]_{\lambda}^{\text{temperature (°C)}}$, concentration (*c* in g/100 mL), and solvent. High resolution mass spectrometry (HRMS) was performed by the Centre régional de spectroscopie de masse de l'Université de Montréal.

(9*H*-fluoren-9-yl)methyl (*R*)2-((1-(tert-butoxy)-1-oxo-3-phenylpropan-2-yl)carbamoyl)-2-(4-(diallylamino)but-2-yn-1-yl)hydrazine-1-carboxylate (5.9)

azaPra **5.7** (100 mg, 0.2 mmol) was dissolved in dioxane (2 mL) in a sealed vessel and treated sequentially with copper (I) iodine (4 mg, 0.02 mmol), paraformaldehyde (30 mg, 0.4 mmol) and diallylamine (34 µL, 0.3 mmol). The reaction mixture was heated for 6 h. After cooling down, the reaction mixture was partitioned between water (10 mL) and EtOAc (10 mL). Layers were separated and the aqueous phase was extracted with EtOAc (2*10 mL). The combined organic layers were washed with sat. NH_4Cl until the blue color disappeared (indicating removal of copper residues) then with water (1* 20 mL) and brine (1* 20 mL). The organic layer was dried over magnesium sulfate and evaporated to a residue which was purified by column chromatography eluting with 0-100 % EtOAc/hexanes. Evaporation of collected fraction gave **5.9** as a pale-yellow foam (95 mg, 79 %): R*f* = 0.34 (5 % MeOH/DCM); $[\alpha]_D^{23}$ 13.6 (*c* 0.64, $CHCl_3$), ^{1}H NMR (500 MHz, $CDCl_3$) δ 1.41 (s, 9H), 3.05-3.09 (m, 6H), 3.32-3.3.35 (m, 2H), 4.21-4.22 (m, 1H), 4.47-4.74 (m, 6H), 5.12-5.22 (m, 5H), 5.75-5.81 (m, 2H), 6.98 (br. s, 1H), 7.07-7.78 (m, 13 H). ^{13}C NMR (125 MHz, $CDCl_3$) δ 28.0, 38.1, 38.5, 41.6, 41.8., 46.9, 55.0, 56.4, 56.5, 82.2, 118.2, 120.1, 126.9, 127.3, 128.0, 128.2, 128.3, 128.4, 129.2, 129.7, 135.2, 141.4, 143.2, 156.4. HRMS calc. for $C_{39}H_{45}N_4O_5$ $[M+H^+]$ 649.3385, found 649.3391.

***tert*-butyl (1-(4-(diallylamino)but-1-yn-1-yl)-2-(diphenylmethylene)hydrazine-1-carbonyl)-*D*-phenylalaninate (5.10)**

Following the protocol for the synthesis of methylaminoalkyne **5.9**, azaPra **5.8** (1.06 g, 2.2 mmol) was reacted with copper (I) iodide (41.9 mg, 0.2 mmol), paraformaldehyde (132 mg, 4.4 mmol) and dialylamine (0.4 mL, 3.3 mmol). The residue was purified by column chromatography eluting with 0-100 % EtOAc/hexanes. Evaporation of the collected fractions gave **5.10** as bright yellow oil: R*f* = 0.26 (80 % EtOAc/hexanes); $[\alpha]_D^{23}$ 47.4 (*c* 1.00, $CHCl_3$), ^{1}H NMR (500 MHz, $CDCl_3$)

δ 1.44 (s, 9H), 3.09-3.10 (m, 3H), 3.17-3.20 (m, 2H), 3.37 (br. s, 1H), 3.40 (dd, *J* = 17.8, 5.6 Hz, 1H), 4.26 (dd, *J* = 18.0, 4.4 Hz, 1H), 4.76-4.80 (m, 1H), 5.13-5.17 (m, 3H), 5.74-5.82 (m, 2H), 7.05-7.11 (m, 1H), 7.22-7.51 (m, 15H). ^{13}C NMR (125 MHz, $CDCl_3$) δ 28.0, 35.3, 38.6, 41.4, 55.0 (two overlapping peaks), 56.1, 68.3, 73.1, 77.3, 81.8, 126.8, 128.2, 128.4, 128.6, 129.1, 129.2, 129.6, 129.7 (two overlapping peak), 130.1, 135.5, 136.5, 138.4, 157.8, 170.8. HRMS calc. for $C_{37}H_{42}N_4O_3Na$ [M+Na$^+$] 613.3149, found 613.3160.

tert-butyl (_R_)-2-(3-((((9_H_-fluoren-9-yl)methoxy)carbonyl)amino)-5-(2-(diallylamino)ethyl)-2-oxo-2,3-dihydro-1_H_-imidazol-1-yl)-3-phenylpropanoate (5.11)

Diallylaminomethyl **5.9** (95 mg, 0.2 mmol) was dissolved in $CHCl_3$ (2 mL) in a sealed vessel and treated with $AgS(O)_3CF_3$ (112 mg, 0.6 mmol). The vessel was capped and heated at 50 °C for 18 h. After cooling down, the reaction mixture was transferred to a separatory funnel and diluted with DCM (10 mL). The organic layer was extracted with sat. $NaHCO_3$ (3* 10 mL), water (1* 10 mL) and brine (1* 10 mL). The organic layer was dried with magnesium sulfate and evaporated to a residue which was purified by column chromatography eluting with 0-100% EtOAc/hexanes. Evaporation of the collected fractions gave imidazolone **5.11** as pale-yellow oil (81 mg, 87 %): R*f* = 0.56 (5 % MeOH/DCM); $[\alpha]_D^{23}$ 28.5 (*c* 0.70, $CHCl_3$), ^{1}H NMR (500 MHz, $CDCl_3$) δ 1.29 (s, 9H), 3.0-3.15 (m, 6H), 3.42-3.59 (m, 2H), 4.03 (br. s, 1H), 4.16-4.28 (m, 1H), 4.36 (t, *J* = 9.9 Hz, 1H), 4.51-4.56 (m, 1H), 4.68-4.69 (m, 1H), 4.87 (br. s, 1H), 5.15-5.19 (m, 4H), 5.56 (s, 1H), 5.76-5.87 (m, 2H), 6.41 (d, *J* = 7.2 Hz, 1H), 7.16-7.79 (m, 13H). ^{13}C NMR (125 MHz, $CDCl_3$) δ 27.9, 28.0, 29.7, 46.8, 51.2, 52.0, 54.8, 56.4, 68.7, 82.0, 117.6, 120.0, 125.3, 126.8, 127.3, 127.9, 128.3, 129.5, 135.4, 136.4, 141.3, 141.8, 143.3, 157.0, 170.6. HRMS calc. for $C_{39}H_{45}N_4O_5$ [M+H$^+$] 649.3385, found 649.3379.

tert-butyl (_R_)-2-(3-((diphenylmethylene)amino)-4-(hydroxymethyl)-5-methyl-2-oxo-2,3-dihydro-1_H_-imidazol-1-yl)-3-phenylpropanoate (5.13)

Alcohol **2.20** (240 mg, 0.4 mmol) was diluted with DCM (4 mL) and cooled to 0 °C using an ice bath. In a separate flask, triphenylphosphine (166 mg, 0.6 mmol) was diluted in DCM (4 mL) and treated with *N*-chlorosuccinimide (84 mg, 0.6 mmol) and imidazole (57 mg, 0.8 mmol). This solution was stirred for 15 minutes and added to the first one. The reaction mixture was allowed

to warm up to RT and stirred for 18 h. Upon confirmation of consumption of starting material by TLC (R*f* = 0.20, 50 % EtOAc/hexanes) water (10 mL) was added to the reaction mixture and stirred for 15 min. Layers were separated and the aqueous layer was extracted with DCM (3* 10 mL). The combined organic layers were washed with sat. $NaHCO_3$ (3* 20 mL), water (1* 20 mL) and brine (1* 20 mL). The organic layer was dried with magnesium sulfate and evaporated to a residue that was purified by column chromatography eluting with 0-100 % EtOAc/hexanes. Evaporation of the collected fraction gave **5.13** as pale-yellow oil (85 mg, 34 %): R*f* = 0.11 (75 % EtOAc, Hexanes); ^{1}H NMR (300 MHz, $CDCl_3$) δ 1.47 (s, 9H), 1.65 (s, 3H), 3.11-3.15 (m, 1H), 3.30-3.38 (m, 1H), 4.33-4.37 (m, 1H), 4.78 (d, *J* = 15.2 Hz, 1H), 4.97 (d, *J* = 15.2 Hz, 1H), 6.24 (br. s, 1H), 6.62-7.60 (m, 15 H); HRMS calc. for $C_{32}H_{35}ClN_5O4$ [M+H$^+$] 588.2372, found 588.2384.

References

1. Ardejani, M. S.; Orner, B. P., Obey the peptide assembly rules. *Science* **2013,** *340* (6132), 561-562.

2. Xu, X.-M.; Carlson, B. A.; Mix, H.; Zhang, Y.; Saira, K.; Glass, R. S.; Berry, M. J.; Gladyshev, V. N.; Hatfield, D. L., Biosynthesis of selenocysteine on its tRNA in eukaryotes. *PLoS biology* **2006,** *5* (1), e4.

3. Miller, G. H.; Kaufman, D. S.; Clarke, S., Amino acid dating. In *Encyclopedia of Quaternary Science: Second Edition*, Elsevier Inc.: 2013; pp 37-48.

4. Fujii, N., D-amino acids in living higher organisms. *Orig. Life Evol. Biosph.* **2002,** *32* (2), 103-127.

5. Smith, L.; Hillman, J., Therapeutic potential of type A (I) lantibiotics, a group of cationic peptide antibiotics. *Curr. Opin. Microbiol.* **2008,** *11* (5), 401-408.

6. Maisel, A. S., B-type natriuretic peptide (BNP) levels: diagnostic and therapeutic potential. *Rev. Cardiovascular Med.* **2001,** *2*, S13-8.

7. Sharma, S.; Verma, I.; Khuller, G., Therapeutic potential of human neutrophil peptide 1 against experimental tuberculosis. *Antimicrob. Agents Chemother.* **2001,** *45* (2), 639-640.

8. Solomon, T. A.; Buckley, J. P., Inhibitory Effects of Central Hypertensive Activity of motensin I and II by 1-Sar-8-ala-angiotensin II (Saralasin Acetate). *J. Pharm. Sci.* **1974,** *63* (7), 1109-1113.

9. Negredo, E.; Ruiz, L.; Paredes, R.; Fuster, D.; Moltó, J.; Clotet, B., Management of antiretroviral drug resistance in HIV-1 infected patients. *Business Briefing: Long-Term Healthcare. London, UK: Touch Briefings* **2004**, 1-7.

10. Prakash, A.; Goa, K. L., Sermorelin. *BioDrugs* **1999,** *12* (2), 139-157.

11. Walker, R. F., Sermorelin: A better approach to management of adult-onset growth hormone insufficiency? *Clin. Interv. Aging* **2006,** *1* (4), 307.

12. Grigsby, P. L.; Poore, K. R.; Hirst, J. J.; Jenkin, G., Inhibition of premature labor in sheep by a combined treatment of nimesulide, a prostaglandin synthase type 2 inhibitor, and atosiban, an oxytocin receptor antagonist. *Am. J. Obstet. Gynecol.* **2000,** *183* (3), 649-657.

13. Olson, D. M.; Zaragoza, D.; Shallow, M.; Cook, J. L.; Mitchell, B.; Grigsby, P.; Hirst, J., Myometrial activation and preterm labour: evidence supporting a role for the prostaglandin F receptor—a review. *Placenta* **2003,** *24*, S47-S54.

14. Spyridonidis, T.; Patsouras, N.; Alexiou, S.; Apostolopoulos, D. J., Imaging myocardial inflammation of various etiologies with 99mTc-depreotide SPET/CT. *Hell. J. Nuc. Med.* **2011,** *14* (3), 260-263.

15. Comi, G.; Martinelli, V.; Rodegher, M.; Moiola, L.; Bajenaru, O.; Carra, A.; Elovaara, I.; Fazekas, F.; Hartung, H.; Hillert, J., Effect of glatiramer acetate on conversion to clinically definite multiple sclerosis in patients with clinically isolated syndrome (PreCISe study): a randomised, double-blind, placebo-controlled trial. *The Lancet* **2009,** *374* (9700), 1503-1511.

16. Craik, D. J.; Fairlie, D. P.; Liras, S.; Price, D., The future of peptide-based drugs. *Chem. Biol. Drug Des.* **2013,** *81* (1), 136-47.

17. Sawyer, T. K., Renaissance in Peptide Drug Discovery - The Third Wave. In *Drug Discovery Series No. 59 Peptide-based Drug Discovery: Challenges and New Therapeutics*, Srivastava, V., Ed. 2017.

18. Vlieghe, P.; Lisowski, V.; Martinez, J.; Khrestchatisky, M., Synthetic therapeutic peptides: science and market. *Drug Discov. Today* **2010,** *15* (1-2), 40-56.

19. Gallop, M. A.; Barrett, R. W.; Dower, W. J.; Fodor, S. P.; Gordon, E. M., Applications of combinatorial technologies to drug discovery. 1. Background and peptide combinatorial libraries. *J. Med. Chem.* **1994,** *37* (9), 1233-1251.

20. Clark, R. J.; Jensen, J.; Nevin, S. T.; Callaghan, B. P.; Adams, D. J.; Craik, D. J., The engineering of an orally active conotoxin for the treatment of neuropathic pain. *Angew. Chem. Int. Ed.* **2010,** *49* (37), 6545-6548.

21. Nakagawa, N.; Obata, T.; Kobayashi, T.; Okada, Y.; Nambu, F.; Terawaki, T.; Aishita, H., In vivo pharmacologic profile of ONO-1078: a potent, selective and orally active peptide leukotriene (LT) antagonist. *Jpn. J. Pharmacol.* **1992,** *60* (3), 217-225.

22. Bailey, P. D.; Boyd, C. R.; Bronk, J. R.; Collier, I. D.; Meredith, D.; Morgan, K. M.; Temple, C. S., How to make drugs orally active: a substrate template for peptide transporter PepT1. *Angew. Chem.* **2000,** *112* (3), 515-518.

23. Linderstrøm-Lang, K. U., *Lane medical lectures: proteins and enzymes*. Stanford University Press: 1952; Vol. 6.

24. Ramachandran, G. N., Stereochemistry of polypeptide chain configurations. *J. Mol. Biol.* **1963,** *7*, 95-99.

25. Cowell, S.; Lee, Y.; Cain, J.; Hruby, V. J., Exploring Ramachandran and chi space: conformationally constrained amino acids and peptides in the design of bioactive polypeptide ligands. *Curr. Med. Chem.* **2004,** *11* (21), 2785-2798.

26. Hruby, V. J.; Li, G.; Haskell-Luevano, C.; Shenderovich, M., Design of peptides, proteins, and peptidomimetics in chi space. *Peptide Sci.* **1997,** *43* (3), 219-266.

27. Beausoleil, E.; Lubell, W. D., Steric effects on the amide isomer equilibrium of prolyl peptides. Synthesis and conformational analysis of N-acetyl-5-tert-butylproline N ‘-methylamides. *J. Am. Chem. Soc.* **1996,** *118* (51), 12902-12908.

28. Meng, H. Y.; Thomas, K. M.; Lee, A. E.; Zondlo, N. J., Effects of *i* and *i*+ 3 residue identity on Cis–Trans isomerism of the aromatici+ 1–prolyli+ 2 amide bond: Implications for type VI β-turn formation. *Peptide Sci.* **2006,** *84* (2), 192-204.

29. Kahn, M., Peptide secondary structure mimetics: recent advances and future challenges. *Synlett* **1993,** *1993* (11), 821-826.

30. Kahn, M. E. a. M., Design, Synthesis, and Application of Peptide Secondary Structure Mimetics. *Mini-Rev. Med. Chem.* **2002**, *2*(5), 447-462.

31. Kaiser, E.; Kezdy, F., Amphiphilic secondary structure: design of peptide hormones. *Science* **1984,** *223* (4633), 249-255.

32. Hutchinson, E. G.; Thornton, J. M., A revised set of potentials for β-turn formation in proteins. *Protein Sci.* **1994,** *3* (12), 2207-2216.

33. Venkatachalam, C., Stereochemical criteria for polypeptides and proteins. V. Conformation of a system of three linked peptide units. *Biopolymers* **1968,** *6* (10), 1425-1436.

34. De Brevern, A. G., Extension of the classical classification of β-turns. *Sci. Rep.* **2016,** *6*, 33191.

35. Kaur, H.; Raghava, G., A neural network method for prediction of β-turn types in proteins using evolutionary information. *Bioinformatics* **2004,** *20* (16), 2751-2758.

36. Gallo, E. A.; Gellman, S. H., Hydrogen-bond-mediated folding in depsipeptide models of. beta.-turns and. alpha.-helical turns. *J. Am. Chem. Soc.* **1993,** *115* (21), 9774-9788.

37. Marshall, G. R., A hierarchical approach to peptidomimetic design. *Tetrahedron* **1993,** *49* (17), 3547-3558.

38. Gerling, U. I.; Brandenburg, E.; Berlepsch, H. v.; Pagel, K.; Koksch, B., Structure analysis of an amyloid-forming model peptide by a systematic glycine and proline scan. *Biomacromolecules* **2011,** *12* (8), 2988-2996.

39. Duclohier, H., Peptaibiotics and peptaibols: an alternative to classical antibiotics? *Chem. Biodivers.* **2007,** *4* (6), 1023-1026.

40. Freidinger, R. M.; Veber, D. F.; Perlow, D. S.; Saperstein, R., Bioactive conformation of luteinizing hormone-releasing hormone: evidence from a conformationally constrained analog. *Science* **1980,** *210* (4470), 656-658.

41. Freidinger, R. M.; Veber, D. F.; Hirschmann, R.; Paege, L. M., Lactam restriction of peptide conformation in cyclic hexapeptides which alter rumen fermentation. *Int. J. Pept. Protein Res.* **1980,** *16* (5), 464-470.

42. Robl, J. A.; Cimarusti, M. P.; Simpkins, L. M.; Weller, H. N.; Pan, Y. Y.; Malley, M.; DiMarco, J. D., Peptidomimetic synthesis: a novel, highly stereoselective route to substituted Freidinger lactams. *J. Am. Chem. Soc.* **1994,** *116* (6), 2348-2355.

43. Perdih, A.; Kikelj, D., The application of Freidinger lactams and their analogs in the design of conformationally constrained peptidomimetics. *Curr. Med. Chem.* **2006,** *13* (13), 1525-1556.

44. Andrew G. Jamieson, N. B., Kim Beauregard, Mandar S. Bodas, Huy Ong, Christiane Quiniou, Sylvain Chemtob, and William D. Lubell, Positional Scanning for Peptide Secondary Structure by systematic solid-phase synthesis of amino lactam peptides. *J. Am. Chem. Soc.* **2009**, *131* (22), 7917-7927.

45. Boutard, N.; Jamieson, A. G.; Ong, H.; Lubell, W. D., Structure–Activity Analysis of the Growth Hormone Secretagogue GHRP-6 by α-and β-Amino γ-Lactam Positional Scanning. *Chem. Biol. Drug Des.* **2010,** *75* (1), 40-50.

46. St-Cyr, D. J.; Jamieson, A. G.; Lubell, W. D., α-Amino-β-hydroxy-γ-lactam for constraining peptide Ser and Thr residue conformation. *Org. Lett.* **2010,** *12* (8), 1652-1655.

47. Geranurimi, A.; Lubell, W. D., Diversity-oriented syntheses of β-substituted α-amino γ-lactam peptide mimics with constrained backbone and side chain residues. *Org. Lett.* **2018,** *20* (19), 6126-6129.

48. Gardner, R. R.; Liang, G.-B.; Gellman, S. H., An Achiral Dipeptide Mimetic That Promotes. beta.-Hairpin Formation. *J. Am. Chem. Soc.* **1995,** *117* (11), 3280-3281.

49. Genin, M. J.; Johnson, R. L., Design, synthesis, and conformational analysis of a novel spiro-bicyclic system as a type II. beta.-turn peptidomimetic. *J. Am. Chem. Soc.* **1992,** *114* (23), 8778-8783.

50. Genin, M. J.; Gleason, W. B.; Johnson, R. L., Design, synthesis, and x-ray crystallographic analysis of two novel spirolactam systems as. beta.-turn mimics. *J. Org. Chem.* **1993,** *58* (4), 860-866.

51. Genin, M. J.; Ojala, W. H.; Gleason, W. B.; Johnson, R. L., Synthesis and crystal structure of a peptidomimetic containing the (R)-4.4-spiro lactam type-II. beta.-turn mimic. *J. Org. Chem.* **1993,** *58* (8), 2334-2337.

52. Hata, M.; Marshall, G. R., Do benzodiazepines mimic reverse-turn structures? *J. Comput. Aided Mol. Des.* **2006,** *20* (5), 321-331.

53. Douchez, A.; Lubell, W. D., Chemoselective alkylation for diversity-oriented synthesis of 1, 3, 4-benzotriazepin-2-ones and pyrrolo [1, 2][1, 3, 4] benzotriazepin-6-ones, potential turn surrogates. *Org. Lett.* **2015,** *17* (24), 6046-6049.

54. Dörr, A. l. A.; Lubell, W. D., γ-Turn mimicry with benzodiazepinones and pyrrolobenzodiazepinones synthesized from a common amino ketone intermediate. *Org. Lett.* **2015,** *17* (14), 3592-3595.

55. Gosselin, F.; Lubell, W. D., An olefination entry for the synthesis of enantiopure α, ω-diaminodicarboxylates and azabicyclo [XY 0] alkane amino acids. *J. Org. Chem.* **1998,** *63* (21), 7463-7471.

56. Cluzeau, J.; Lubell, W. D., Design, synthesis, and application of azabicyclo [XY 0] alkanone amino acids as constrained dipeptide surrogates and peptide mimics. *Peptide Sci.* **2005,** *80* (2-3), 98-150.

57. Atmuri, N. P.; Lubell, W. D., Insight into Transannular Cyclization Reactions To Synthesize Azabicyclo [X,Y,Z] alkanone Amino Acid Derivatives from 8-, 9-, and 10-Membered Macrocyclic Dipeptide Lactams. *J. Org. Chem.* **2015,** *80* (10), 4904-4918.

58. Vagner, J.; Qu, H.; Hruby, V. J., Peptidomimetics, a synthetic tool of drug discovery. *Curr. Opin. Chem. Biol.* **2008,** *12* (3), 292-296.

59. Mir, F. M.; Atmuri, N. P.; Bourguet, C. B.; Fores, J. R.; Hou, X.; Chemtob, S.; Lubell, W. D., Paired Utility of Aza-Amino Acyl Proline and Indolizidinone Amino Acid Residues for Peptide Mimicry: Conception of Prostaglandin F2α Receptor Allosteric Modulators That Delay Preterm Birth. *J. Med. Chem.* **2019,** *62* (9), 4500-4525.

60. Gante, J., Azapeptides. *Synthesis* **1989,** *21* (06), 405-413.

61. Gante, J.; Krug, M.; Lauterbach, G.; Weitzel, R.; Hiller, W., Synthesis and properties of the first all-aza analogue of a biologically active peptide. *J. Pept. Sci.* **1995,** *1* (3), 201-206.

62. Zega, A., Azapeptides as pharmacological agents. *Curr. Med. Chem.* **2005,** *12* (5), 589-597.

63. Proulx, C.; Sabatino, D.; Hopewell, R.; Spiegel, J.; García Ramos, Y.; Lubell, W. D., Azapeptides and their therapeutic potential. *Future Med. Chem.* **2011,** *3* (9), 1139-1164.

64. Chingle, R.; Proulx, C.; Lubell, W. D., Azapeptide synthesis methods for expanding side-chain diversity for biomedical applications. *Acc. Chem. Res.* **2017,** *50* (7), 1541-1556.

65. André, F.; Boussard, G.; Bayeul, D.; Didierjean, C.; Aubry, A.; Marraud, M., Aza-peptides II. X-Ray structures of aza-alanine and aza-asparagine-containing peptides. *J. Pept. Res.* **1997,** *49* (6), 556-562.

66. Marraud, M.; Aubry, A., Crystal structures of peptides and modified peptides. *Peptide Sci.* **1996,** *40* (1), 45-83.

67. Lee, H. J.; Lee, K. B.; Ahn, I. A.; Ro, S.; Choi, K. H.; Choi, Y. S., Role of azaamino acid residue in β-turn formation and stability in designed peptide. *J. Pept Res.* **2000,** *56* (1), 35-46.

68. Benatalah, Z.; Aubry, A.; Boussard, G.; Marraud, M., Evidence for a β-turn in an azadipeptide sequence: Synthesis and crystal structure of ButCO-Pro-AzaAla-NHPri. *Int. J. Pept. Protein Res.* **1991,** *38* (6), 603-605.

69. Reynolds, C. H.; Hormann, R. E., Theoretical study of the structure and rotational flexibility of diacylhydrazines: Implications for the structure of nonsteroidal ecdysone agonists and azapeptides. *J. Am. Chem. Soc.* **1996,** *118* (39), 9395-9401.

70. Melendez, R. E.; Lubell, W. D., Aza-amino acid scan for rapid identification of secondary structure based on the application of N-Boc-Aza1-dipeptides in peptide synthesis. *J. Am. Chem. Soc.* **2004,** *126* (21), 6759-6764.

71. Chrisp, P.; Goa, K. L., Goserelin. *Drugs* **1991,** *41* (2), 254-288.

72. Gassman, J. M.; Magrath, J., An active-site titrant for chymotrypsin, and evidence that azapeptide esters are less susceptible to nucleophilic attack than ordinary esters. *Bioorg. Med. Chem. Lett.* **1996,** *6* (15), 1771-1774.

73. Bourguet, C. B.; Sabatino, D.; Lubell, W. D., Benzophenone semicarbazone protection strategy for synthesis of aza-glycine containing aza-peptides. *Peptide Sci.* **2008,** *90* (6), 824-831.

74. Garcia-Ramos, Y.; Proulx, C.; Lubell, W. D., Synthesis of hydrazine and azapeptide derivatives by alkylation of carbazates and semicarbazones. *Can. J. Chem.* **2012,** *90* (11), 985-993.

75. Proulx, C.; Lubell, W. D., N-Amino-imidazolin-2-one Peptide Mimic Synthesis and Conformational Analysis. *Org. Lett.* **2012,** *14* (17), 4552-4555.

76. Traore, M.; Doan, N. D.; Lubell, W. D., Diversity-oriented synthesis of azapeptides with basic amino acid residues: aza-lysine, aza-ornithine, and aza-arginine. *Org. Lett.* **2014,** *16* (13), 3588-91.

77. Garcia-Ramos, Y.; Lubell, W. D., Synthesis and alkylation of aza-glycinyl dipeptide building blocks. *J. Pept. Sci.* **2013,** *19* (12), 725-729.

78. Proulx, C.; Lubell, W. D., Copper-catalyzed N-arylation of semicarbazones for the synthesis of aza-arylglycine-containing aza-peptides. *Org. Lett.* **2010,** *12* (13), 2916-2919.

79. Proulx, C.; Lubell, W. D., Aza-1, 2, 3-triazole-3-alanine synthesis via copper-catalyzed 1, 3-dipolar cycloaddition on aza-progargylglycine. *J. Org. Chem.* **2010,** *75* (15), 5385-5387.

80. Doan, N. D.; Hopewell, R.; Lubell, W. D., N-aminoimidazolidin-2-one peptidomimetics. *Org. Lett.* **2014,** *16* (8), 2232-5.

81. St-Cyr, D. J.; García-Ramos, Y.; Doan, N.-D.; Lubell, W. D., Aminolactam, N-aminoimidazolone, and N-aminoimdazolidinone peptide mimics. In *Peptidomimetics I*, Springer: 2017; pp 125-175.

82. Proulx, C.; Lubell, W. D., Analysis of N-amino-imidazolin-2-one peptide turn mimic 4-position substituent effects on conformation by X-ray crystallography. *Peptide Sci.* **2014,** *102* (1), 7-15.

83. Poupart, J.; Doan, N.-D.; Berube, D.; Hamdane, Y.; Medena, C.; Lubell, W. D., Palladium-Catalyzed Arylation of N-aminoimidazol-2-ones Towards Synthesis of Constrained Phenylalanine Dipeptide Mimics. *Heterocycles* **2019,** *99* (1), 279-293.

84. García-Ramos, Y.; Proulx, C.; Camy, C.; Lubell, W. D., Synthesis and purification of enantiomerically pure N-aminoimidazolin- 2-one dipeptide. *Proceedings of the 32nd Europ. Peptide Symp.* **2012**.

85. Chignen Possi, K.; Mulumba, M.; Omri, S.; Garcia-Ramos, Y.; Tahiri, H.; Chemtob, S.; Ong, H.; Lubell, W. D., Influences of Histidine-1 and Azaphenylalanine-4 on the Affinity, Anti-inflammatory, and Antiangiogenic Activities of Azapeptide Cluster of Differentiation 36 Receptor Modulators. *J. Med. Chem.* **2017,** *60* (22), 9263-9274.

86. Poupart, J.; Mulumba, M.; Doan, N. D.; Ong, H.; Lubell, W. D., Application of *N*-Aminoimidazol-2-one Turn Mimics to Study the Backbone and Side-chain Orientations of Peptide-based CD36 Modulators. *In preparation* **2019**.

87. Akee, R. K.; Carroll, T. R.; Yoshida, W. Y.; Scheuer, P. J.; Stout, T. J.; Clardy, J., Two imidazole alkaloids from a sponge. *J. Org. Chem.* **1990,** *55* (6), 1944-1946.

88. Fu, X.; Barnes, J. R.; Do, T.; Schmitz, F. J., New imidazole alkaloids from the sponge Leucetta chagosensis. *J. Nat. Prod.* **1997,** *60* (5), 497-498.

89. Smith, R. C.; Reeves, J. C., Antioxidant properties of 2-imidazolones and 2-imidazolthiones. *Biochem. Pharmacol.* **1987,** *36* (9), 1457-1460.

90. Gadwood, R. C.; Kamdar, B. V.; Dubray, L. A. C.; Wolfe, M. L.; Smith, M. P.; Watt, W.; Mizsak, S. A.; Groppi, V. E., Synthesis and biological activity of spirocyclic benzopyran imidazolone potassium channel openers. *J. Med. Chem.* **1993,** *36* (10), 1480-1487.

91. Naylor, E. M.; Parmee, E. R.; Colandrea, V. J.; Perkins, L.; Brockunier, L.; Candelore, M. R.; Cascieri, M. A.; Colwell Jr, L. F.; Deng, L.; Feeney, W. P., Human β3 andrenergic receptor agonists containing imidazolidinone and imidazolone benzenesulfonamides. *Bioorg. Med. Chem. Lett.* **1999,** *9* (5), 755-758.

92. Pande, K.; Kalsi, R.; Bhalla, T.; Barthwal, J., Some newer imidazolones and their anti-inflammatory activity. *Die Pharmazie* **1987,** *42* (4), 269.

93. Kamal, A.; Ramakrishna, G.; Raju, P.; Viswanath, A.; Ramaiah, M. J.; Balakishan, G.; Pal-Bhadra, M., Synthesis and anti-cancer activity of chalcone linked imidazolones. *Bioorg. Med. Chem. Lett.* **2010,** *20* (16), 4865-4869.

94. Khan, K. M.; Mughal, U. R.; Ambreen, N.; Samreen; Perveen, S.; Choudhary, M. I., Synthesis and leishmanicidal activity of 2, 3, 4-substituted-5-imidazolones. *J. Enzyme Inhib. Med. Chem.* **2010,** *25* (1), 29-37.

95. Lima, H. M.; Lovely, C. J., Synthesis of 2-imidazolones and 2-iminoimidazoles. *Org. Lett.* **2011,** *13* (21), 5736-5739.

96. Ruiz, J.; Mesa, A. F., From Diphosphino-Functionalized 1, 3-Dialkylimidazolium Cations to Imidazolones through Dehydrogenative C-N Coupling. *Chem. Eur. J.* **2014,** *20* (1), 102-105.

97. Brazier, S. A.; McCombie, H., CCXLVIII.—The condensation of α-keto-β-anilino-αβ-diphenylethane and its homologues with phenylcarbimide and with phenylthiocarbimide.*J. Chem. Soc. Perkin Trans. 1* **1912,** *101*, 2352-2358.

98. Carling, R. W.; Moore, K. W.; Moyes, C. R.; Jones, E. A.; Bonner, K.; Emms, F.; Marwood, R.; Patel, S.; Patel, S.; Fletcher, A. E., 1-(3-Cyanobenzylpiperidin-4-yl)-5-methyl-4-phenyl-1, 3-dihydroimidazol-2-one: a selective high-affinity antagonist for the human dopamine D4 receptor with excellent selectivity over ion channels. *J. Med. Chem.* **1999,** *42* (14), 2706-2715.

99. Göhner, M.; Haiss, P.; Kuhn, N.; Ströbele, M.; Zeller, K.-P., The 1: 1 Adduct of 1, 3-Diisopropyl-4, 5-dimethyl-2, 3-dihydroimidazol-2-ylidene and Nitrous Oxide. *Zeitschrift für Naturforschung B* **2013,** *68* (5-6), 539-545.

100. Pereshivko, O. P.; Peshkov, V. A.; Peshkov, A. A.; Jacobs, J.; Van Meervelt, L.; Van der Eycken, E. V., Unexpected regio-and chemoselectivity of cationic gold-catalyzed cycloisomerizations of propargylureas: access to tetrasubstituted 3, 4-dihydropyrimidin-2 (1 H)-ones. *Org. Bioorg. Chem.* **2014,** *12* (11), 1741-1750.

101. Peshkov, V. A.; Pereshivko, O. P.; Sharma, S.; Meganathan, T.; Parmar, V. S.; Ermolat'ev, D. S.; Van der Eycken, E. V., Tetrasubstituted 2-imidazolones via Ag (I)-catalyzed cycloisomerization of propargylic ureas. *J. Org. Chem.* **2011,** *76* (14), 5867-5872.

102. Zuliani, A.; Ranjan, P.; Luque, R.; Van der Eycken, E. V., Heterogeneously catalyzed synthesis of imidazolones via cycloisomerizations of propargylic ureas using Ag and Au/Al SBA-15 systems. *ACS Sustain. Chem. Eng.* **2019,** *7* (5), 5568-5575.

103. Huguenot, F.; Delalande, C.; Vidal, M., Metal-free 5-exo-dig cyclization of propargyl urea using TBAF. *Tetrahedron Lett.* **2014,** *55* (33), 4632-4635.

104. Yasuhara, A.; Kanamori, Y.; Kaneko, M.; Numata, A.; Kondo, Y.; Sakamoto, T., Convenient synthesis of 2-substituted indoles from 2-ethynylanilines with tetrabutylammonium fluorideJ. Chem. Soc. Perkin Trans. *1* **1999,** (4), 529-534.

105. Casnati, A.; Perrone, A.; Mazzeo, P. P.; Bacchi, A.; Mancuso, R.; Gabriele, B.; Maggi, R.; Maestri, G.; Motti, E.; Stirling, A. s., Synthesis of Imidazolidin-2-ones and Imidazol-2-ones via Base-Catalyzed Intramolecular Hydroamidation of Propargylic Ureas under Ambient Conditions. *J. Org. Chem.* **2019,** *84* (6), 3477-3490.

106. Yedage, S. L.; Bhanage, B. M., tert-Butyl Nitrite-Mediated Synthesis of N-Nitrosoamides, Carboxylic Acids, Benzocoumarins, and Isocoumarins from Amides. *J. Org. Chem.* **2017,** *82* (11), 5769-5781.

107. Dufour, E.; Storer, A. C.; Menard, R., Peptide aldehydes and nitriles as transition state analog inhibitors of cysteine proteases. *Biochemistry* **1995,** *34* (28), 9136-9143.

108. Sarubbi, E.; Seneci, P. F.; Angelastro, M. R.; Peet, N. P.; Denaro, M.; Islam, K., Peptide aldehydes as inhibitors of HIV protease. *FEBS Lett.* **1993,** *319* (3), 253-256.

109. Zhu, L.; George, S.; Schmidt, M. F.; Al-Gharabli, S. I.; Rademann, J.; Hilgenfeld, R., Peptide aldehyde inhibitors challenge the substrate specificity of the SARS-coronavirus main protease. *Antivir. Res.* **2011,** *92* (2), 204-212.

110. Thompson, R. C., Use of peptide aldehydes to generate transition-state analogs of elastase. *Biochemistry* **1973,** *12* (1), 47-51.

111. Abeles, R. H.; Maycock, A. L., Suicide enzyme inactivators. *Acc. Chem. Res.* **1976,** *9* (9), 313-319.

112. La-Venia, A.; Ventosa-Andrés, P.; Krchňák, V., Peptidomimetics via Iminium Ion Chemistry on Solid Phase: Single, Fused, and Bridged Heterocycles. In *Peptidomimetics II*, Springer: 2015; pp 105-126.

113. Krchňák, V.; Holladay, M. W., Solid phase heterocyclic chemistry. *Chem. Rev.* **2002,** *102* (1), 61-92.

114. Todd, M. H.; Ndubaku, C.; Bartlett, P. A., Amino acid derived heterocycles: Lewis acid catalyzed and radical cyclizations from peptide acetals. *J. Org. Chem.* **2002,** *67* (12), 3985-3988.

115. Moulin, A.; Martinez, J.; Fehrentz, J. A., Synthesis of peptide aldehydes. *J. Pept. Sci.* **2007,** *13* (1), 1-15.

116. Triana, V.; Derda, R., Tandem Wittig/Diels–Alder diversification of genetically encoded peptide libraries. *Org. Biomol. Chem.* **2017,** *15* (37), 7869-7877.

117. Ben-Efraim, D., The prototropic rearrangement of secondary propargylic amines. *Tetrahedron* **1973,** *29* (24), 4111-4125.

118. Navarro-Vázquez, A., Why base-catalyzed isomerization of N-propargyl amides yields mostly allenamides rather than ynamides. *Beilstein J. Org. Chem.* **2015,** *11* (1), 1441-1446.

119. Huang, J.; Xiong, H.; Hsung, R. P.; Rameshkumar, C.; Mulder, J. A.; Grebe, T. P., The First Successful Base-Promoted Isomerization of Propargyl Amides to Chiral Ynamides. Applications in Ring-Closing Metathesis of Ene− Ynamides and Tandem RCM of Diene− Ynamides. *Org. Lett.* **2002,** *4* (14), 2417-2420.

120. Buncel, E.; Menon, B., Carbanion mechanisms. 6. Metalation of arylmethanes by potassium hydride/18-crown-6 ether in tetrahydrofuran and the acidity of hydrogen. *J. Am. Chem. Soc.* **1977,** *99* (13), 4457-4461.

121. Reeve, W.; Erikson, C. M.; Aluotto, P. F., A new method for the determination of the relative acidities of alcohols in alcoholic solutions. The nucleophilicities and competitive reactivities of alkoxides and phenoxides. *Can. J. Chem.* **1979,** *57* (20), 2747-2754.

122. Fosgerau, K.; Hoffmann, T., Peptide therapeutics: current status and future directions. *Drug Discov. today* **2015,** *20* (1), 122-128.

123. Sawyer, T. K., Renaissance in Peptide Drug Discovery: The Third Wave. In *Peptide-based Drug Disc.*, 2017; pp 1-34.

124. Ung, P.; Winkler, D. A., Tripeptide motifs in biology: targets for peptidomimetic design. *J. Med. Chem* **2011,** *54* (5), 1111-1125.

125. Cooper, W. J.; Waters, M. L., Molecular recognition with designed peptides and proteins. *Curr. Opin. Chem. Biol.* **2005,** *9* (6), 627-631.

126. Loughlin, W. A.; Tyndall, J. D.; Glenn, M. P.; Hill, T. A.; Fairlie, D. P., Beta-Strand Mimetics. *Chem. Rev.* **2011,** *110* (6), PR32-PR69.

127. Freidinger, R. M., Synthesis of. gamma.-lactam-constrained tryptophyl-lysine derivatives. *J. Org. Chem.* **1985,** *50* (19), 3631-3633.

128. Freidinger, R. M.; Perlow, D. S.; Veber, D. F., Protected lactam-bridged dipeptides for use as conformational constraints in peptides. *J. Org. Chem.* **1982,** *47* (1), 104-109.

129. Trevino, S. R.; Schaefer, S.; Scholtz, J. M.; Pace, C. N., Increasing protein conformational stability by optimizing β-turn sequence. *J. Mol. Biol.* **2007,** *373* (1), 211-218.

130. Makwana, K. M.; Mahalakshmi, R., Comparative analysis of cross strand aromatic–Phe interactions in designed peptide β-hairpins. *Org. Biomol. Chem.* **2014,** *12* (13), 2053-2061.

131. Jacquot, D. E.; Zöllinger, M.; Lindel, T., Total synthesis of the marine natural product rac-dibromophakellstatin. *Angew. Chem. Int. Ed.* **2005,** *44* (15), 2295-2298.

132. Halab, L.; Lubell, W. D., Use of steric interactions to control peptide turn geometry. Synthesis of type VI β-turn mimics with 5-tert-butylproline. *J. Org. Chem.* **1999,** *64* (9), 3312-3321.

133. Zondlo, N. J., Aromatic–proline interactions: Electronically tunable CH/π interactions. *Acc. Chem. Res.* **2012,** *46* (4), 1039-1049.

134. Newberry, R. W.; Raines, R. T., The n→ π* Interaction. *Acc. Chem. Res.* **2017,** *50* (8), 1838-1846.

135. Halab, L.; Lubell, W. D., Effect of sequence on peptide geometry in 5-tert-butylprolyl type VI β-turn mimics. *J. Am. Chem. Soc.* **2002,** *124* (11), 2474-2484.

136. Wilmot, C.; Thornton, J., β-Turns and their distortions: a proposed new nomenclature. *Protein Eng. Des. Sel.* **1990,** *3* (6), 479-493.

137. Sanbonmatsu, K. Y.; García, A. E., Structure of Met-enkephalin in explicit aqueous solution using replica exchange molecular dynamics. *Proteins* **2002,** *46* (2), 225-234.

138. Devynck, M.-A.; Pernollet, M.-G.; Meyer, P.; Fermandjian, S.; Fromageot, P., Angiotensin receptors in smooth muscle cell membranes. *Nature New Biol.* **1973,** *245* (141), 55.

139. Holladay, L. A.; Puett, D., Somatostatin conformation: evidence for a stable intramolecular structure from circular dichroism, diffusion, and sedimentation equilibrium. *Proc. Natl. Acad. Sci.* **1976,** *73* (4), 1199-1202.

140. Cann, J. R.; Stewart, J. M.; Matsueda, G. R., Circular dichroism study of the secondary structure of bradykinin. *Biochemistry* **1973,** *12* (19), 3780-3788.

141. Gibson, S. E.; Guillo, N.; Tozer, M. J., Towards control of χ-space: Conformationally constrained analogues of Phe, Tyr, Trp and His. *Tetrahedron* **1999,** *55* (3), 585-615.

142. Lu, J.; Tan, X.; Chen, C., Palladium-catalyzed direct functionalization of imidazolinone: Synthesis of dibromophakellstatin. *J. Am. Chem. Soc.* **2007,** *129* (25), 7768-7769.

143. Momany, F.; Bowers, C.; Reynolds, G.; Hong, A.; Newlander, K., Conformational energy studies and in vitro and in vivo activity data on growth hormone-releasing peptides. *Endocrinology* **1984,** *114* (5), 1531-1536.

144. Howard, A. D.; Feighner, S. D.; Cully, D. F.; Arena, J. P.; Liberator, P. A.; Rosenblum, C. I.; Hamelin, M.; Hreniuk, D. L.; Palyha, O. C.; Anderson, J., A receptor in pituitary and hypothalamus that functions in growth hormone release. *Science* **1996,** *273* (5277), 974-977.

145. Momany, F.; Bowers, C.; Reynolds, G.; Chang, D.; Hong, A.; Newlander, K., Design, synthesis, and biological activity of peptides which release growth hormone in vitro. *Endocrinology* **1981,** *108* (1), 31-39.

146. Kojima, M.; Hosoda, H.; Date, Y.; Nakazato, M.; Matsuo, H.; Kangawa, K., Ghrelin is a growth-hormone-releasing acylated peptide from stomach. *Nature* **1999,** *402* (6762), 656.

147. Hosoda, H.; Kojima, M.; Kangawa, K., Biological, physiological, and pharmacological aspects of ghrelin. *J. Pharmacol. Sci.* **2006,** *100* (5), 398-410.

148. Bodart, V.; Bouchard, J.; McNicoll, N.; Escher, E.; Carriere, P.; Ghigo, E.; Sejlitz, T.; Sirois, M.; Lamontagne, D.; Ong, H., Identification and characterization of a new growth hormone–releasing peptide receptor in the heart. *Circulation Res.* **1999,** *85* (9), 796-802.

149. Collot-Teixeira, S.; Martin, J.; McDermott-Roe, C.; Poston, R.; McGregor, J. L., CD36 and macrophages in atherosclerosis. *Cardiovascular Res.* **2007,** *75* (3), 468-477.

150. Ong, H.; Tremblay, A.; Febbraio, M.; Silverstein, R.; Avallone, R.; Iken, K.; Wang, Y.; Bujold, K.; Demers, A.; Sirois, M. In *Growth hormone-releasing peptides as inhibitors of fatty streaks formation: A new therapy for atherosclerosis*, Program and Abstracts of the 85th Annual Meeting of The Endocrine Society, Philadelphia, 2003; pp 19-22.

151. Jager, R. D.; Mieler, W. F.; Miller, J. W., Age-related macular degeneration. *New Eng. J. Med.* **2008,** *358* (24), 2606-2617.

152. Proulx, C.; Picard, E.; Boeglin, D.; Pohankova, P.; Chemtob, S.; Ong, H.; Lubell, W. D., Azapeptide analogues of the growth hormone releasing peptide 6 as cluster of differentiation 36 receptor ligands with reduced affinity for the growth hormone secretagogue receptor 1a. *J. Med. Chem.* **2012,** *55* (14), 6502-6511.

153. Mellal, K.; Omri, S.; Mulumba, M.; Tahiri, H.; Fortin, C.; Dorion, M.-F.; Pham, H.; Ramos, Y. G.; Zhang, J.; Pundir, S., Immunometabolic modulation of retinal inflammation by CD36 ligand. *Scientific reports* **2019,** *9* (1), 1-18.

154. Sabatino, D.; Proulx, C.; Pohankova, P.; Ong, H.; Lubell, W. D., Structure–Activity Relationships of GHRP-6 Azapeptide Ligands of the CD36 Scavenger Receptor by Solid-Phase Submonomer Azapeptide Synthesis. *J. Am. Chem. Soc.* **2011,** *133* (32), 12493-12506.

155. Evans, B. E.; Bock, M. G.; Rittle, K. E.; DiPardo, R. M.; Whitter, W. L.; Veber, D. F.; Anderson, P. S.; Freidinger, R. M., Design of potent, orally effective, nonpeptidal antagonists of the peptide hormone cholecystokinin. *Proc. Natl. Acad. Sci.* **1986,** *83* (13), 4918-4922.

156. Evans, B.; Rittle, K.; Bock, M.; DiPardo, R.; Freidinger, R.; Whitter, W.; Lundell, G.; Veber, D.; Anderson, P.; Chang, R., Methods for drug discovery: development of potent, selective, orally effective cholecystokinin antagonists. *J. Am. Chem. Soc.* **1988,** *31* (12), 2235-2246.

157. Stigers, K. D.; Soth, M. J.; Nowick, J. S., Designed molecules that fold to mimic protein secondary structures. *Curr. Opin. Chem. Biol.* **1999,** *3* (6), 714-723.

158. Yésica García-Ramos; Caroline Proulx; Christophe Camy; Lubell, W. D., Synthesis and purification of enantiomerically pure *N*-aminoimidazolin- 2-one dipeptide. *Proceedings of the 32nd Europ. Peptide Symp. (2012)* **2012**.

159. Poupart, J.; Youhsra, H.; Lubell, W. D., Synthesis of enantiomerically enriched 4,5-disubstitued N-aminoimidazol-2-ones (Nai) peptide turn mimics. *In revision* **2019**.

160. Yamamoto, H.; Futatsugi, K., "Designer acids": combined acid catalysis for asymmetric synthesis. *Angew. Chem.* **2005,** *44* (13), 1924-42.

161. Zhang, J.; Proulx, C.; Tomberg, A.; Lubell, W. D., Multicomponent diversity-oriented synthesis of aza-lysine-peptide mimics. *Org. Lett.* **2013,** *16* (1), 298-301.

162. Chingle, R.; Ohm, R. G.; Chauhan, P. S.; Lubell, W. D., Aza-propargylglycine installation by aza-amino acylation: Synthesis and Ala-scan of an azacyclopeptide CD36 modulator. *Peptide Sci.* **2019,** *111* (1), e24102.

163. Kim, S.; Lee, P. H., Cyclization of Allenyne-1, 6-diols Catalyzed by Gold and Silver Salts: An Efficient Selective Synthesis of Dihydrofuran and Furan Derivatives. *Adv. Synth. Catal.* **2008,** *350* (4), 547-551.

164. Bailey, J. L.; Sudini, R. R., Synthesis of 2, 4-and 2, 4, 5-substituted oxazoles via a silver triflate mediated cyclization. *Tetrahedron lett.* **2014,** *55* (27), 3674-3677.

165. Mantovani, A. C.; Pesarico, A. P.; Sampaio, T. B.; Nogueira, C. W.; Zeni, G., Synthesis of pharmacologically active 1-amino-isoquinolines prepared via silver triflate-catalyzed cyclization of o-alkynylbenzaldoximes with isocyanates. *Eur. J. Phar. Sci.* **2014,** *51*, 196-203.

166. Frégeau, G. S., R.; Elimam, H.; Esposito, C.L.,; Ménard, L.; de Graça, S.D.; Proulcx, C.; Zanh, J.: Febbraio, M.; Soto, Y.; Lubell, W.D.: Ong, H.: Marleau, S., Atheroprotective and atheroregressive potential of azapeptide derivatives of GHRP-6 as selective CD36 ligands in apolipoprotein E-deficient mice. *In revision* **2019**.

167. Marcotte, F.-A.; Lubell, W. D., An effective new synthesis of 4-aminopyrrole-2-carboxylates. *Org. Lett.* **2002,** *4* (15), 2601-2603.

168. Sprung, M. A., A Summary of the Reactions of Aldehydes with Amines. *Chem. Rev.* **1940,** *26* (3), 297-338.

169. Otera, J., *Modern carbonyl chemistry*. John Wiley & Sons: 2008.

170. Taylor, J. E.; Jones, M. D.; Williams, J. M.; Bull, S. D., Friedel− Crafts Acylation of Pyrroles and Indoles using 1, 5-Diazabicyclo [4.3. 0] non-5-ene (DBN) as a Nucleophilic Catalyst. *Org. Lett.* **2010,** *12* (24), 5740-5743.

171. Al-awar, R. S.; Ray, J. E.; Schultz, R. M.; Andis, S. L.; Kennedy, J. H.; Moore, R. E.; Liang, J.; Golakoti, T.; Subbaraju, G. V.; Corbett, T. H., A convergent approach to cryptophycin 52 analogues: synthesis and biological evaluation of a novel series of fragment A epoxides and chlorohydrins. *J. Med. Chem.* **2003,** *46* (14), 2985-3007.

172. Still, W. C.; Kahn, M.; Mitra, A., Rapid chromatographic technique for preparative separations with moderate resolution. *J. Org. Chem.* **1978,** *43* (14), 2923-2925.

Annexes

Annex 1: NMR Spectra for chapter 2

Compound 2.16c

^{1}H-NMR, 500 MHz, $CDCl_3$

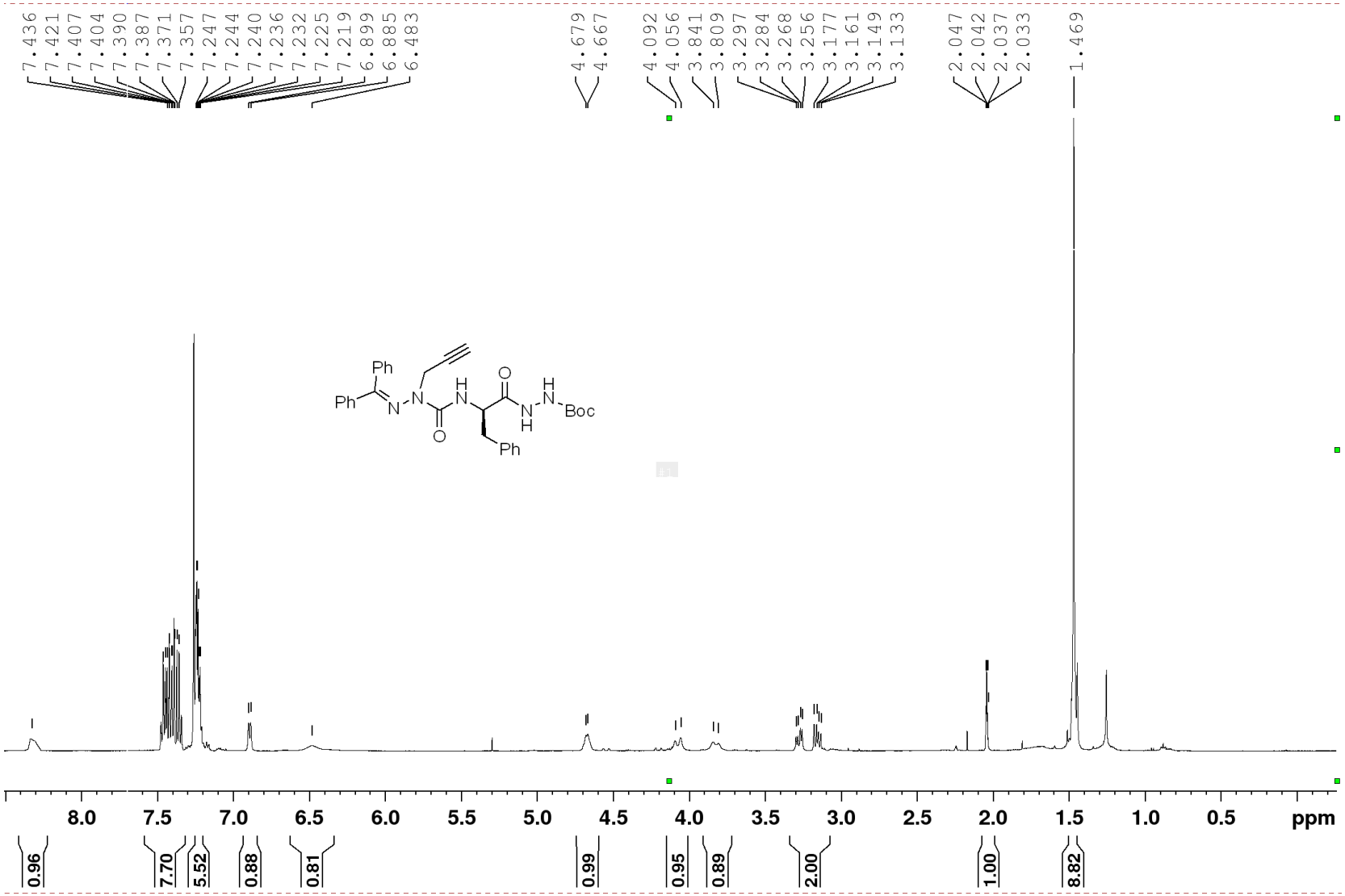

^{13}C-NMR, 75 MHz, $CDCl_3$

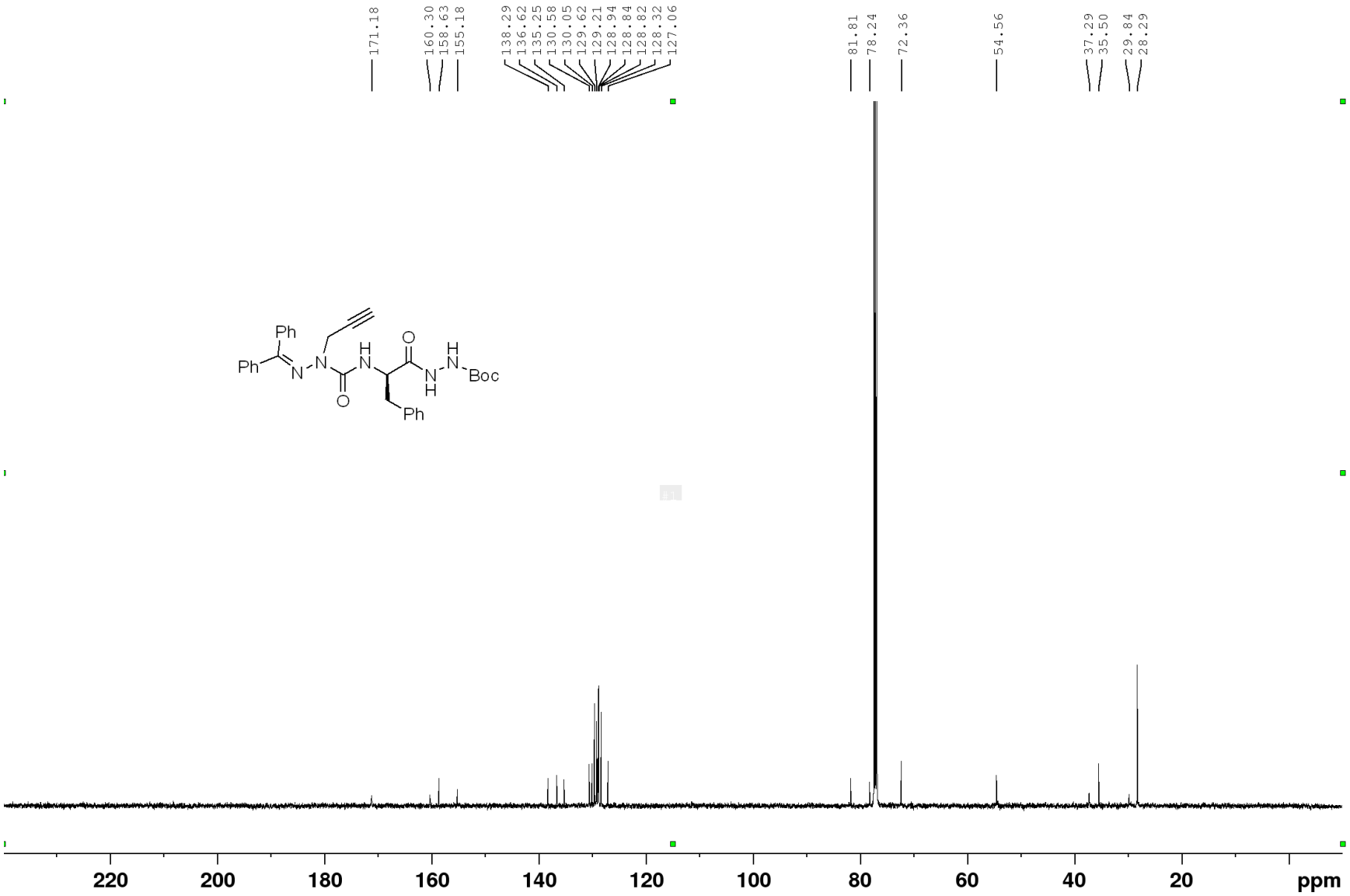

Compound 2.17b

^{1}H-NMR, 500 MHz, $CDCl_3$

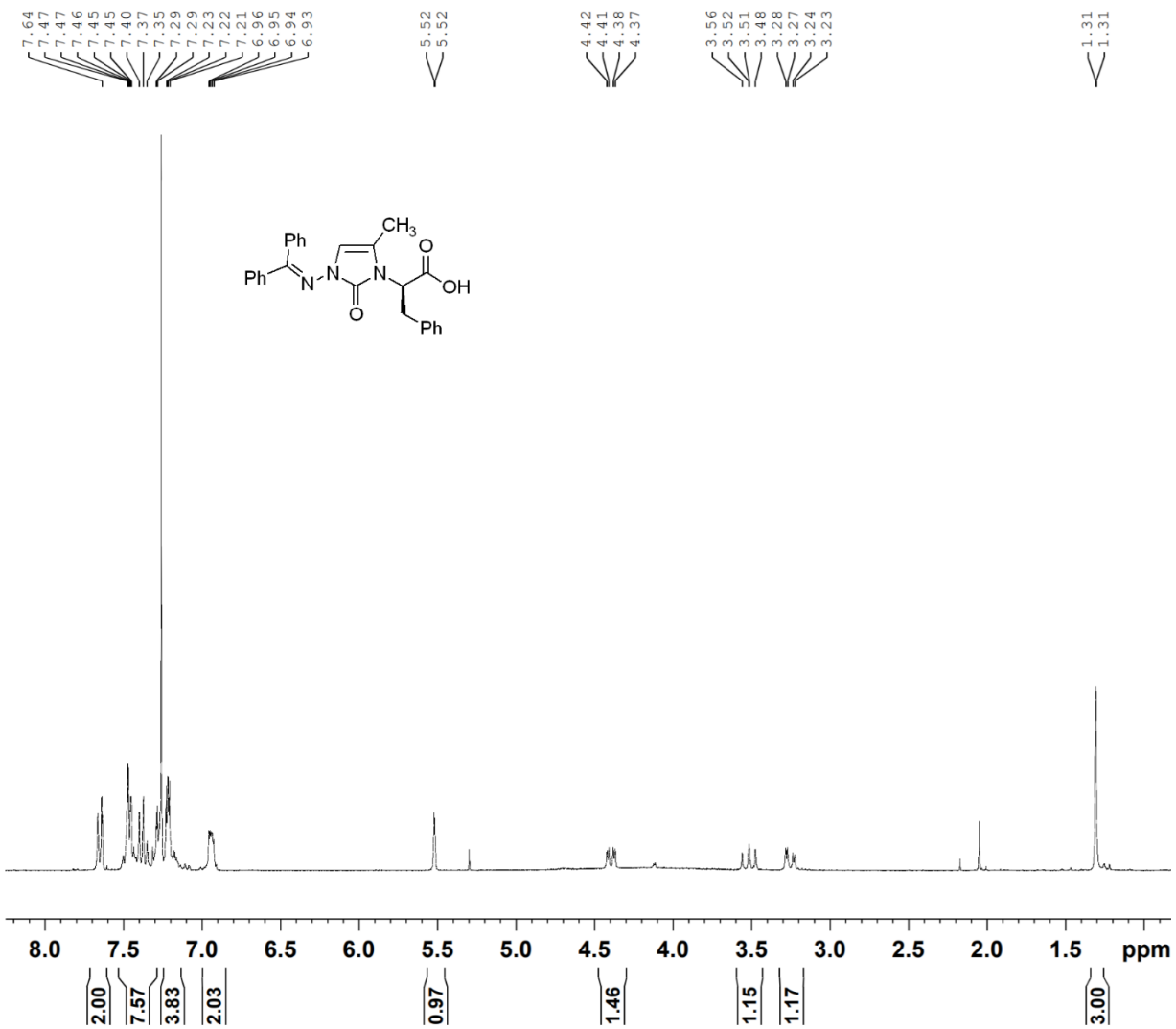

^{13}C-NMR, 125 MHz, $CDCl_3$

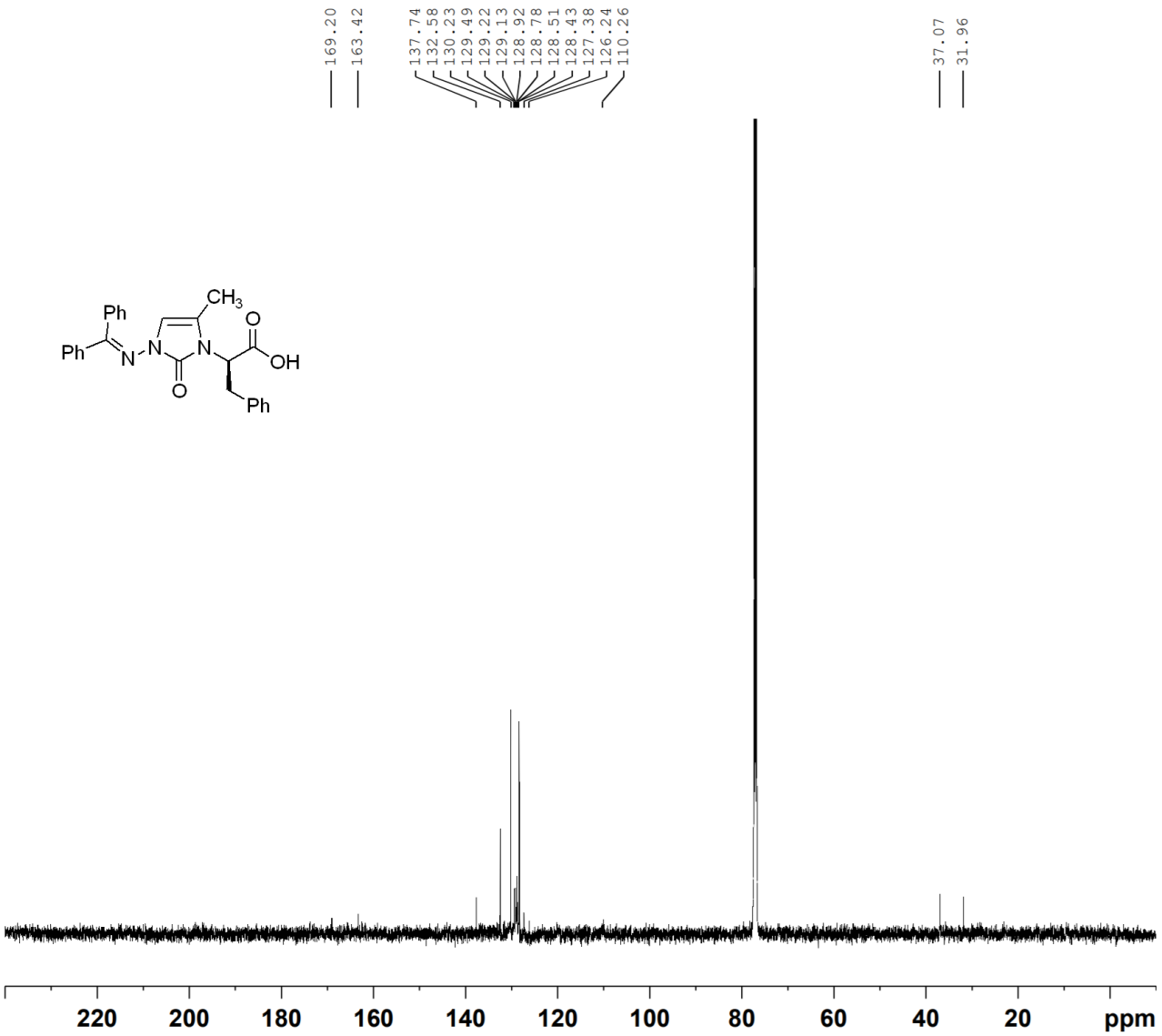

Compound 2.17c

^{1}H-NMR, 400 MHz, $CDCl_3$

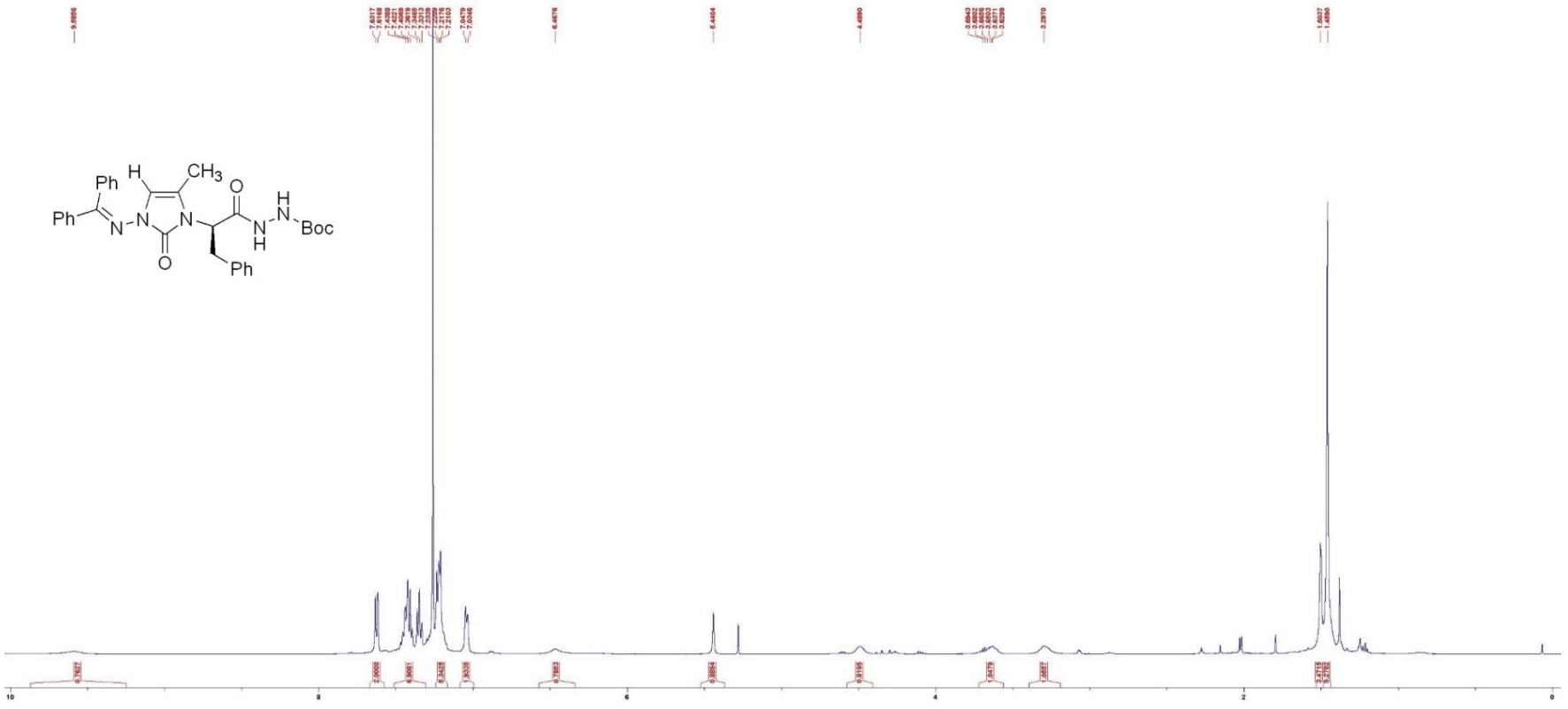

^{13}C-NMR, 75 MHz, $CDCl_3$

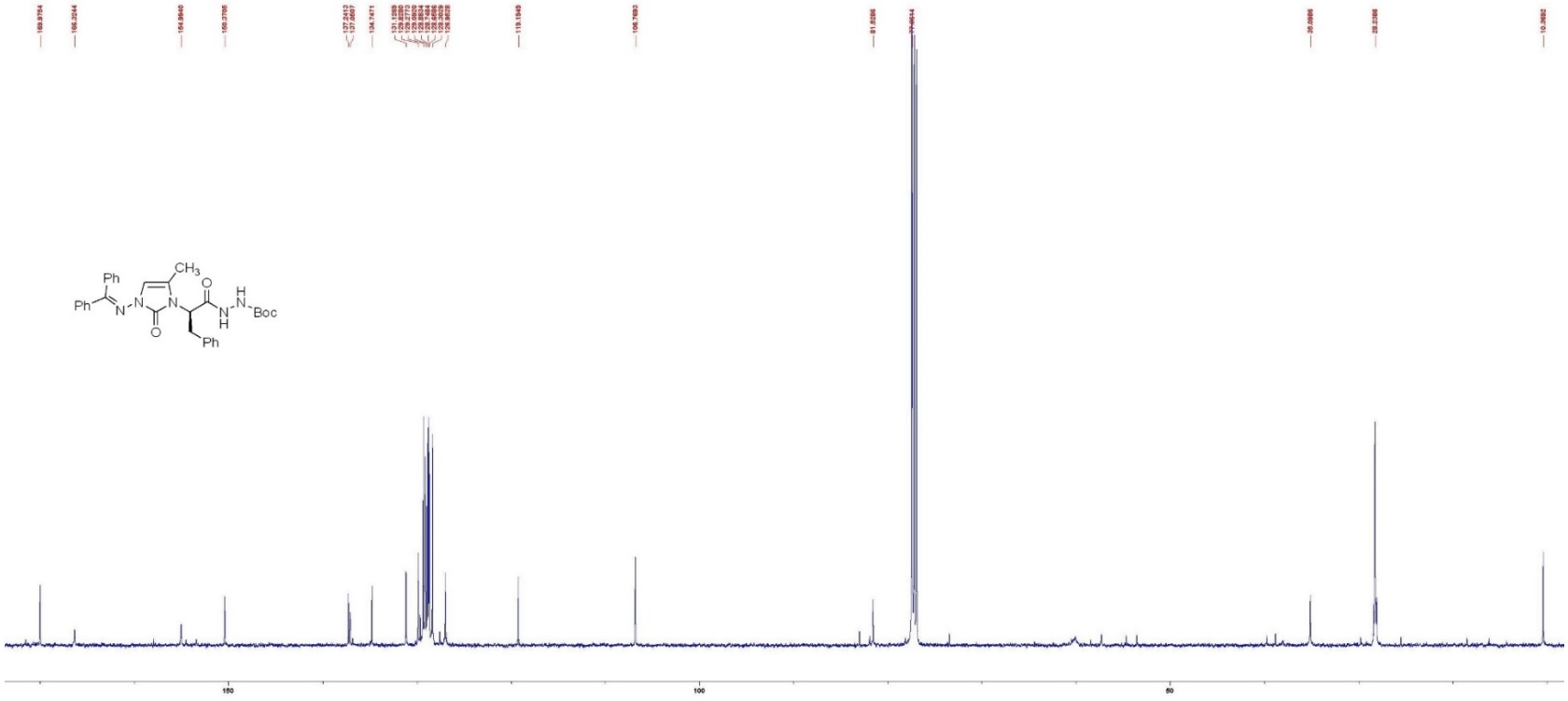

Compound 2.19a

^{1}H-NMR, 500 MHz, $CDCl_3$

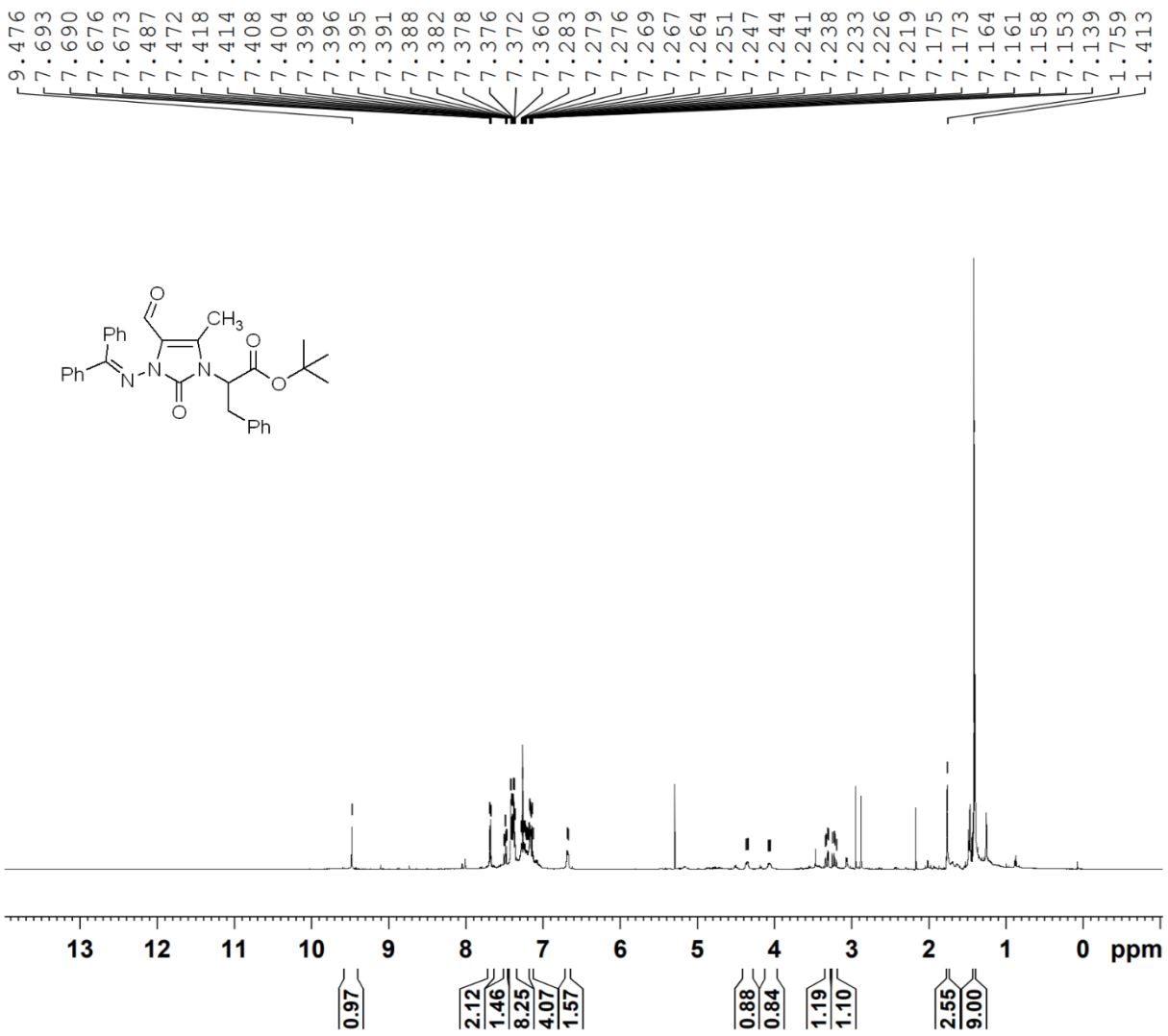

^{13}C-NMR, 125 MHz, $CDCl_3$

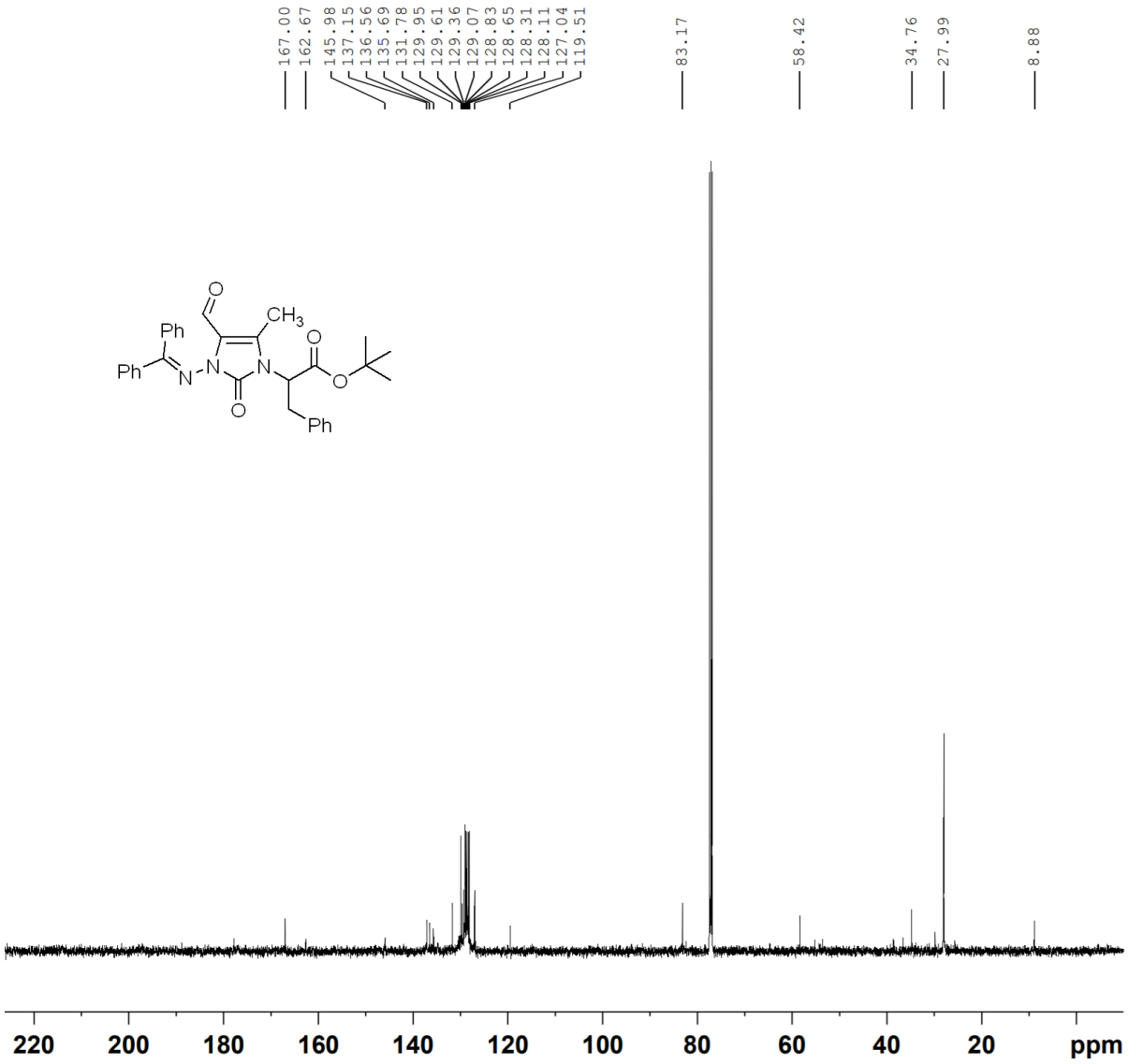

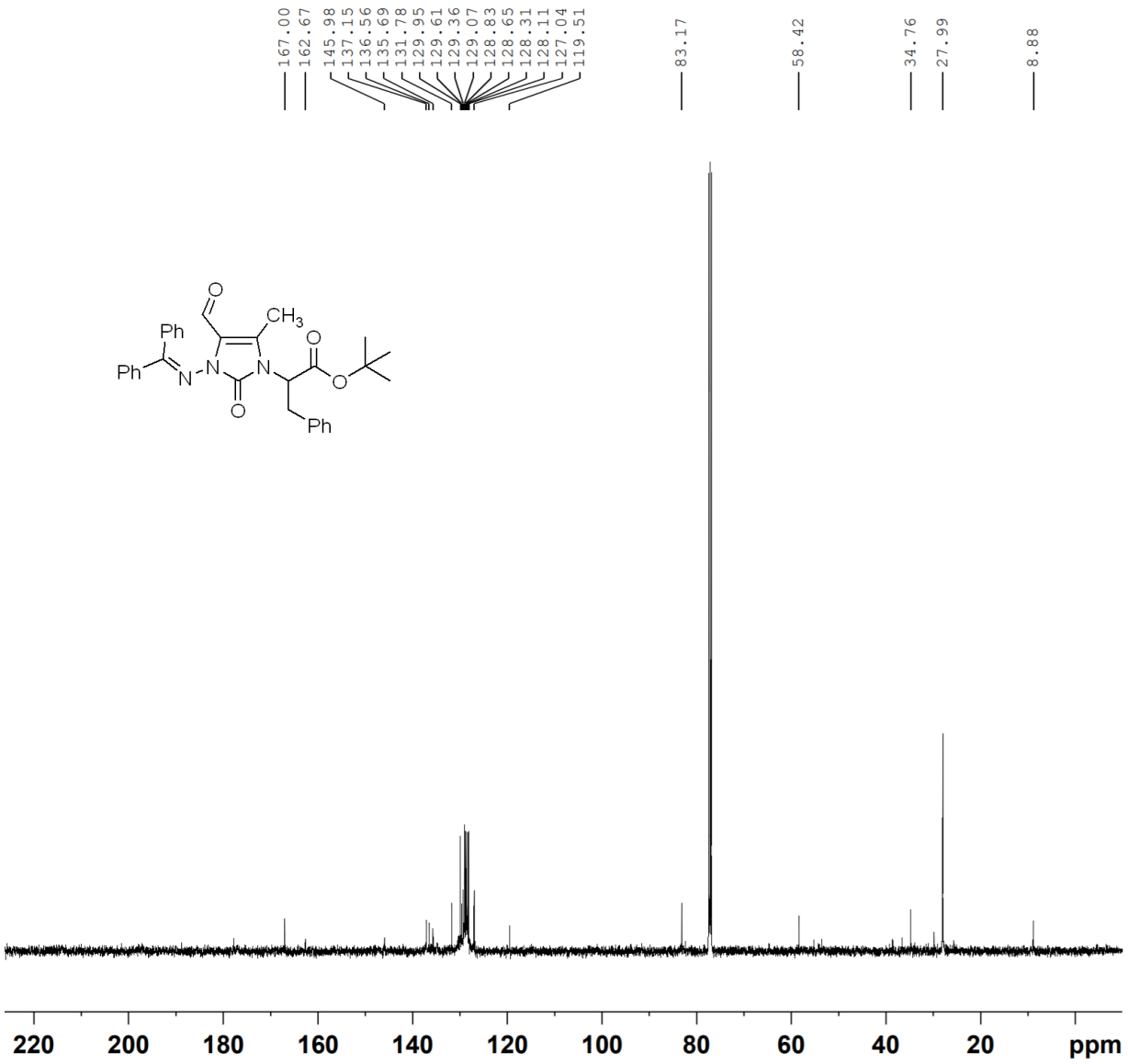
167.00
162.67
145.98
137.15
136.56
135.69
131.78
129.95
129.61
129.36
129.07
128.83
128.65
128.31
128.11
127.04
119.51
83.17
58.42
34.76
27.99
8.88
O
CH3
Ph
Ph
N
N
N
O
O
O
Ph
220
200
180
160
140
120
100
80
60
40
20
ppm

Compound 2.19b

^{1}H-NMR, 300 MHz, $CDCl_3$

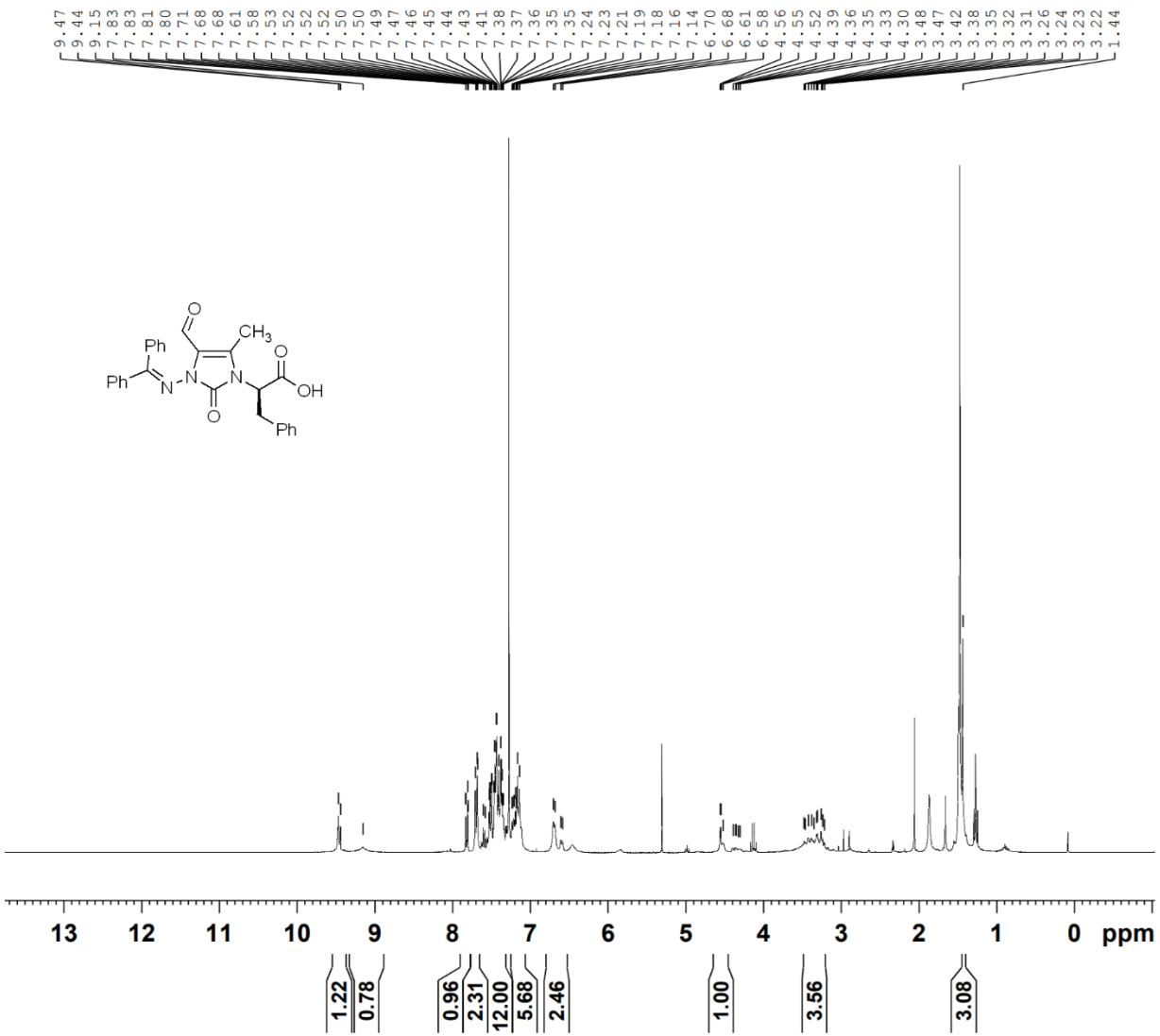

^{13}C-NMR, 125 MHz, $CDCl_3$

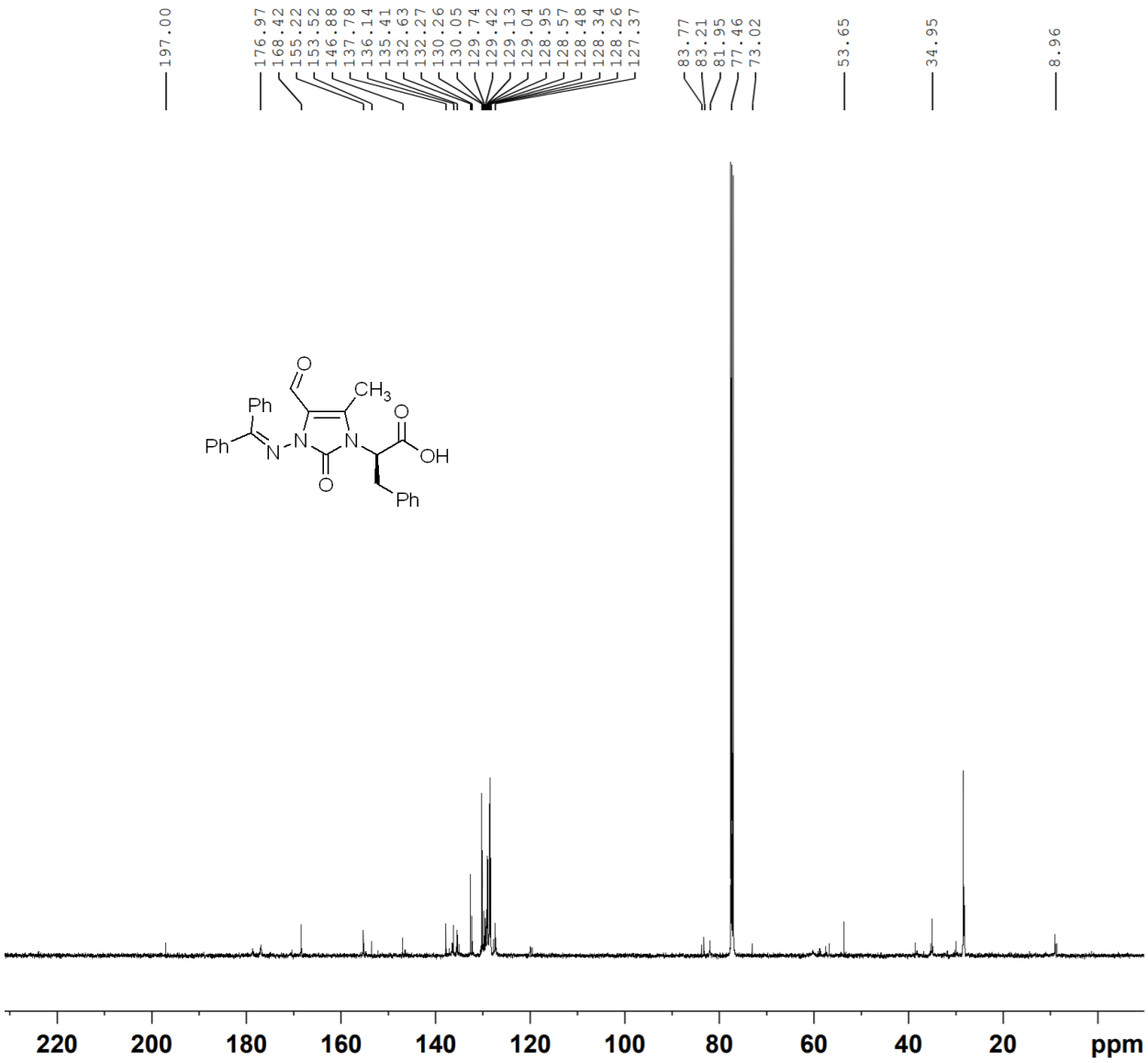

Compound 2.19c

^{1}H-NMR, 500 MHz, $CDCl_3$

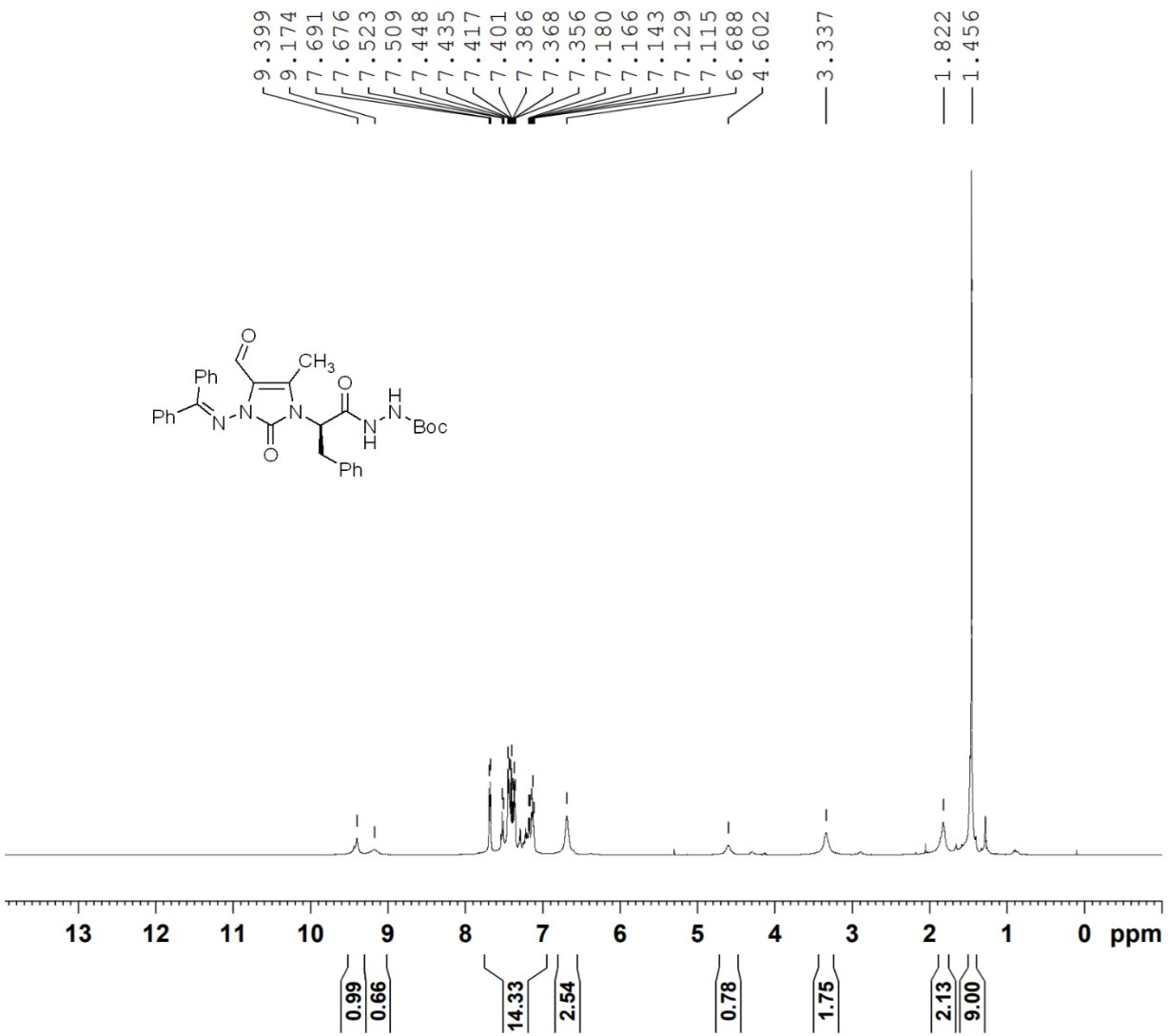

^{13}C-NMR, 125 MHz, $CDCl_3$

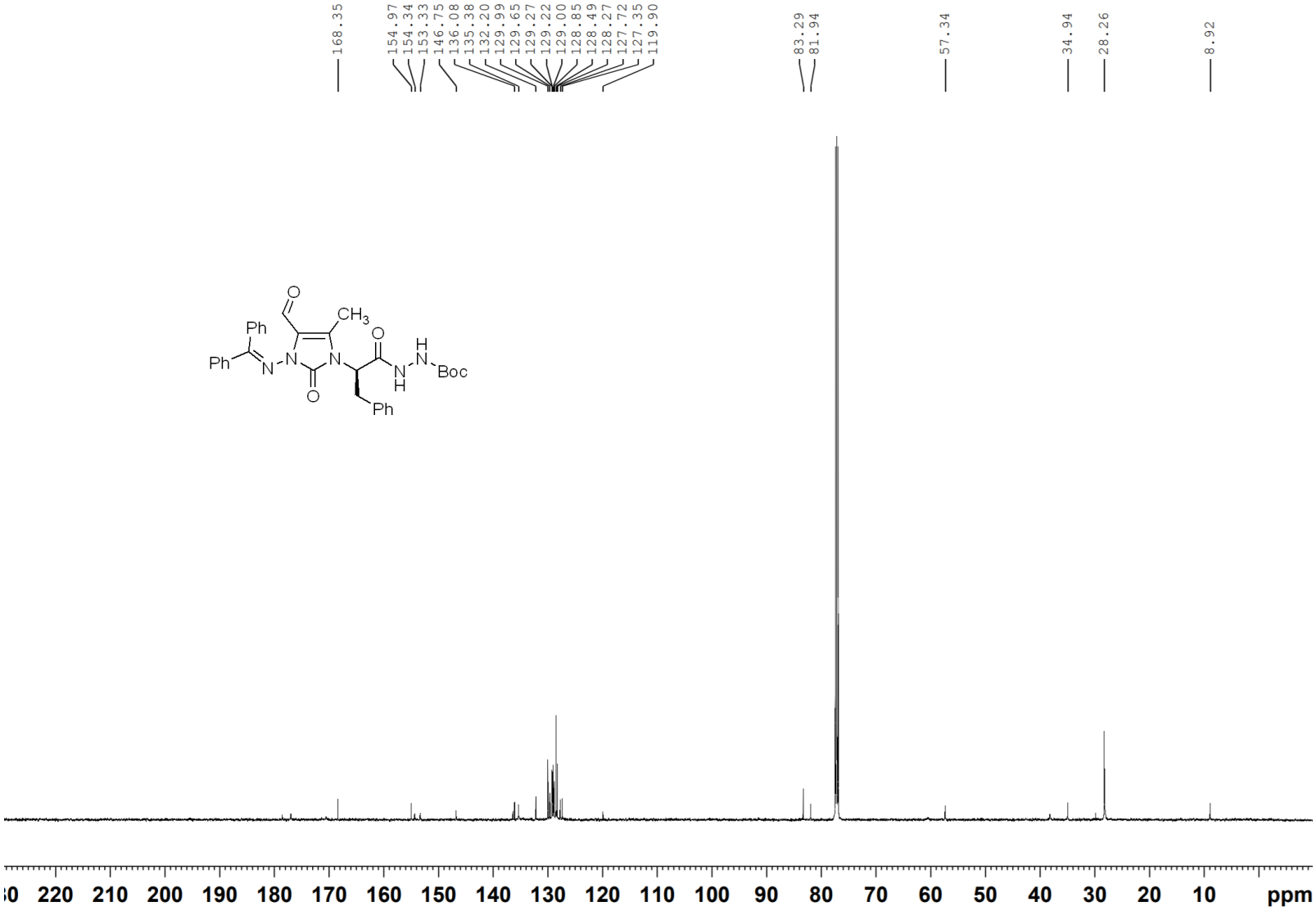

Compound 2.19d

^{1}H-NMR, 400 MHz, $CDCl_3$

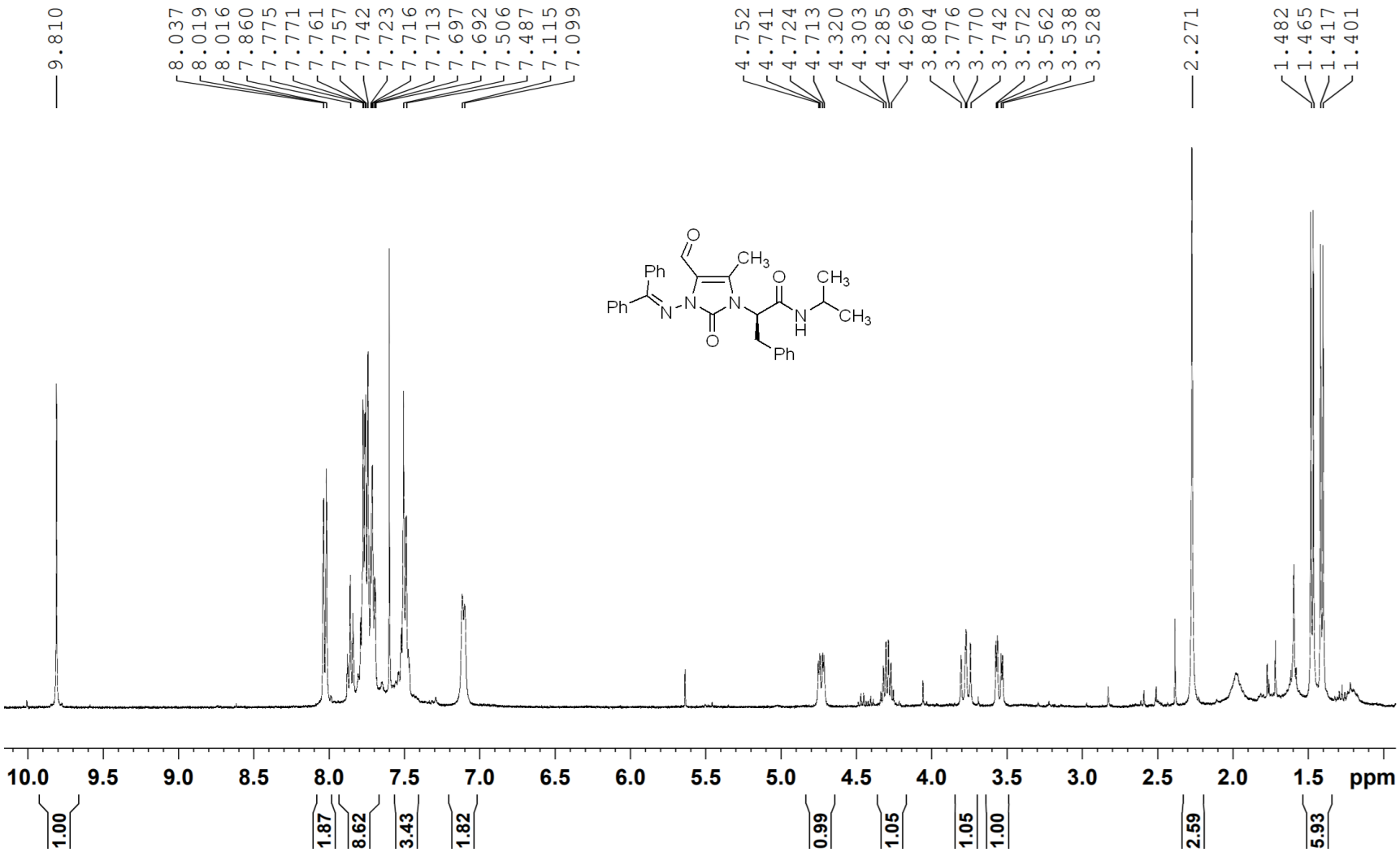

^{13}C-NMR, 125 MHz, $CDCl_3$

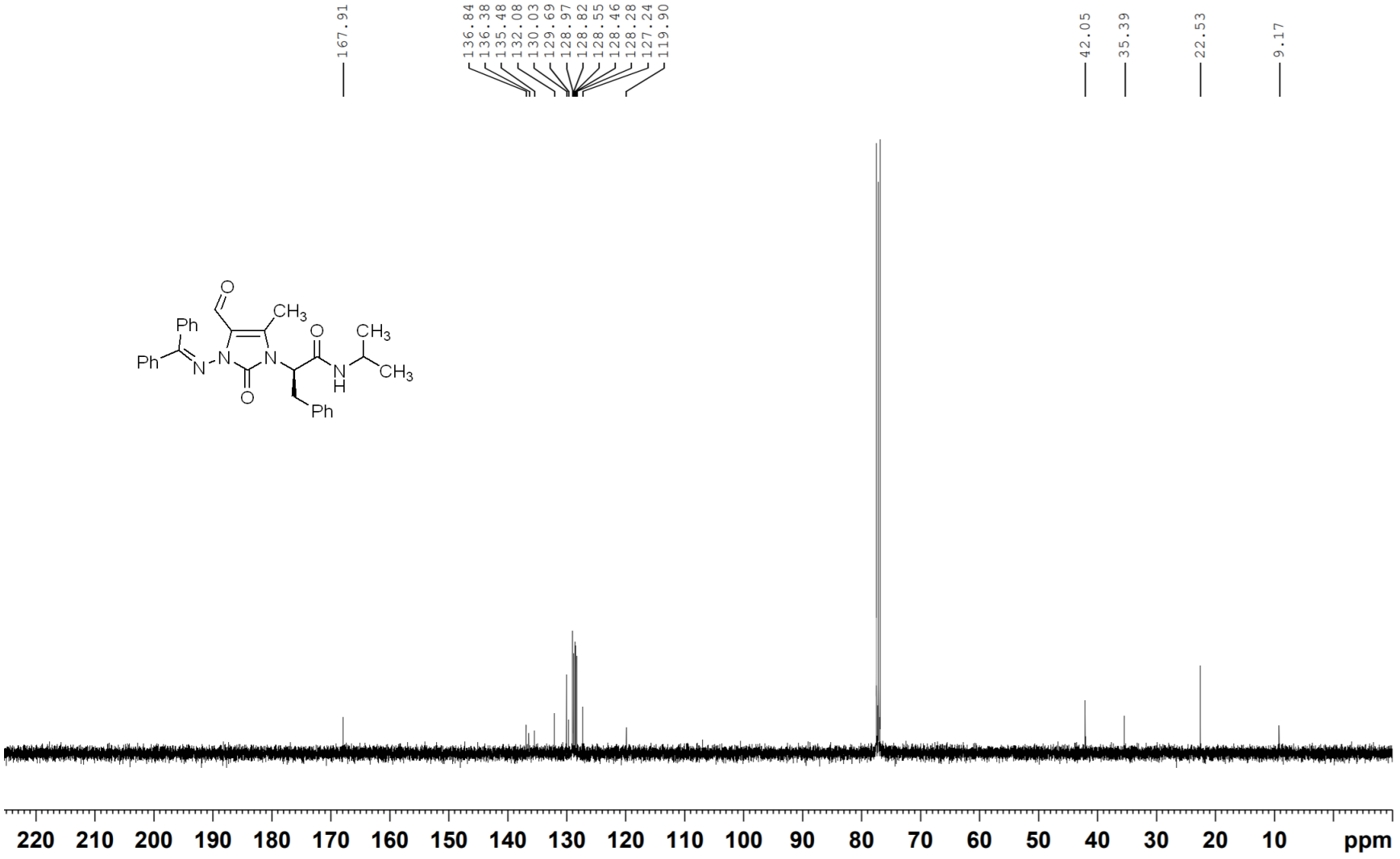

Compound 2.20

^{1}H-NMR, 300 MHz, $CDCl_3$

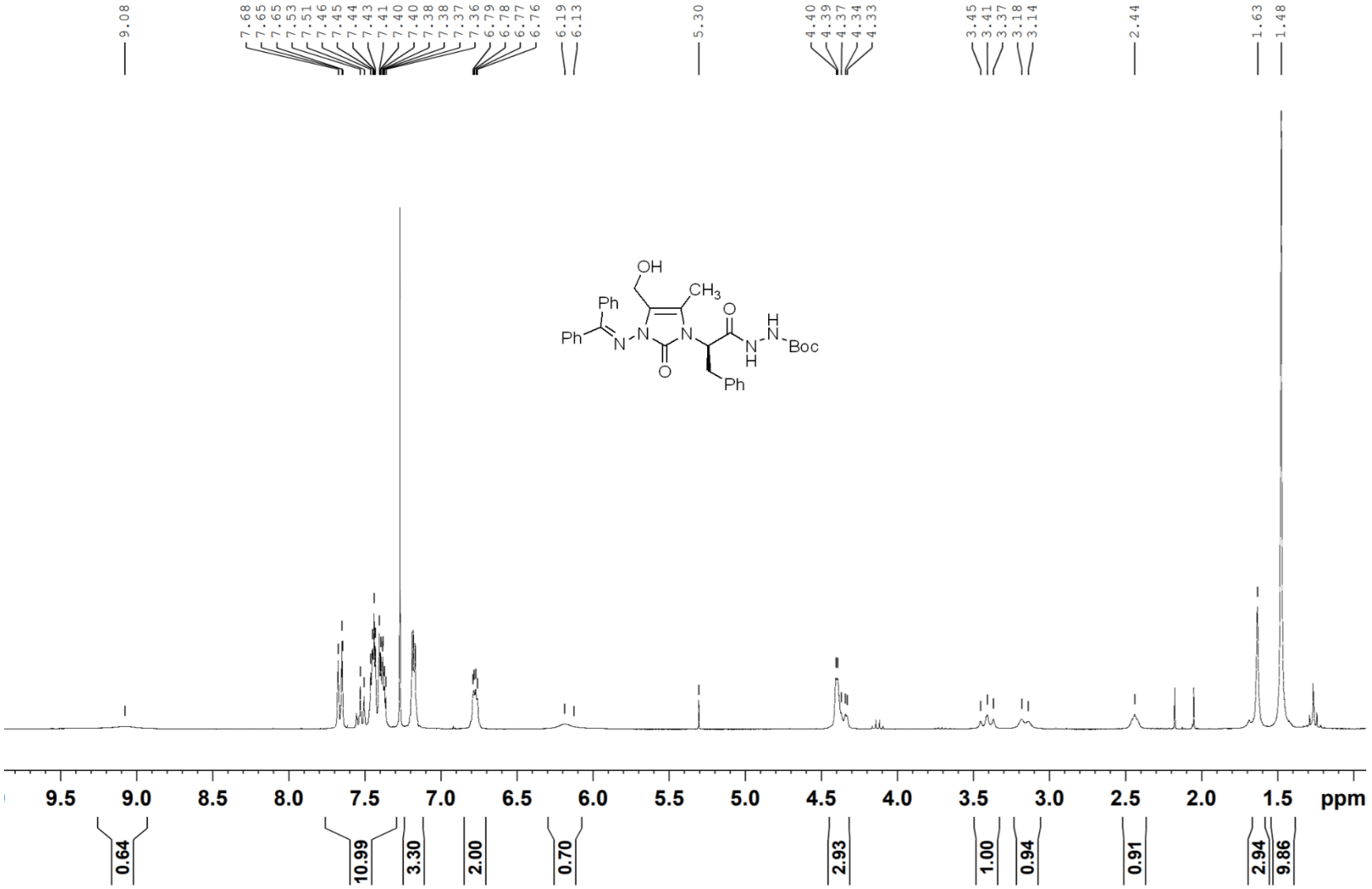

^{13}C-NMR, 75 MHz, $CDCl_3$

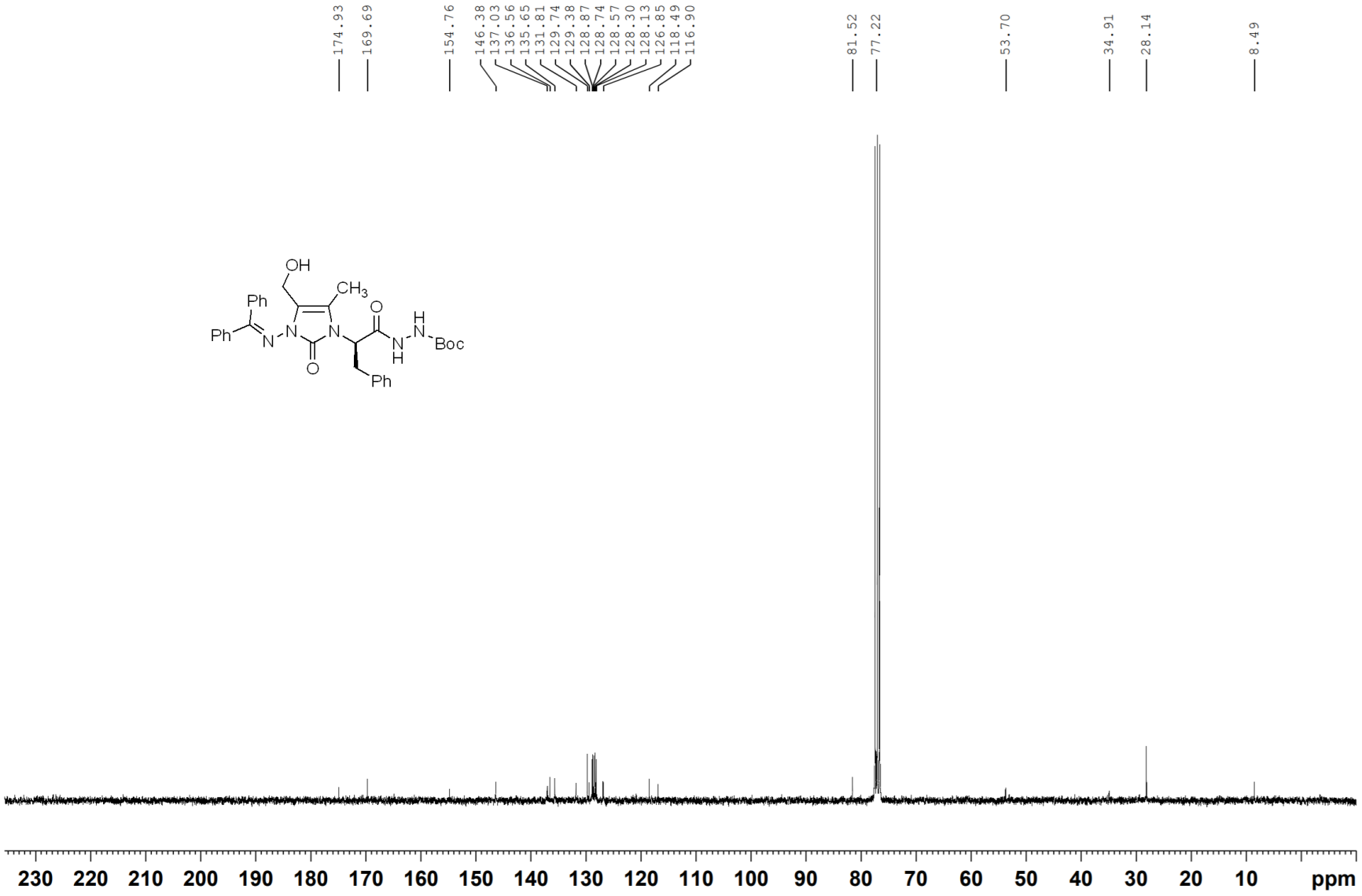

Compound 2.21

^{1}H-NMR, 400 MHz, $CDCl_3$

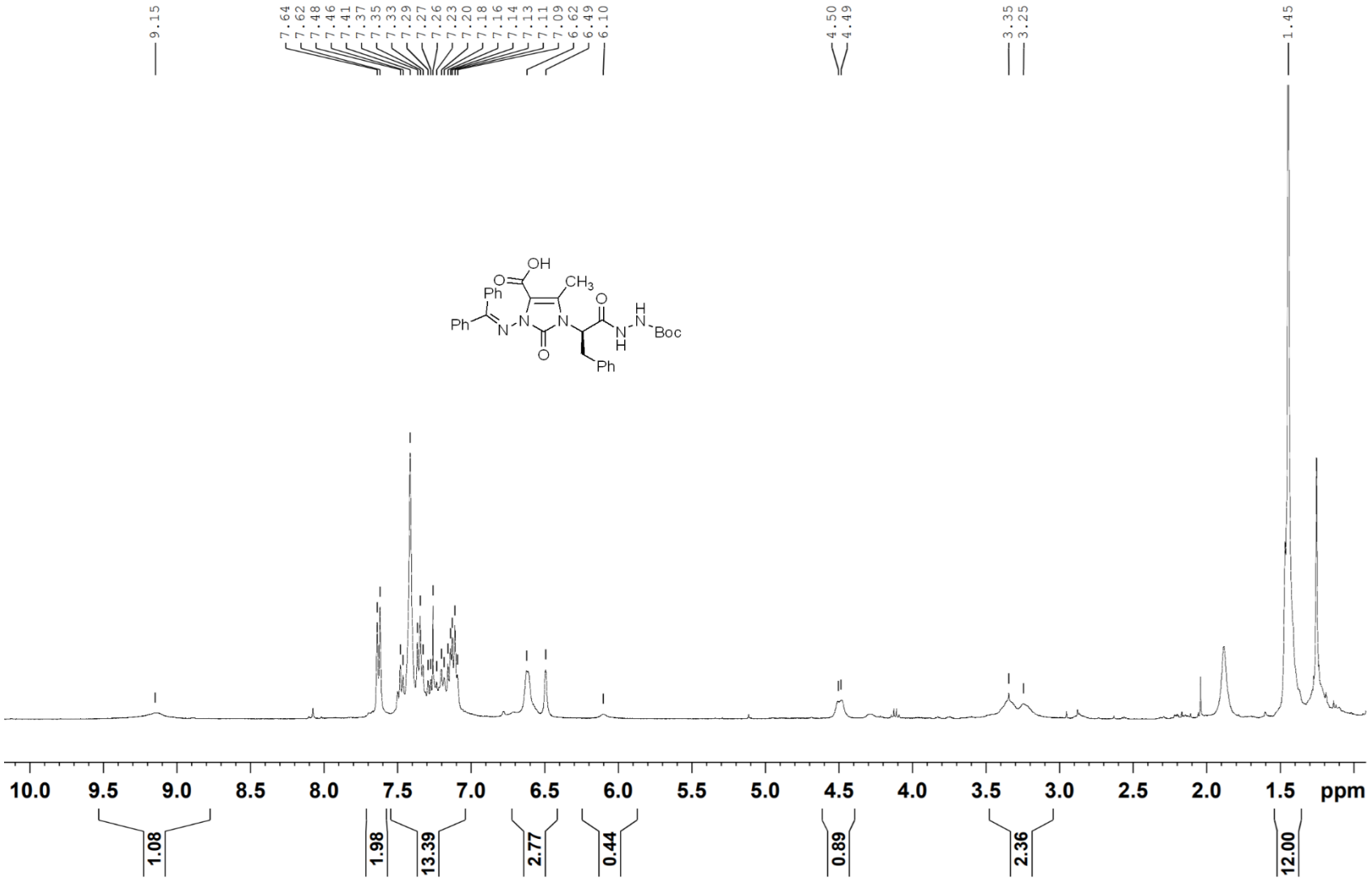

^{13}C-NMR, 75 MHz, $CDCl_3$

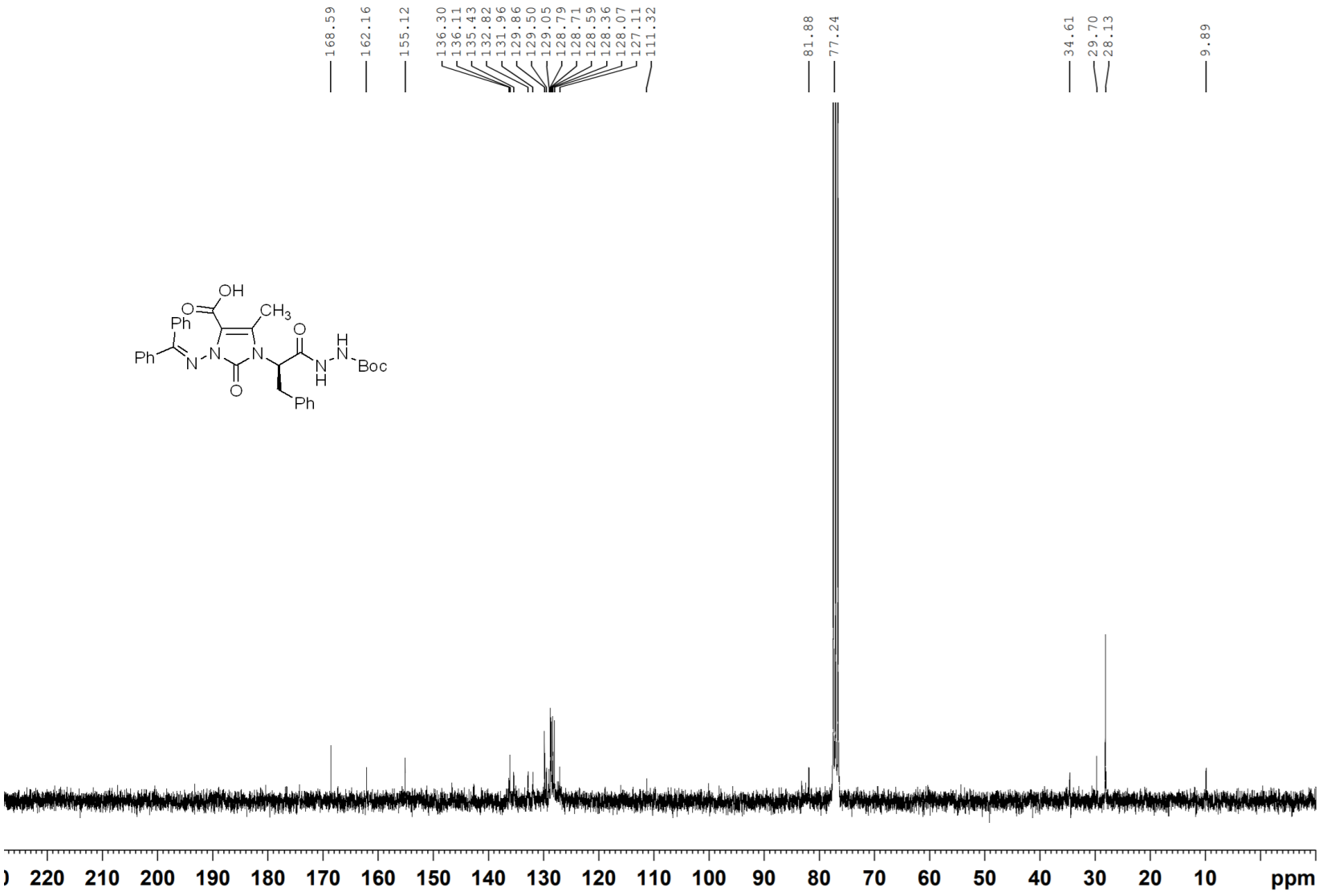

Compound 2.22

^{1}H-NMR, 300 MHz, $CDCl_3$

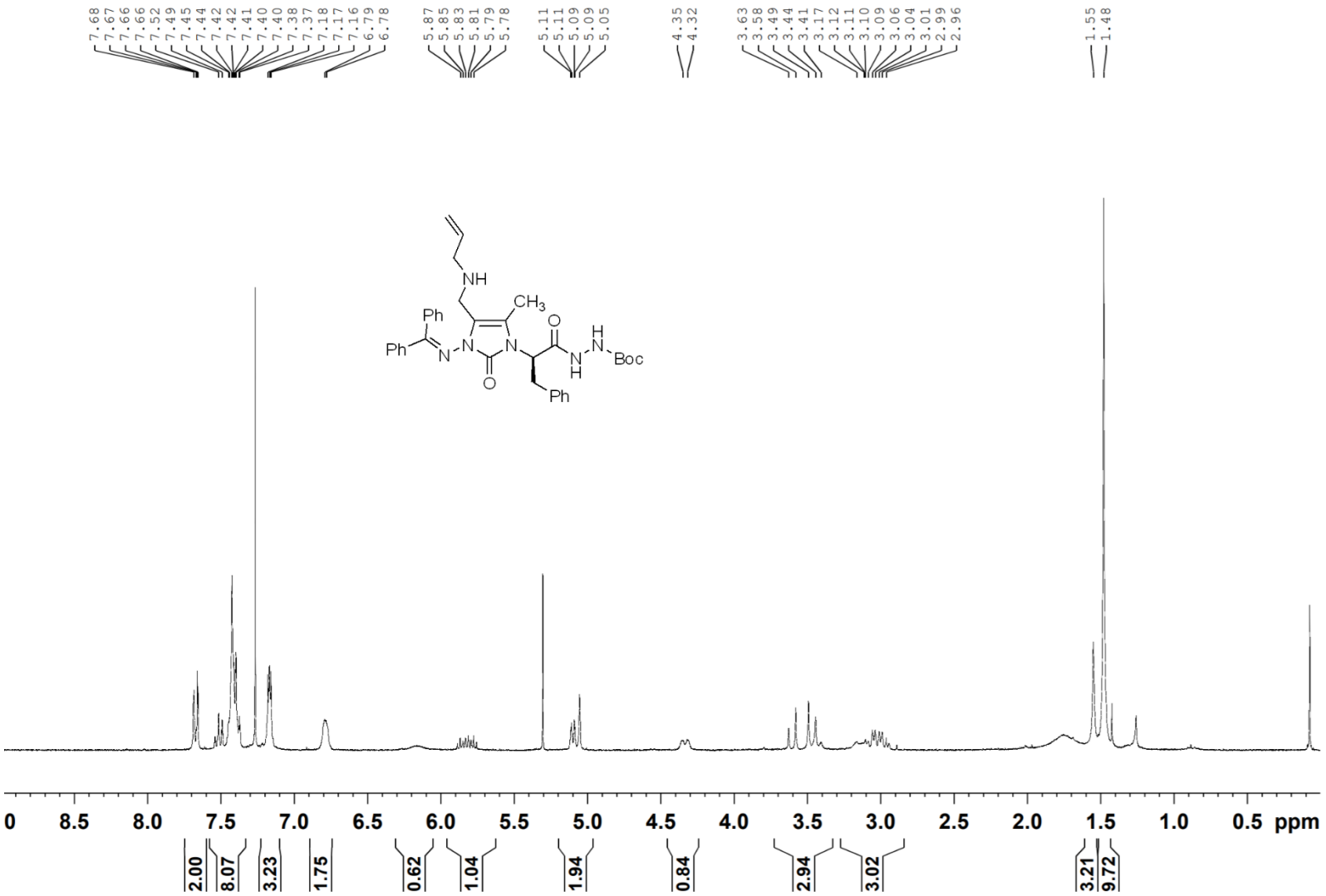

^{13}C-NMR, 125 MHz, $CDCl_3$

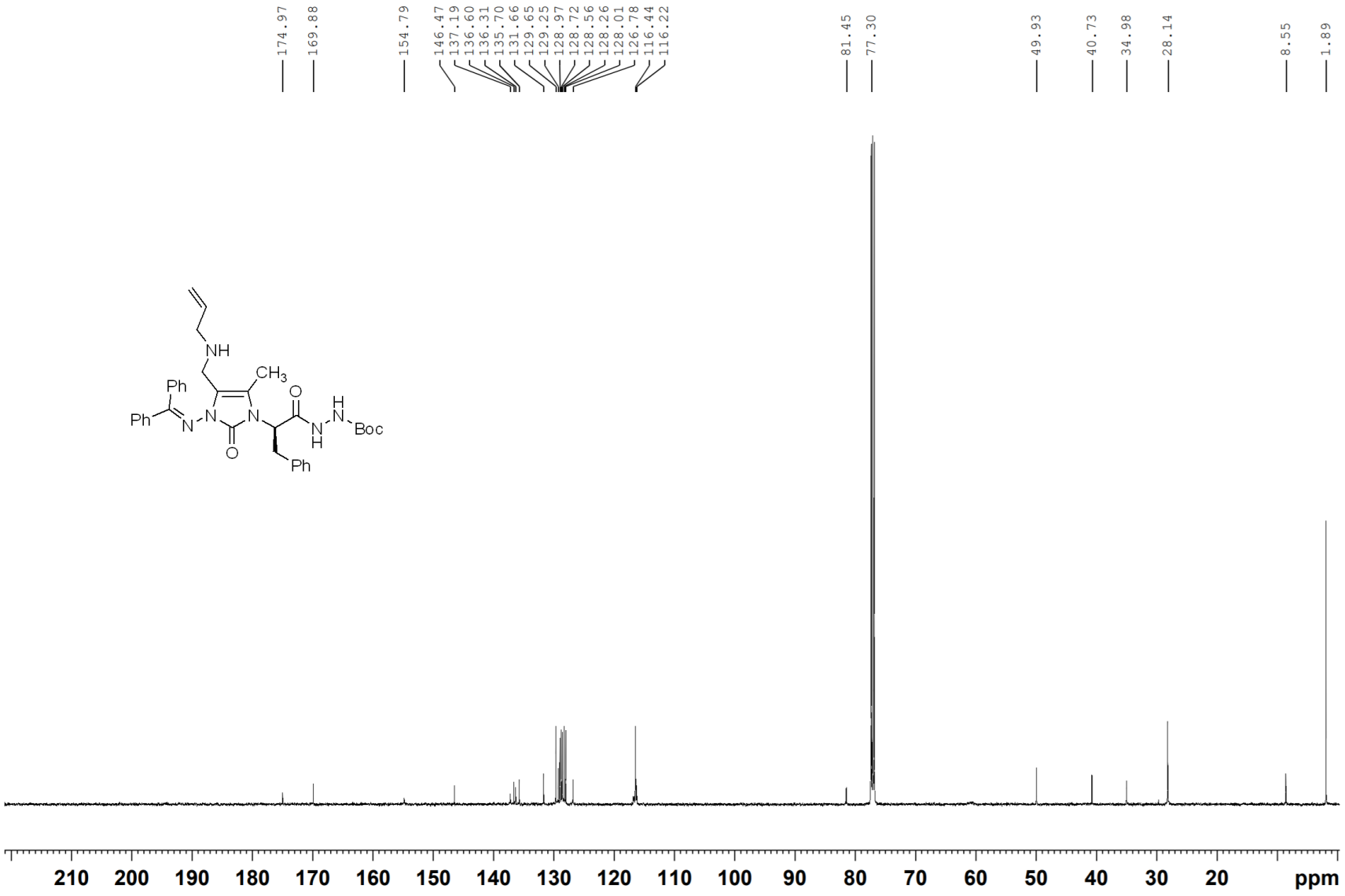

Compound 2.23

^{1}H-NMR, 300 MHz, $CDCl_3$

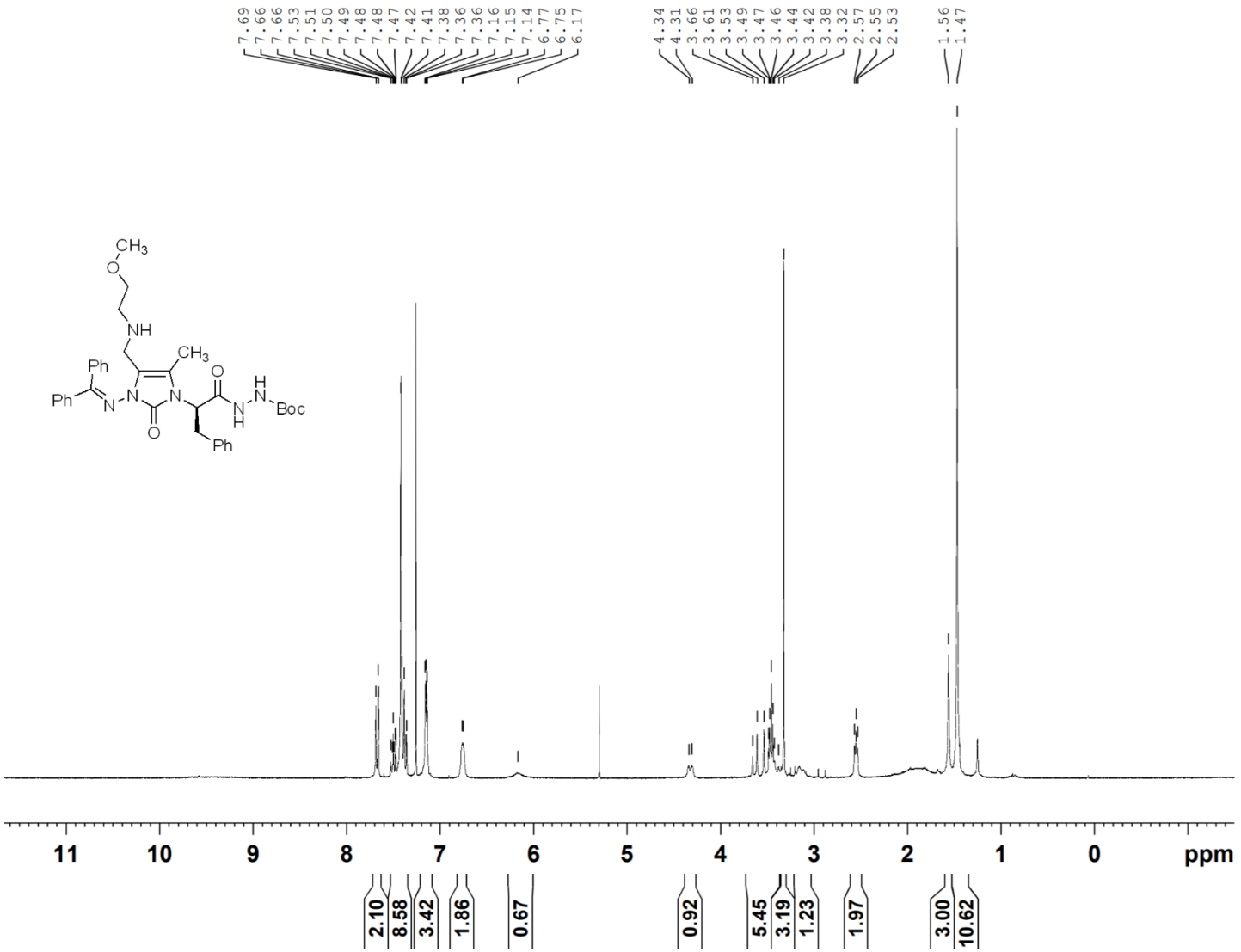

^{13}C-NMR, 100 MHz, $CDCl_3$

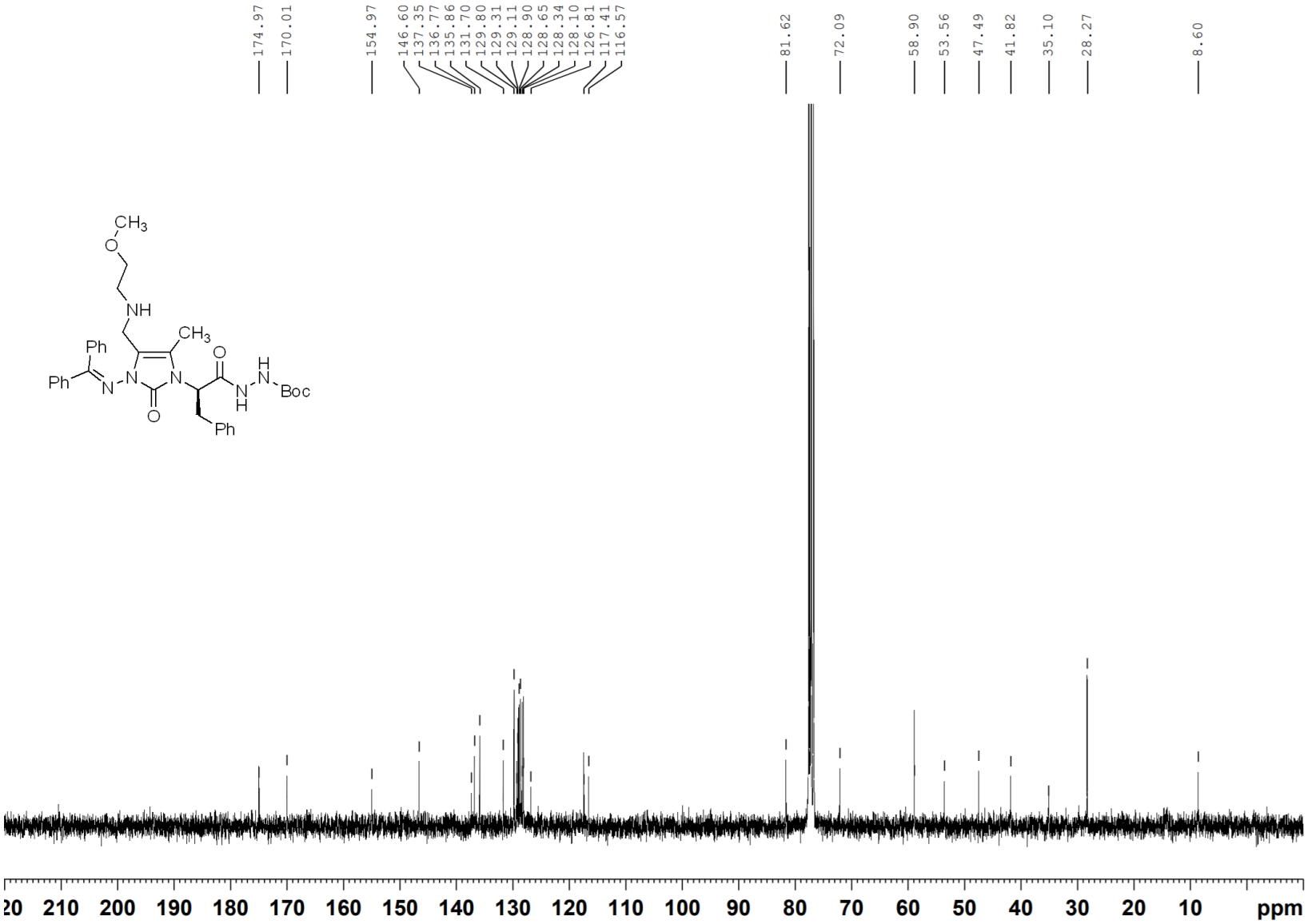

Compound 2.24

^{1}H-NMR, 500 MHz, $CDCl_3$

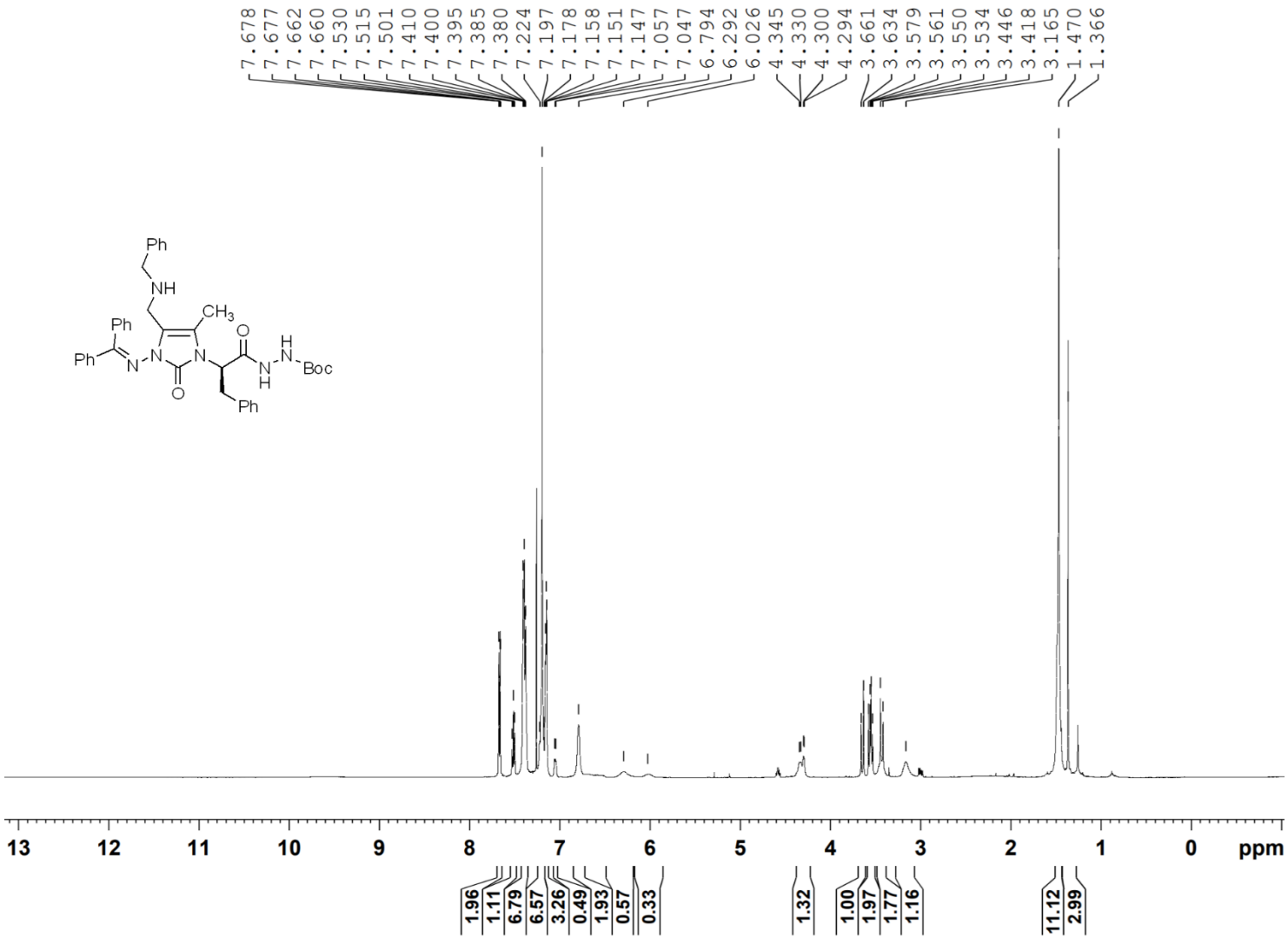

^{13}C-NMR, 125 MHz, $CDCl_3$

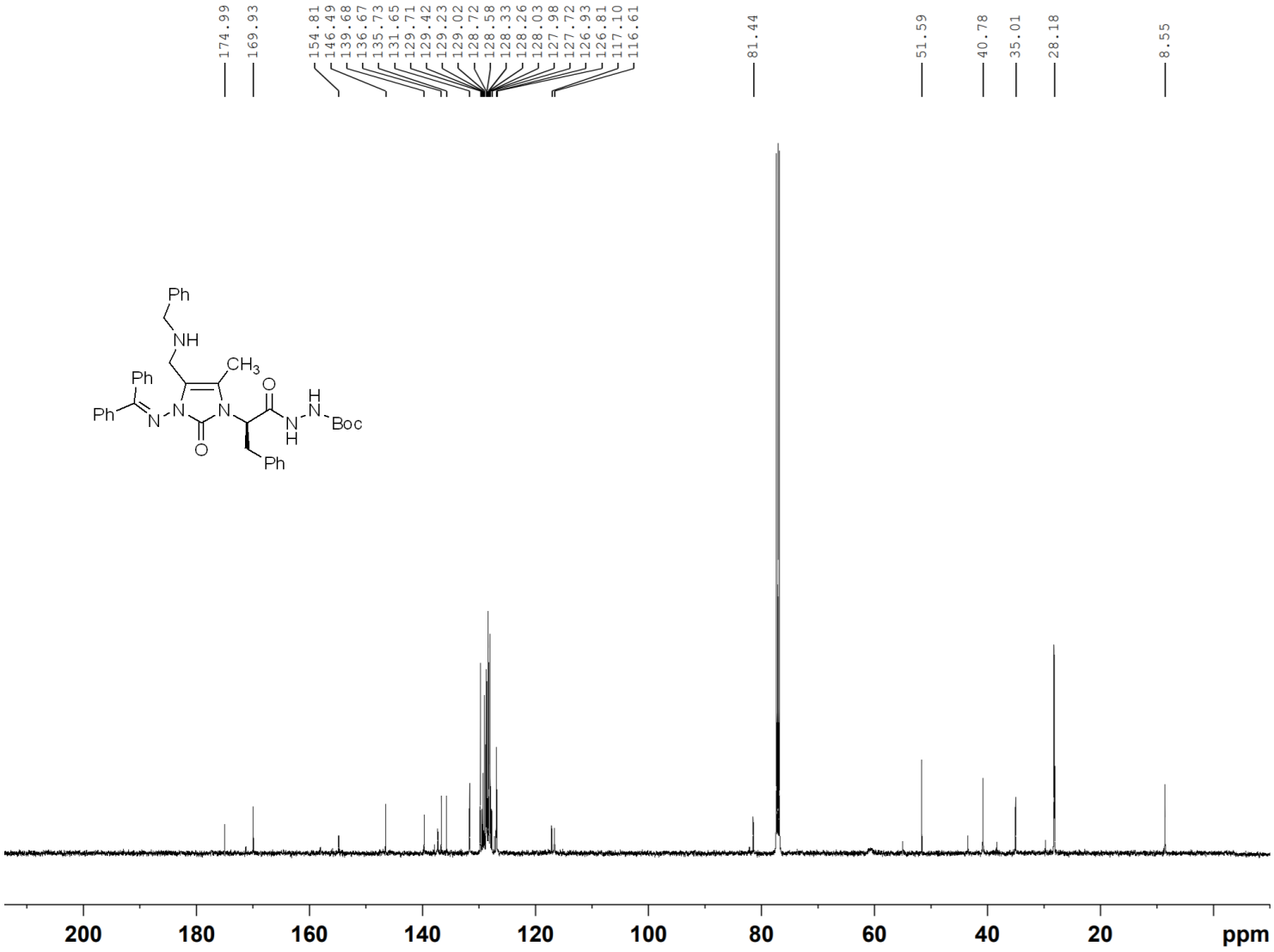

Compound 2.25

^{1}H-NMR, 500 MHz, $CDCl_3$

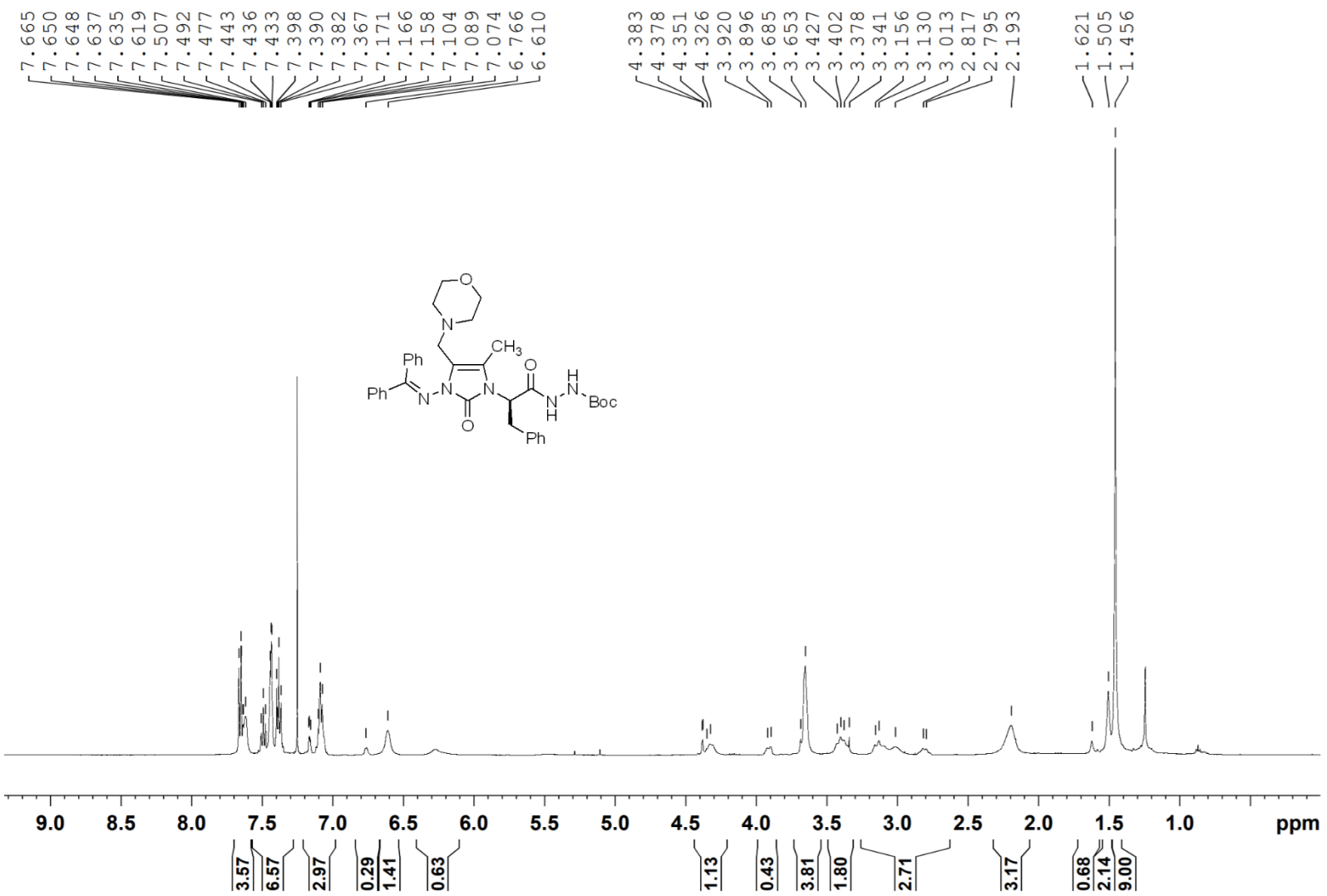

^{13}C-NMR, 125 MHz, $CDCl_3$

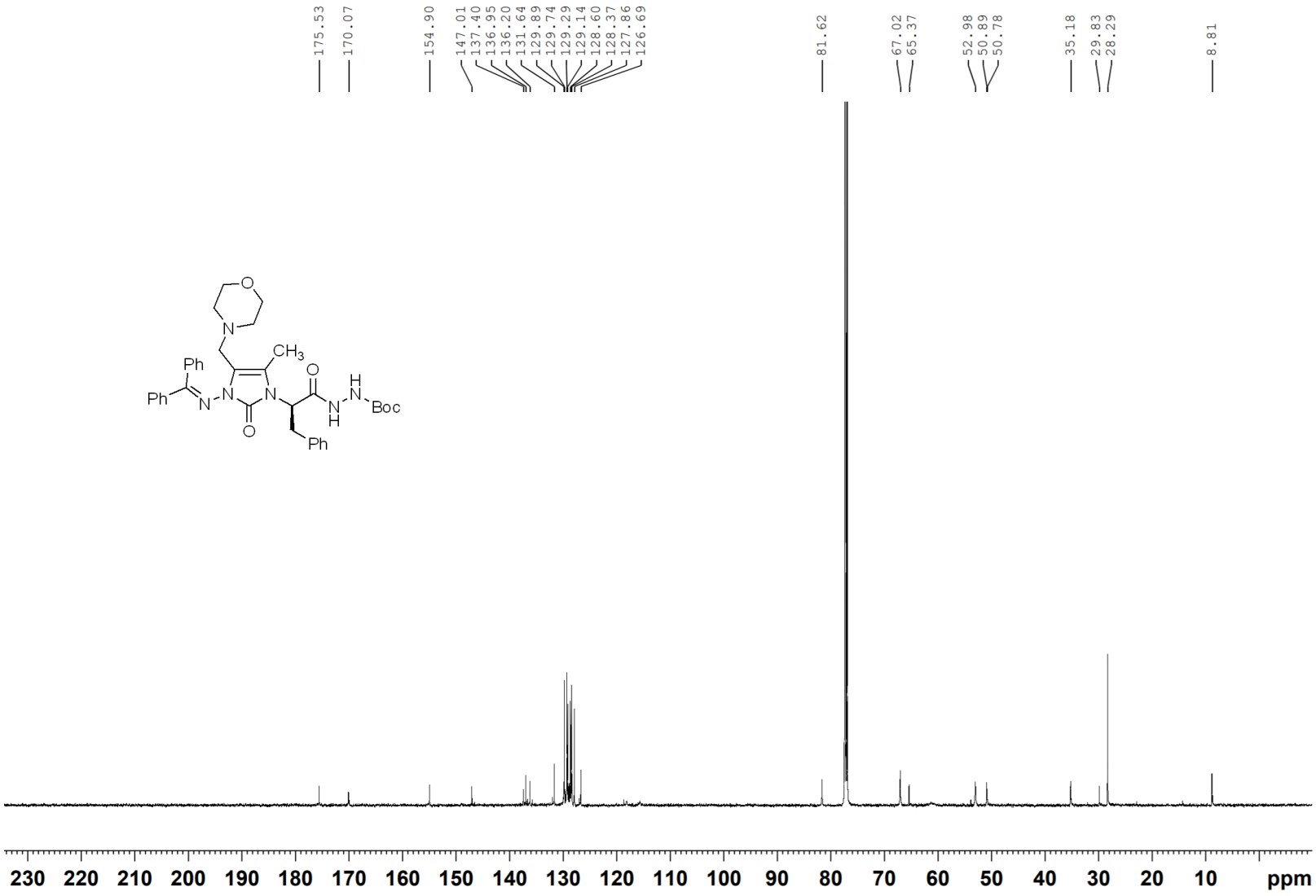

Compound 2.26

^{1}H-NMR, 300 MHz, $CDCl_3$

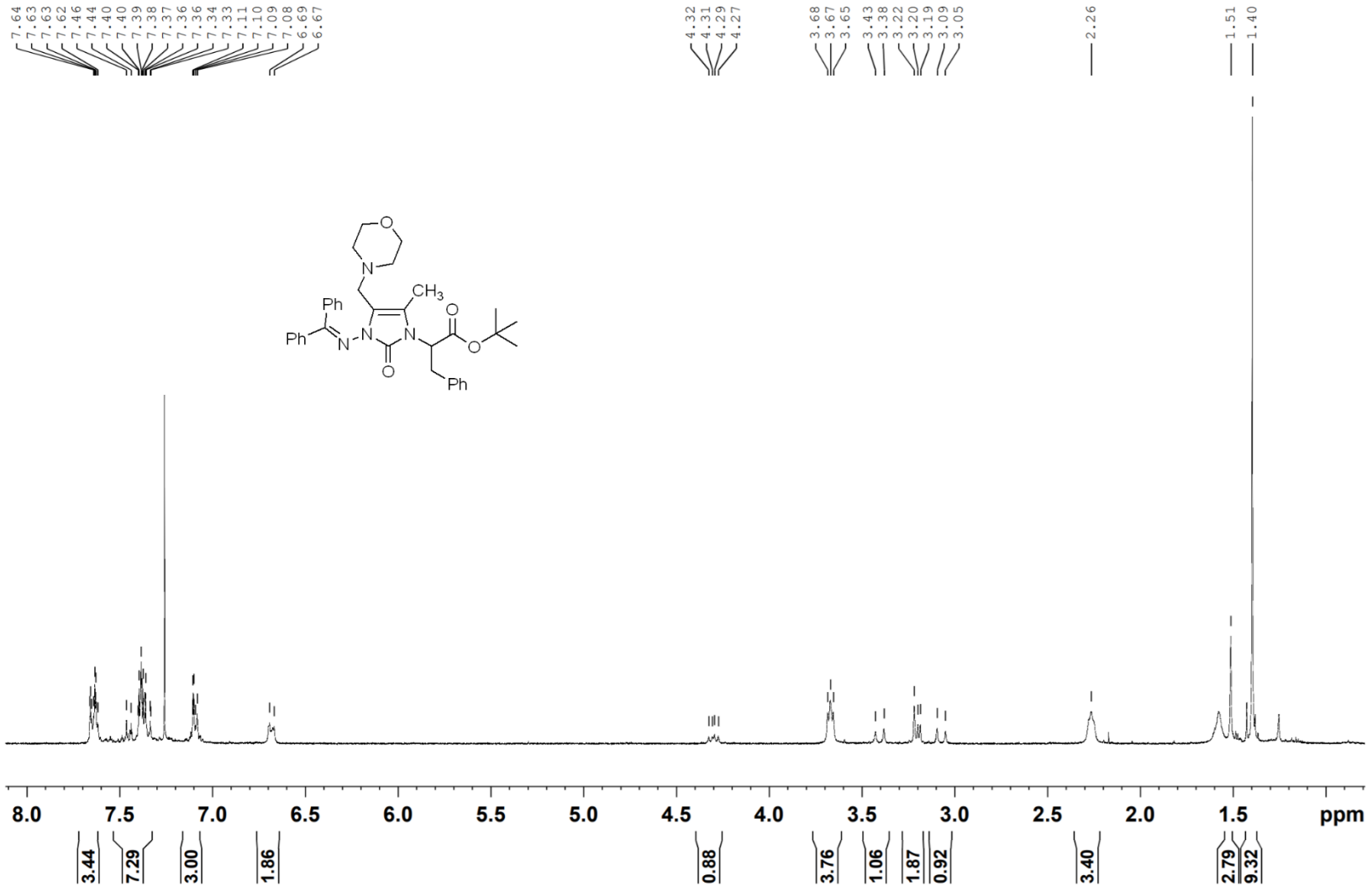

^{13}C-NMR, 100 MHz, $CDCl_3$

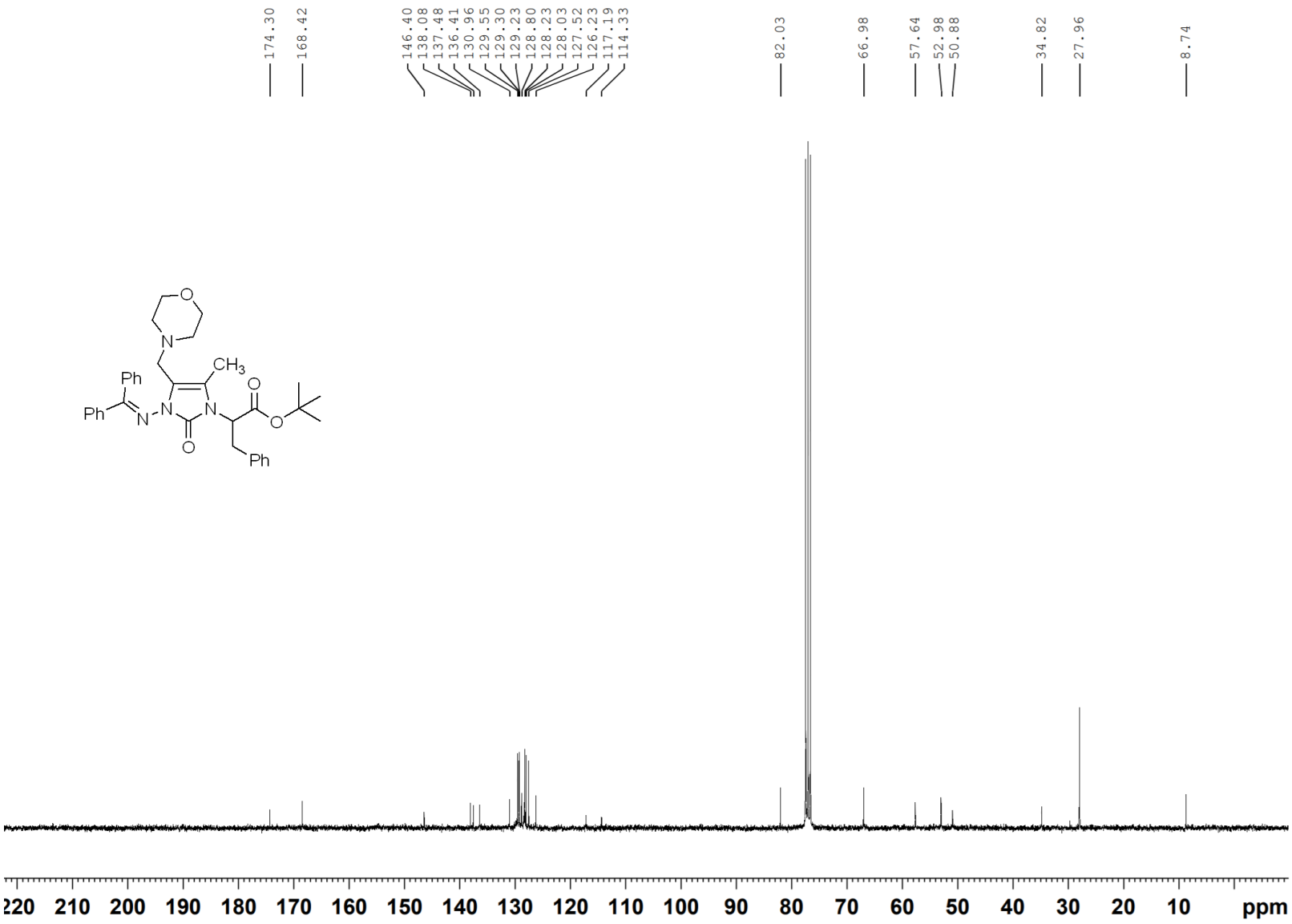

Annex 2: NMR Spectra for chapter 3

Compound 3.17

^{1}H-NMR, 400 MHz, $CDCl_3$

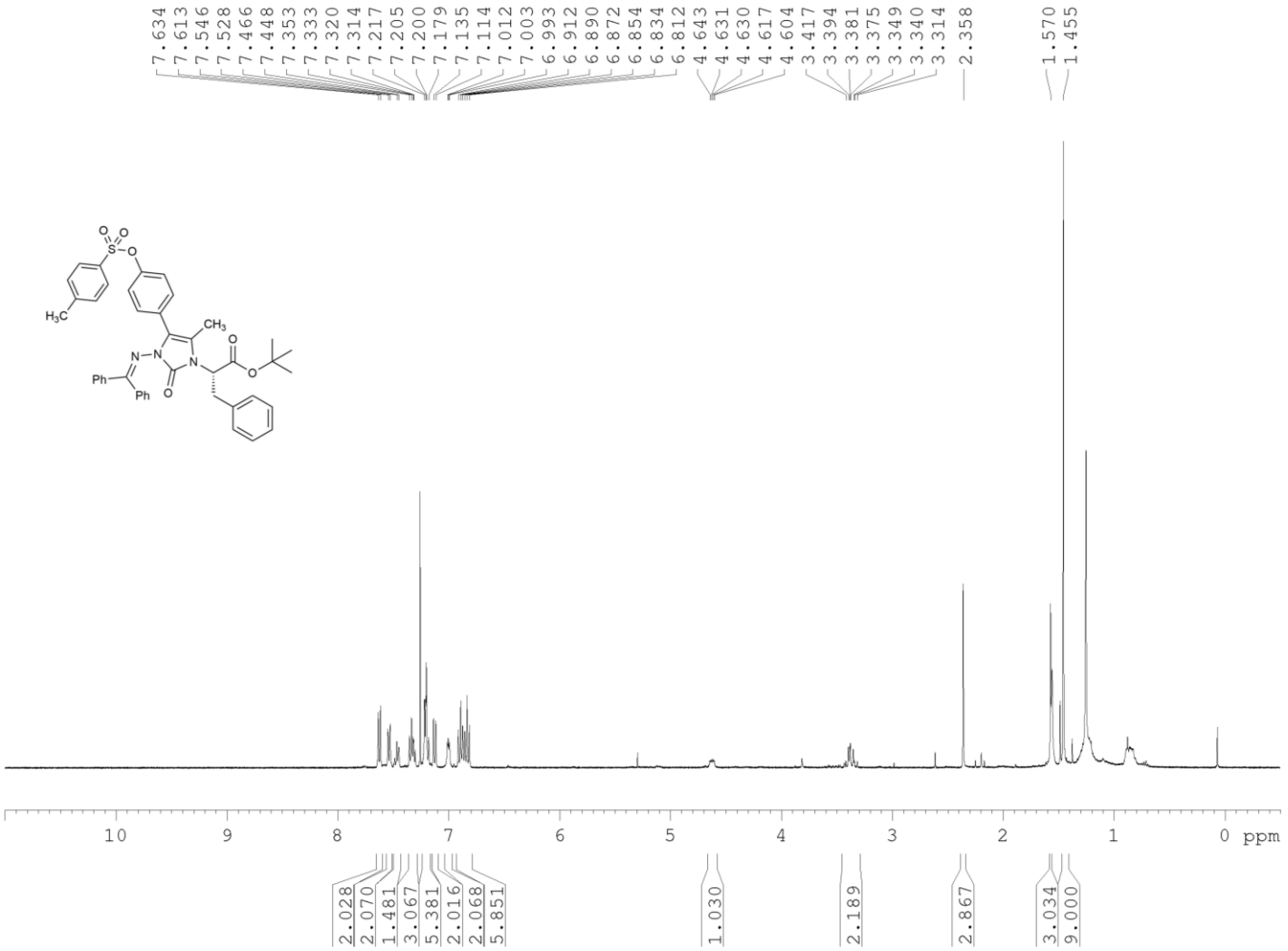

^{13}C-NMR, 75 MHz, $CDCl_3$

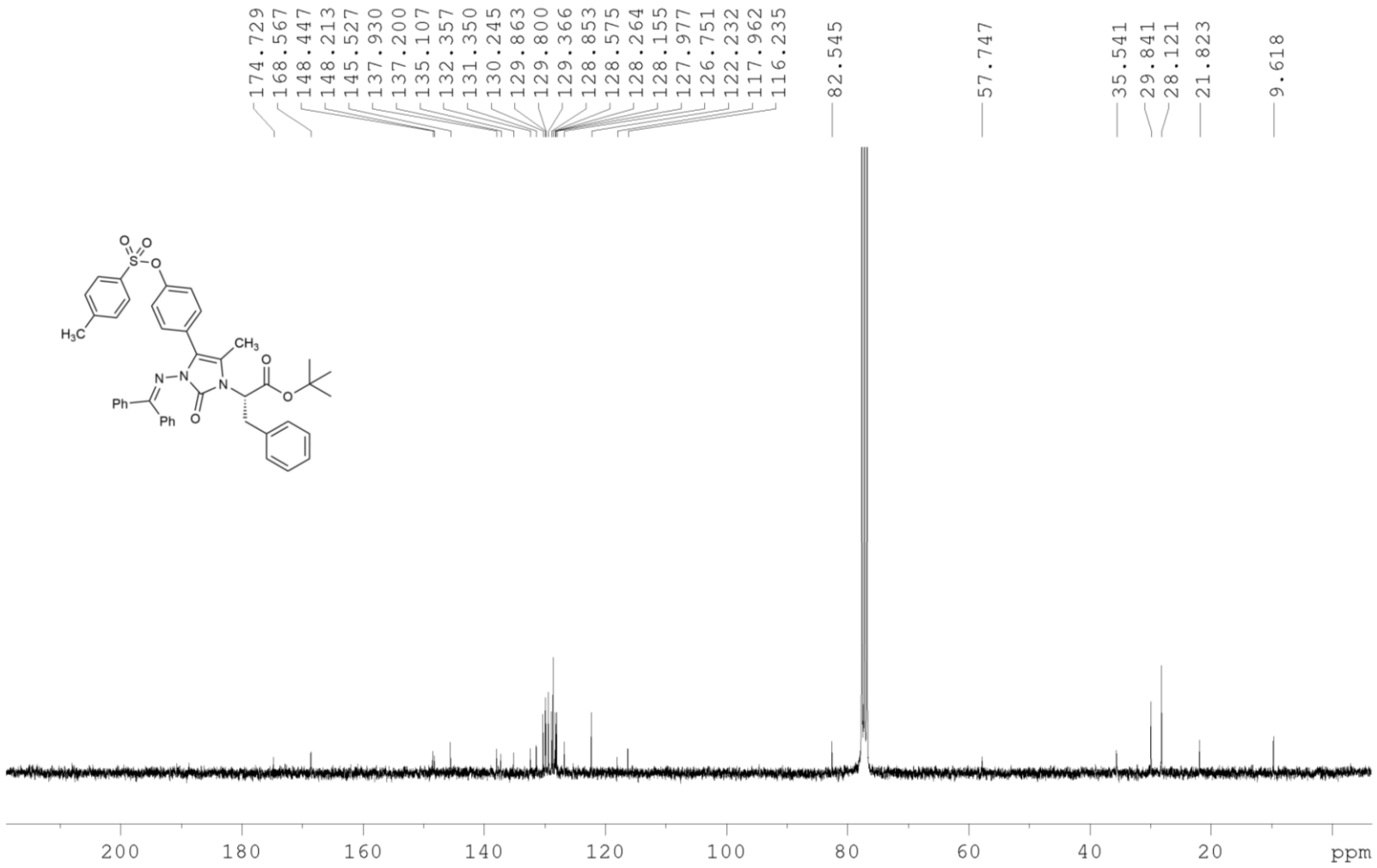

Compound 3.18

^{1}H-NMR, 400 MHz, $CDCl_3$

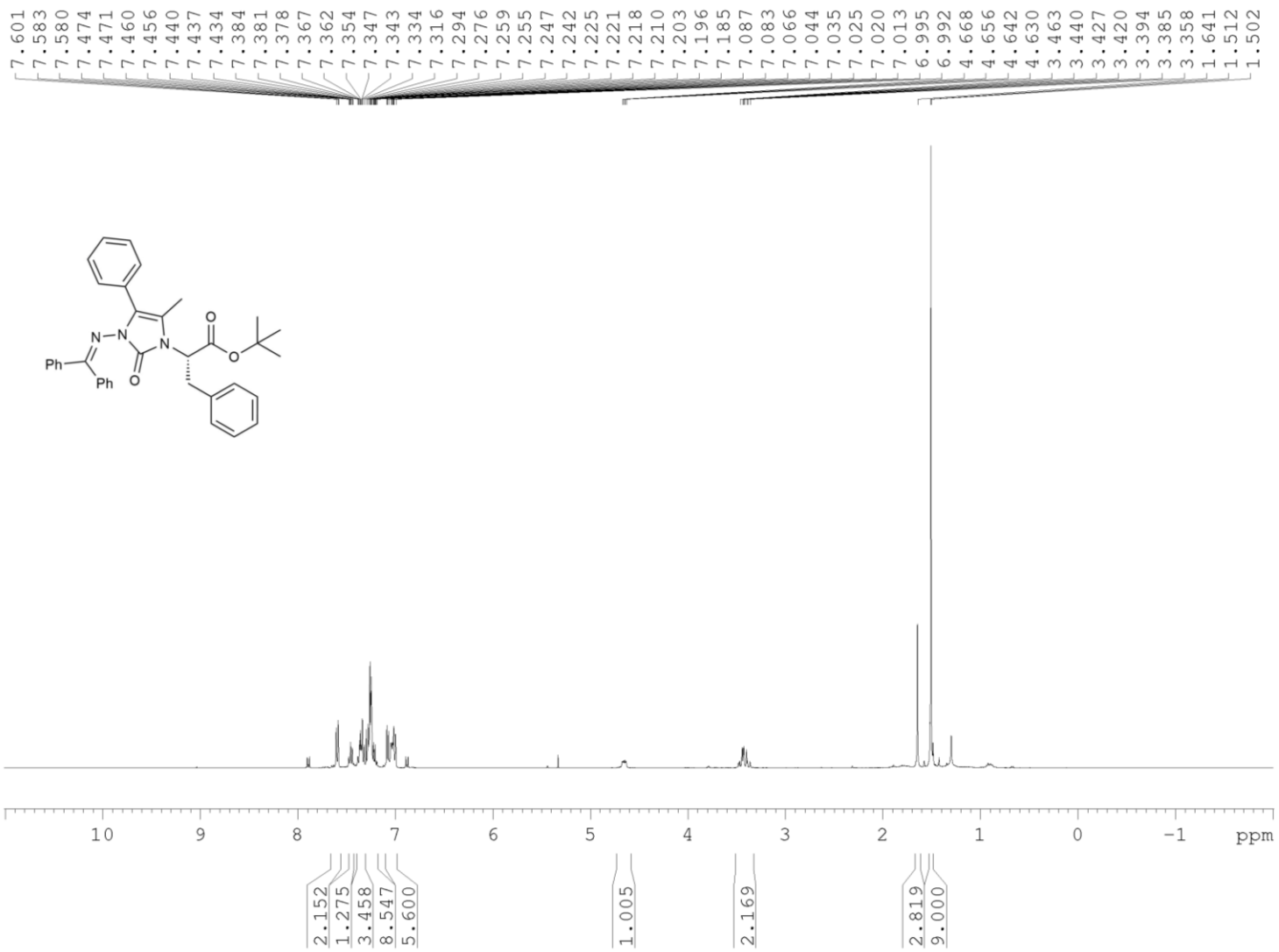

^{13}C-NMR, 101 MHz, $CDCl_3$

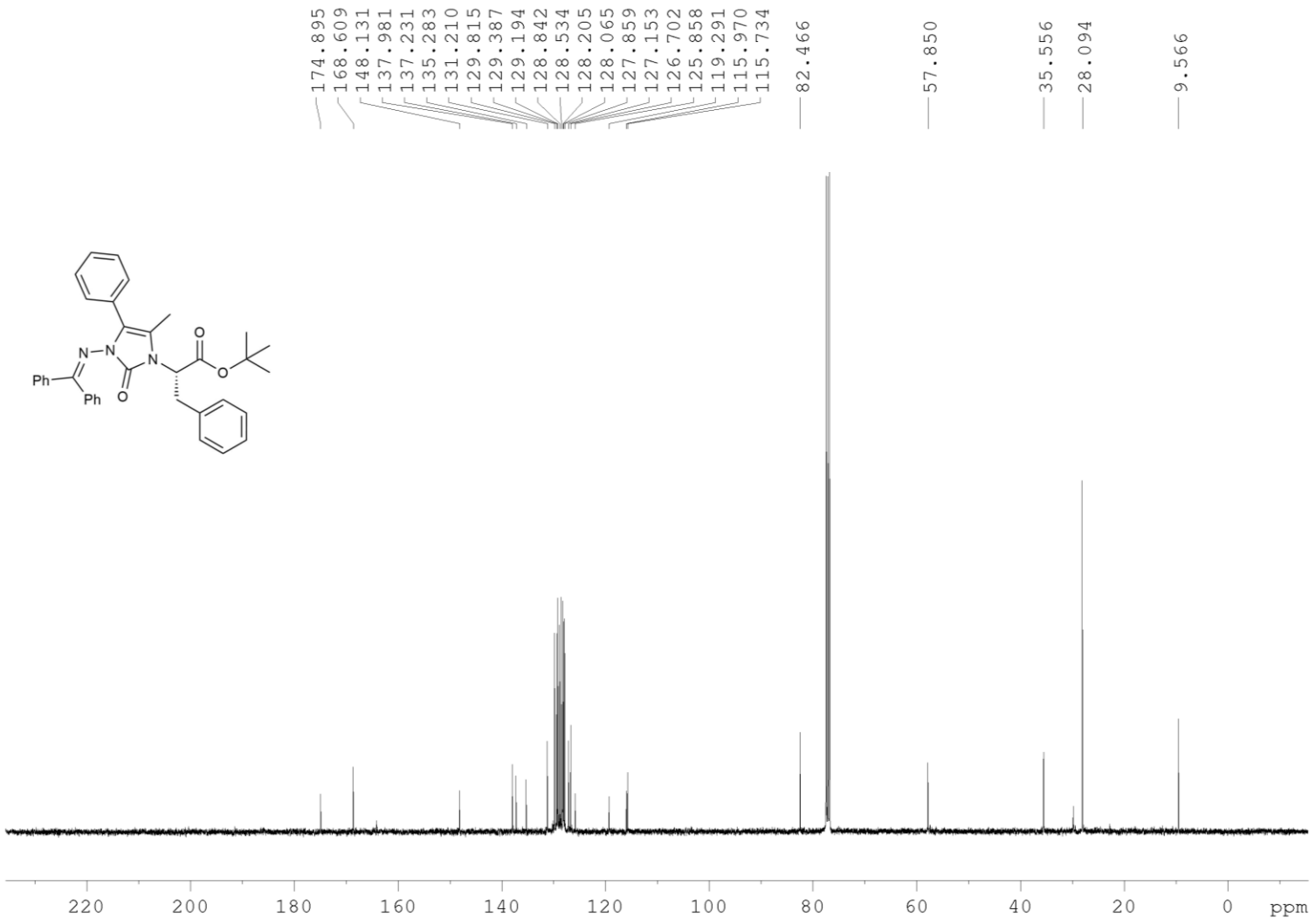

Compound 3.19

^{1}H-NMR, 400 MHz, $CDCl_3$

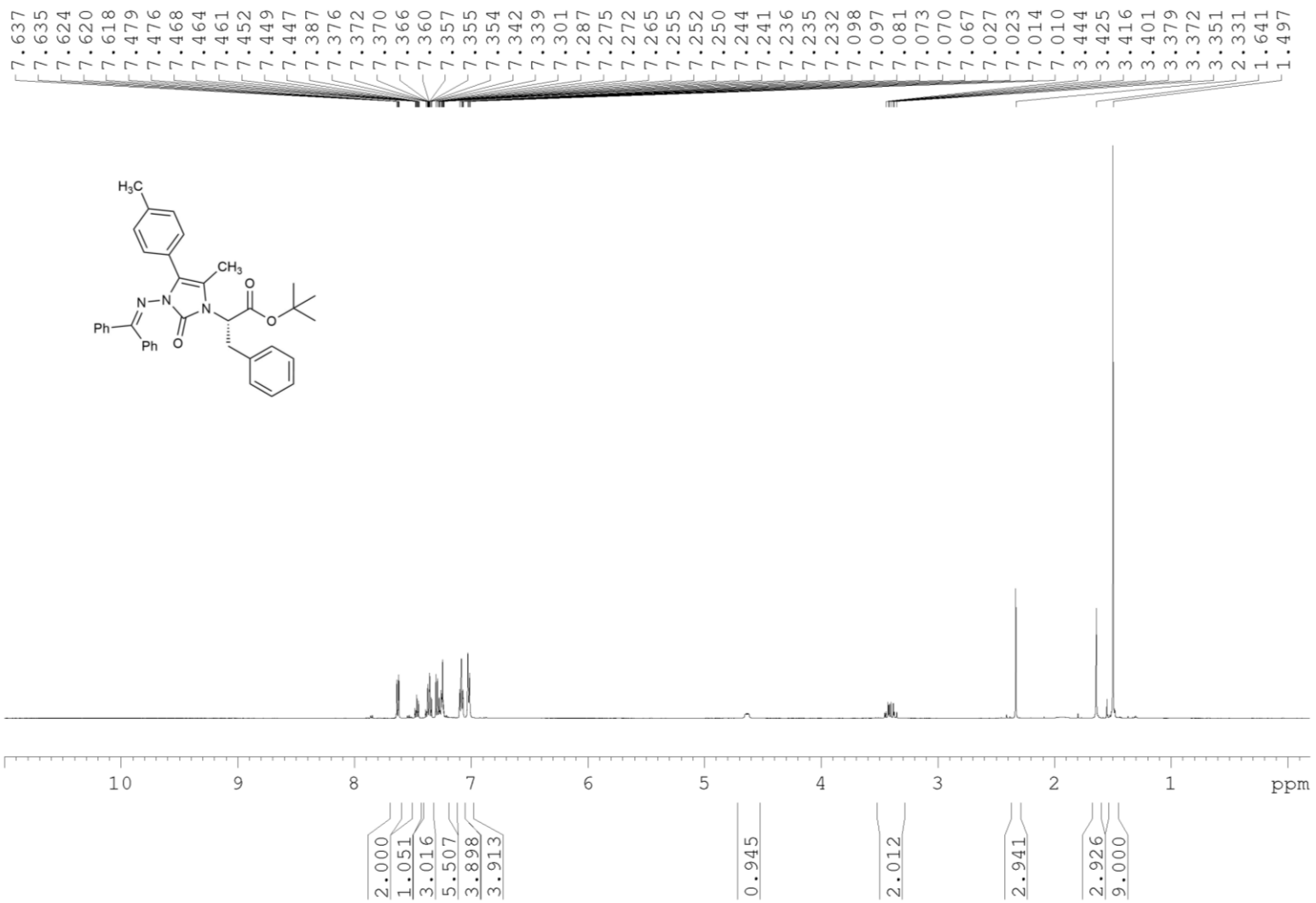

^{13}C-NMR, 101 MHz, $CDCl_3$

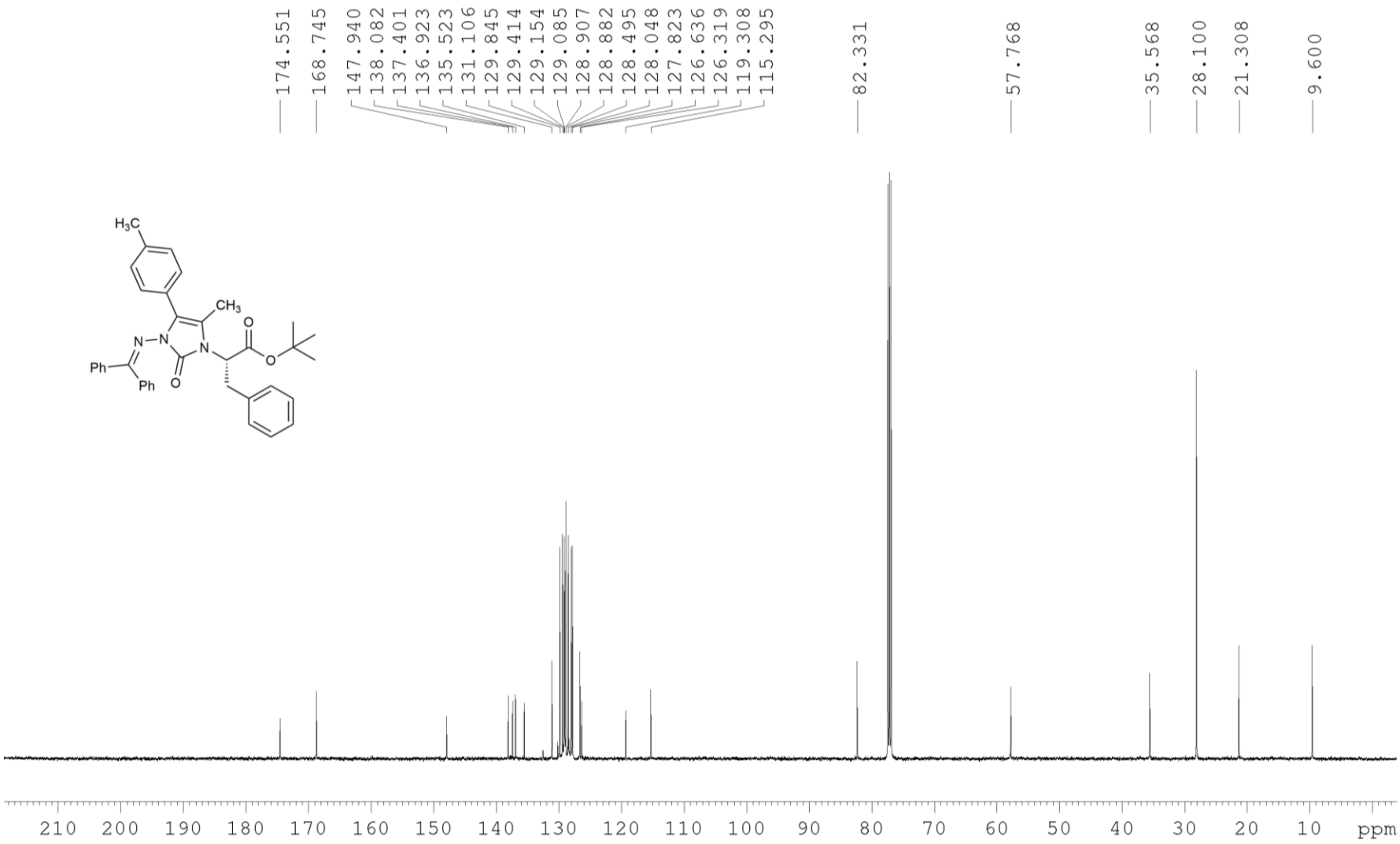

Compound 3.20

^{1}H-NMR, 400 MHz, $CDCl_3$

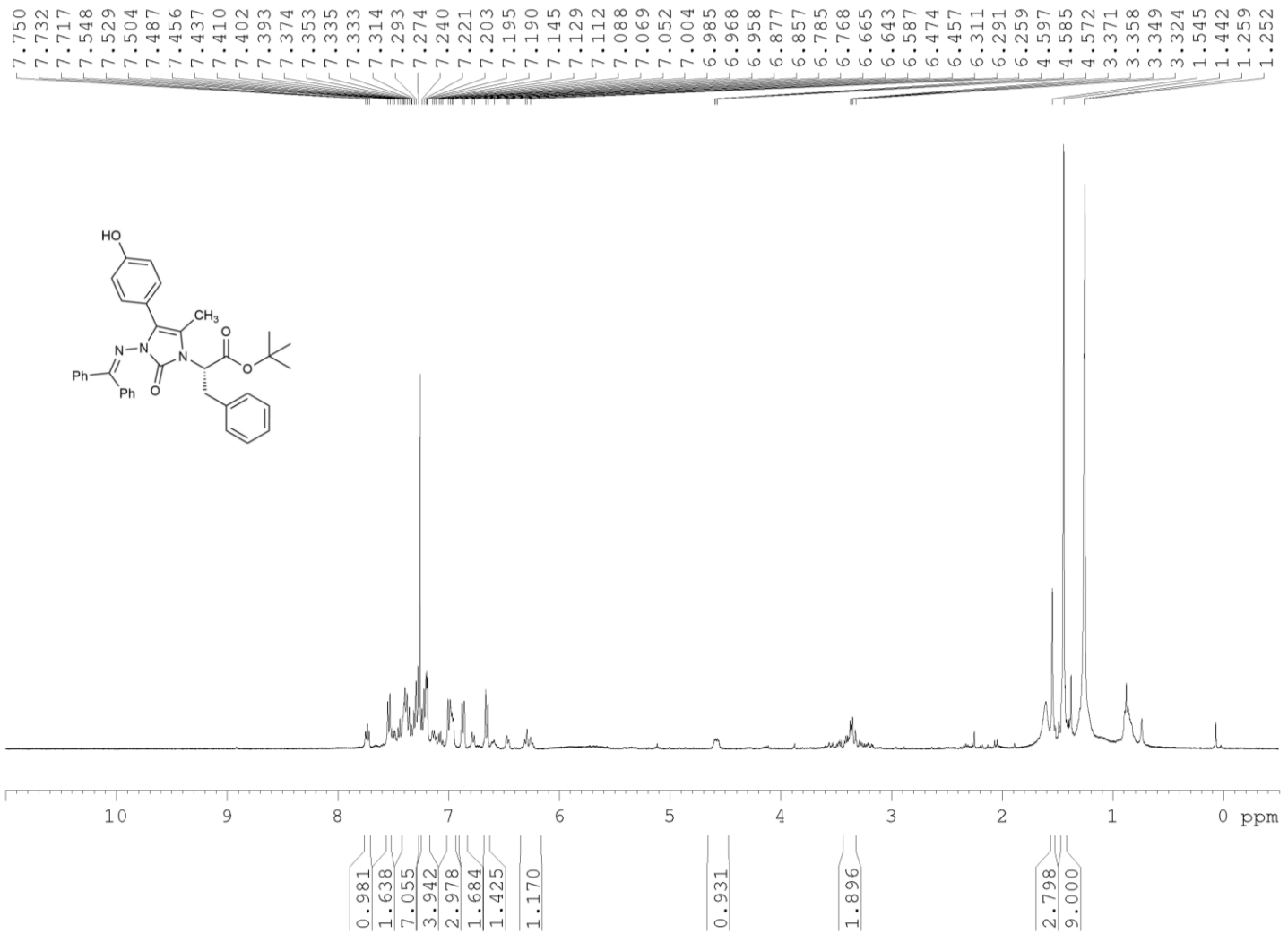

^{13}C-NMR, 75 MHz, $CDCl_3$

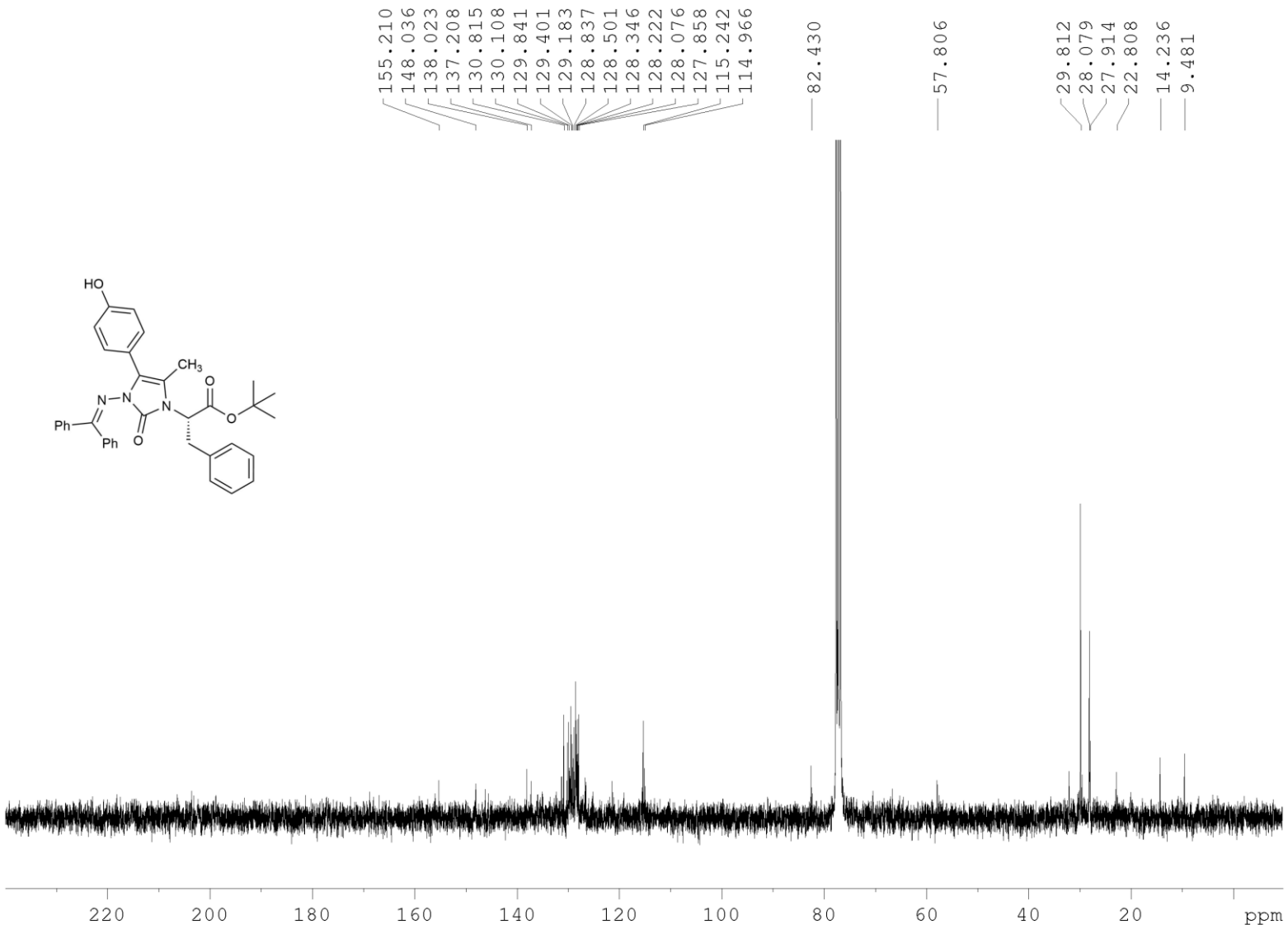

Compound 3.21

^{1}H-NMR, 300 MHz, $CDCl_3$

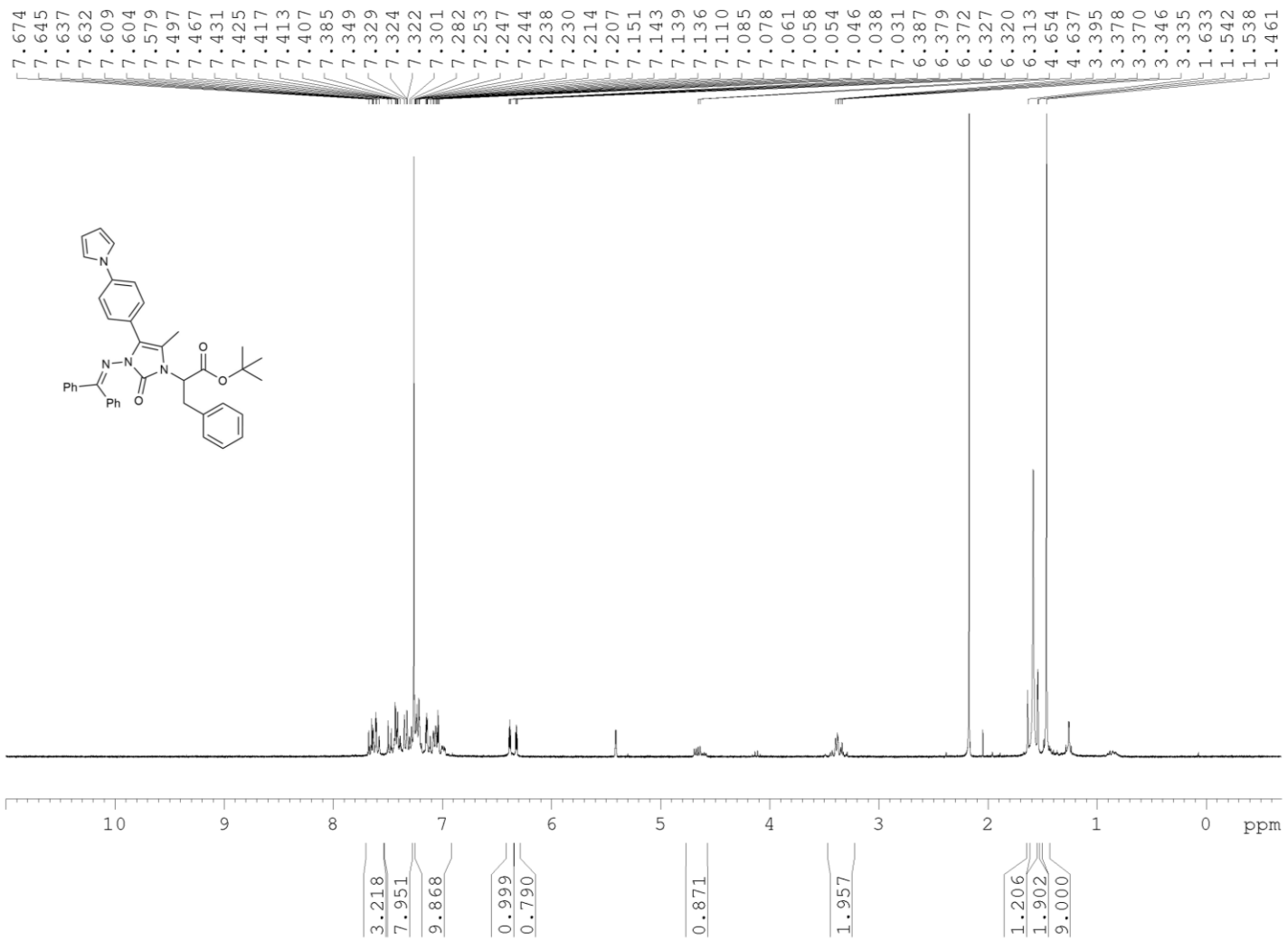

^{13}C-NMR, 176 MHz, DMSO-d_6

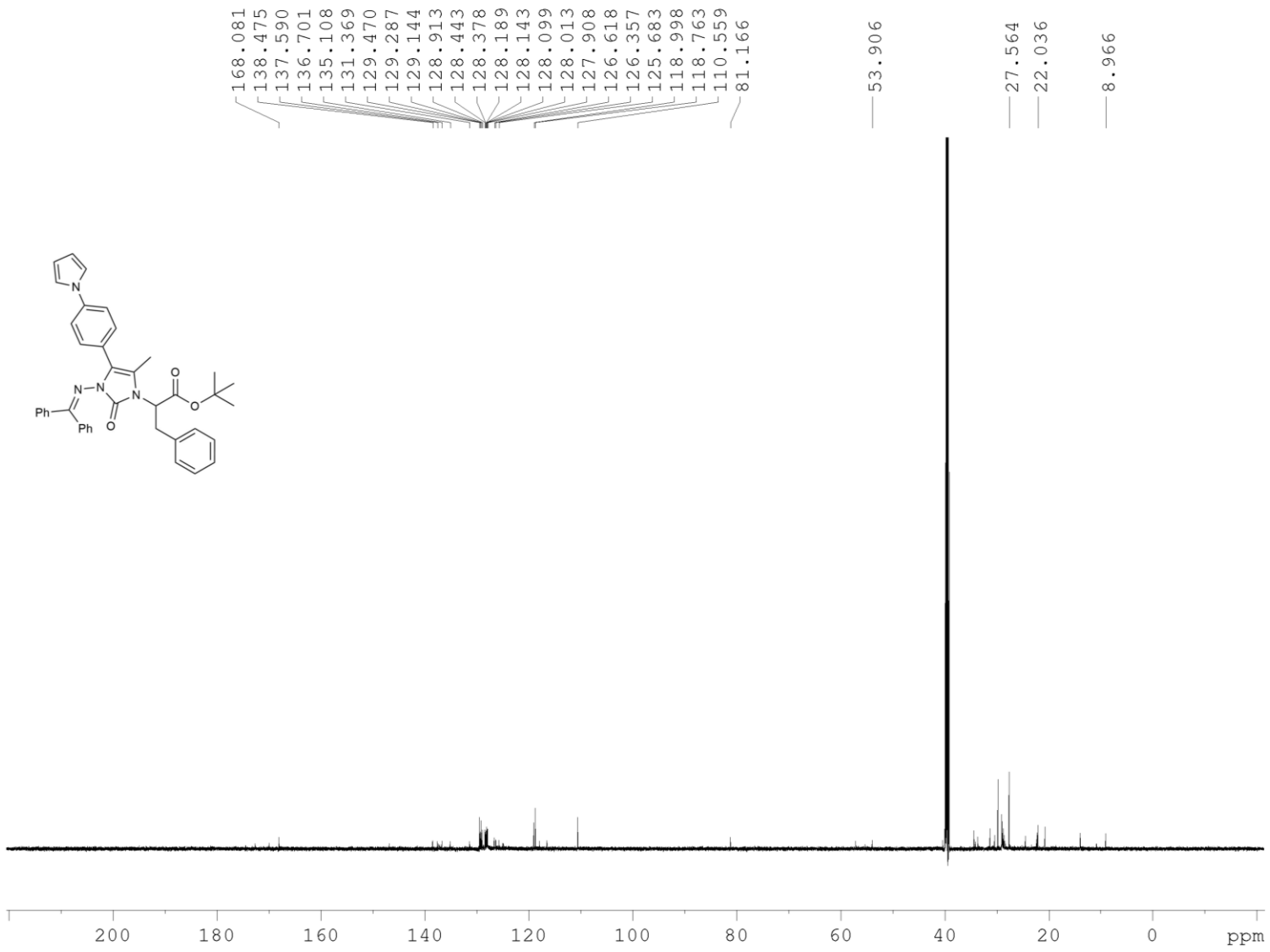

Compound 3.22

^{1}H-NMR, 500 MHz, $CDCl_3$

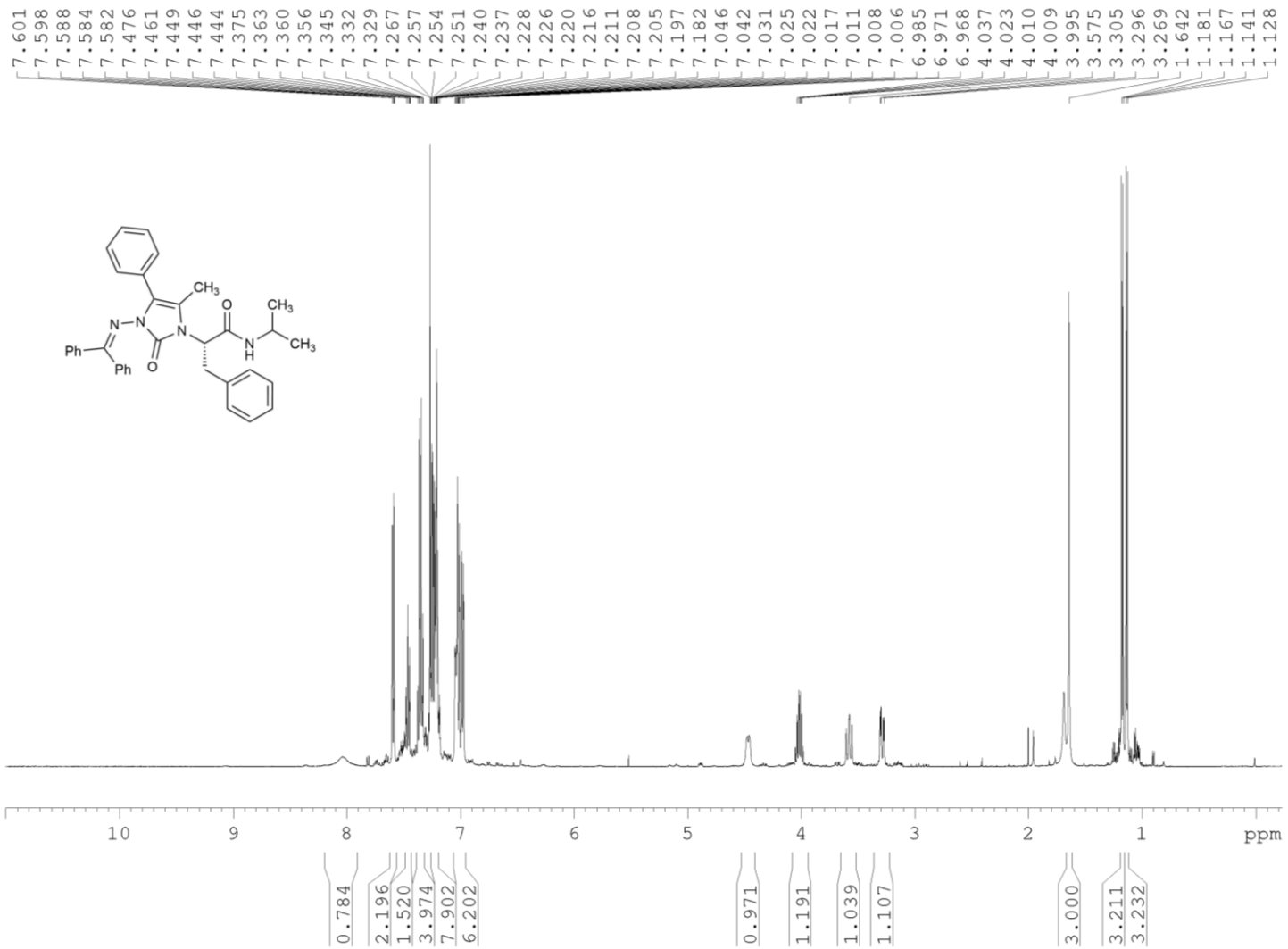

^{13}C-NMR, 126 MHz, $CDCl_3$

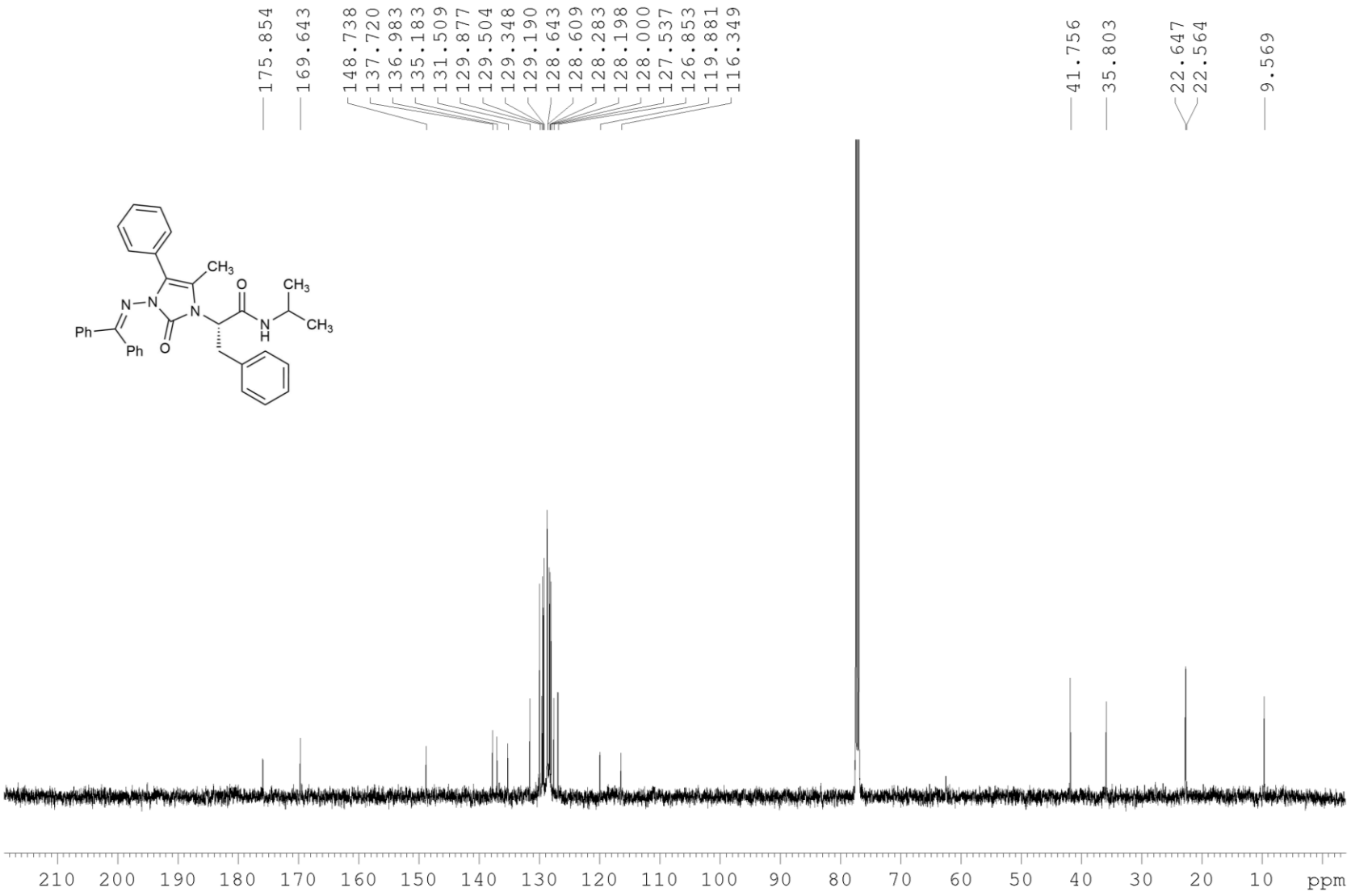

Compound 3.23

^{1}H-NMR, 500 MHz, $CDCl_3$

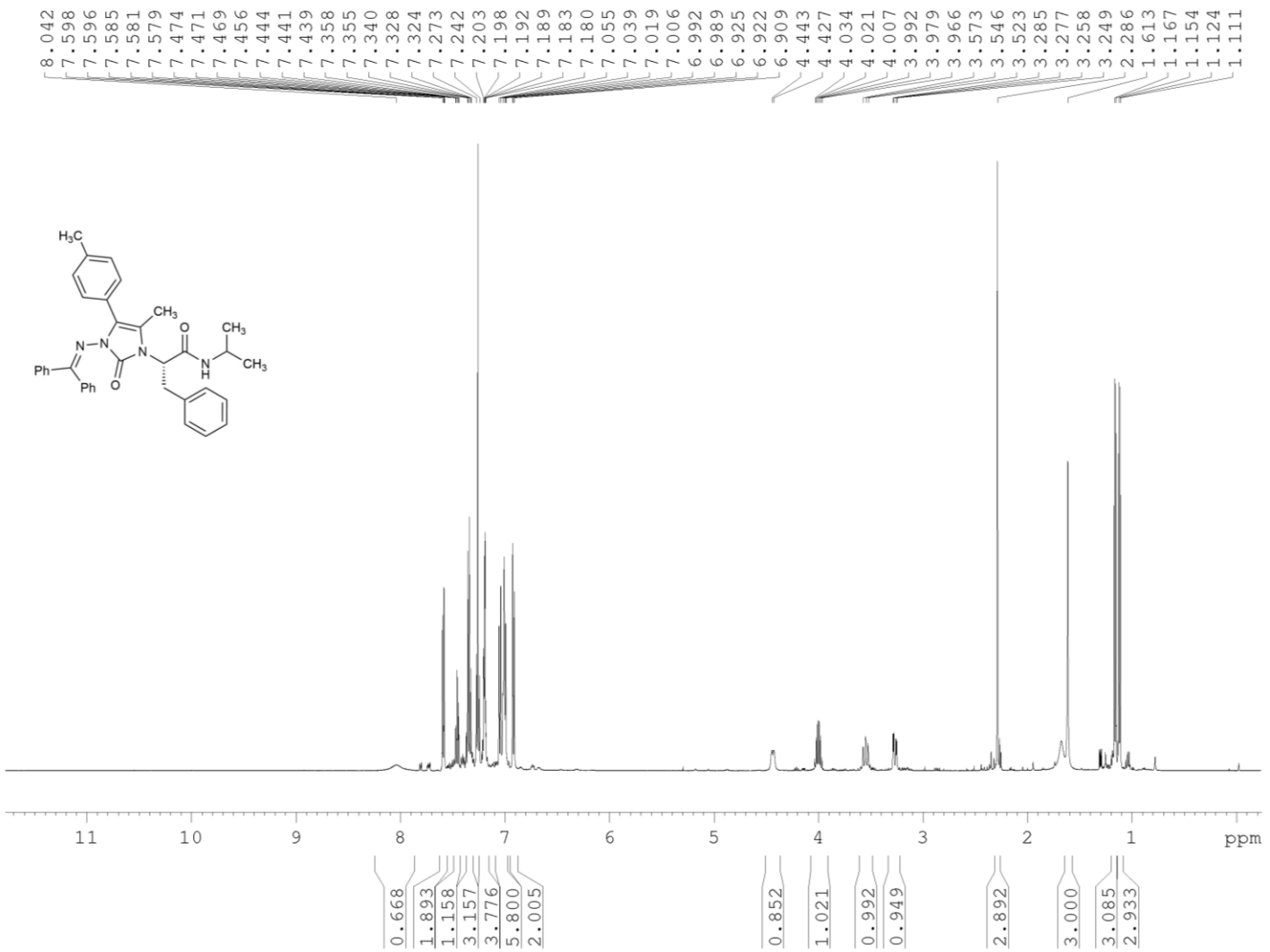

^{13}C-NMR, 126 MHz, $CDCl_3$

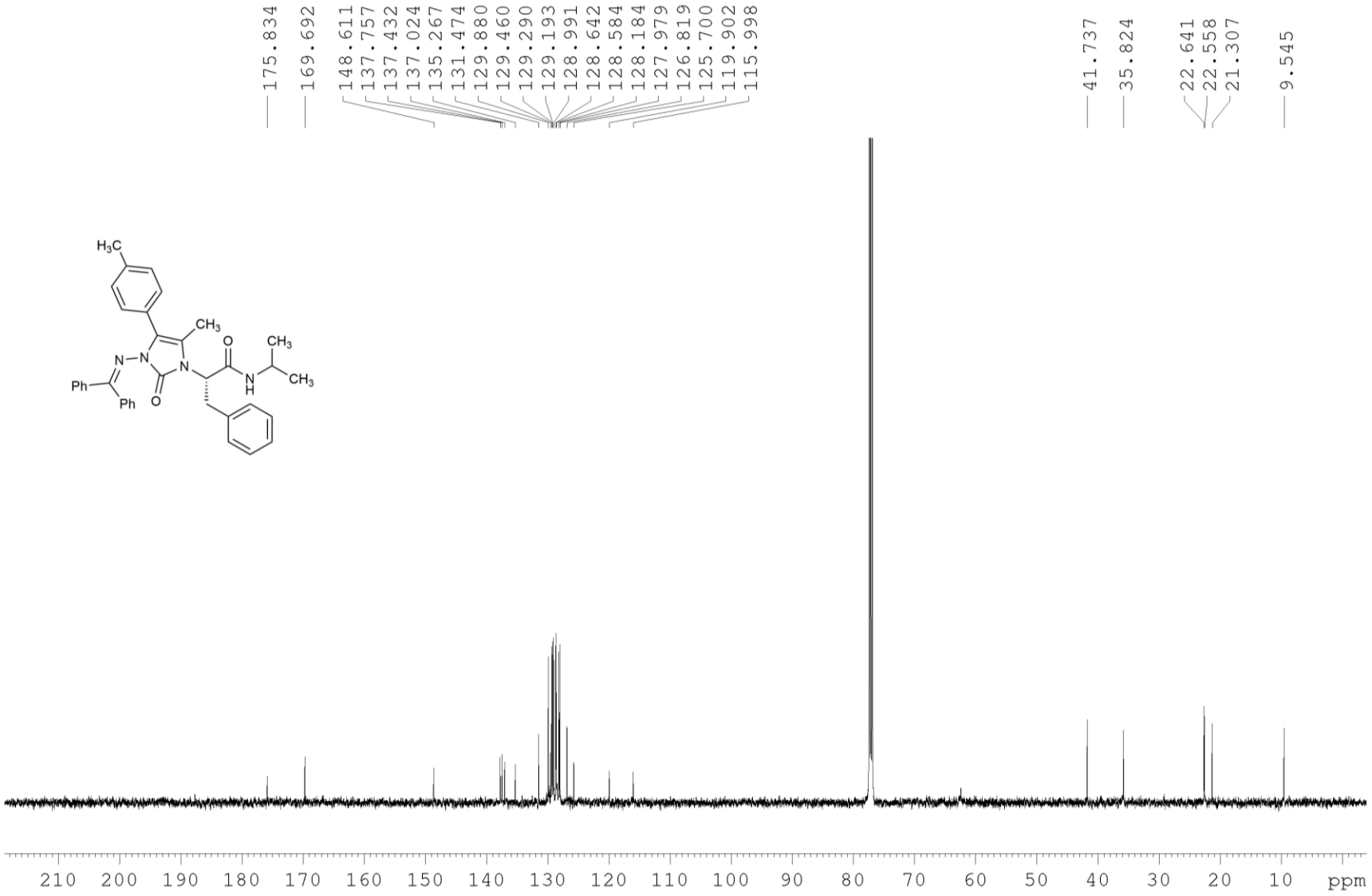

Compound 3.24

^{1}H-NMR, 500 MHz, $CDCl_3$

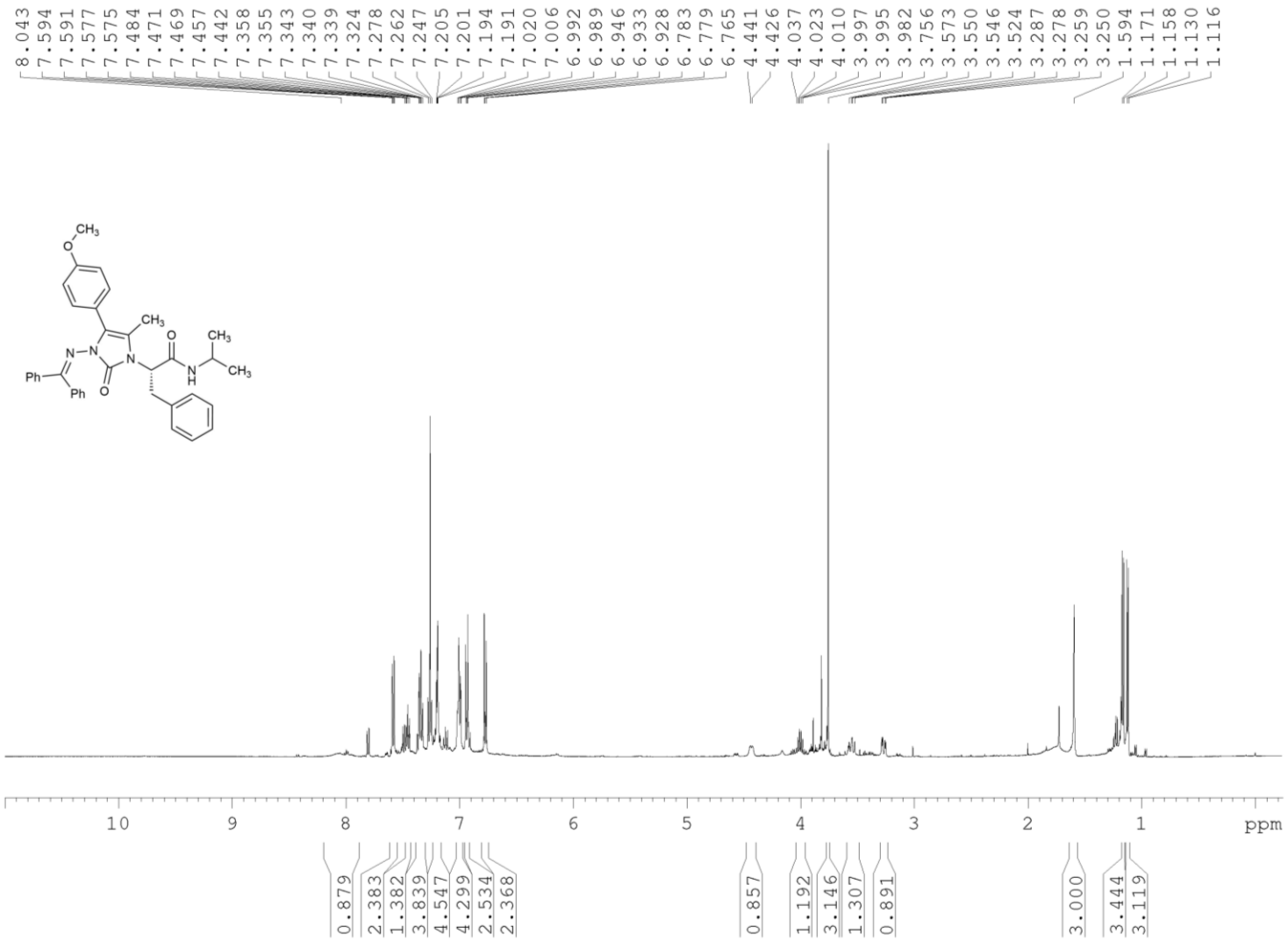

^{13}C-NMR, 126 MHz, $CDCl_3$

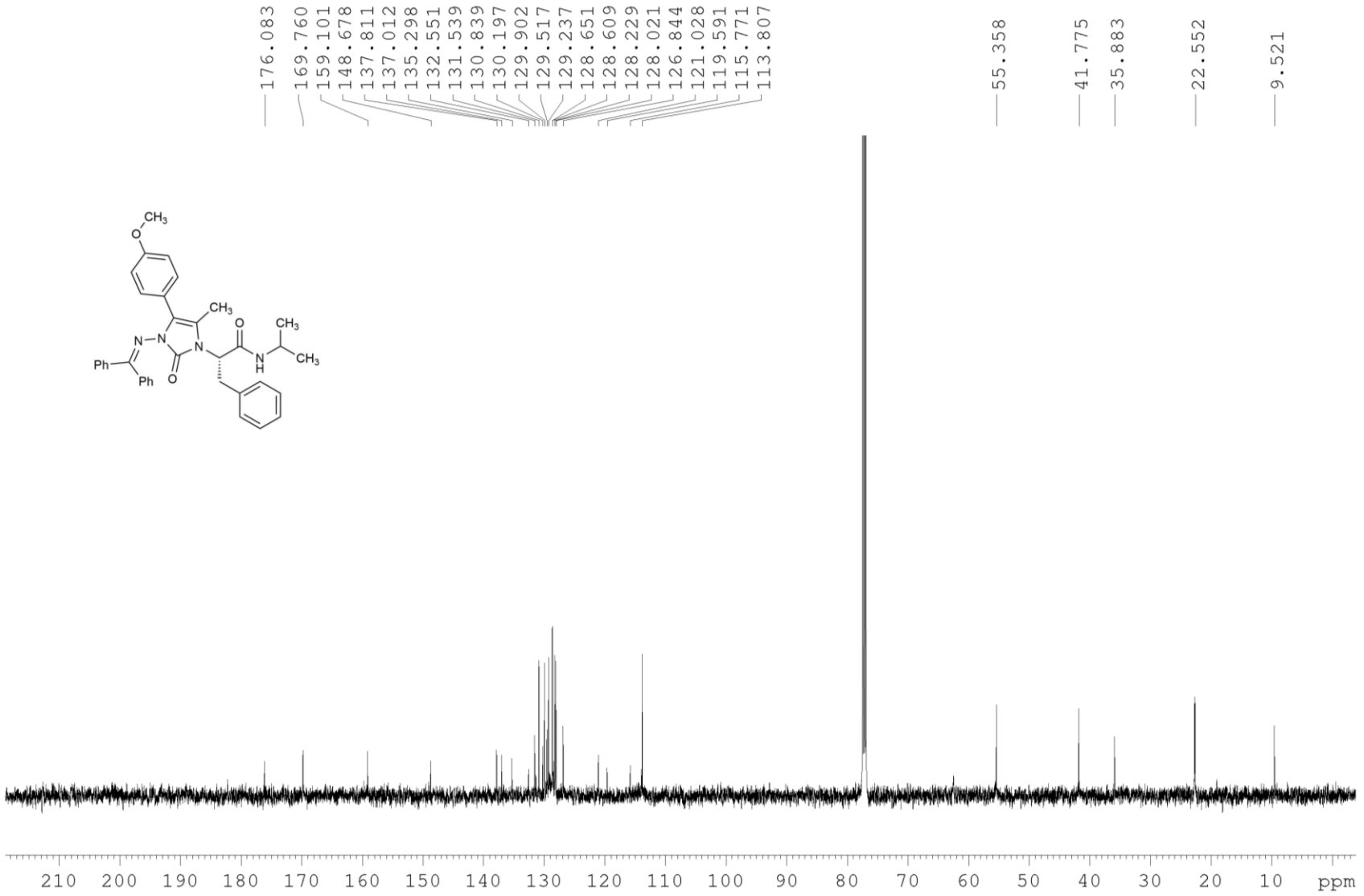

Compound 3.25

^{1}H-NMR, 500 MHz, $CDCl_3$

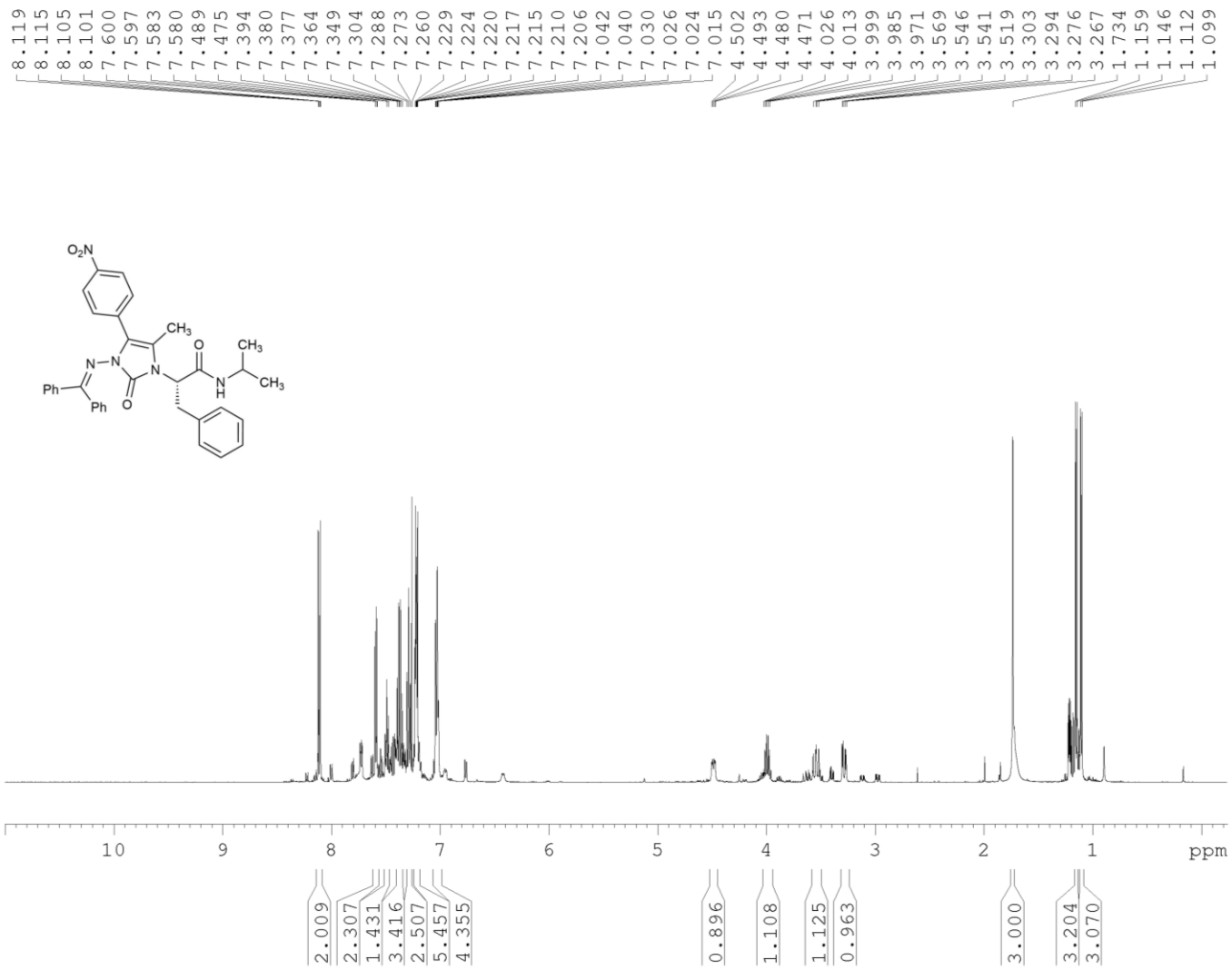

^{13}C-NMR, 126 MHz, $CDCl_3$

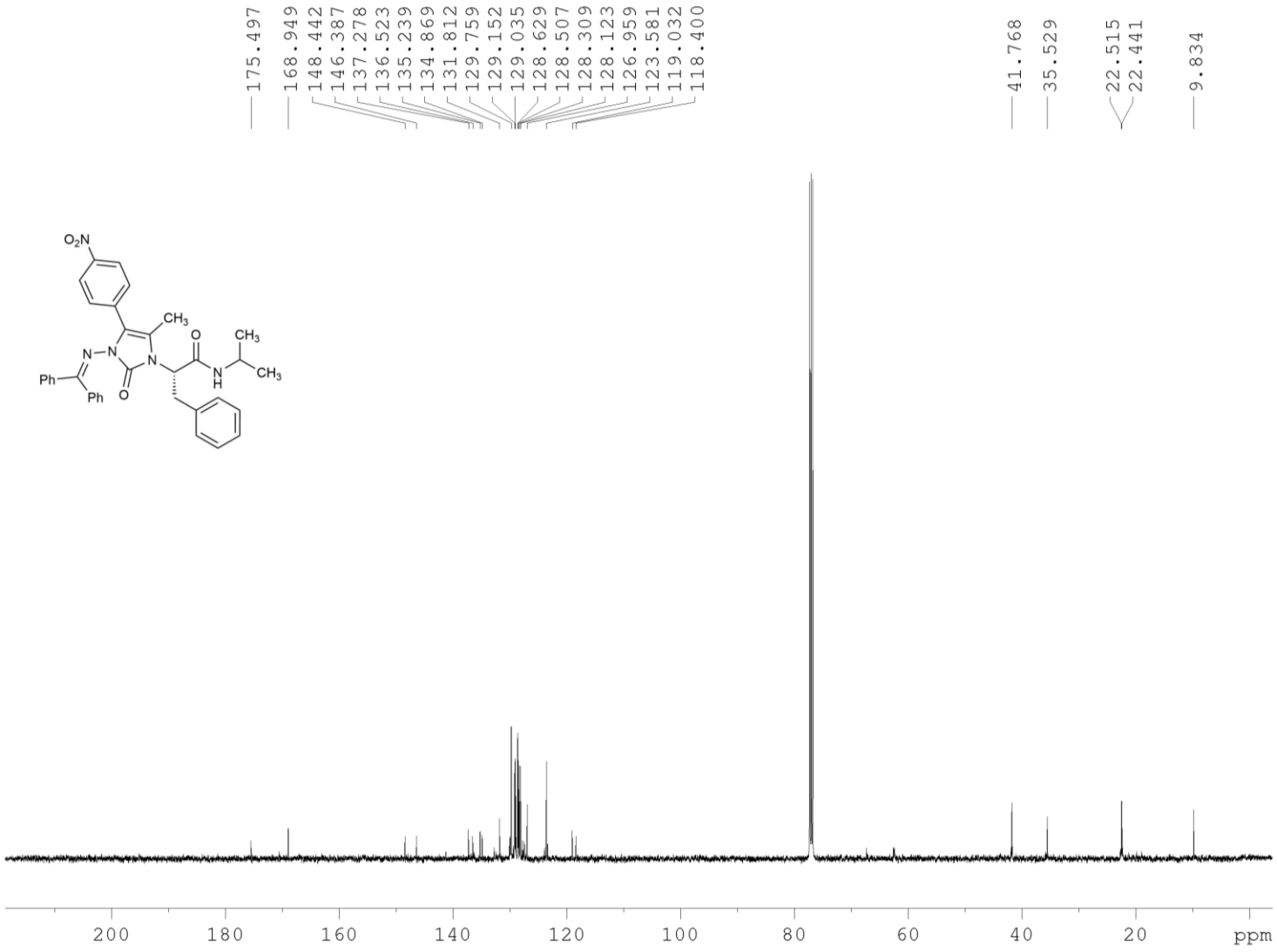

Compound 3.26

^{1}H-NMR, 500 MHz, $CDCl_3$

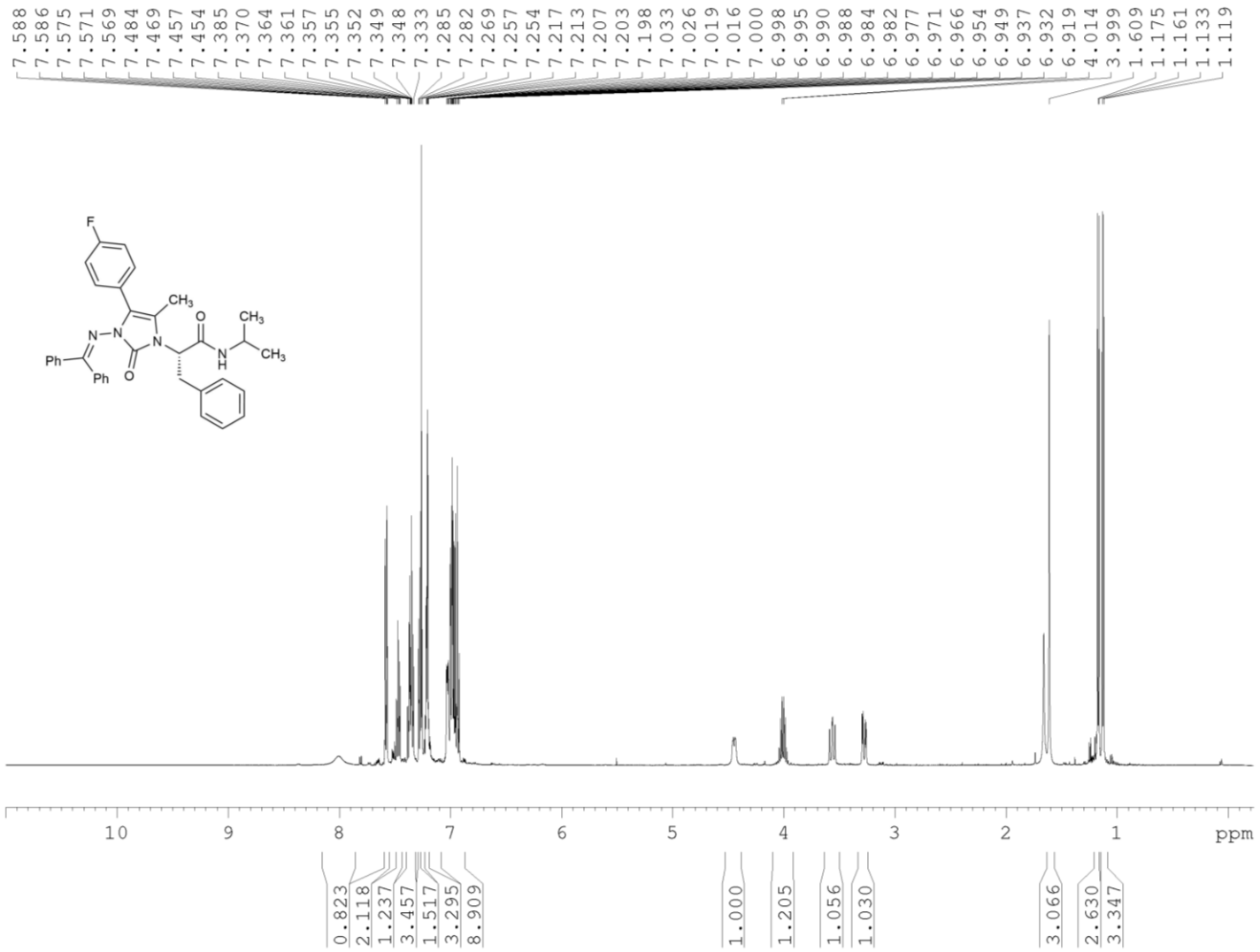

^{13}C-NMR, 126 MHz, $CDCl_3$

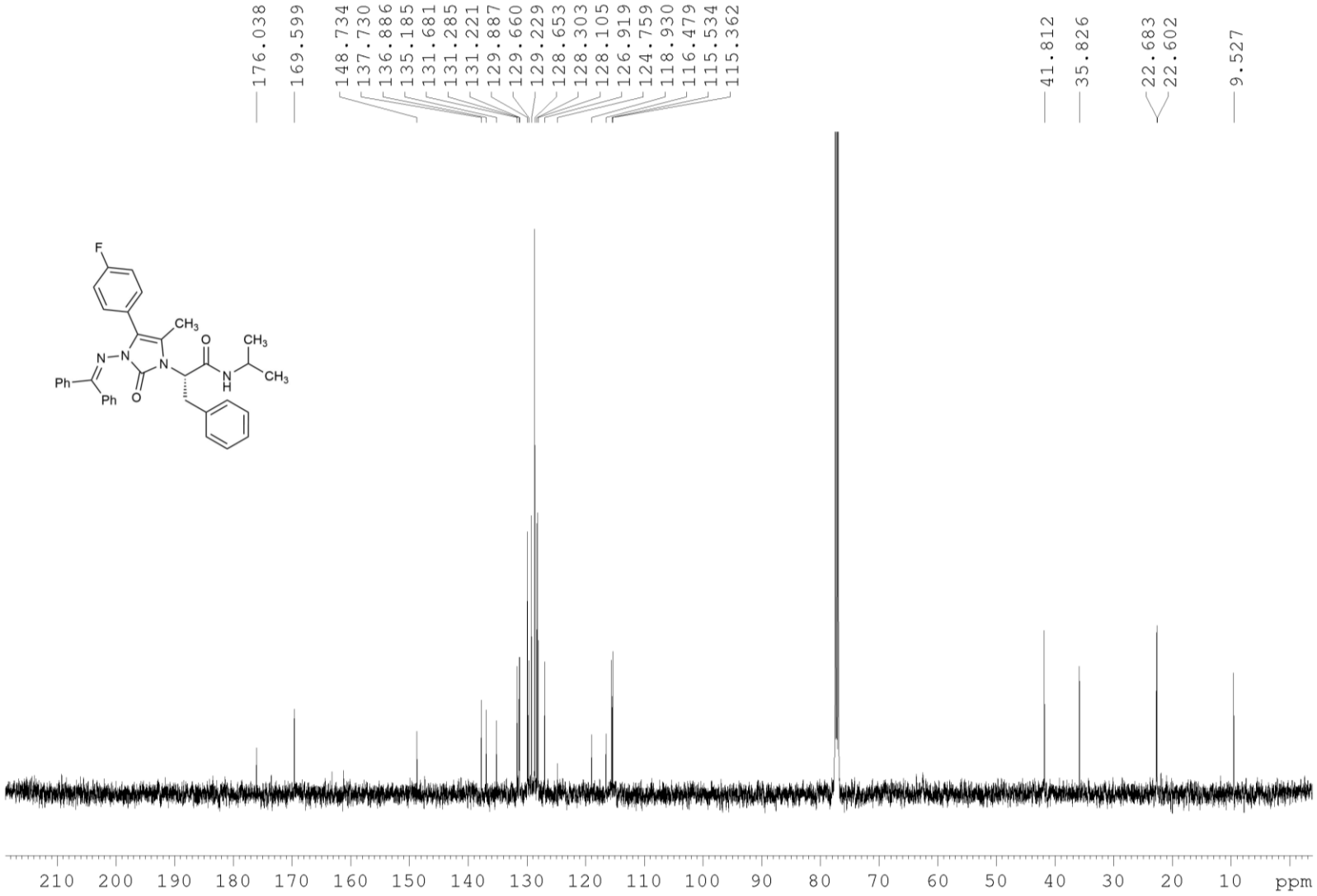

Compound 3.27

^{1}H-NMR, 400 MHz, $CDCl_3$

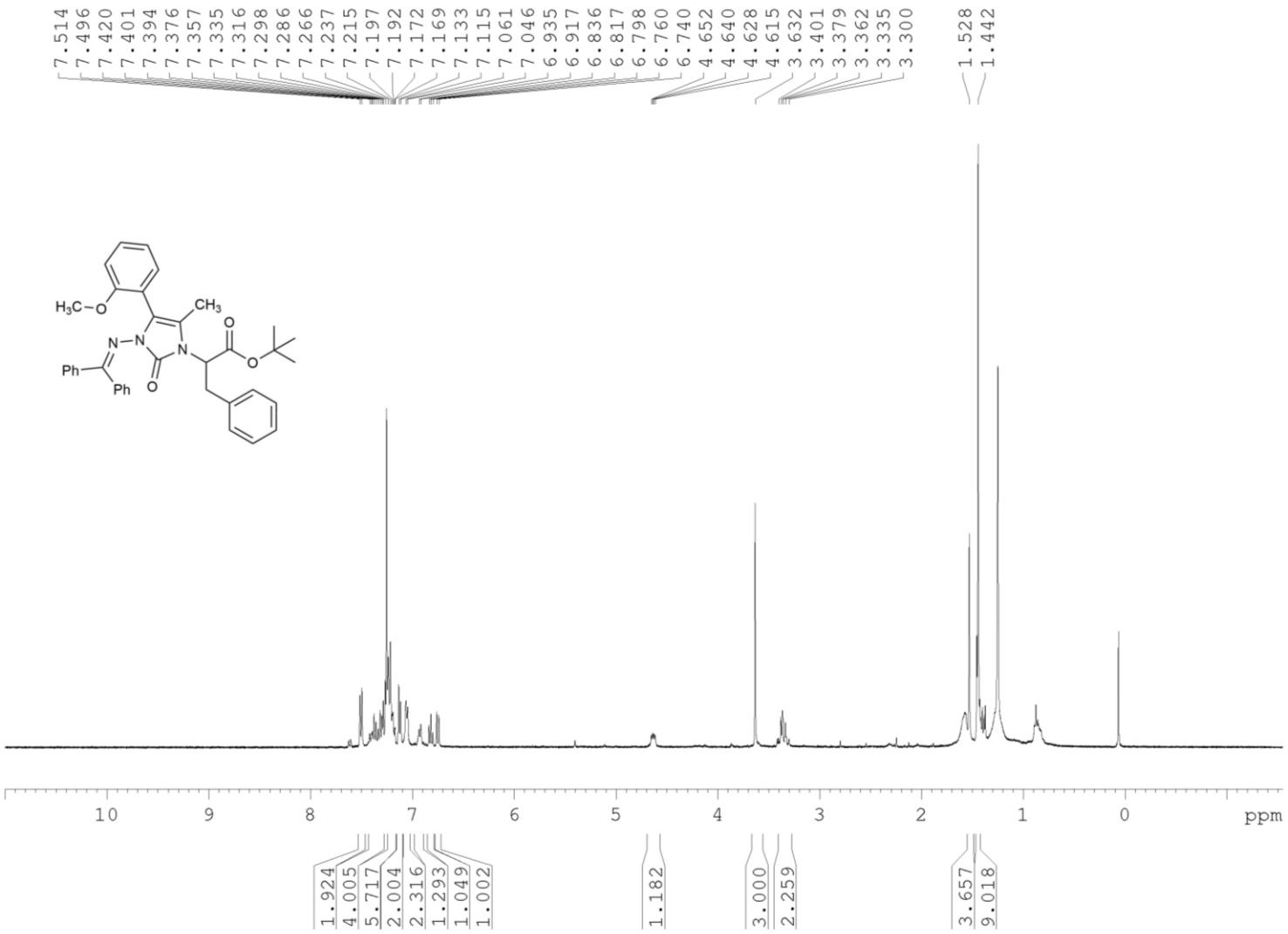

^{13}C-NMR, 75 MHz, $CDCl_3$

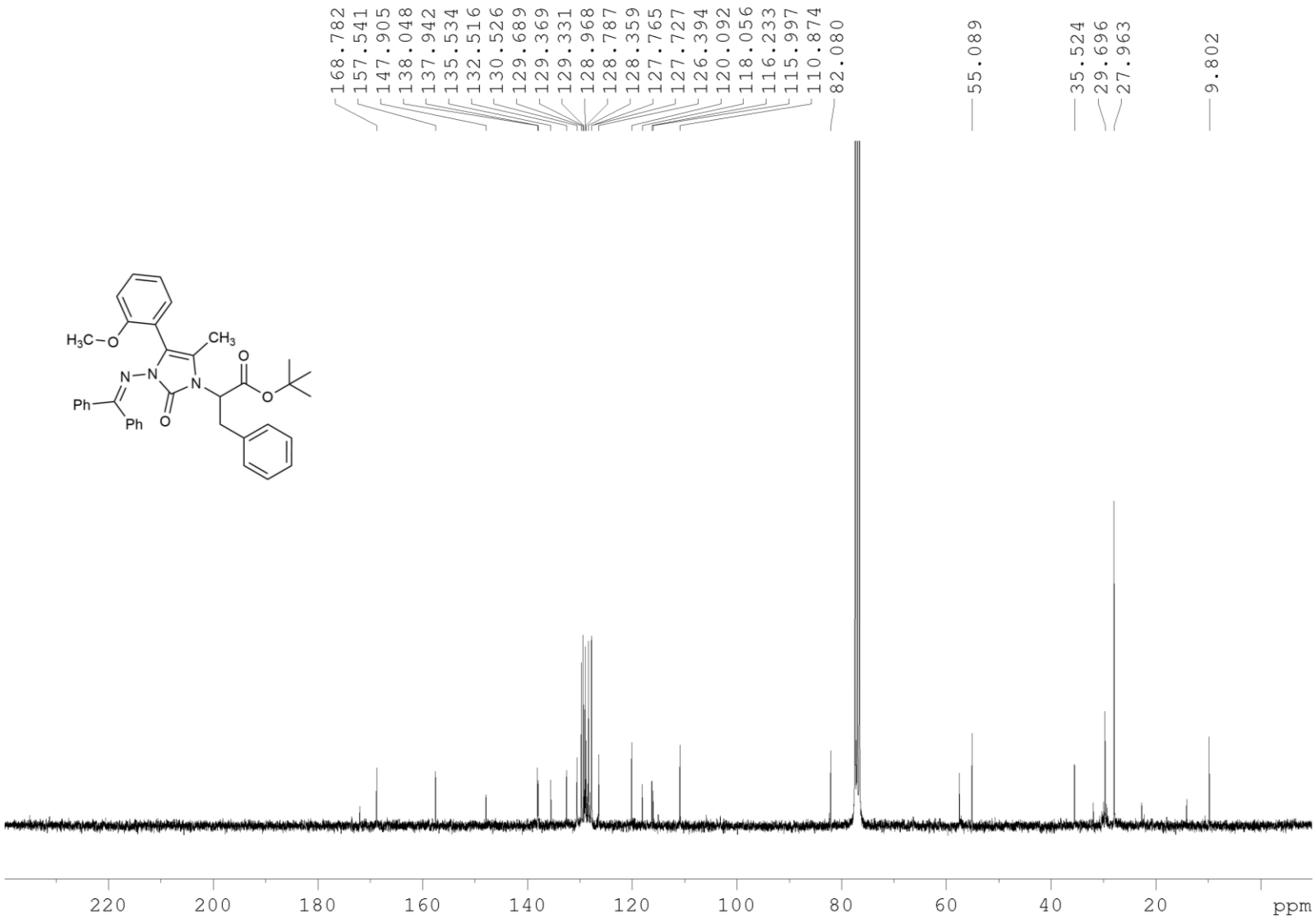

Compound 3.28

^{1}H-NMR, 500 MHz, $CDCl_3$

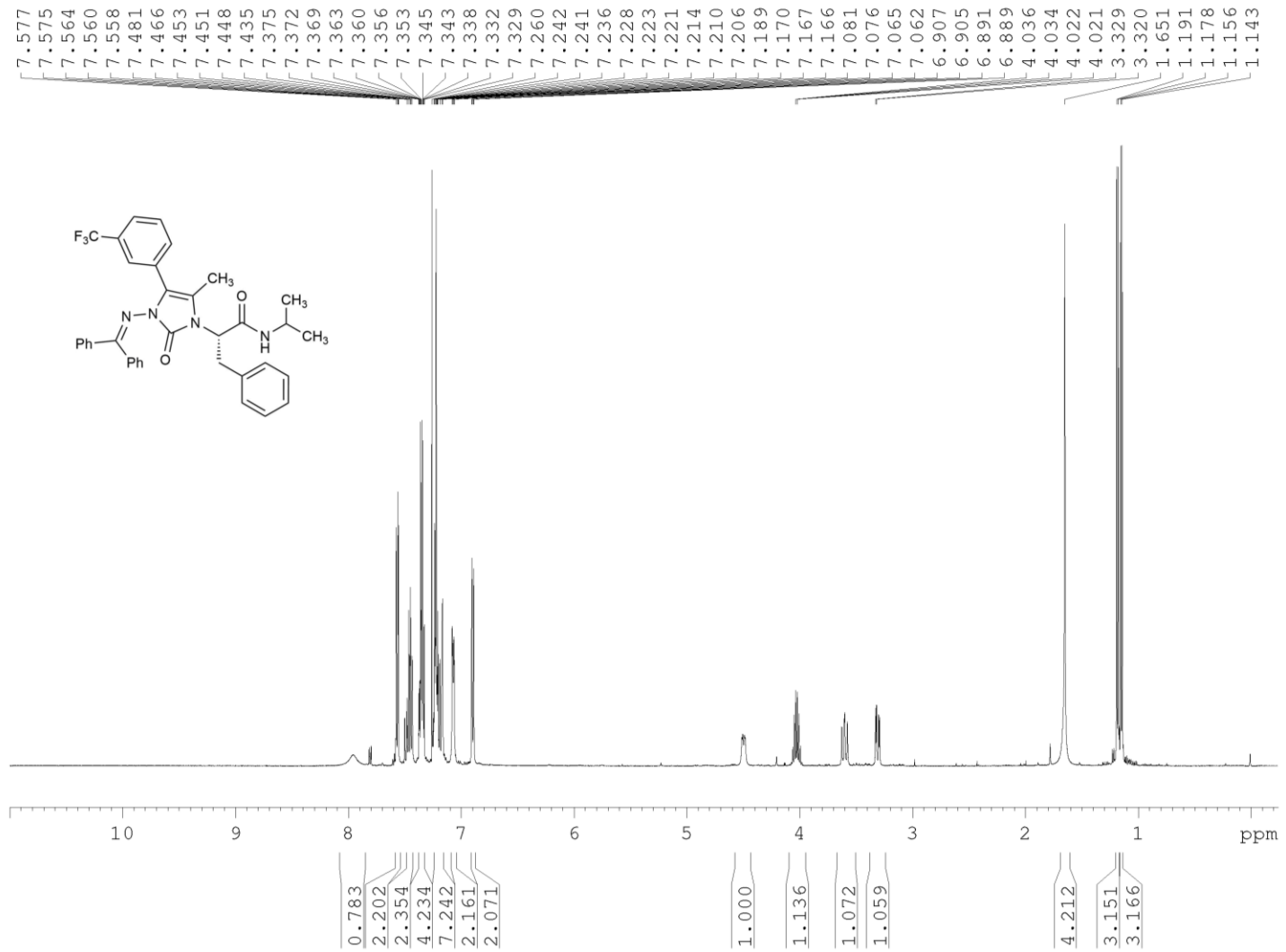

^{13}C-NMR, 126 MHz, $CDCl_3$

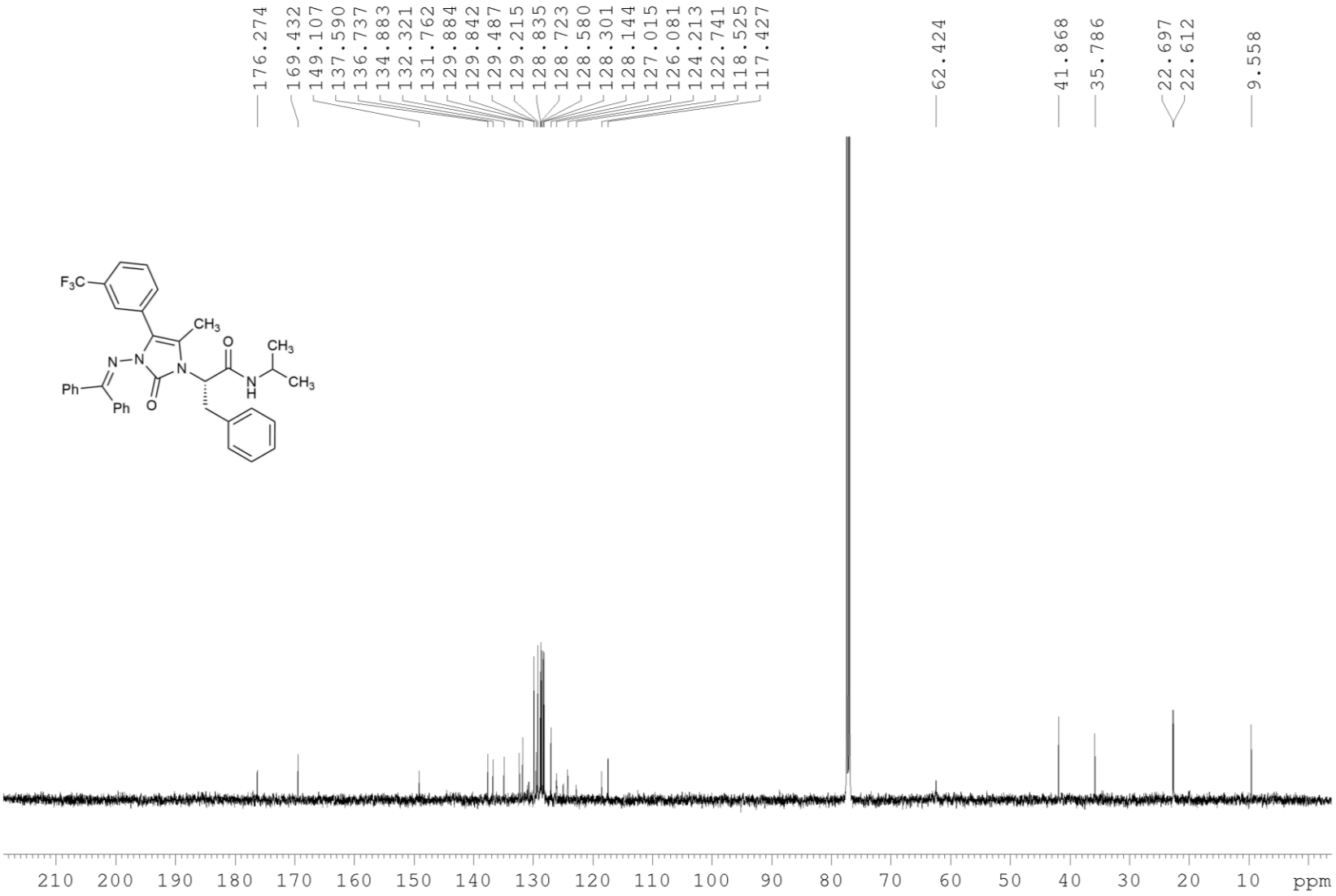

Compound 3.30

^{1}H-NMR, 300 MHz, $CDCl_3$

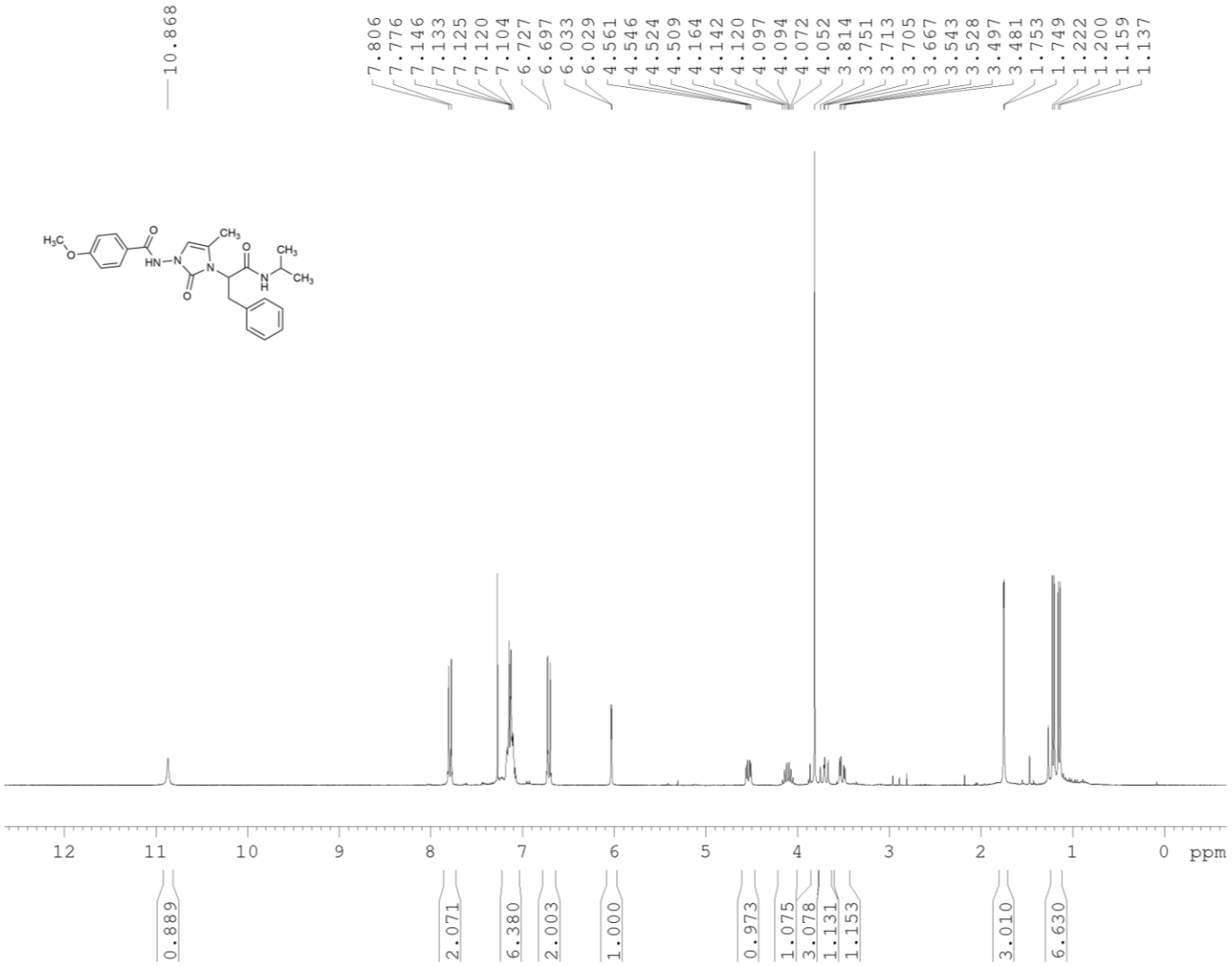

^{13}C-NMR, 75 MHz, $CDCl_3$

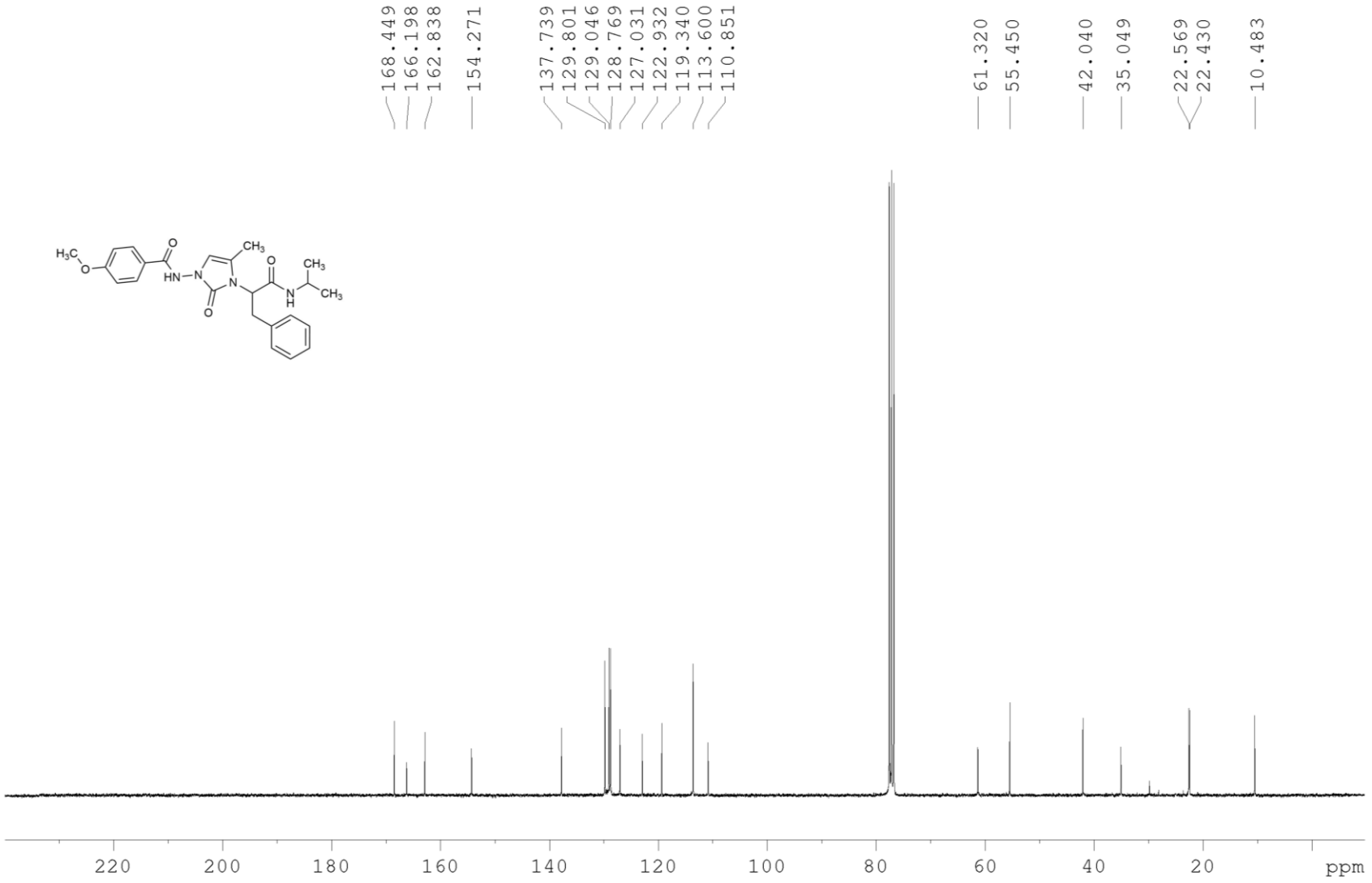

Compound 3.31

^{1}H-NMR, 300 MHz, $CDCl_3$

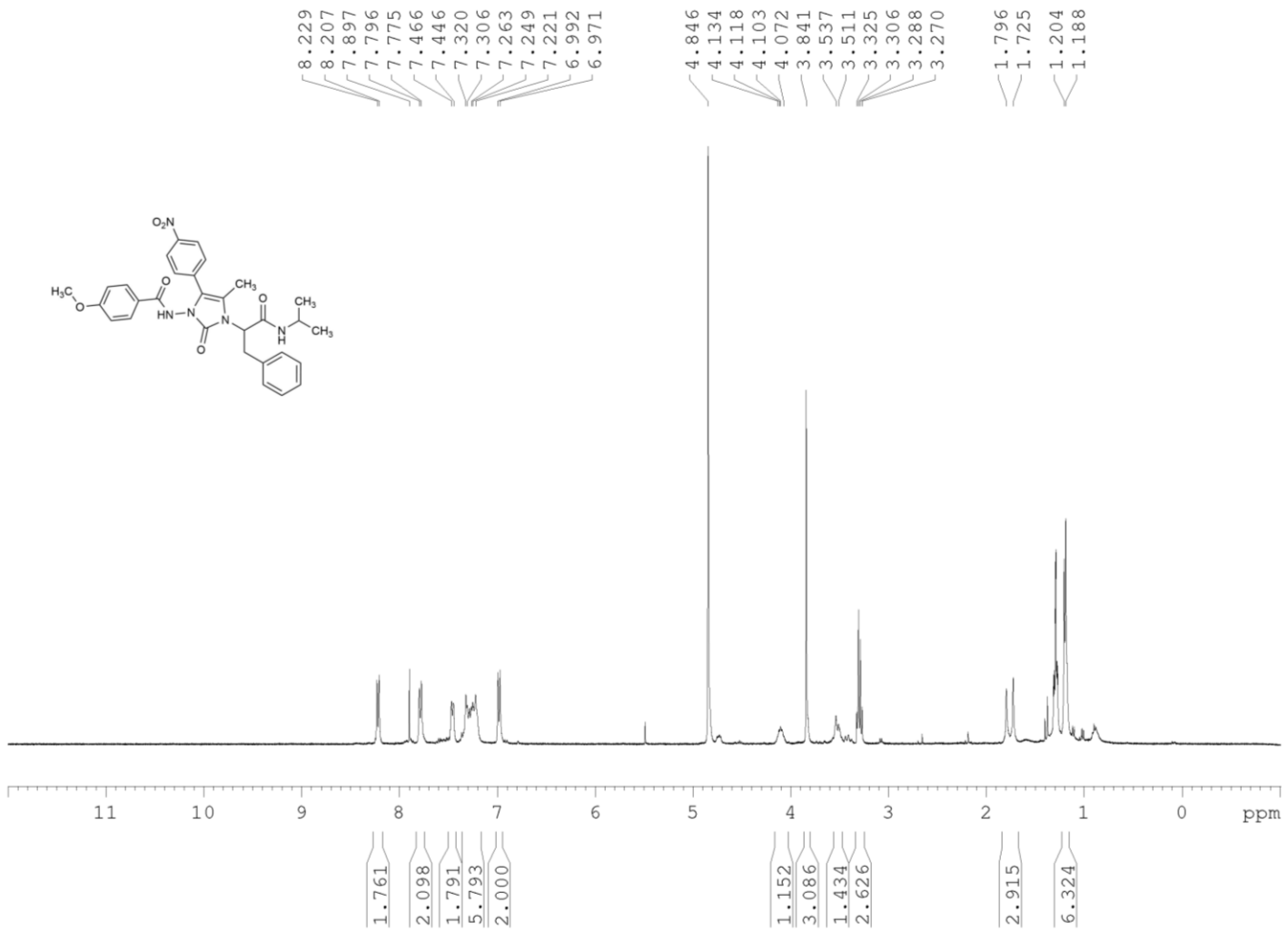

^{13}C-NMR, 75 MHz, $CDCl_3$

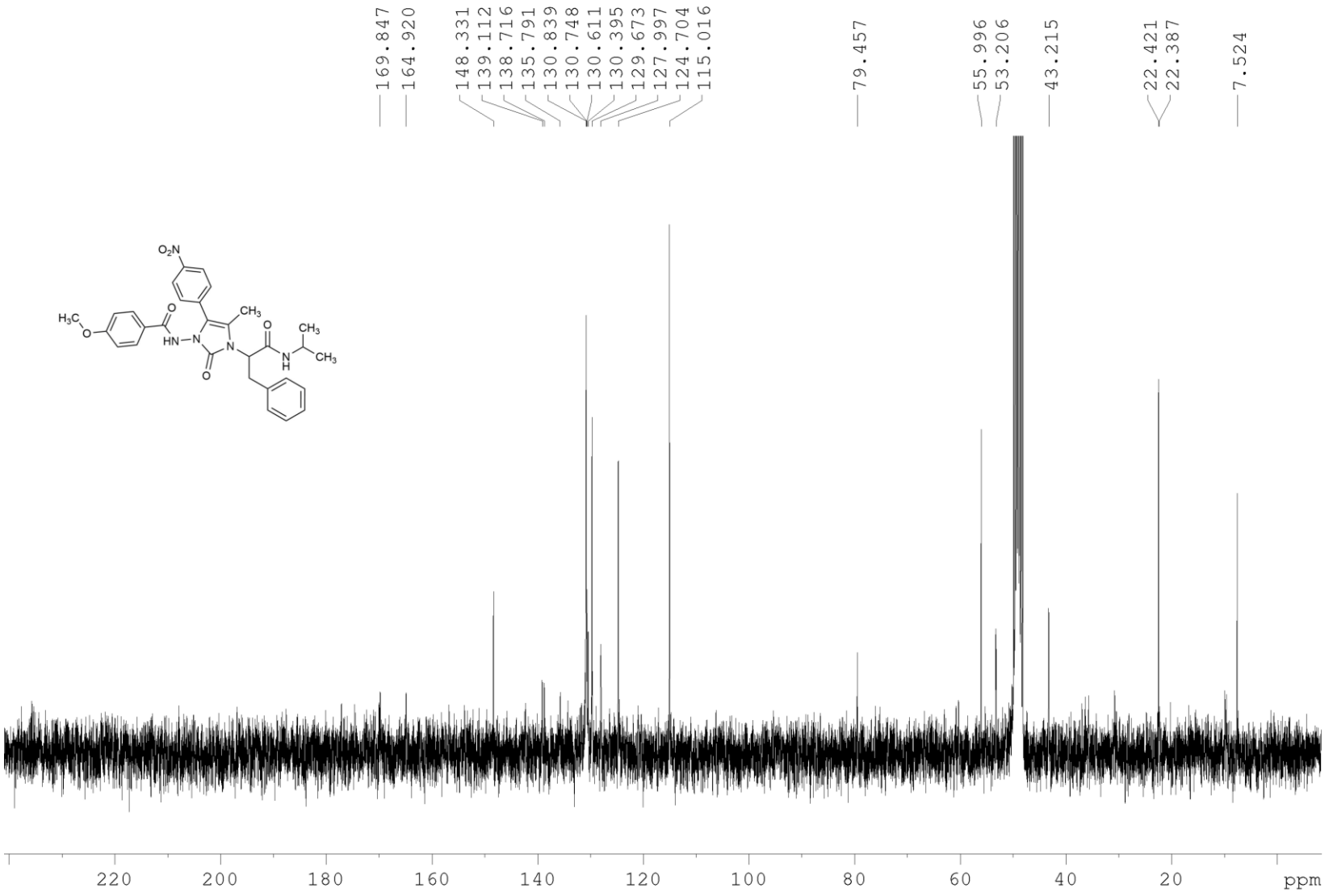

Annex 3: NMR Spectra for chapter 4

tert-Butyl (4-iodophenyl) carbonate

^{1}H-NMR, 500 MHz, $CDCl_3$

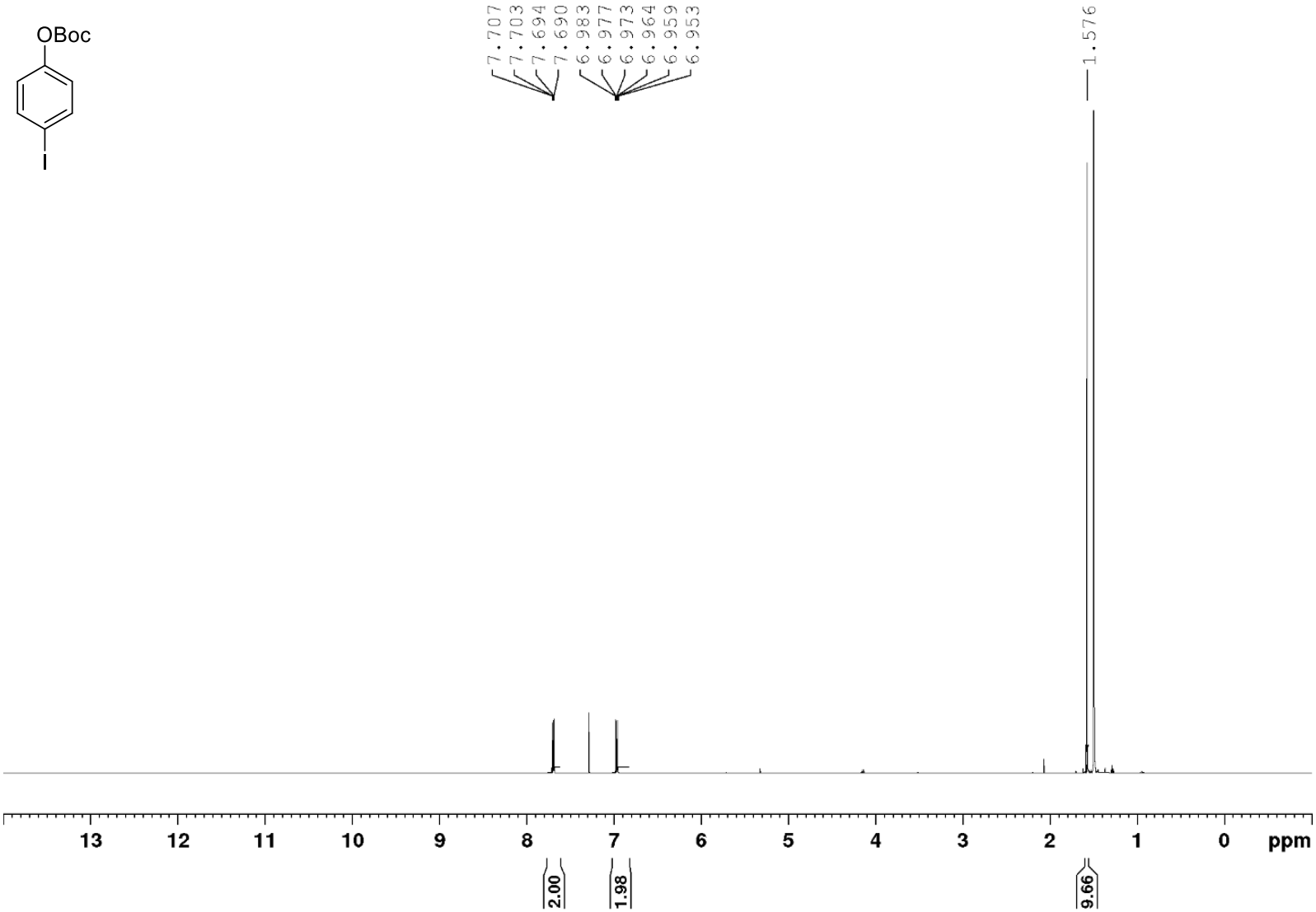

^{13}C-NMR, 125 MHz, $CDCl_3$

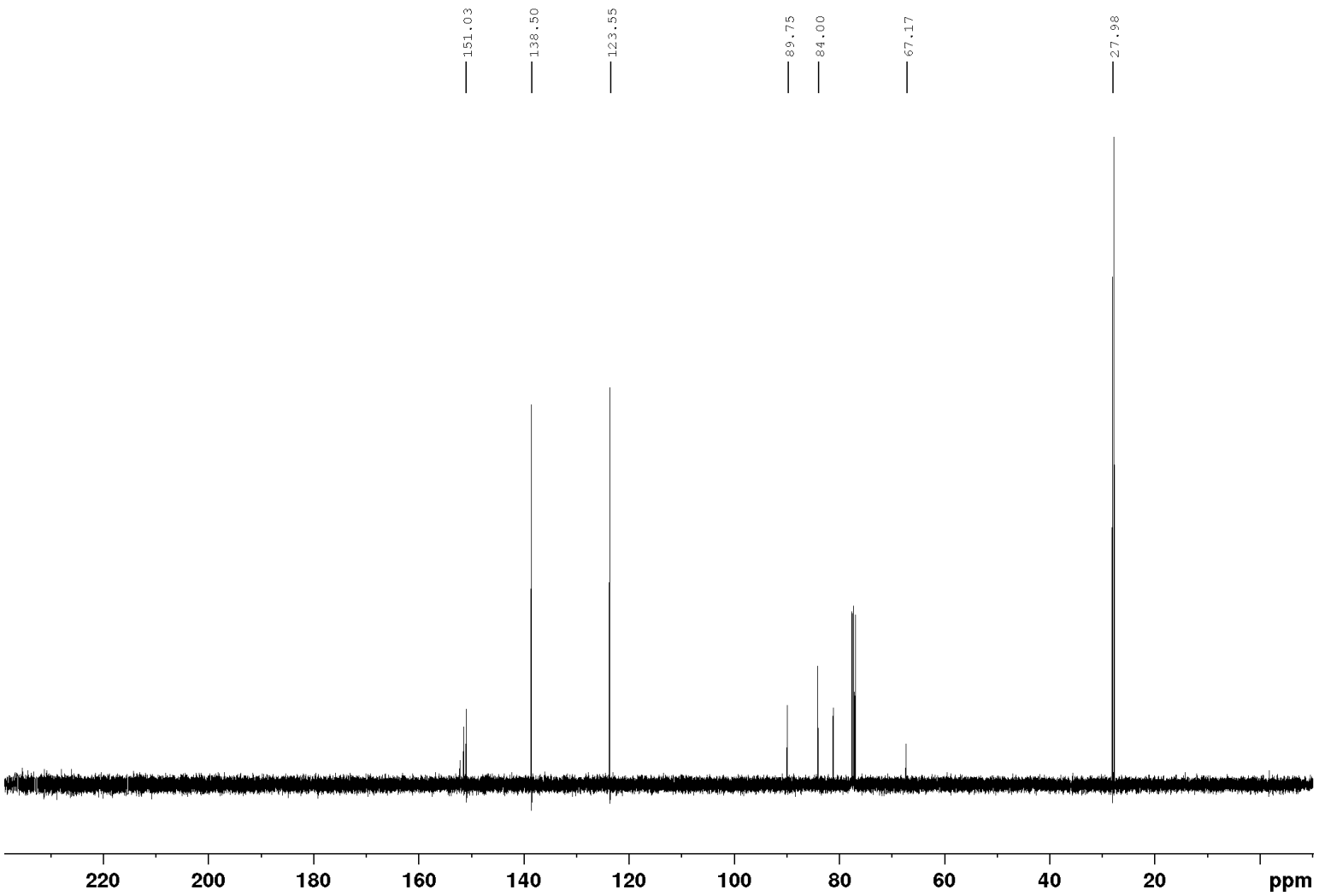

Annex 4: NMR Spectra for chapter 5

Compound 5.9

^{1}H-NMR, 500 MHz, $CDCl_3$

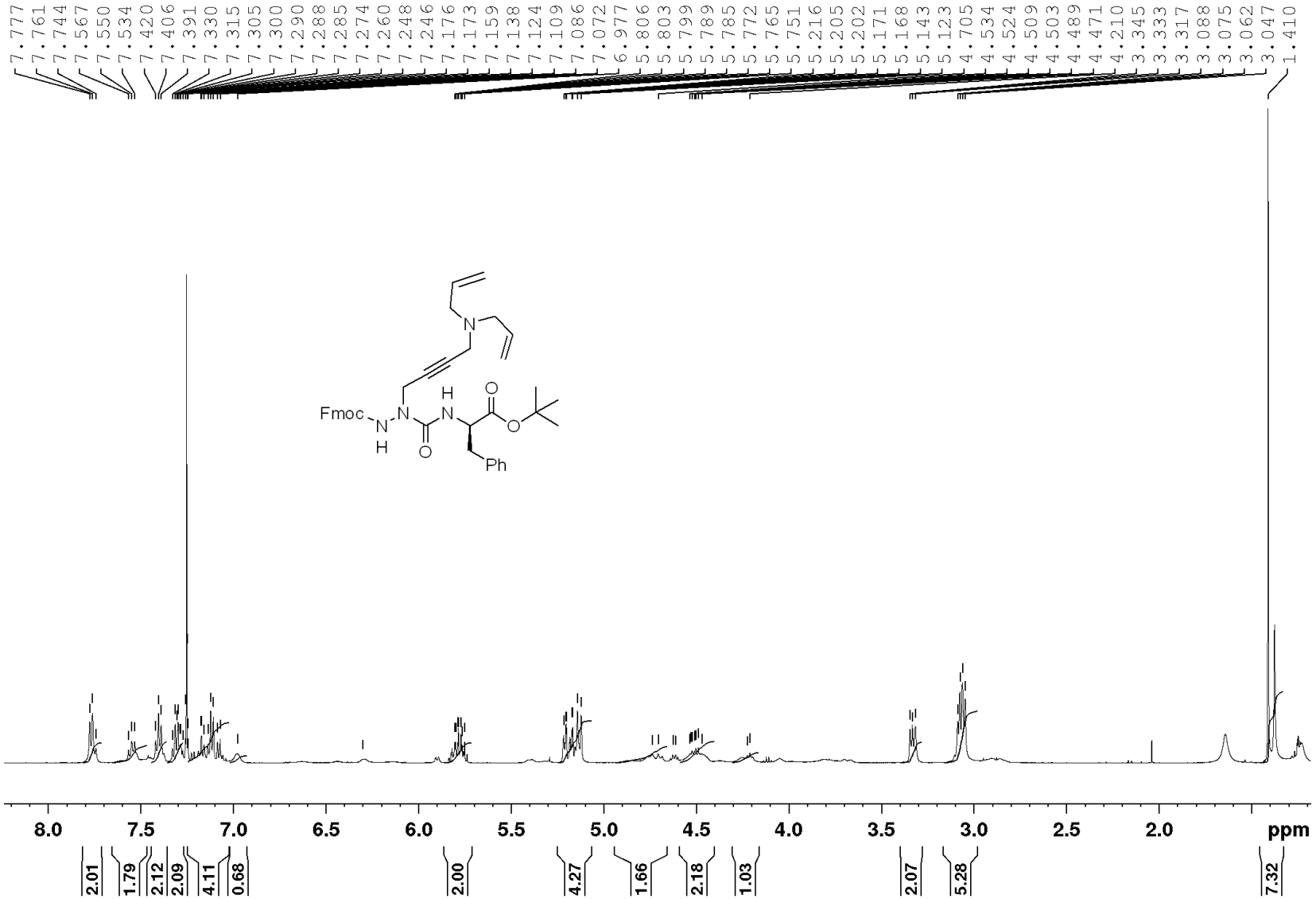

^{13}C-NMR, 125 MHz, $CDCl_3$

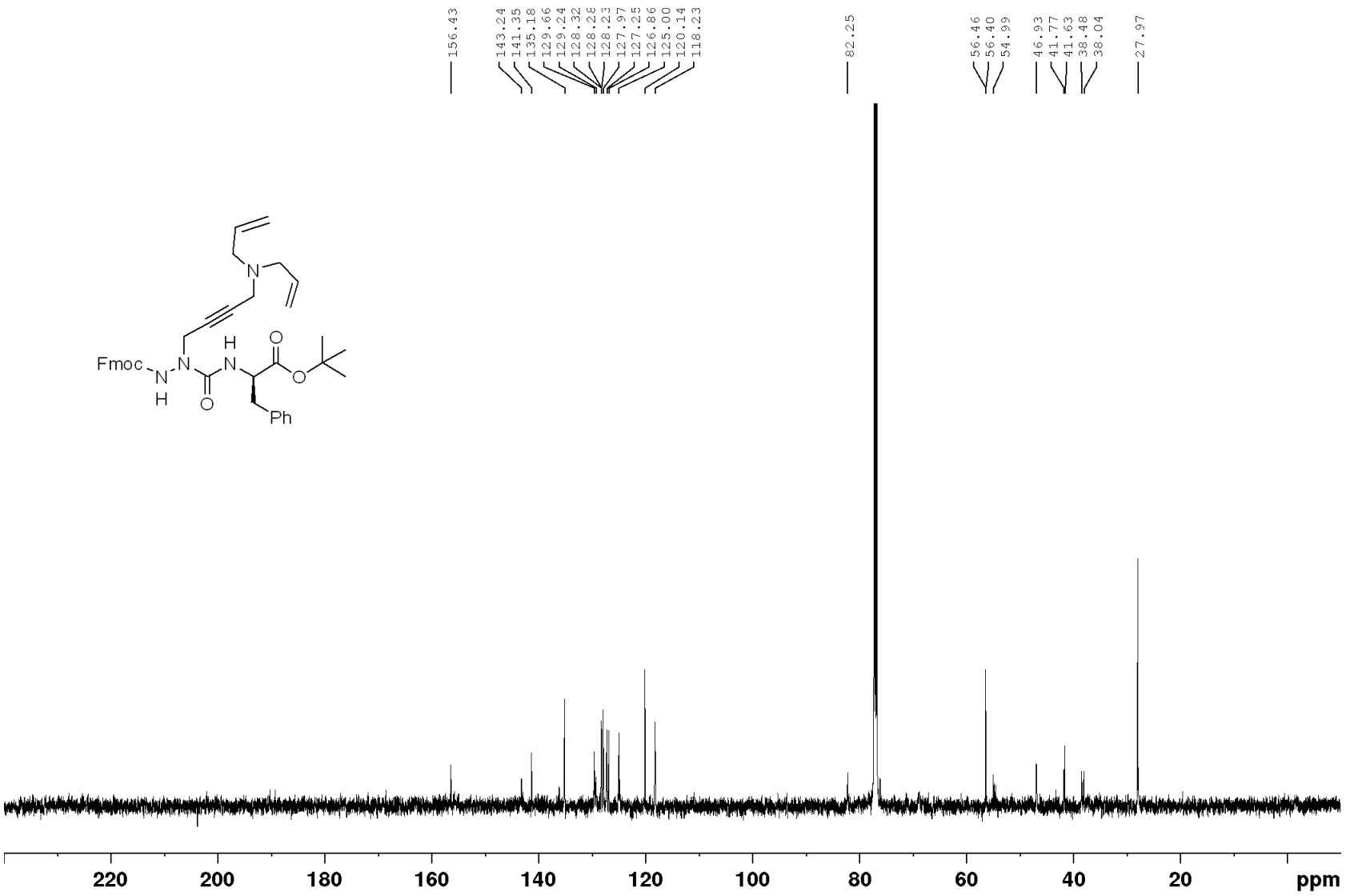

Compound 5.10

^{1}H-NMR, 500 MHz, $CDCl_3$

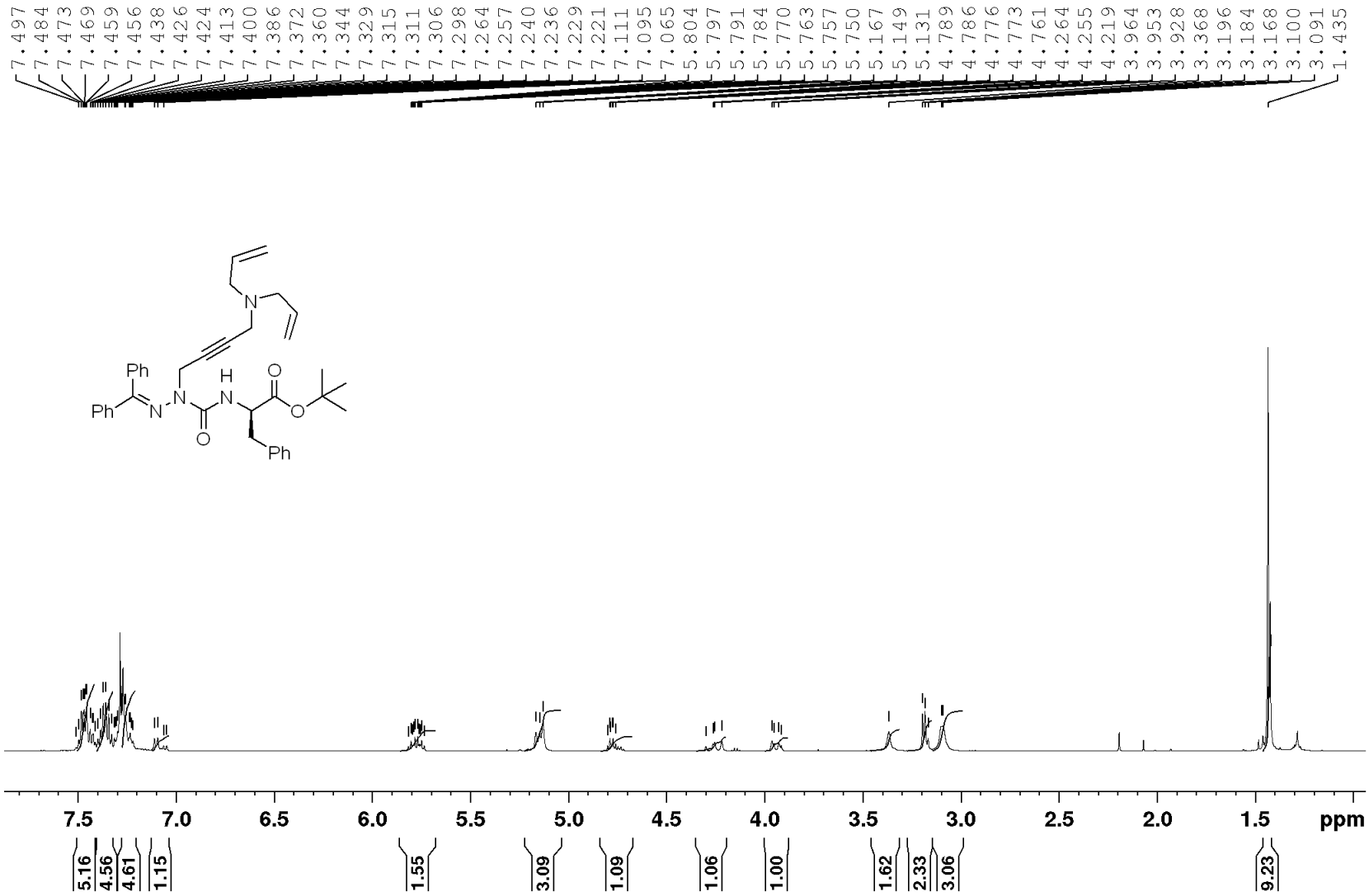

^{13}C-NMR, 125 MHz, $CDCl_3$

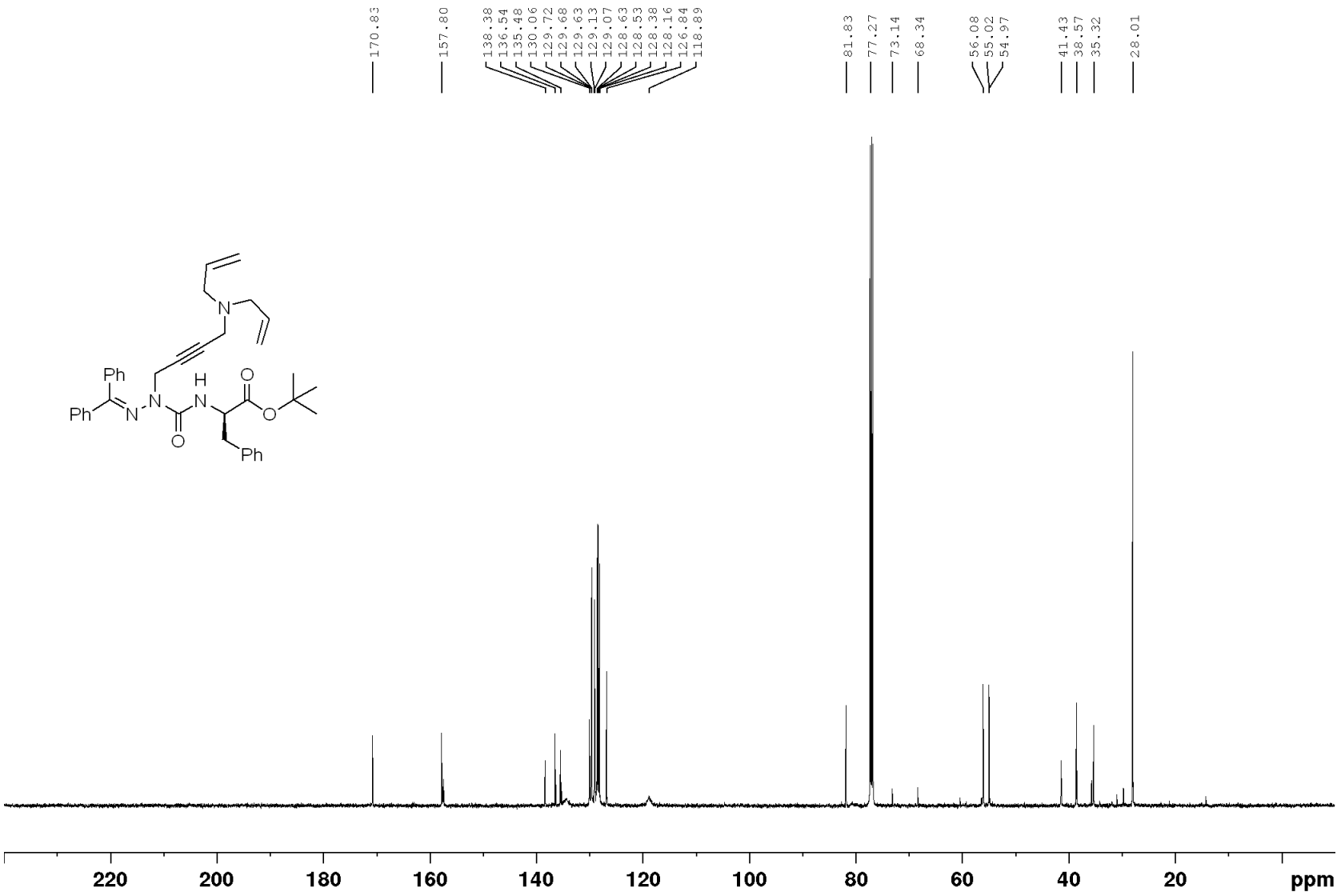

Compound 5.11

^{1}H-NMR, 500 MHz, $CDCl_3$

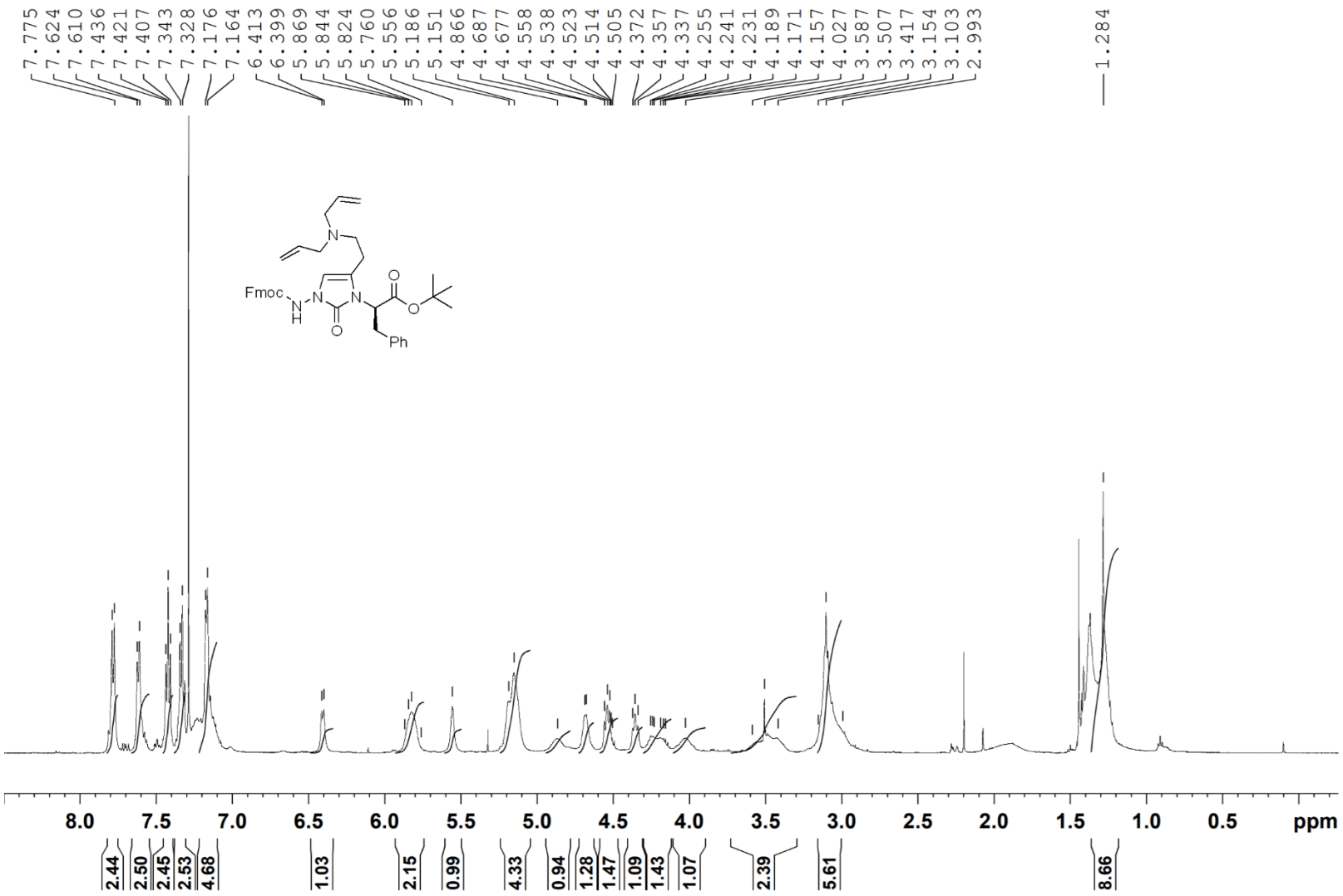

^{13}C-NMR, 125 MHz, $CDCl_3$

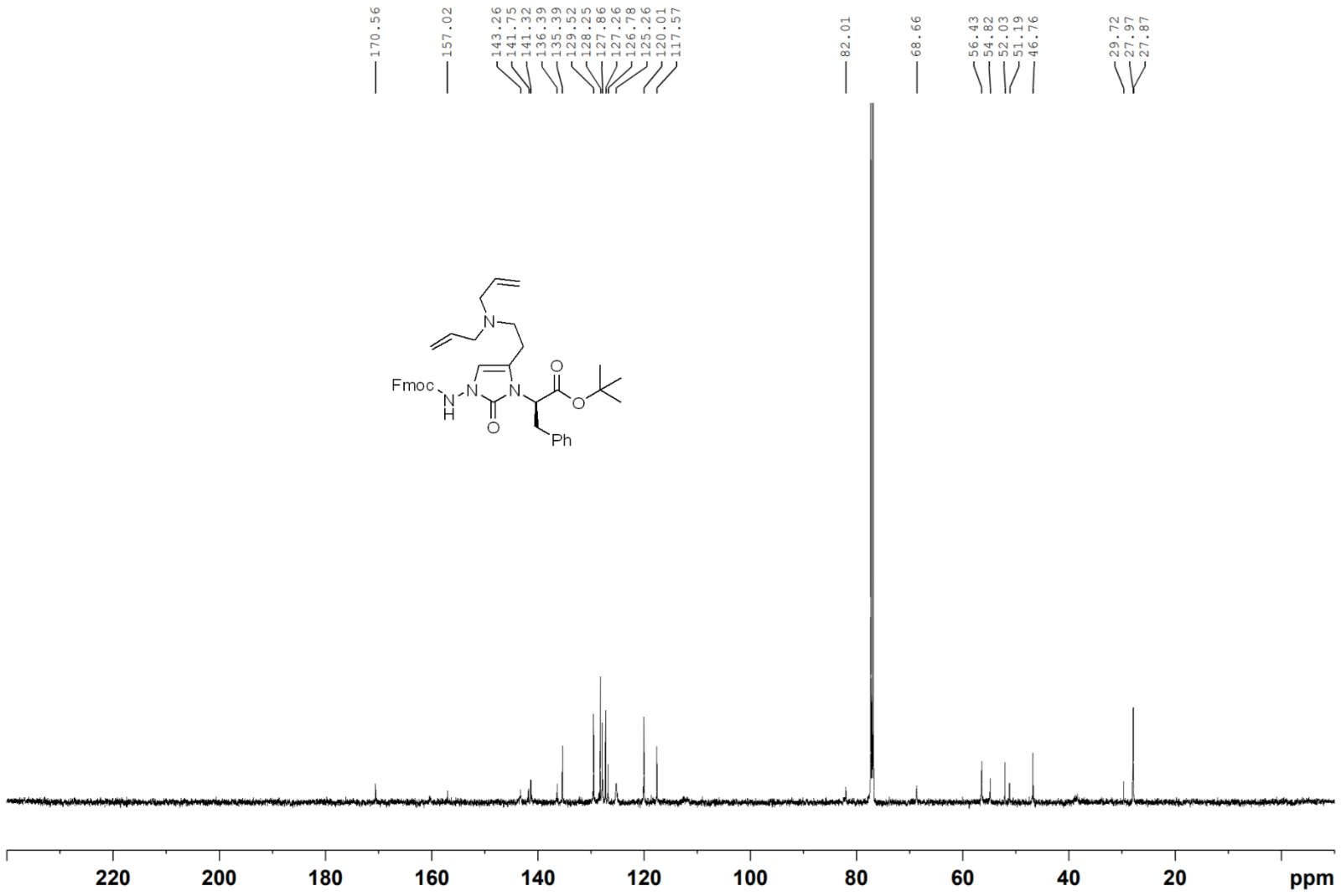

Compound 5.13

^{1}H-NMR, 300 MHz, $CDCl_3$

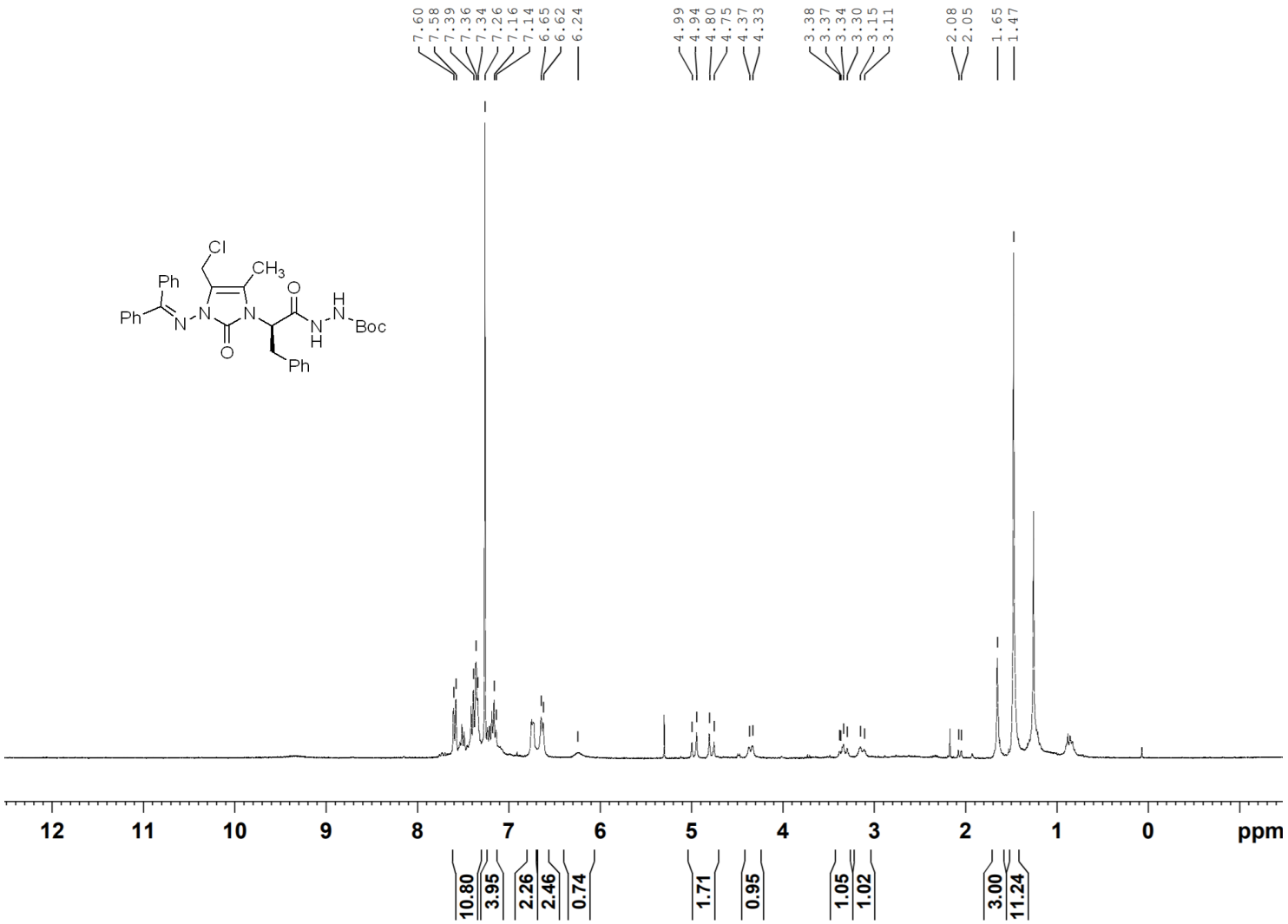

Annex 5: LC-MS for chapter 4

LC-MS data for peptides **4.9** to **4.12**

System A) 10%-90% MeCN (+0.1% FA) in H_2O (+0.1% FA) over 15 min

System B) 10%-90% MeOH (+0.1% FA) in H_2O (+0.1% FA) over 15 min

UV detection at 214 or 254 nm

Peptide 4.9

System A)

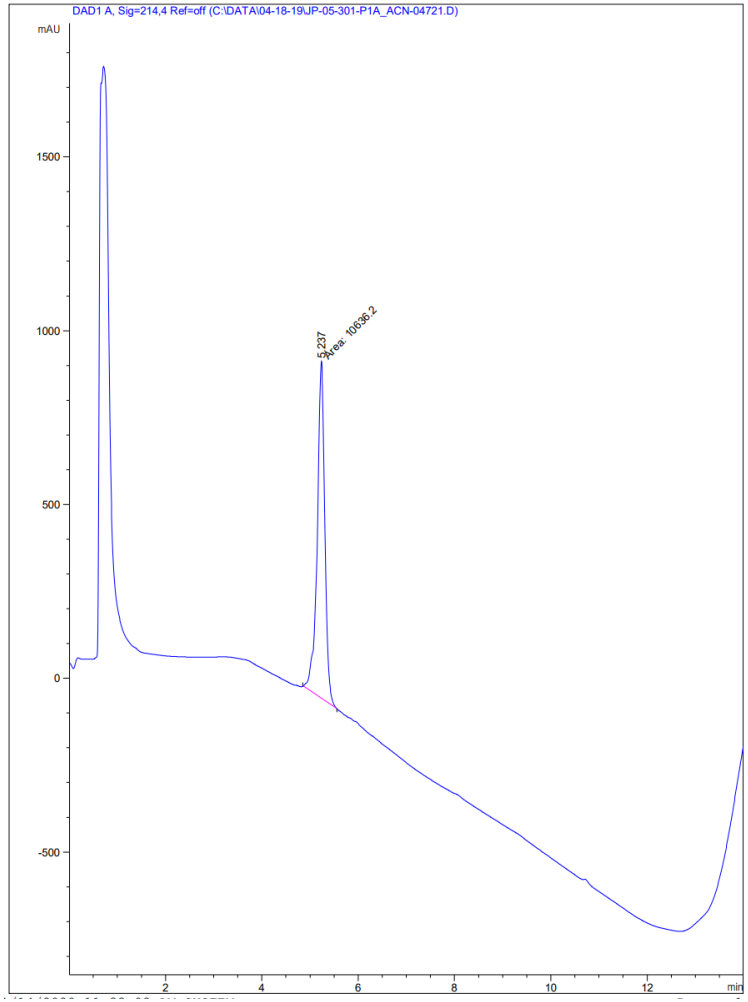

System B)

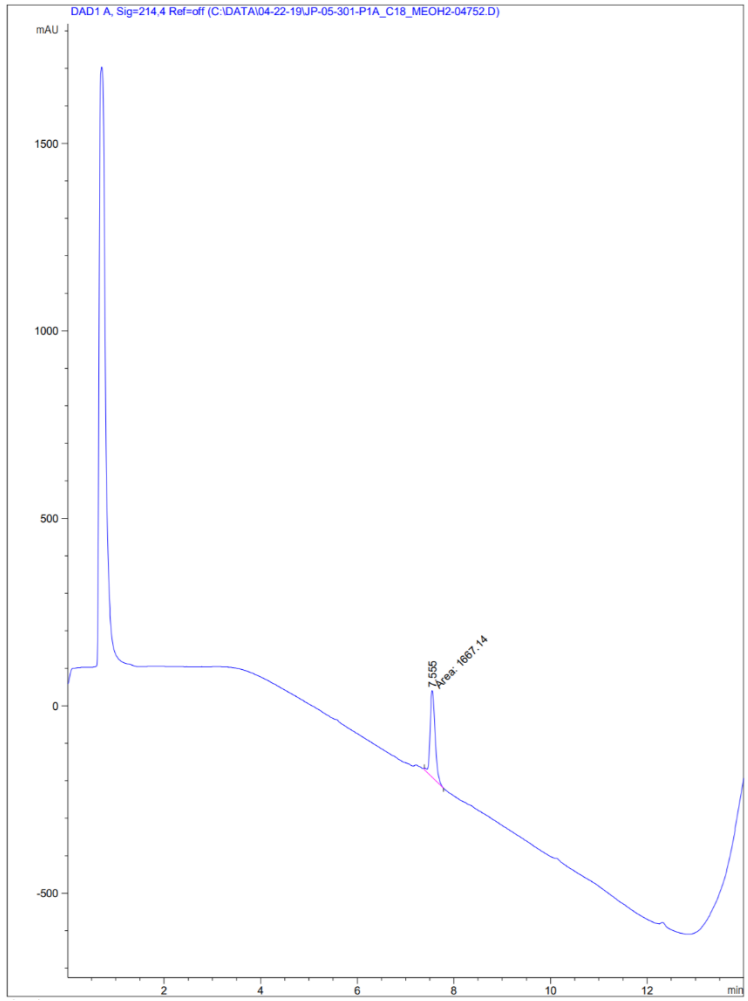

HRMS

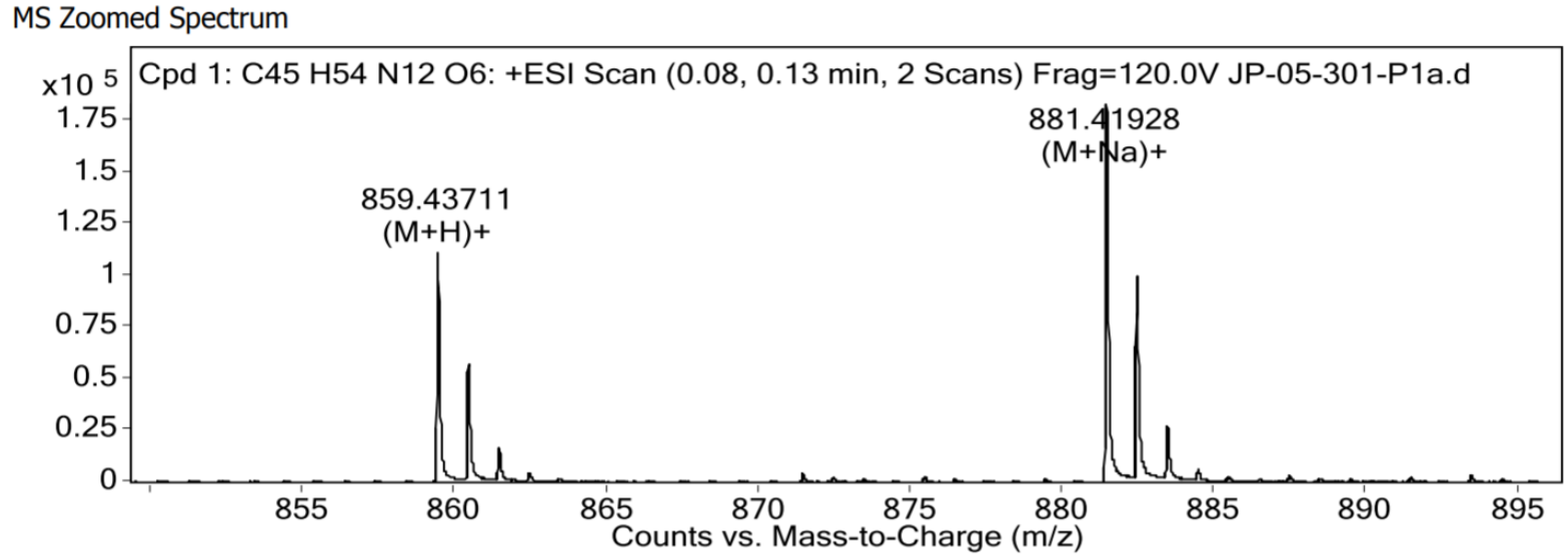
MS Zoomed Spectrum
Cpd 1: C45 H54 N12 O6: +ESI Scan (0.08, 0.13 min, 2 Scans) Frag=120.0V JP-05-301-P1a.d
x10 5
1.75
1.5
1.25
1
0.75
0.5
0.25
0
859.43711
(M+H)+
881.41928
(M+Na)+
855
860
865
870
875
880
885
890
895
Counts vs. Mass-to-Charge (m/z)

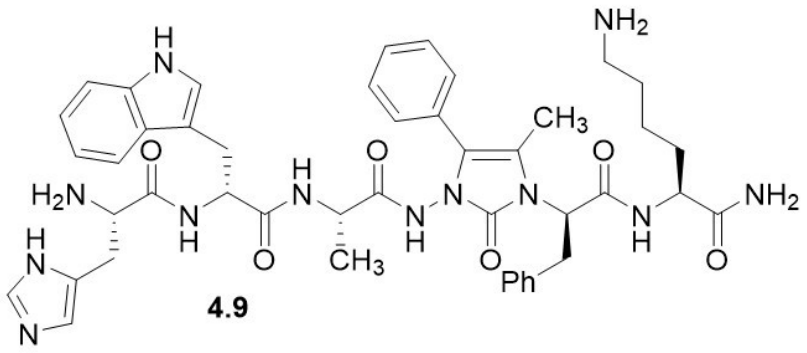
NH2
H
N
CH3
O
O
O
H2N
N
H
N
H
N
N
N
N
H
NH2
H
N
O
CH3
O
Ph
O
N

4.9

Peptide 4.10

System A)

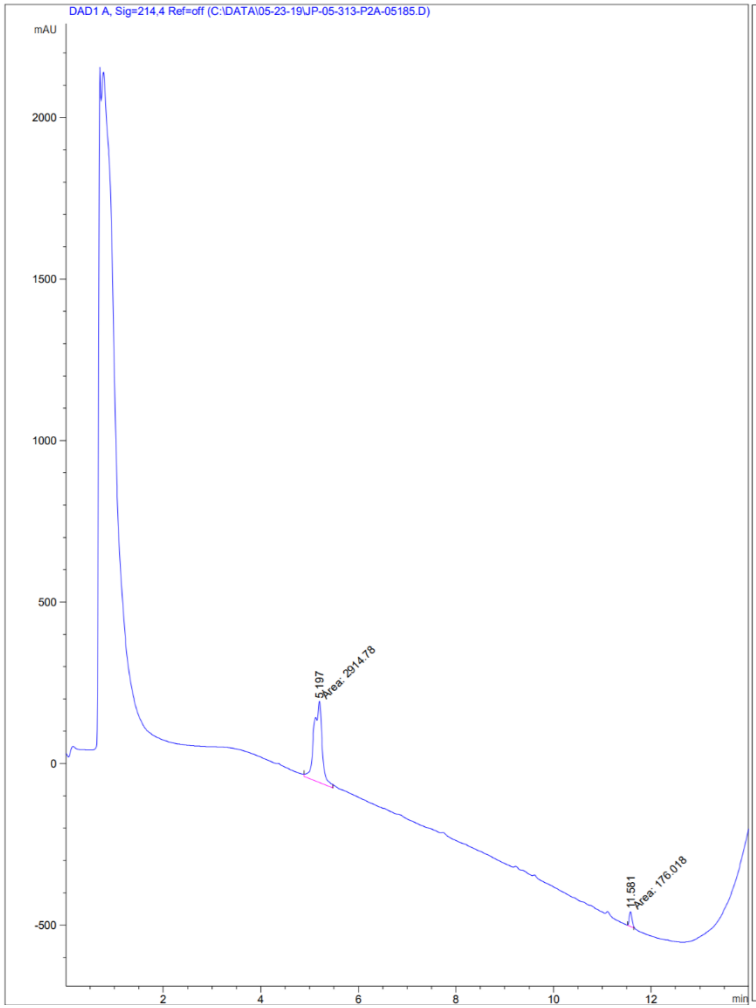

System B)

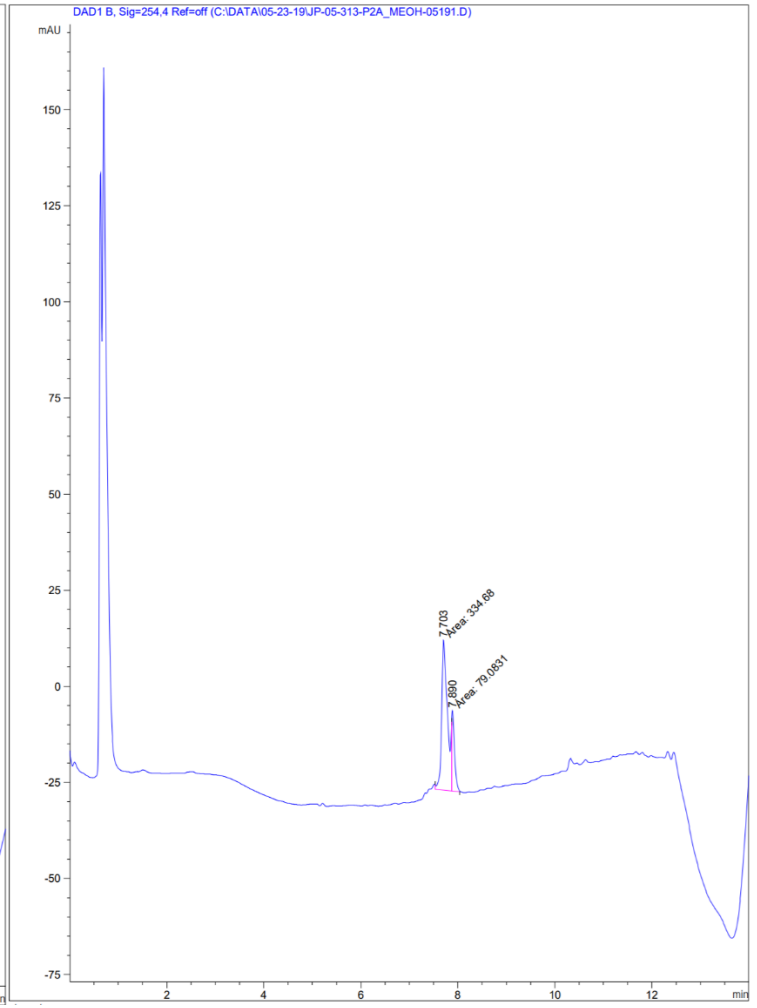

HRMS

MS Zoomed Spectrum

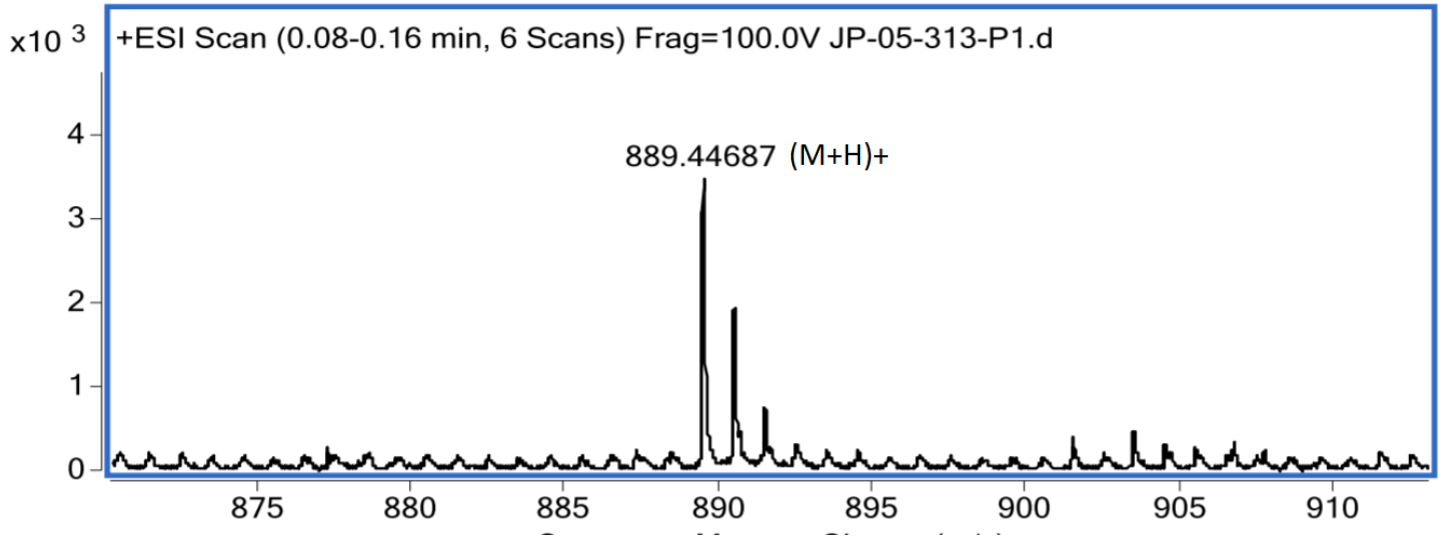

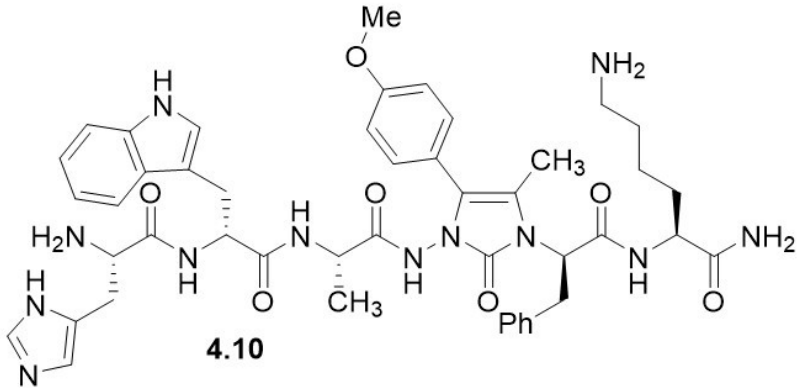

4.10

Peptide 4.11

System A)

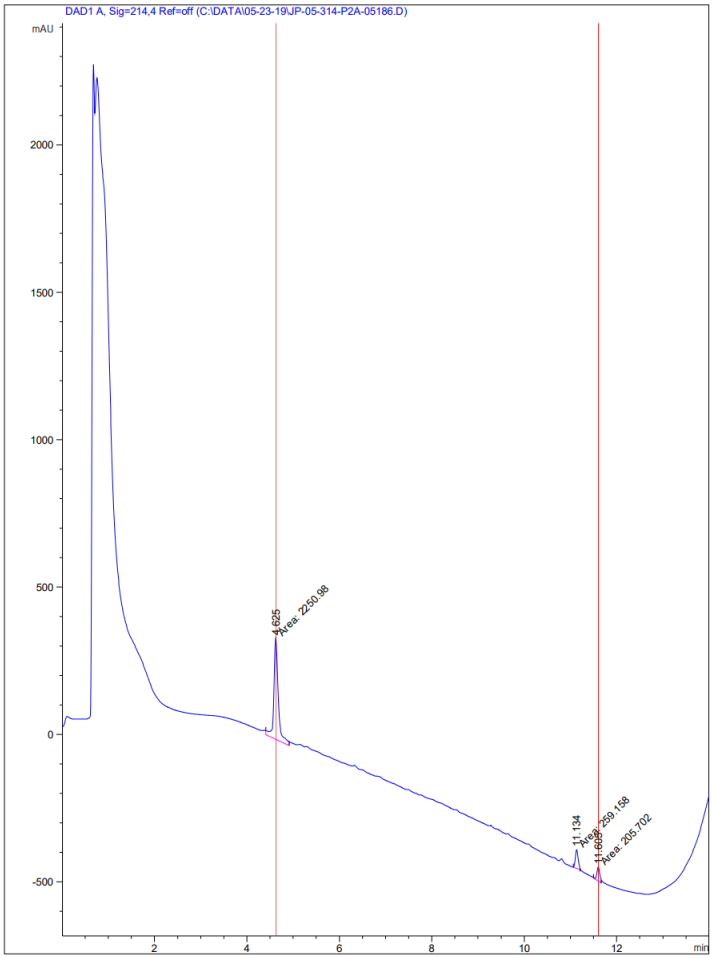

System B)

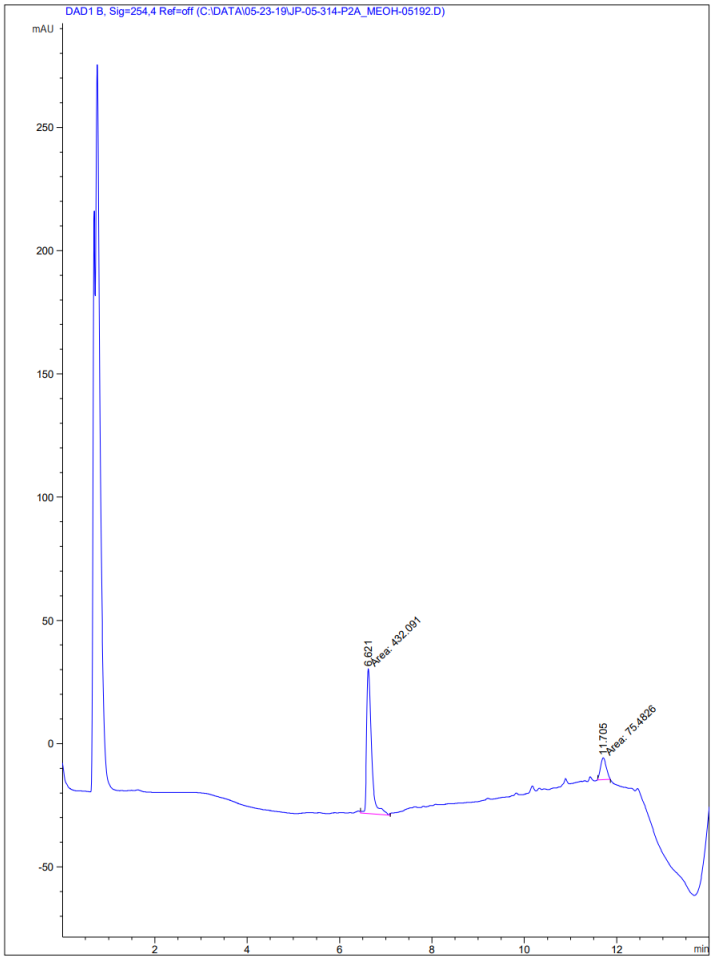

HRMS

MS Zoomed Spectrum

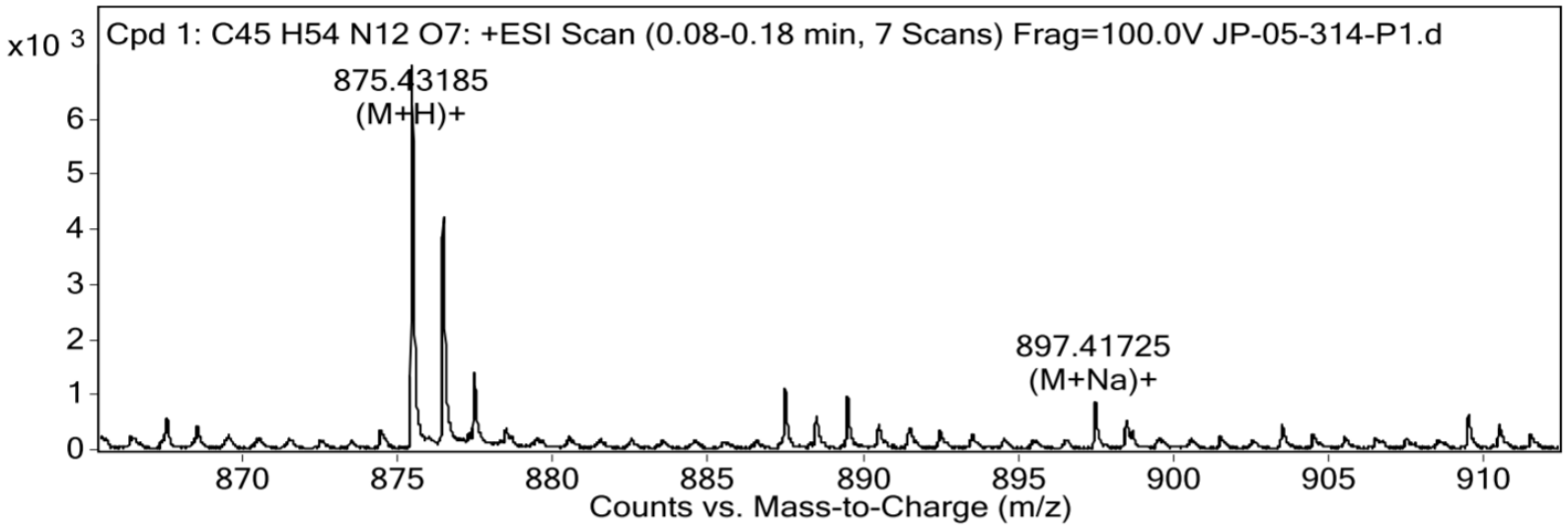

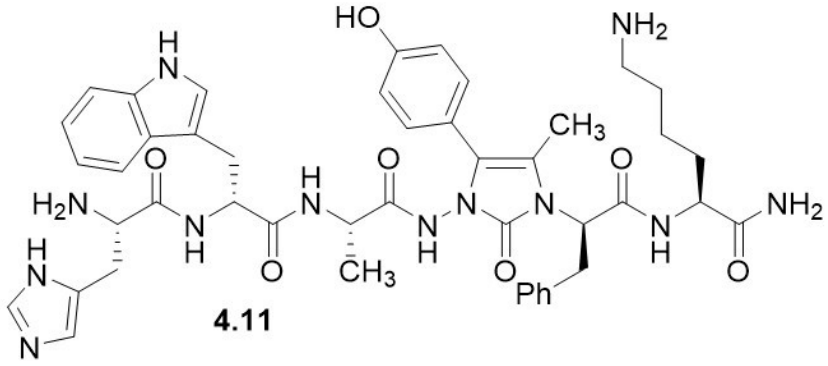

4.11

Peptide 4.12

System A)

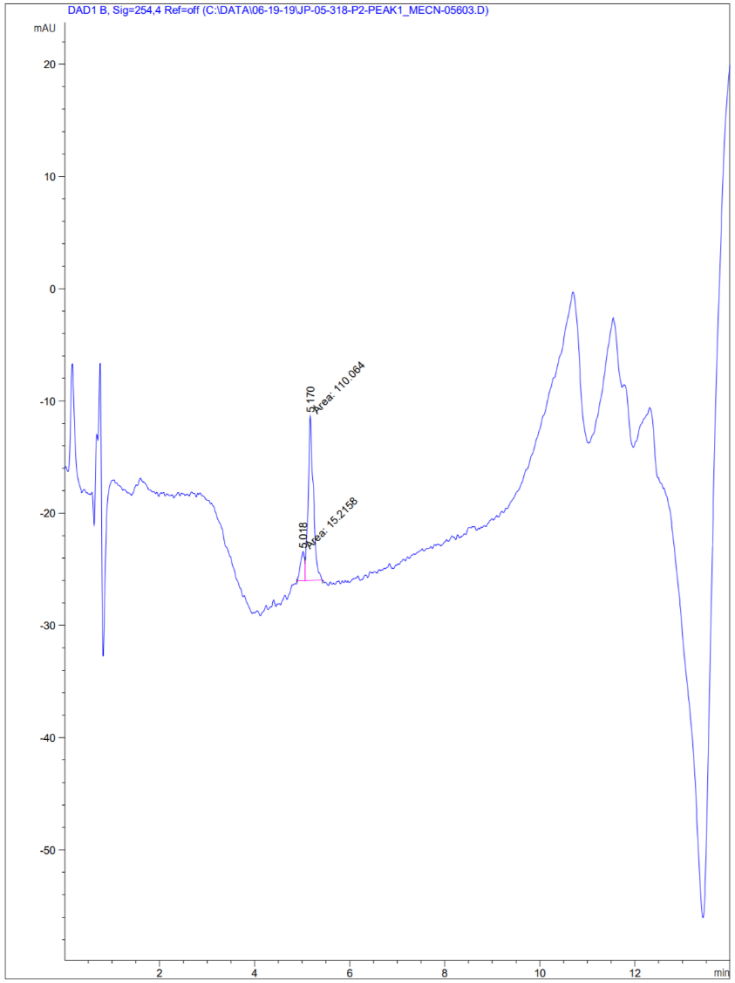

System B)

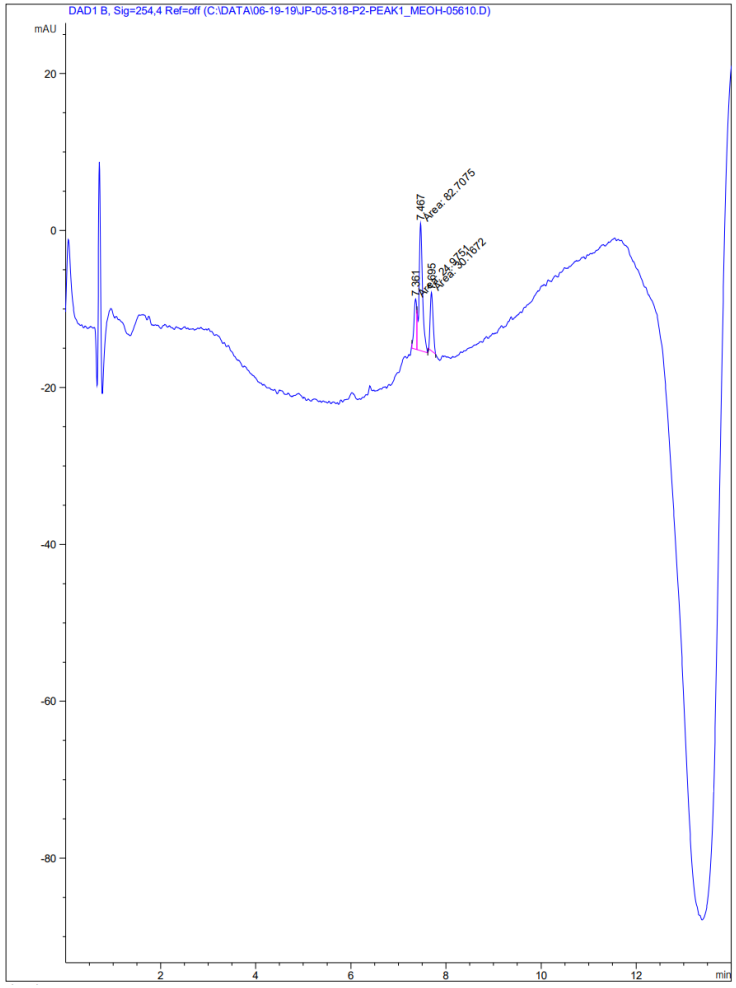

HRMS

MS Zoomed Spectrum

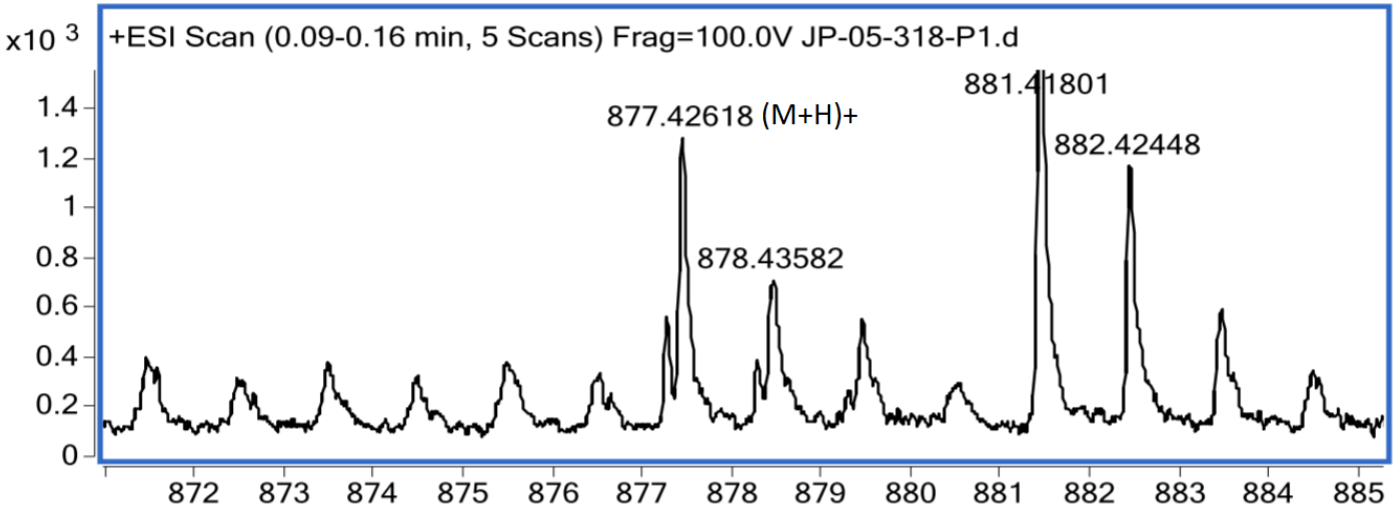

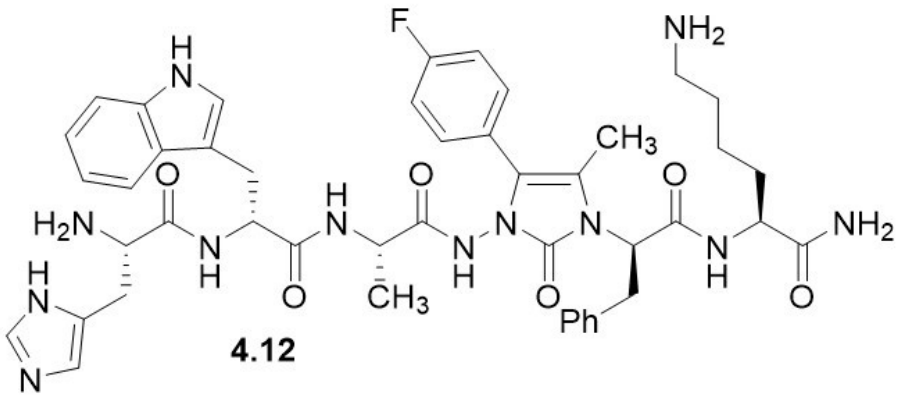

4.12